FRACTIONAL MATHEMATICAL MODEL FOR DYNAMICS OF INFECTIOUS DISEASES

Thesis Submitted
in Partial Fulfilment of the Requirements for the
Degree of

DOCTOR OF PHILOSOPHY

by

Swati
(Roll No. 2K19/Ph.D./AM/06)

Under the Supervision of
Dr. NILAM
Associate Professor

Department of Applied Mathematics

DELHI TECHNOLOGICAL UNIVERSITY
(Formerly Delhi College of Engineering)
Shahbad Daulatpur, Main Bawana Road, Delhi-110042, India

April 2025

© DELHI TECHNOLOGICAL UNIVERSITY, DELHI, 2025
ALL RIGHTS RESERVED.

DELHI TECHNOLOGICAL UNIVERSITY
(Formerly Delhi College of Engineering)
Shahbad Daulatpur, Main Bawana Road, Delhi-42

CANDIDATE'S DECLARATION

I, Swati, hereby certify that the work which is being presented in the thesis entitled "Fractional mathematical model for dynamics of infectious diseases" in partial fulfilment of the requirements for the award of the Degree of Doctor of Philosophy, submitted in the Department of Applied Mathematics, Delhi Technological University is an authentic record of my own work carried out during the period from August 2019 to October 2024 under the supervision of Dr. Nilam.

The matter presented in the thesis has not been submitted by me for the award of any other degree of this or any other Institute.

Place: Delhi (Swati)

Date: 30 October 2024

DELHI TECHNOLOGICAL UNIVERSITY
(Formerly Delhi College of Engineering)
Shahbad Daulatpur, Main Bawana Road, Delhi-42

CERTIFICATE

Certified that **Swati (**enrolment no 2K19/Ph.D./AM/06) has carried out her research work presented in this thesis entitled **"Fractional mathematical model for dynamics of infectious diseases"** for the award of **Doctor of Philosophy** from Department of Applied Mathematics, Delhi Technological University, Delhi, under my supervision. The thesis embodies results of original work, and studies are carried out by the student herself, and the contents of the thesis do not form the basis for the award of any other degree to the candidate or to anybody else from this or any other University/Institution.

(Dr. Nilam)

Supervisor and Associate Professor
Department of Applied Mathematics
Delhi Technological University
Main Bawana Road,
Delhi-110042, India)

(Prof. R.K. Srivastava)

Professor and Head
Department of Applied Mathematics

Date: 30 October 2024

ACKNOWLEDGMENTS

This thesis would have not been possible without the guidance and the help of several individuals who have extended their valuable assistance in the preparation and completion of the thesis.

I wish to express my deep and sincere gratitude to my supervisor Dr. Nilam, Associate Professor, Department of Applied Mathematics, Delhi Technological University (DTU), Delhi for her inspiring guidance and support during my research work and preparation of this thesis. It is indeed a great pleasure for me to work under her supervision. She does not only offer me guidance and necessary support for the successful completion of this work but also served to boost my moral. Her understanding, encouragement and personal guidance have provided a good basis for the present thesis.

I sincerely thank Prof. R. K. Srivastava, Professor and Head, Department of Applied Mathematics, DTU, for providing necessary facilities and valuable suggestions during theprogress of my work. I extend my sincere thanks to Prof. Rinku Sharma, Dean, PG, DTU for his everlasting support.

I would like to take this opportunity to thank the Hon'ble Vice Chancellor, DTU, Delhi, for providing necessary facilities during the research work. I am also thankful to the members of DRC and SRC, who allow me to do this work. I sincerely thank all faculty members of the Department of Applied Mathematics and other departments of DTU for their constant support and encouragement.

I also express my thanks to all the people working in the field of Mathematical Epidemiology whose research works provided me a platform to carry out my research work.

I want to thank Dr. Ankit Sharma, DTU, Delhi for spending his invaluable time in this work.

I owe my gratitude to all the Ph. D. fellows of my department that in one way or another shared with me the daily life at work. I wish to express my warm thanks

to Dr. Vijay Kumar Yadav, Dr. Abhishek Kumar, Dr. Kanica Goel, Mr. Anil Kumar Rajak, Mr. Abhay Srivastava, Mr. Sunil Kumar Meena and Ms. Priya Yadav.

I wish to record my profound gratitude to my parents and my parents-in-law who provided me with all kinds of support and help for my academic achievements. I am deeply grateful to my husband (Mr. Ashwani Kumar Singh) for his endless patience, thank you for being my greatest source of strength and for sharing this journey with me.

I would like to express my thanks to my sisters (Ms. Bharti and Ms. Jyoti), brother (Mr. Akhilesh Kumar Rajpuri), sister-in-law (Ms. Monika Gautam) and all my family members for their heartiest cooperations and affections. I would like to express my special thanks to my little sweet son (Advik Singh) and my nephews & niece for their hugs, laughter, and unconditional love. You may not have fully understood this journey, but your presence has been my greatest source of strength and joy.

Thank you!!!

Dedicated to my father

FRACTIONAL MATHEMATICAL MODEL FOR DYNAMICS OF INFECTIOUS DISEASES

SWATI

ABSTRACT

This thesis presents a comprehensive study of fractional-order differential models used for analysing the dynamics of infectious diseases. The fractional-order framework generalizes classical models with the inclusion of derivatives not being integer, thus capturing memory effects that describe long-term dependencies in disease spread and dynamics. We have also introduced time delays to account for incubation periods or delayed interventions seen in the real-world delay between disease spread and treatment. Such delays have major impacts on both epidemic progress and the timing of control measures, such as quarantine, vaccination or therapeutic intervention. In this work, we developed and evaluated fractional-order models for infectious diseases, including delayed versions of SIR and SIQR models. We investigated the system's positiveness, boundedness, stability, bifurcation, and long-term behavior with various fractional orders and time delays. This study examined how these characteristics affect crucial epidemiological indicators including the basic reproduction number (R_0). Numerical simulations are used to describe the spread of diseases like COVID-19, demonstrating that time delays along with fractional dynamics provide a more accurate description of disease behaviour over time.

Keywords: Epidemic; Fractional order differential equations (FODE); Basic Reproduction number, Incidence rates; Treatment rates; Bifurcation; Stability Analysis

TABLE OF CONTENTS

Page No.

Title **i**

Candidate's Declaration **iii**

Certificate **v**

Acknowledgement **vii**

ABSTRACT ..... **xi**

LIST OF TABLES ..... **xvii**

LIST OF FIGURES ..... **xix**

CHAPTER 1 ..... **1**

INTRODUCTION **1**

1.1 Infectious Diseases 1
1.1.1 Modes of Transmission 2
1.1.2 Disease prevention and control 3
1.2 Mathematical Modeling of Infectious Diseases 4
1.2.1 Deterministic and Stochastic Models 7
1.2.2 Delay differential equation 7
1.3 Basic Reproduction Number 8
1.3.1 Next generation matrix method 9
1.4 Fractional Calculus 9
1.4.1 Fractional Order Epidemiology 10
1.4.2 Fractional order Delay Differential Equations 10
1.5 Stability Analysis 11
1.6 Limit Cycle 11
1.7 Bifurcation 11
1.7.1 Saddle-node bifurcation 11
1.7.2 Transcritical bifurcation 12
1.7.3 Hopf bifurcation 12
1.8 Thesis Organization 12

CHAPTER 2 ..... **17**

FRACTIONAL ORDER SIR EPIDEMIC MODEL WITH BEDDINGTON – DE ANGELIS INCIDENCE AND HOLLING TYPE II TREATMENT RATE FOR COVID-19 ..... **17**

2.1 Introduction 18
2.2 Formulation of Fractional order epidemic Model 19
2.3 Basic Properties of the Model 20
2.4 Mathematical analysis of the model 22
2.4.1 Equilibria and their stability 22
2.4.2 Determination of Basic Reproduction Number 23

2.4.3 Analysis of local stability behaviour DFE (Q^d)..... 23
2.4.4 EEP (Q^e) existence and study of local equilibrium 25
2.4.5 Global stability analysis of DFE (Q^d) and Endemic equilibrium (Q^e)..... 27
2.5 Numerical Simulation 29
2.6 Conclusion..... 48

CHAPTER 3 51

FRACTIONAL ORDER MODEL USING CAPUTO FRACTIONAL DERIVATIVE TO ANALYSE THE EFFECTS OF SOCIAL MEDIA ON MENTAL HEALTH DURING COVID-19 51

3.1 Introduction..... 52
3.2 Formulation of Fractional order Mathematical Model..... 53
3.3 Basic Properties of the Model..... 54
3.4 Mathematical analysis of the model..... 56
3.4.1 Equilibria and their Stability..... 56
3.4.2 Disease free equilibria (DFE): 57
3.4.3 Endemic equilibria (EE): 57
3.4.4 Computation of Basic Reproduction Number..... 58
3.4.5 Local stability analysis of DFE (D^f) and EEP (D^e)..... 59
3.4.6 Global stability analysis of DFE (D^f) and EEP (D^e) 61
3.5 Numerical Simulations..... 63
3.6 Conclusion..... 71

CHAPTER 4 73

CAPUTO FRACTIONAL DERIVATIVE MODEL FOR IMPACT OF AWARENESS ON INFECTIOUS DISEASE 73

4.1 Introduction..... 74
4.2 Formulation of Fractional order Mathematical Model..... 76
4.3 Basic Properties of the Model..... 77
4.4 Mathematical analysis of the model..... 79
4.4.1 Equilibria and their stability..... 79
4.4.2 Determination of Basic Reproduction Number 80
4.4.3 Analysis of local stability behavior..... 81
4.4.3.1 Local stability analysis of DFE ($B^{\mathbf{0}}$)..... 81
4.4.3.2 EEP (B^*) existence and study of local equilibrium..... 81
4.4.4 Global Stability Analysis of Disease free equilibrium (B^0) and Endemic equilibrium point (B^*)..... 84
4.5 Numerical Simulation 86
4.6 Conclusion..... 98

CHAPTER 5 99

THE BEHAVIOR OF THE FRACTIONAL ORDER DELAY DIFFERENTIAL SIR EPIDEMIC MODEL WITH HOLLING TYPE II TREATMENT RATE AND CROWLEY-MARTIN RATE OF INCIDENCE 99

5.1 Introduction..... 100
5.2 Formulation of Fractional order Mathematical Model..... 101

5.3 Basic Properties of the Model 103
5.4 Mathematical analysis of the model 104
5.4.1 Disease Free Equilibria and Stability Analysis 104
5.4.2 Existence and stability analysis of endemic equilibrium 106
5.5 Numerical Simulations 111
5.6 Conclusion 119

CHAPTER 6 121

BIFURCATION ANALYSIS OF A DOUBLE DELAYED SIQR FRACTIONAL ORDER MODEL INCORPORATING HOLLING TYPE-II TREATMENT RATE AND MONOD-HALDANE INCIDENCE RATE 121

6.1 Introduction 122
6.2 Formulation of Fractional order Mathematical Model 123
6.3 Basic Properties of the Model 124
6.4 Mathematical analysis of the model 126
6.4.1 Stability Analysis and Hopf Bifurcation 126
6.4.1.1 Existence and Stability Analysis of Disease Free Equilibrium 126
6.4.1.2 Existence and Stability Analysis of Endemic Equilibrium Point 129
6.5 Numerical Simulations 143
6.5.1 $\tau_1 > 0$ and $\tau_2 = 0$ 143
6.5.2 $\tau_1 = 0$ and $\tau_2 > 0$ 144
6.5.3 $\tau_1 > 0$ and $\tau_2 > 0$ 144
6.5.3.1 $\tau_1 > 0$, $\tau_2 > 0$ and $\tau_1 \in (0, \tau_1^0)$ 144
6.5.3.2 $\tau_1 > 0$, $\tau_2 > 0$ and $\tau_2 \in (0, \tau_2^0)$ 145
6.6 Conclusion 177

CHAPTER 7 179

CONCLUSION, FUTURE SCOPE AND SOCIAL IMPACT 179

7.1 Conclusion 179
7.2 Future Scope 181
7.3 Social Impact 181

REFERENCES 183

APPENDIX 197

LIST OF PUBLICATIONS 199

LIST OF CONFERENCES 201

PLAGIARISM VERIFICATION 207

CURRICULUM VITAE 211

LIST OF TABLES

Table 2.1 Parameters with their descriptions 20
Table 2.2 Model parameters with their values 30
Table 3.1 Model parameters with their values 63
Table 4.1 The parameters and their Illustrations 76
Table 4.2 Model parameters with their values 86
Table 6.1 Model parameters and variables 123

LIST OF FIGURES

Figure 2.1. Basic Reproduction number vs Infected Population 32
Figure 2.2 Result of varying fractional order ρ on susceptibles 33
Figure 2.3 Result of varying fractional order ρ on infectives 33
Figure 2.4 Result of varying fractional order ρ on recovered 34
Figure 2.5 (i) Effect of varying measures taken by susceptibles on susceptibles with $\rho = 0.6$ and no measures taken by infectives 34
Figure 2.5(ii) Effect of varying measures taken by susceptibles on susceptibles with $\rho = 0.8$ and no measures taken by infectives 35
Figure 2.5(iii) Effect of varying measures taken by susceptibles on susceptibles with $\rho = 1.0$ and no measures taken by infectives 35
Figure 2.6(i) Effect of varying preventive measures taken by susceptibles on infectives with $\rho = 0.6$ and no measures taken by infectives 36
Figure 2.6 (ii) Effect of varying preventive measures taken by susceptibles on infectives with $\rho = 0.8$ and no measures taken by infectives 36
Figure 2.6 (iii) Effect of varying preventive measures taken by susceptibles on infectives with $\rho = 1.0$ and no measures taken by infectives 37
Figure 2.7a (i) Effect of varying measures taken by infectives on infectives with $\rho = 0.6$ and no measures taken by susceptibles 37
Figure 2.7a (ii) Effect of varying measures taken by infectives on infectives with $\rho = 0.8$ and no measures taken by susceptibles 38
Figure 2.7a (iii) Effect of varying measures taken by infectives on infectives with $\rho = 1$ and no measures taken by susceptibles 38
Figure 2.7b (i) Effect of varying measures taken by infectives on infectives with $\rho = 0.6$ 39
Figure 2.7b (ii) Effect of varying measures taken by infectives on infectives with $\rho = 0.8$ 39
Figure 2.7b (iii) Effect of varying measures taken by infectives on infectives with $\rho = 1$ 40
Figure 2.8a (i) Effect of varying measures taken by infectives on susceptibles with $\rho = 0.6$ and no measures taken by susceptibles 40
Figure 2.8a (ii) Effect of varying measures taken by infectives on susceptibles with $\rho = 0.8$ and no measures taken by susceptibles 41
Figure 2.8a (iii) Effect of varying measures taken by infectives on susceptibles with $\rho = 1.0$ and no measures taken by susceptibles 41
Figure 2.8b (i) Effect of varying measures taken by infectives on susceptibles with $\rho = 0.6$ 42
Figure 2.8b (ii) Effect of varying measures taken by infectives on susceptibles with $\rho = 0.8$ 42
Figure 2.8b (iii) Effect of varying measures taken by infectives on susceptibles with $\rho = 1$ 43
Figure 2.9a (i) Effect of lockdown on infectives with $\rho = 0.4$ 43
Figure 2.9a (ii) Effect of lockdown on infectives with $\rho = 0.8$ 44
Figure 2.9a (iii) Effect of lockdown on infectives with $\rho = 1$ 44

Figure 2.9b (i) Effect of lockdown on susceptibles with $\rho = 0.6$ 45
Figure 2.9b (ii) Effect of lockdown on susceptibles with $\rho = 0.8$ 45
Figure 2.9b (iii) Effect of lockdown on susceptibles with $\rho = 1$ 46
Figure 2.10 (i) Effect of immigration on infectives 46
Figure 2.10 (ii) Effect of immigration on susceptibles 47
Figure 2.11 Effect of transmission of disease on basic reproduction number R_0 47
Figure 2.12 Effect of measures taken by susceptibles on basic reproduction number R_0 48
Figure 3.1 Effect of memory on susceptibles 65
Figure 3.2 Effect of memory on infectives 65
Figure 3.3 Effect of limitation in treatment availability on infectives for fractional order ρ = 0.50 66
Figure 3.4 Effect of limitation in treatment availability on infectives for fractional order ρ = 1.0 66
Figure 3.5 Effect of varying cure rates on infectives for ρ = 0.60 67
Figure 3.6 Effect of varying cure rates on infectives for ρ = 0.80 67
Figure 3.7 Effect of varying cure rates on infectives for ρ = 1 68
Figure 3.8 Effect of varying inhibition rate due to infection on infectives for ρ = 1. 68
Figure 3.9 Effect of varying inhibition rate due to infection on infectives for ρ = 0.80 69
Figure 3.10 Effect of varying inhibition rate due to infection on infectives for ρ = 0.60 69
Figure 3.11 Phase portrait of the system for fractional order ρ = 0.90 70
Figure 3.12 Phase portrait of the system for fractional order ρ = 0.70 70
Figure 4.1 Effect of awareness on Infectives for u = 0 and u = 25% 88
Figure 4.2 Effect of awareness on Infectives for u = 0 and u = 50 % 88
Figure 4.3 Effect of awareness on Infectives for u = 0 and u = 75% 89
Figure 4.4 Effect of awareness on Susceptibles for u = 0 and u = 25% 89
Figure 4.5 Effect of awareness on Susceptibles for u = 0 and u = 50% 90
Figure 4.6 Effect of awareness on Susceptibles for u = 0 and u = 75% 90
Figure 4.7 Percentage of decrement in infected population for different u 91
Figure 4.8 Percentage of increment in susceptible population for different u 91
Figure 4.9 Effect of varying treatment rates on infectives with u = 40% 92
Figure 4.10 Effect of varying treatment rates on infectives with u =20% 92
Figure 4.11 Effect of varying treatment rates on infectives with u = 0 93
Figure 4.12 Effect of varying Inhibition rate due to infection on Infectives with u = 0 93
Figure 4.13 Effect of varying Inhibition rate due to infection on Infectives with u = 20% 94
Figure 4.14 Effect of varying Inhibition rate due to infection on Infectives with u = 40% 94
Figure 4.15 Effect of varying Inhibition rate due to infection on Susceptibles with u = 0 95
Figure 4.16 Effect of varying Inhibition rate due to infection on Susceptibles with u = 20% 95
Figure 4.17 Effect of varying Inhibition rate due to infection on Susceptibles with u = 30% 96

Figure 4.18 Phase Portrait for fractional order 0.8 96
Figure 4.19 Phase Portrait for fractional order 0.9 97
Figure 4.20 Phase Portrait for Integer order system with order 1.0 97
Figure 5.1 Effect of varying fractional orders on Susceptibles 112
Figure 5.2 Effect of varying fractional orders on infectives 112
Figure 5.3 Effect of varying γ_1 on infectives when fractional order ρ = 0.85 113
Figure 5.4 Effect of varying γ_2 on infectives when fractional order ρ = 0.85 113
Figure 5.5 Time series for susceptible population when $\rho = 0.85$, $\tau = 4.1 < \tau^0$ ... 114
Figure 5.6 Time series for infected population when $\rho = 0.85$, $\tau = 4.1 < \tau^0$ 114
Figure 5.7 Time series for susceptible population when $\rho = 0.85$, $\tau = 4.5 > \tau^0$ ... 115
Figure 5.8 Time series for infected population when $\rho = 0.85$, $\tau = 4.5 > \tau^0$ 115
Figure 5.9 Time series for susceptible population when $\rho = 0.8$, 0.9 and 1, $\tau = 3.7$ 116
Figure 5.10 Time series for infected population when $\rho = 0.8$, 0.9 and 1, $\tau = 3.7$ 116
Figure 5.11 Time series for susceptible population when $\rho = 0.8$, 0.9 and 1, $\tau = 4$ 117
Figure 5.12 Time series for infected population when $\rho = 0.8$, 0.9 and 1, $\tau = 4$ ... 117
Figure 5.13 Effect of varying γ_1 on infectives when fractional order ρ = 0.8 and $\tau = 3.3$ 118
Figure 5.14 Effect of varying γ_2 on infectives when fractional order ρ = 0.8 and $\tau = 3.3$ 118
Figure 5.15 Effect of varying α_1 on susceptibles when fractional order ρ = 0.8 and $\tau = 3.3$ 119
Figure 6.1 (i) Time series for the susceptible population when $\rho = 0.85, \tau_1 = 13.2 < \tau_1^0$ 145
Figure 6.1 (ii) Time series for the infected population when $\rho = 0.85, \tau_1 = 13.2 < \tau_1^0$ 146
Figure 6.1 (iii) Time series for the quarantine population when $\rho = 0.85, \tau_1 = 13.2 < \tau_1^0$ 146
Figure 6.1 (iv) Time series for the recovered population when $\rho = 0.85, \tau_1 = 13.2 < \tau_1^0$ 147
Figure 6.2 (i) Time series for the susceptible population when $\rho = 0.85, \tau_1 = 22.3 > \tau_1^0$ 147
Figure 6.2 (ii) Time series for the infected population when $\rho = 0.85, \tau_1 = 22.3 > \tau_1^0$ 148
Figure 6.2 (iii) Time series for the quarantine population when $\rho = 0.85, \tau_1 = 22.3 > \tau_1^0$ 148
Figure 6.2 (iv) Time series for the recovered population when $\rho = 0.85, \tau_1 = 22.3 > \tau_1^0$ 149
Figure 6.3 (i) Time series for the susceptible population when $\rho = 0.7, 0.8, 0.9 \; and \; 1, \tau_1 = 9$ 149
Figure 6.3 (ii) Time series for the infected population when $\rho = 0.7, 0.8, 0.9 \; and \; 1, \tau_1 = 9$ 150
Figure 6.3 (iii) Time series for the quarantine population when $\rho = 0.7, 0.8, 0.9 \; and \; 1, \tau_1 = 9$ 150

Figure 6.3 (iv) Time series for the recovered population when $\rho = 0.7, 0.8, 0.9\ and\ 1, \tau_1 = 9$ 151
Figure 6.4 (i) Time series for the susceptible population when $\rho = 0.7, 0.8, 0.9\ and\ 1, \tau_1 = 12$ 151
Figure 6.4 (ii) Time series for the infected population when $\rho = 0.7, 0.8, 0.9\ and\ 1, \tau_1 = 12$ 152
Figure 6.4 (iii) Time series for the quarantine population when $\rho = 0.7, 0.8, 0.9\ and\ 1, \tau_1 = 12$ 152
Figure 6.4 (iv) Time series for the recovered population when $\rho = 0.7, 0.8, 0.9\ and\ 1, \tau_1 = 12$ 153
Figure 6.5 (i) Time series for the susceptible population when $\rho = 0.85, \tau_2 = 15 < \tau_2^0$ 153
Figure 6.5 (ii) Time series for the infected population when $\rho = 0.85, \tau_2 = 15 < \tau_2^0$ 154
Figure 6.5 (iii) Time series for the quarantine population when $\rho = 0.85, \tau_2 = 15 < \tau_2^0$ 154
Figure 6.5 (iv) Time series for the recovered population when $\rho = 0.85, \tau_2 = 15 < \tau_2^0$ 155
Figure 6.6 (i) The time series of the system when $\rho = 0.85, \tau_2 = 26 > \tau_2^0$ 155
Figure 6.6 (ii) Time series for the infected population when $\rho = 0.85, \tau_2 = 26 > \tau_2^0$ 156
Figure 6.6 (iii) Time series for the quarantine population when $\rho = 0.85, \tau_2 = 26 > \tau_2^0$ 156
Figure 6.6 (iv) Time series for the recovered population when $\rho = 0.85, \tau_2 = 26 > \tau_2^0$ 157
Figure 6.7 (i) Time series for the susceptible population when $\rho = 0.7, 0.8, 0.9\ and\ 1, \tau_2 = 8$ 157
Figure 6.7 (ii) Time series for the infected population when $\rho = 0.7, 0.8, 0.9\ and\ 1, \tau_2 = 8$ 158
Figure 6.7 (iii) Time series for the quarantine population when $\rho = 0.7, 0.8, 0.9\ and\ 1, \tau_2 = 8$ 158
Figure 6.7 (iv) Time series for the recovered population when $\rho = 0.7, 0.8, 0.9\ and\ 1, \tau_2 = 8$ 159
Figure 6.8 (i) Time series for the susceptible population when $\rho = 0.7, 0.8, 0.9\ and\ 1, \tau_2 = 12$ 159
Figure 6.8 (ii) Time series for the infected population when $\rho = 0.7, 0.8, 0.9\ and\ 1, \tau_2 = 12$ 160
Figure 6.8 (iii) Time series for the quarantine population when $\rho = 0.7, 0.8, 0.9\ and\ 1, \tau_2 = 12$ 160
Figure 6.8 (iv) Time series for the recovered population when $\rho = 0.7, 0.8, 0.9\ and\ 1, \tau_2 = 12$ 161
Figure 6.9 (i) Time series for the susceptible population when $\rho = 0.85, \tau_1 = 9, \tau_2 = 18 < \tau_3^0$ 161
Figure 6.9 (ii) Time series for the infected population when $\rho = 0.85, \tau_1 = 9, \tau_2 = 18 < \tau_3^0$ 162

Figure 6.9 (iii) Time series for the quarantine population when $\rho = 0.85, \tau_1 = 9, \tau_2 = 18 < \tau_3^0$ 162
Figure 6.9 (iv) Time series for the recovered population when $\rho = 0.85, \tau_1 = 9, \tau_2 = 18 < \tau_3^0$ 163
Figure 6.10 (i) Time series for the susceptible population when $\rho = 0.85, \tau_1 = 9, \tau_2 = 24.5 > \tau_3^0$ 163
Figure 6.10 (ii) Time series for the infected population when $\rho = 0.85, \tau_1 = 9, \tau_2 = 24.5 > \tau_3^0$ 164
Figure 6.10 (iii) Time series for the quarantine population when $\rho = 0.85, \tau_1 = 9, \tau_2 = 24.5 > \tau_3^0$ 164
Figure 6.10 (iv) Time series for the recovered population when $\rho = 0.85, \tau_1 = 9, \tau_2 = 24.5 > \tau_3^0$ 165
Figure 6.11 (i) Time series for the susceptible population when $\rho = 0.6, 0.7, 0.8 \; and \; 0.9, \tau_2 = 13.5$ 165
Figure 6.11 (ii) Time series for the infected population when $\rho = 0.6, 0.7, 0.8 \; and \; 0.9, \tau_2 = 13.5$ 166
Figure 6.11 (iii) Time series for the quarantine population when $\rho = 0.6, 0.7, 0.8 \; and \; 0.9, \tau_2 = 13.5$ 166
Figure 6.11 (iv) Time series for the recovered population when $\rho = 0.6, 0.7, 0.8 \; and \; 0.9, \tau_2 = 13.5$ 167
Figure 6.12 (i) Time series for the susceptible population when $\rho = 0.7, 0.8, 0.85 \; and \; 0.86, \tau_2 = 19.5$ 167
Figure 6.12 (ii) Time series for the infected population when $\rho = 0.7, 0.8, 0.85 \; and \; 0.86, \tau_2 = 19.5$ 168
Figure 6.12 (iii) Time series for the quarantine population when $\rho = 0.7, 0.8, 0.85 \; and \; 0.86, \tau_2 = 19.5$ 168
Figure 6.12 (iv) Time series for the recovered population when $\rho = 0.7, 0.8, 0.85 \; and \; 0.86, \tau_2 = 19.5$ 169
Figure 6.13 (i) Time series for the susceptible population when $\rho = 0.85, \tau_2 = 18, \tau_1 = 9 < \tau_4^0$ 169
Figure 6.13 (ii) Time series for the infected population when $\rho = 0.85, \tau_2 = 18, \tau_1 = 9 < \tau_4^0$ 170
Figure 6.13 (iii) Time series for the quarantine population when $\rho = 0.85, \tau_2 = 18, \tau_1 9 < \tau_4^0$ 170
Figure 6.13 (iv) Time series for the recovered population when $\rho = 0.85, \tau_2 = 18, \tau_1 = 9 < \tau_4^0$ 171
Figure 6.14 (i) Time series for the susceptible population when $\rho = 0.85, \tau_2 = 18, \tau_1 = 23 > \tau_4^0$ 171
Figure 6.14 (ii) Time series for the infected population when $\rho = 0.85, \tau_2 = 18, \tau_1 = 23 > \tau_4^0$ 172
Figure 6.14 (iii) Time series for the quarantine population when $\rho = 0.85, \tau_2 = 18, \tau_1 = 23 > \tau_4^0$ 172
Figure 6.14 (iv) Time series for the recovered population when $\rho = 0.85, \tau_2 = 18, \tau_1 = 23 > \tau_4^0$ 173
Figure 6.15 (i) Time series for the susceptible population when $\rho = 0.7, 0.8, 0.9 \; and \; 1.0, \tau_1 = 9$ 173

Figure 6.15 (ii) Time series for the infected population when $\rho = 0.7, 0.8, 0.9 \; and \; 1.0, \tau_1 = 9$ 174
Figure 6.15 (iii) Time series for the quarantine population when $\rho = 0.7, 0.8, 0.9 \; and \; 1.0, \tau_1 = 9$ 174
Figure 6.15 (iv) Time series for the recovered population when $\rho = 0.7, 0.8, 0.9 \; and \; 1.0, \tau_1 = 9$ 175
Figure 6.16 (i) Time series for the susceptible population when $\rho = 0.7, 0.8, 0.9 \; and \; 1.0, \tau_1 = 15$ 175
Figure 6.16 (ii) Time series for the infected population when $\rho = 0.7, 0.8, 0.9 \; and \; 1.0, \tau_1 = 15$ 176
Figure 6.16 (iii) Time series for the quarantine population when $\rho = 0.7, 0.8, 0.9 \; and \; 1.0, \tau_1 = 15$ 176
Figure 6.16 (iv) Time series for the recovered population when $\rho = 0.7, 0.8, 0.9 \; and \; 1.0, \tau_1 = 15$ 177

CHAPTER 1

INTRODUCTION

Infectious diseases have always threatened public health, ranging from influenza to malaria and tuberculosis, ending most recently in the COVID-19 outbreak that highlighted the essentiality of having strong epidemiological models. The desire to understand the dynamics of infectious disease transmission, persistence and control has led to the use of a range of mathematical models. For example, the Susceptible-Infectious-Recovered (SIR) framework is well known compartmental models that have been widely used for describing disease dynamics. But these classical models typically use integer-order derivatives, which might not completely characterize the long memory, and the complicated dynamics present in the biological systems that describe disease transfer. In this case, fractional calculus provides an interesting enhancement of the classical models. Through utilizing the fractional-order derivatives, which provide a generalization of the concept of differentiation to non-integer orders, they enable the model to account for memory effects commonly observed in real-world epidemic processes. Fractional models permit domains where the influence of lasting past states on future dynamics are unresolved: a generality that affords more nuance (and so complexity) to capturing the subtle and at times, non-intuitive, dynamics required for describing certain diseases.

This is an introductory chapter which provides summary of findings during mechanisms of epidemic transmission in the field of mathematical epidemiology. The current chapter aims to provide some background on the infection mechanisms, epidemic control mechanism, role of mathematical models in epidemiology and motivation of the work performed as part of this thesis. Additionally, the current chapter provides a preview of the work completed.

1.1 Infectious Diseases

Infectious diseases have always been one of the biggest threats to human health, and they have long been considered a threat to human health. It is well known that factors associated to the disease, including the infectious agent, the mechanism of transmission, susceptibility, and the available treatment options, all have a role in the spread of communicable diseases. Infectious agents continue to adapt and change many emerge as novel infectious diseases while others re-emerge again from dormant states after slumbering for decades. Some of the diseases that have been identified are

lyme disease (1975), hepatitis C (1989), hepatitis E (1990) and hantavirus (1993). Climate change is causing diseases like yellow fever, dengue fever, and malaria to reappear and spread to new places. Sometimes new outbreaks of cholera, plague, and haemorrhagic fevers occur. Since December 2019, Wuhan, China had seen an increase in the number of cases of novel coronavirus-infected pneumonia (NCIP), which was first discovered on December 31 in the same year. The COVID-19 pandemic was a public health emergency of global concern which needs a sophisticated strategy. The emerging and reemerging diseases have led to a revived interest in infectious diseases

1.1.1 Modes of Transmission

Infectious diseases spread by a variety of modes, specific to the pathogen, environment and human behavior. Modes of transmission include:

- Direct Contact Transmission: This happens if an infected person touches or exchanges body fluids with another person by contact with skin, by touching, kissing, shaking hands or sexual contact direct from one person to another. Examples: HIV, Zika virus or Syphilis.

- Indirect Contact Transmission: Infected individuals can transfer infectious pathogens by contaminating objects or surfaces. Example diseases include MRSA, norovirus, and rhinovirus (common cold).

- Droplet Transmission: Droplets exhaled by an infected person while coughing, sneezing, or talking might be inhaled by people around. Droplets usually travel small distances. Example diseases: COVID-19, influenza, tuberculosis.

- Vector-borne Transmission: Pathogens are transmitted to humans via the bites of infected insects or animals (vectors). Examples: Malaria (mosquitoes), dengue (mosquitoes), Lyme disease (ticks), plague (fleas) etc are some of the examples of diseases.

- Waterborne Transmission: Spread when the pathogens are taken in through water that is contaminated. Example diseases: Cholera, typhoid fever, hepatitis A.

- Zoonotic Transmission: Transmissions of diseases from animals to humans, either through direct contact or via contact with an intermediate pathway (vector, contaminated food, and environment). Example: Rabies, avian influenza, and hantavirus.

It is important to know the mode of transmission as it determines the clinical manifestations and control measures including hygiene, vaccination, quarantine, or vector control.

1.1.2 Disease prevention and control

Limiting contacts is a highly effective strategy for managing epidemics. But in today's world with more social connections, this strategy is difficult to implement. The two most often used preventative measures that may reduce disease spread and improve control are immunization and treatment. Over the past ten years, the population's behavior has changed, screening and preventive services have been expanded, and disease management and immunization programs have all worked together to curb the spread of infection.

The primary motivation for people to prevent infections is that prevention is possible and effective if implemented correctly. Effective measures can be implemented to prevent disease and minimize the harms caused by infectious diseases. Preventive measures for infections are available but not given to a significant proportion of those in need, or they are out of reach. The course of treatment is a crucial part of an all-encompassing strategy for preventing harm to the health. Treatment for infected persons reduces mortality and morbidity among the susceptible population, prevents further transmission, lowers overall healthcare and societal expenditures, and improves productivity. To attain the best results, the treatments must be well-organized and of the highest standards. A chance to slow the rate at which infections spread across society is provided by the availability of efficient treatment services.

Vaccination, also known as an immunization, is used to strengthen the immune system's resistance to a specific infection. A pathogen's physical characteristics are like those of the material used in vaccinations. Essentially, one can consider an antibody to be a fake pathogen devoid of the ability to replicate and spread the disease. It could very well be composed of a broken or weakened pathogen. Immunizations can activate the host's immune system and cause the development of antibodies against the pathogens, helping the host recall them as foreign invaders, because they resemble harmful microorganisms. This way, the immune system eliminates the real bacterium whenever it is encountered inside the host. We refer to this phenomenon as immunity or resistance. Thus, as soon as an antibody to a disease is available, it is an ideal tool for protecting the whole population against the pathogen. Antibodies have, in fact, saved millions of lives(Rahman et al., 2016) however, as there was no primary measles immunization at that time, prior to the vaccine's introduction in 1963 about 400,000 measles incidences got reported annually throughout the United States. The risk of death or serious morbidity through diseases like polio, rubella or mumps amongst children used to be massive too. With proper immunization, these diseases will no longer be prevalent.

1.2 Mathematical Modelling of Infectious Diseases

Infectious diseases continue to pose a substantial threat to human existence. Consequently, understanding the dynamics of disease progression is critical for disease control or elimination. Mathematical models can be used to explore the dynamics of infectious diseases. Mathematical modeling of infectious diseases carries an importance as it provides advancement in understanding the mechanisms for the disease spread and makes health decisions more cost-effective and reliable than the experimental studies. We may use the model to predict the future path of an outbreak to a significant extent, allowing us to evaluate control methods. As a result, new fields, such as mathematical epidemiology, have emerged. Models employ fundamental assumptions and parameters to predict whether a disease will spread or die out in the community.

The first ever mathematical modeling was being traced back to the 18th century when in 1766, Daniel Bernoulli formulated a smallpox model to predict the effect of control measures on smallpox-infected population (Hethcote, 2006). However, because of the advent of numerous diseases in society, mathematical models have taken on a new platform in the twentieth century, following the model established by Kermack and Mckendrick (Kermack & Mckendrick, 1927), which indicates whether an outbreak of smallpox would occur. They (Hethcote, 2006; Anderson & May, 1991) have addressed a wide range of biological phenomena, including infection phases, vertical transmission, disease vectors, age structure, social and sexual mixing groups, spatial spread, chemotherapy, immunization, isolate, passive immunity, steady loss of vaccine, and disease-acquired immunity. Some models focused on diseases such as measles, rubella, chickenpox, diphtheria, cancer, smallpox, malaria, rabies, herpes, syphilis, and HIV/AID (Hethcote, 2000, Anderson & May, 1991, Longini & Halloran, 2005; Usher, 1994). The disease transmission models describe the transmission process and track the afflicted individuals. Models can identify the population remaining uninfected at the end of an epidemic. The concept of population compartments is often used in epidemic models (Hethcote, 2000, Anderson & May 1991, Diekmannn and Heesterbeek, 2000, Murray, 1989).

For mathematical convenience, these compartments are typically labelled by their initial letter, with S, E, I, and R signifying the susceptible, exposed, infected, and recovered populations, respectively. People who are vulnerable against infection are termed as susceptible and have been placed into the S (susceptible) compartment. A person who is currently infected but does not show symptoms or cannot infect others has been placed in the E (exposed) compartment. Once an infected person begins contaminating others, he or she is termed infected and assigned to compartment I (infected). Finally, once an individual has been cured from the disease he or she is transferred to the R (recovered) compartment. A recovered individual either stays there if he or she achieves permanent recovery or becomes susceptible again and moves back into the S compartment, depending on the disease.

Various models can be built by addressing these compartments in terms of pathogens and infections, such as SIS, SIR, SIRS, and so on. If an infected person becomes susceptible again after treatment, a SEIS or SIS model might be appropriate for disease dynamics. Bacterial diseases could be considered SIS models. However, if recovery is long-lasting and the healed persons are no longer susceptible to the pathogen, as seen in viral infection, an SIR-type model would be acceptable. In these demonstrative exercises, the population is homogeneously mixed, with persons contracting diseases or being cured at consistent rates.

The following ordinary differential equations provided a basic SIR epidemic model(Kermack & Mckendrick, 1927).

$$\begin{aligned} \frac{dS}{dt} &= \frac{-\beta SI}{N} \\ \frac{dI}{dt} &= \frac{\beta SI}{N} - \gamma I \\ \frac{dR}{dt} &= \gamma I \end{aligned} \tag{1.1}$$

where β is the transmission rate and γ is the recovery rate. This simple model depicts how sub-populations of susceptible, infected, and recovered classes evolve without regard for the host population's demographics. Several aspects have been incorporated into model (1.1) to capture the most significant characteristics of the situation under consideration; nevertheless, doing so has increased the model's complexity and rendered the analysis difficult, even unattainable. Therefore, when employing a mathematical modeling approach to explore disease dynamics, establishing a balance between a model's rationality and mathematical tractability always remains a crucial issue.

The bilinear or mass action incidence rate, shown by the parameter $\beta S(t)I(t)$, in model (1.1) illustrates how incidence rises as the number of susceptible and infected individuals increases. This transmission rate is calculated by multiplying the frequency of interpersonal interaction by the probability that an infectious person will infect a vulnerable person. Several further nonlinear saturated incidence rates that are frequently employed by different researchers are as follows:

Holling type II: The expression $F(S, I) = \frac{\beta SI}{1+\gamma I}$, S, β, $\gamma > 0$, is known as Holling functional type II incidence rate (Holling, 1959) introduced this incidence rate, which is also known as the saturated incidence rate. Holling type II is best suitable for the condition stated as: “For each outbreak of the disease, its incidence is first very low and then develops slowly as infection increases. Furthermore, due to the crowding

effect, when the number of infected persons is very big, the infection reaches its peak" (Dubey, 2016).

Holling type III: The expression for Holling Type III incidence rate is given by $F(S,I) = \frac{\beta I^2}{1+\gamma I^2}, S, \beta, \gamma > 0$. Holling type III defines the condition in which incidence of infection first grows very fast initially with increase in infectives and then it grows slowly and finally settles down to maximum saturated value. After this condition, any increase in infection will not affect the infection rate.

Beddington-DeAngelis functional type: The expression $F(S,I) = \frac{\beta SI}{1+\alpha S+\gamma I}, \beta, \alpha, \gamma > 0$ is known as Beddington-DeAngelis type incidence rate. Here β is the transmission rate, α is a measure of inhibition effect, such as preventive measures taken by susceptible and γ is a measure of inhibition effect such as treatment with respect to infectives (Dubey et.al., 2015). This incidence was introduced by Beddington (Beddington, 1975) and DeAngelis (Deangelis et al., 1975) independently. "This incidence rate considers the effect of inhibition among infectives in case of the low density of population (Dubey et al., 2015)".

Crowley-Martin functional type: The Crowley-Martin type of functional response was introduced by P.H. Crowley and E.K. Martin (Crowley & Martin, 1989) and is expressed as $F(S,I) = \frac{\beta SI}{(1+\alpha S)(1+\gamma I)}, \beta, \alpha, \gamma > 0$. "From the expression, we observe that like the Beddington-DeAngelis type incidence rate, one can easily derive other forms of incidence rates. The important difference between Beddington-DeAngelis type and Crowley-Martin type incidence rate is that the later considers the effect of inhibition among infectives even in case of high density of susceptible population while the former neglects this"(Dubey et al., 2015).

Treatment is essential for curing diseases and preventing the emergence of resistant pathogens. As a result, the treatment rate must be carefully considered in the epidemic model. In 2004, Wang and Ruan (W. Wang & Ruan, 2004) investigated the impact of treatment capacity on disease transmission dynamics using the SIR epidemic model with bilinear incidence rate and constant treatment rate. This type of treatment rate is appropriate when there are few infectives and treatment resources are plentiful, but it is improper when there are many infected individuals and treatment resources are scarce. Therefore, in 2012, Zhou and Fan (L. Zhou & Fan, 2012) improved the treatment rate by considering a saturated treatment rate and explored the SIR epidemic model to understand the effect of the limited medical resources and their supply efficiency on the transmission of infectious diseases. To regulate the disease, most researchers concentrate on a nonlinear form of treatment rate. Dubey et al (Dubey et al., 2013) added the nonlinear treatment rate as Holling Type II, Holling Type III, and Holling Type IV into their model and offered nonlinear dynamics to manage the

epidemic. In this thesis, we have investigated the effects of different nonlinear treatment rates on disease transmission models. The authors emphasized that, in addition to the nonlinearity in the incidence and treatment rates, public awareness is a significant strategy for reducing disease transmission. Many authors have explored how knowledge and awareness affect the spread of epidemics. (Al-Dmour et al., 2020; Goel et al., 2020; Kumar et al., 2019; Manzoni et al., 2021; Misra et al., 2011; Naik, 2020)

1.2.1 Deterministic and Stochastic Models

Usually, differential and difference equations are used to determine the model in deterministic models. For handling big populations, deterministic models have been employed. The infectious population and susceptible population sizes in these kinds of models are always continuous functions of time. Different compartments in the model, each denoting a different epidemic stage, are depicted. Deterministic model has non-random parameters and variables. When there is a very small population, the deterministic model is invalid. Therefore, to analyse the small size population with random variable, the stochastic model has been applied. The probability distribution's interrelationships and dynamics are explained by this model. There are two different kinds of stochasticity: environmental and demographic. Demographic stochasticity occurs when a person is vulnerable to occurrences with equal probabilities. In environmental stochasticity, the model is governed by the circumstance with fluctuation in probability. The outcome of the stochastic model may differ depending on the random variable evaluated.

1.2.2 Delay differential equations

The evaluation of past and currently ongoing epidemics and the formulation of structure for future-cost control interventions jointly depend on delay differential equation (DDE). It may be stated that when a disease first appears, there will be a delay in recognizing it. Therefore, the time delay is an essential parameter in the dynamical behavior of infectious diseases, which may lead to a change in the dynamical system's behavior. Delay differential equations (DDEs) are known to allow richer dynamics than ordinary differential equations and therefore provide a more realistic representation of time delays in real-world problems. This was well established by Driver (Driver, 1977). Usually, time delays are used to describe that a person may not be infectious soon after being infected. The contagious disease latency period, defined as the span between pathogen exposure and infection (while after exposed in which the pathogen is presence in an active but not detectable, dormant stage without clinical symptoms or signs of infection given a host), can be modeled by DDE. There are several reasons for the delay, particularly when it comes to epidemiology. The two most significant reasons to think about time delay are (i) the infection's latency in a vector and (ii) the infection's latency in an infected host. In

these instances, a period must pass as the level of infection of infected host (or the vector will reach a high enough threshold to continue transmission). Delay is hard to quantify mathematically because the usual way of incorporating it into a mathematical model leads to delay differential equations, and these are challenging from an analytical standpoint. Several researchers have examined disease transmission models with latent or incubation period since many diseases (e.g., flu, tuberculosis, H1N1) have an incubatory period where a host is considered infected but is not yet able to pass the infection on to another individual. DDEs (delay differential equations) has been widely applied to describe time effects of infectious period in SIR, SIS, SEIR and other epidemic models (Alshorman et al., 2017; Deng et al., 2007; Goel & Nilam, 2019; Hattaf, Lashari et al., 2013; Hattaf, Yousfi, et al., 2013; Hattaf & Yousfi, 2016; A. Kumar & Nilam, 2019; M. Li & Liu, 2014; Rihan et al., 2019; Tipsri & Chinviriyasit, 2014; K. Wang et al., 2007). In (Rakkiyappan et al., 2019), examined a virus infection based on a system of nonlinear differential equations with multiple time delays. The authors (Wei et al., 2008) considered the vector borne epidemic model with time delay. (Meng et al., 2010) talked about a situation where the incidence is delayed in the infected but not in the susceptible; in other words, the bilinear incidence rate is $\beta S(t)I(t-\tau)$ with an incubation period of τ. The current rate of new infective human cases depends on both the current population of susceptible humans, and on the current population of infective mosquitoes.

1.3 Basic Reproduction Number

The basic reproduction number R_0 in epidemiology is stated as "the average number of secondary infections generated by a single infected individual over the course of his/her infectious period in an entirely susceptible community"(Van Den Driessche & Watmough, 2002). This parameter is heavily influenced by contact rate; the higher the number of effective contacts, the higher the chance of catching a new disease. The other factor is the duration of infectiousness: a person who can spread an infection to others for longer periods of time will be in contact with more people while infected and so is likely to infect more. According to widely used infection models, when R_0>1, the infection will eventually be able to spread through the population, in other words, an epidemic will occur, while it is not if R_0< 1. In general, the higher the value of R_0, the harder it is to control epidemic. This threshold property provides important information on how diseases spread or are controlled. There exist various approaches for calculating the basic reproduction number R_0 (Diekmann et al., 1990). To determine the basic reproduction number R_0, we used the next generation matrix method approach (Van Den Driessche & Watmough, 2002) in the thesis.

1.3.1 Next generation matrix method

The basic reproduction number for a compartmental model of the spread of infectious diseases is computed in epidemiology using the next-generation matrix. The method was given by Diekmann et al. (Diekmann et al., 1990) and van den Driessche and Watmough (Van Den Driessche & Watmough, 2002). Using a next-generation matrix, the entire population is split into p compartments with $p < q$ infected compartments to get the fundamental reproduction number. Let x_i, $i = 1,2,3, \dots p$ be the number of infected individuals in the i^{th} infected compartment at time t caused by the j^{th} infected individual. Now the epidemic model is $\frac{dx_i}{dt} = F_i(x) - V_i(x)$, where $V_i(x) = [V_i^-(x) - V_i^+(x)]$. In these equations, $F_i(x)$ represents the rate of new infections in compartment i, V_i^+ represents the rate of transfer of individuals into compartment i by all other means, and V_i^- represents the rate of transfer of individuals out of the compartment i. Let x_0 be the disease-free equilibrium. The values of the parts of the Jacobian matrix $F(x)$ and $V(x)$ are $DF(x_0) = \begin{pmatrix} F & 0 \\ 0 & 0 \end{pmatrix}$ and $DV(x_0) = \begin{pmatrix} V & 0 \\ J_3 & J_4 \end{pmatrix}$ respectively. Here F and V are $p \times p$ matrices, defined as, $F = \frac{\partial F_i(x_0)}{\partial x_j}$ and $V = \frac{\partial V_i(x_0)}{\partial x_j}$. Now the matrix FV^{-1} is known as the next generation matrix. The basic reproduction of the model is then given by the eigenvalue of FV^{-1} with the largest absolute value.

1.4 Fractional Calculus

Fractional calculus (FC) was originally mentioned by Gottfried Wilhelm Leibniz, one of the founders of classical calculus, in a letter to L'Hôpital dated September 30, 1695. L'Hôpital inquired of Leibniz what would happen if the derivative's order, which was formerly an integer, was changed to a fraction. Leibniz replied: “It will lead to a paradox, from which one day useful consequences will be drawn.” The notation $\frac{d^n y}{dx^n}$, for $n = \frac{1}{2}$ was introduced by Leibniz (Ross, 1975). Fractional calculus sparked the interest of other mathematicians, including Euler, Laplace, Fourier, Lacroix, Weyl, Grunwald, Abel, Riemann, and Liouville, who all contributed to its growth in the pure theoretical realm of mathematics. FC theory is defined as the application of conventional differentiation and integration to arbitrary orders. FC has a history dating back over 320 years. Fractional calculus is not as popular as other branches of research due to a lack of problem-solving strategies and intricacy. In recent years, due to its applicability in the fields of science and engineering, the FC has been a popular topic among researchers, resulting in many theoretical and numerical results.

1.4.1 Fractional Order Epidemiology

Fractional calculus can be used to describe memory and hereditary properties of a system, more attractively than integer-order differential equations. This ability is especially applicable in cases of epidemiology, where previous states affect future dynamics. Here in human population memory refers to personal understanding. Therefore, epidemic development and control process could not be considered as such in the human level without memory effect. Because the dynamics of the system depend on both the present state and history of the system, the classical SIR model fails to describe many disease processes. The dynamic process based on fractional order derivative carries memory of the past and current state. Thus, fractional order systems may be a more realistic choice for the modeling of such dynamics in epidemiological compartmental models. This generalization provides a broader basis for the modeling of different physical, biological and engineering systems particularly possessing memory, hereditary attributes or nonlinear diffusion properties. Several models have been proposed to explore the dynamics of epidemics using fractional order derivatives (Angstmann et al., 2016; Hoan et al., 2020; Naik, 2020; Owoyemi et al., 2020; Rostamy & Mottaghi, 2016)

1.4.2 Fractional order Delay Differential Equations

A Fractional-order Delay Differential Equation (FODDE) is an extension of a standard differential equation that uses fractional calculus to quantify the memory and hereditary properties in systems. These are particularly useful in epidemic modeling because the transmission dynamics frequently involve dependencies on past states of the system. This is important for diseases that have incubation times, immunity delays or behavioral memory effects.

Epidemic models with fractional-order derivatives and time delays have recently gained popularity(Chinnathambi & Rihan, 2018; Deng et al., 2007; S. Liu et al., 2020). Most real-world occurrences are inevitably influenced by memory or temporal delay. The authors (Naim et al., 2022) investigated the effect of dual time delay and Caputo fractional derivative on the long-run behavior of a viral system with the non-cytolytic immune hypothesis and discovered that fractional order can significantly improve the dynamics and strengthen the infection model's stability. Authors in (S. Liu et al., 2020) investigate the bifurcation analysis of a fractional order SIQR model with double delay.

1.5 Stability Analysis

When a higher level of nonlinearity is applied to address real-world problems, mathematical models become more complicated. It is difficult to develop an explicit solution for these models. Approximate solutions with fixed parameters can be determined via numerical simulations, but the general solution may not be known. Stability analysis is an especially valuable method for determining a solution's long-term behavior when the general solution is difficult to obtain. Local and global model solutions are the two most common forms found in literature. While global stability describes the behavior of the solution across the domain, local stability concentrates on the behavior of the model solution around the equilibrium point.

1.6 Limit Cycle

An isolated closed trajectory is called a limit cycle According to Strogatz (Strogatz, 2018), the term "isolated" refers to trajectories that spiral either toward or away from the limit cycle and are not closed to their neighbours. We refer to the limit cycle as steady or attractive if all nearby trajectories approach it. If not, the limit cycle is either unstable or, in rare circumstances, half-stable.

1.7 Bifurcation

When the stability behavior or dynamics of equilibrium points change, then it refers to Bifurcation and the point at which bifurcation occur is called Bifurcation point (Strogatz, 2018). The bifurcation term has been introduced by Poincare (Guckenheimer & Holmes, 1983) to say about the “splitting” of equilibrium solutions in a family of differential equations. Bifurcation can cause changes in equilibrium point, stability condition and periodic orbit as well. Examples of different types of bifurcations are: Transcritical, Hopf bifurcation and Saddle-node bifurcation.

1.7.1 Saddle-node bifurcation

Any dynamical system's ability to create or destroy equilibrium points is governed by this fundamental mechanism. Two equilibrium points in this bifurcation-one of which is a saddle point and the other a stable node-collision and mutual annihilation occur at the bifurcating point.

1.7.2 Transcritical bifurcation

In this bifurcation, two equilibriums of the system collide and switch their stable points. In this case, as the parameter traverses critical value one equilibrium point converts from unstable to stable and another from stable to unstable. However, in this case there is no equilibrium point being created or disappearing.

1.7.3 Hopf bifurcation

At the critical value of the bifurcation parameter, a limit cycle is created, and an equilibrium point loses stability in this bifurcation. In this instance, the imaginary axis is crossed from the left half-plane to the right half-plane by two entirely imaginary eigenvalues. Consequently, the system has a limit cycle. There are essentially two forms of Hopf bifurcation depending on the structure of the limit cycle. Supercritical Hopf bifurcation occurs when the limit cycle is orbitally stable; subcritical Hopf bifurcation occurs when the limit cycle is orbitally unstable.

1.8 Thesis Organization

The thesis entitled “Fractional Mathematical Model for dynamics of Infectious Diseases” contains seven chapters followed by conclusion & future scope and bibliography. The thesis is organized as follows:

Chapter 1

The first chapter is an introductory section that provides a comprehensive overview of a fractional-order mathematical model for analysing the dynamics of infectious diseases, including the fundamental terminologies, significant concepts and various types of models. Traditional integer-order models frequently fail to capture the complexity and memory effects associated with disease transmission. This study uses fractional calculus, which allows for non-integer orders of differentiation and integration, to improve disease modeling and prediction for treatment possibilities including time delays to better reflect real-world events. This chapter aims to provide a chronological overview of the development of epidemiology and the rationale behind the research conducted in the thesis.

Chapter 2

In this work, an attempt has been made to study and investigate a non-linear, non-integer SIR epidemic model for COVID-19 by incorporating Beddington-De Angelis incidence rate and Holling type II saturated cure rate. Beddington-De Angelis incidence rate has been chosen to observe the effects of measure of inhibition taken by both: susceptible and infective. This includes measure of inhibition taken by susceptible as wearing proper mask, personal hygiene and maintaining social distance and the measure of inhibition taken by infectives may be quarantine or any other available treatment facility. Holling type II treatment rate has been considered for the model for its ability to capture the effects of available limited treatment facilities in case of COVID-19. To include the neglected effect of memory property in integer order system, Caputo form of non-integer derivative has been considered, which exists in most biological systems. It has been observed that the model is well posed i.e., the solution with a positive initial value is reviewed for non-negativity and boundedness.
Basic reproduction number R_0 is determined by next generation matrix method. Routh Hurwitz criteria has been used to determine the presence and stability of equilibrium points and then stability analyses have been conducted. It has been observed that the disease-free equilibrium Q^d is stable for $R_0 < 1$ i.e., there will be no infection in the population and the system tends towards the disease-free equilibrium Q^d and for $R_0 > 1$, it becomes unstable, and the system will tend towards endemic equilibrium Q^e. Further, global stability analysis is carried out for both the equilibria using R_0. Lastly numerical simulations to assess the effects of various parameters on the dynamics of disease has been performed.

The work of this chapter has been published entitled "**Fractional order SIR epidemic model with Beddington-De Angelis incidence and Holling type II treatment rate for COVID-19**" in Journal of Applied Mathematics and Computing, 2021 (Springer). https://doi.org/10.1007/s12190-021-01658-y Impact Factor-2.4, Indexing: SCIE

Chapter 3

During COVID-19 outbreak, the large population was exposed to social media. Since it was a new virus and no specific information was available about its dynamics, therefore people were dependent on social media to gather more and more information. Social media has its pros and cons, which have an impact on the life of human being which was more in case of COVID-19 due to restricted interaction during the period of pandemic. In this article the effects of social media on the mental health of people have been investigated with the help of Holling type II and Monod Haldane rates in the form of incidence and treatment rates, respectively. The model exhibits two types of equilibria viz. disease-free equilibrium (DFE) and endemic equilibrium (EE), which has been confirmed by the Fractional Routh-Hurwitz criterion. Further

stability behavior has been also analysed under certain sufficient conditions that depends on R_0, a Basic Reproduction number, which is determined by the method of next generation matrix. The findings indicate that the fractional derivative order has a considerable influence on the dynamic process. The difference between fractional and integer order derivatives is illustrated by the memory effect. Finally, numerical simulations have been performed to examine the effect of various parameters on the dynamics of social media on mental health.

The work of this chapter has been published entitled "**Fractional order model using Caputo fractional derivative to analyse the effects of social media on mental health during COVID-19**" in Alexandria Engineering Journal, 2024 (Elsevier). https://doi.org/10.1016/j.aej.2024.02.049 Impact Factor- 6.2, Indexing: SCIE

Chapter 4

In Chapter 4, a mathematical model of infectious diseases that is non-integer SIR-type is studied. This model considers the psychological changes in individuals that are caused by a concurrent rise in public awareness. Here, a nonlinear, non-integer model has been developed by considering the Monod-Haldane incidence rate, the Holling type III treatment rate, and the Caputo derivative. Numerical simulations have been performed to verify the theoretical analysis's consistency. As the fractional derivative order parameter is increased, each solution approaches equilibrium more quickly. Furthermore, it has been observed that raising media knowledge reduces the number of infected people, hence lowering the peak of the epidemic.

The work presented in this chapter has been communicated with title "**Caputo Fractional derivative model for impact of awareness on infectious disease**".

Chapter 5

Time delays and fractional order are critical components of biological memory systems. Non-integer order enhances the model's behaviour; however, time lag has major implication on the occurrence of Hopf bifurcation and system stability. This work examines the dynamics of fractionally ordered delay differential Susceptibles-Infectives-Recovered epidemiological model with Holling functional type II treatment rate and Crowley-Martin (CM) functional type incidence. To acquire a more practical understanding of the epidemic's dynamics, the incidence rate was delayed by the latency time. We examine the sufficient requirements for steady-state

stability and Hopf bifurcation in the presence of time delay. The model exhibits a Hopf bifurcation at the threshold parameters. When time delays exceed critical values, the model goes through Hopf bifurcation. Some numerical simulations are offered to support the theoretical findings. Numerical studies demonstrate that combining fractional order with time delays in the epidemic model affects the behavior and improves the model's stability

The work presented in this chapter has been communicated with title "**The behavior of the fractional order delay differential SIR epidemic model with Holling type II treatment rate and Crowley-Martin rate of incidence**".

Chapter 6

Fractional order and time delays are required for biological systems with memory. In this chapter, we analyse a double delayed fractional order susceptible-infected-quarantine-recovered epidemic model with saturated incidence and treatment rates. The model incorporates two time delays: one for the duration of the incubation period and another for people's resistance to isolation. The model experiences Hopf bifurcation when delays exceed critical values. The application of the acquired results is demonstrated by providing a few numerical simulation examples.

The work presented in this chapter has been communicated with title "**Bifurcation analysis of a double delayed SIQR fractional order model incorporating Holling Type-II treatment rate and Monod-Haldane incidence rate**".

Chapter 7

Chapter 7 is conclusive in nature. This thesis is comprising of 7 chapters in which Introduction of the work is given in chapter 1. Chapter 2, 3 and 4 aimed to incorporate fractional calculus into the modeling process of infectious diseases to capture the memory effects observed in disease transmission with different incidence and treatment rates. By incorporating memory effects into the analysis, this thesis lays the groundwork for more sophisticated models that can better inform public health strategies and improve our response to disease outbreaks. Chapter 5 and 6 is an advancement of chapters 2, 3 and 4 with the inclusion of time delays, expanding the model to incorporate more diverse types of delays. The inclusion of fractional calculus with time delays in the mathematical model resulted in a significantly improved representation of infectious disease dynamics.

This thesis provides a valuable framework for future research and practical applications, highlighting the importance of considering both memory effects and time

delays in disease modeling. By improving the ability to predict and manage outbreaks, this work contributes to more effective public health strategies and a deeper understanding of disease dynamics. Future research could focus on simplifying the computational aspects of the fractional model to make it more accessible for real-time applications. Additionally, exploring the integration of the fractional model with other types of data, such as genetic information or environmental factors, could provide a more comprehensive understanding of disease dynamics.

CHAPTER 2

FRACTIONAL ORDER SIR EPIDEMIC MODEL WITH BEDDINGTON – DE ANGELIS INCIDENCE AND HOLLING TYPE II TREATMENT RATE FOR COVID-19

In this chapter, an attempt has been made to study and investigate a non-linear, non-integer SIR epidemic model for COVID-19 by incorporating Beddington-DeAngelis incidence rate and Holling type II saturated cure rate. Beddington-De Angelis incidence rate has been chosen to observe the effects of measure of inhibition taken by both: susceptible and infective. This includes measure of inhibition taken by susceptible as wearing proper mask, personal hygiene and maintaining social distance and the measure of inhibition taken by infectives may be quarantine or any other available treatment facility. Holling type II treatment rate has been considered for the present model for its ability to capture the effects of available limited treatment facilities in case of COVID-19. To include the neglected effect of memory property in integer order system, Caputo form of non-integer derivative has been considered, which exists in most biological systems. It has been observed that the model is well posed which means that the solution with a positive initial value is reviewed for non negativity and boundedness. Basic reproduction number R_0 is determined by next generation matrix method. Routh Hurwitz criteria have been used to determine the presence and stability of equilibrium points and then stability analyses have been conducted. It has been observed that the disease-free equilibrium Q^d is stable for $R_0 < 1$ i.e., there will be no infection in the population and the system tends towards the disease-free equilibrium Q^d and for $R_0 > 1$, it becomes unstable, and the system will tend towards endemic equilibrium Q^e. Further, global stability analysis is carried out for both the equilibria using R_0. Lastly numerical simulations to assess the effects of various parameters on the dynamics of disease has been performed.

2.1 Introduction

The current outbreak of coronavirus disease COVID-19 got reported first from Wuhan, China on 31st Dec 2019. On March 11, 2020, WHO announced that the spread of coronavirus infection COVID-19 would be described as pandemic. On March 13, 2020, WHO declared Europe the centre of the pandemic outbreak. Since March 2020, while new cases appear to be evolved in China, the number of cases in rest of the world has been rising exponentially. Many governments have adopted stringent steps to avoid the spread of this new virus, such as travel bans, demanding social distance and shutting schools, bars, restaurants, and other businesses. The transmission rate is heterogeneous across countries and far exceeds the rate of recovery which allows for a rapid spread. Since the proper treatment facilities are not available for corona virus, therefore the only way to stabilize the outbreak is perhaps to reduce the rate of transmission by limiting exposure of public gathering or social distancing.

The complex behavior of infectious disorders has long been explored as good health is among the most significant concerns in the physical world. The epidemic dynamics are investigated by several mechanisms. A mathematical description of the dynamics helps us to explore the complexity of the disease critically, to analyse statistical and model data, to make predictions about newly emerging diseases like COVID-19 and to determine the efficacy of the steps taken.

Kermack and Mckendrick (Kermack & Mckendrick, 1927) developed the first compartmental model for the study of the disease dynamics, many researchers then presented numerous mathematical models such as SIR, SIRS, SEIR, SEIRS etc. (where S, I, E and R represents the susceptible, infected, exposed, and recovered individuals) (Dubey et al., 2013; A. Kumar, Kumar, et al., 2020; A. Kumar & Nilam, 2019, 2018; M. Li & Liu, 2014).

In recent times, infectious simulation research has been diverted to fractional differential research due to its ability to offer a convincing analysis of certain nonlinear dynamics, the study of fractional order differential equations in the past decades has received a significant attention of researchers. Since, 2019 novel coronavirus is discovered, many research articles in modeling of COVID-19 transmission have used ordinary differential equations to study its dynamics (Bardina et al., 2020; Din & Algehyne, 2021; Palladino et al., 2020). Though there are reasons that the non-integer models give better fit to the actual data, numerous models have been developed to study the dynamics of COVID-19 using fractional order derivatives (Debasis Mukherjee & Maji, 2020; Owoyemi et al., 2020; Rajagopal et al., 2020; Rezapour et al., 2020).

Motivated by the above-mentioned literature, we formulated a fractional order SIR model for COVID-19 pandemic with nonlinear incidence rate known as Beddington-DeAngelis type incidence rate and Holling type II saturated treatment rate. To incorporate the effects of measure of inhibition taken by susceptible such as wearing proper mask, personal hygiene and maintaining social distancing and the measure of inhibition taken by infectives can be quarantine, Beddington-DeAngelis incidence rate has been chosen (Beddington, 1975). For any outbreak of new disease, treatment capacity is first very low and then grows slowly with improvement of hospital's conditions, availability of effective drugs, vaccines etc which are also the conditions arises in case of COVID-19. Since Holling type II function (W. Wang, 2006; W. Wang & Ruan, 2004) follow the same pattern, therefore it has been chosen as treatment rate for the present study. The fractional order derivative is taken in Caputo-sense. We evaluated the model mathematically first, and then the simulations have been performed for the model.

2.2 Formulation of Fractional order epidemic Model

Several disease models were suggested and evaluated during the last few years. Here we are proposing a fractional order epidemic model for COVID-19 by using the Caputo fractional derivative with order ρ, where $0 < \rho \leq 1$. Whole population N(t) is categorized into three classes namely susceptible S(t), infectives I(t) and recovered R(t). We assume that recovered individuals cannot become infected again and, they cannot infect the susceptible population again. The Caputo derivative is described in definition 1in Appendix. Under these assumptions we proposed a Caputo-fractional order SIR model represented by the following non-linear differential equations:

$$\left.\begin{aligned} {}_0^cD_t^{\rho}\, S(t) &= \mu - \lambda\, S(t) - \frac{\beta\, S(t)I(t)}{1+\beta_1 S(t)+\beta_2\, I(t)} \\ {}_0^cD_t^{\rho} I(t) &= \frac{\beta\, S(t)I(t)}{1+\beta_1\, S(t)+\beta_2\, I(t)} - (\lambda+\alpha+\gamma)I(t) - \frac{\sigma\, I(t)}{1+\delta\, I(t)} \\ {}_0^cD_t^{\rho} R(t) &= \gamma\, I(t) - \lambda R(t) + \frac{\sigma\, I(t)}{1+\delta\, I(t)} \end{aligned}\right\} \tag{2.1}$$

with non-negative initial conditions: $S(0) = S_0 \geq 0, I(0) = I_0 \geq 0$ and $R(0) = R_0 \geq 0$, where the different model parameters are defined likewise:

Table 2.1 Parameters with their descriptions

S.No.	Parameter	Description
1	β	Coefficient of transmission between susceptible S and infected persons I
2	λ	Natural mortality rate of people in each class
3	μ	Constant rate of recruitment is susceptible due to immigration
4	α	Infection mortality rate in infected people
5	γ	Rate of recovery in contaminated persons
6	β_1	Measure of inhibition (preventive measures taken by susceptibles such as wearing proper mask, maintaining personnel hygiene, maintaining social distance etc)
7	β_2	Measure of inhibition (preventive measures taken by infectives such as treatment of infective individuals, quarantine)
8	σ	Treatment rate of disease
9	δ	Rate of limitation in treatment availability

2.3 Basic Properties of the Model

Let $\mathbb{R}^3_+ := \{X \epsilon \mathbb{R}^3 : X \geq 0\}$ and $X(t) = \big(S(t), I(t), R(t)\big)^T$ on non-negative solutions, the lemmas needed to prove the theorem are mentioned in Appendix.

Theorem 2.1 There exists a unique non-negative solution for fractional differential equation given by system (2.1) for $t \geq 0$ and the solution will remain in region $M = \{(S, I, R) \in R^3_+ : 0 < S + I + R \leq \overline{D}\ , \overline{D}\ \geq C_E \frac{\mu}{\lambda}\}$ for $t \geq 0$.

Proof. First, we check that all the solutions of the model (2.1) with its initial conditions are non-negative.
Suppose that $S(0) > 0$ for $t = 0$. Now we show that $S(t) \geq 0$ for all $t \geq 0$. We will prove this by contradiction, let $S(t) \leq 0$ for all $t \geq 0$. Then, there exists a $\tau_1 > 0$ such that $S(t) > 0$ for that $0 \leq t < \tau_1$, $S(t) = 0$ at $t = \tau_1$, and $S(t) < 0$ for $\tau_1 < t < \tau_1 + \epsilon_1$ with sufficiently small $\epsilon_1 > 0$. Now taking first equation of model (2.1), we obtain ${}_0^C D^\rho\, S(t)|_{t=\tau_1} = \mu > 0$. From Lemma 2, for any $0 < \epsilon_1 \ll 1$, we have $S(\tau_1 + \epsilon_1) = S(\tau_1) + \frac{1}{\Gamma(\alpha)} D^\rho S(\xi)\ (\epsilon_1)^\rho$. Thus, we get $S(\tau_1 + \epsilon_1) \geq 0$, which is in contradiction to the fact that $S(t) < 0$ for $\tau_1 < t < \tau_1 + \epsilon_1$. Hence, we have $S(t) \geq 0$ for all $t \geq 0$.
Next, we prove that $I(t) \geq 0$ for all $t \geq 0$. Once again, we do it by contradiction. Assume that $I(t) \geq 0$ is not true, then there exists a $\tau_2 > 0$ such that $I(t) > 0$ for that

$0 \leq t < \tau_2$, $I(t) = 0$ at $t = \tau_2$, and $I(t) < 0$ for $\tau_2 < t < \tau_2 + \epsilon_2$ with sufficiently small $\epsilon_2 > 0$. Then we obtain

$$ {}_0^C D^\rho \, I(t)|_{t=\tau_2} = 0. $$

From Lemma 2, for any $0 < \epsilon_2 \ll 1$, we have $I(\tau_2 + \epsilon_2) = I(\tau_2) + \frac{1}{\Gamma(\alpha)} D^\rho I(\xi) \, (\epsilon_2)^\rho$. Thus, we get $I(\tau_2 + \epsilon_2) \geq 0$, which is in contradiction to the fact that $I(t) < 0$ for $\tau_2 < t < \tau_2 + \epsilon_2$. Hence, we have $I(t) \geq 0$ for all $t \geq 0$. Similarly, we can prove that $R(t) \geq 0$ for all $t \geq 0$. Thus, it is concluded that all the solutions of model (2.1) with initial conditions are non-negative.

Now we prove boundedness of solutions.
Adding all the equations of the model (2.1), we obtain:

$$ D_t^\rho N = \mu - \lambda N - \alpha I $$

Where $N = S + I + R$. As $I(t) \geq 0$, we have

$$ D_t^\rho N \leq \mu - \lambda N. $$

Now consider the initial value problem $D_t^\rho \bar{N} = \mu - \lambda \bar{N}$, $\bar{N}(0) = \bar{N}_0$. Using comparison principle (Lu & Zhu, 2018) we obtain the following inequality:
$N(t) \leq \bar{N}(t)$ for all $t \geq 0$. Now applying Laplace transform to the initial value problem we obtain $s^\rho L[\bar{N}(t)] - s^{\rho-1}\bar{N}_0 = \frac{\mu^\rho}{s} - \lambda L[\bar{N}(t)]$

$$ \Rightarrow L[\bar{N}(t)] = \frac{s^{\rho-1}\bar{N}_0}{s^\rho + \lambda} + \frac{\mu^\rho s^{-1}}{s^\rho + \lambda} $$

Using Lemma 3, we obtain

$$ L\left[E_{\rho,1}(-\lambda t^\rho)\right] = \frac{s^{\rho-1}}{s^\rho + \lambda} $$

$$ L\left[t^\rho E_{\rho,\rho+1}(-\lambda t^\rho)\right] = \frac{s^{-1}}{s^\rho + \lambda} $$

Applying inverse Laplace transform in the above two equations, we get

$$ \bar{N}(t) = \bar{N}_0 E_{\rho,1}(-\lambda t^\rho) + \mu t^\rho E_{\rho,\rho+1}(-\lambda t^\rho), $$

using $D_t^\rho N \leq \mu - \lambda N$

we have $N(t) \leq N_0 E_{\rho,1}(-\lambda t^\rho) + \mu t^\rho E_{\rho,\rho+1}(-\lambda t^\rho)$,

By Lemma 4, we obtain

$$ |N(t)| \leq \frac{N_0 C_E}{1 + \lambda t^\rho} + \frac{\mu t^\rho C_E}{1 + \lambda t^\rho} $$

Where C_E is constant given in Lemma 4. Hence, as $t \to \infty$, we have $N(t) \leq \overline{D}$ with $\overline{D} \geq C_E \frac{\mu}{\lambda}$. Thus, the solutions are bounded and will remain in region M for $t \geq 0$. Therefore, theorem 2.1 is proved and solution remains in $\mathbb{R}^3_+$.

2.4 Mathematical analysis of the model

This section performs stability analysis of the disease free equilibrium point and the endemic equilibrium point.

2.4.1 Equilibria and their stability

As in the above non-linear model of three equations, for stability analysis it is logical to consider only the first two equations because these are independent of the third equation. The model is therefore reduced to:

$$\left.\begin{aligned} {}_0^cD_t^{\rho}\, S(t) &= \mu - \lambda\, S(t) - \frac{\beta\, S(t)I(t)}{1+\beta_1 S(t)+\beta_2\, I(t)} \\ {}_0^cD_t^{\rho} I(t) &= \frac{\beta\, S(t)I(t)}{1+\beta_1\, S(t)+\beta_2\, I(t)} - (\lambda+\alpha+\gamma)I(t) - \frac{\sigma\, I(t)}{1+\delta\, I(t)} \end{aligned}\right\} \tag{2.2}$$

Where $a = \lambda + \alpha + \gamma$

To find the equilibrium points, set the right side of the system (2.2) to zero, we get

$$\left.\begin{aligned} \mu - \lambda\, S(t) - \frac{\beta\, S(t)I(t)}{1+\beta_1 S(t)+\beta_2\, I(t)} &= 0 \\ \frac{\beta\, S(t)I(t)}{1+\beta_1\, S(t)+\beta_2\, I(t)} - (\lambda+\alpha+\gamma)I(t) - \frac{\sigma\, I(t)}{1+\delta\, I(t)} &= 0 \end{aligned}\right\} \tag{2.3}$$

Thus, solving the above system, we obtain the two equilibria points called disease free equilibrium point (DFE) and endemic equilibrium point (EEP) specified as

(i) DFE: $Q^d = (S^d, I^d) = \left(\frac{\mu}{\lambda}, 0\right)$ showing no illness in the environment and all the people are susceptible only

(ii) EEP: $Q^e = (S^e, I^e)$ which is described in the later section.

Now, to obtain the behaviour of stability of these two equilibria, Basic Reproduction Number R_0 is required to be computed(Van Den Driessche & Watmough, 2002).

2.4.2 Determination of Basic Reproduction Number

To compute the Basic Reproduction number R_0 using the next generation matrix method, we assume that

$$D_t^{\rho} x = P(x) - R(x)$$

Where $x = (S, I)^T$, $P(x)$ represents the matrix of new infections coming and $R(x)$ represents the matrix of transfer of individuals entering and leaving from the compartments.

The Jacobian matrices of $P(x)$ and $R(x)$ are evaluated at disease free equilibrium point Q^d and are given by

$$P = \begin{pmatrix} \frac{\beta\mu}{\lambda + \beta_1\mu} & 0 \\ 0 & 0 \end{pmatrix}$$

$$R = \begin{pmatrix} \sigma + a & 0 \\ \frac{\beta\mu}{\lambda + \beta_1\mu} & \lambda \end{pmatrix}$$

$$PR^{-1} = \begin{pmatrix} \frac{\beta\mu}{(a+\sigma)(\lambda + \mu\beta_1)} & 0 \\ 0 & 0 \end{pmatrix}$$

This matrix PR^{-1} is known as next generation matrix and the spectral radius of this matrix is the basic reproduction number R_0 (Ye & Xu, 2019). R_0 for our model is

$$R_0 = \rho(PR^{-1}) = \frac{\beta\mu}{(\lambda + \beta_1\mu)(\sigma + a)}$$

The basic reproduction number R_0 is the average number of secondary cases caused by an infective in a fully susceptible population. The value of R_0 depends on both the disease and the host population.

2.4.3 Analysis of local stability behaviour DFE (Q^d)

Now we are concerned about the local stability of disease-free equilibrium point (DFE Q^d**)**. We claim the following theorem for this and prove this:

Theorem 2.2 $Q^d=(S^d, I^d) = \left(\frac{\mu}{\lambda}, 0\right)$,the disease- free equilibrium of model (2.2) is locally asymptotically stable when the Basic Reproduction number $R_0 < 1$ and unstable otherwise.

Proof. The local stability behaviour of the DFE point of the non-linear system (2.3) is computed by linearizing the system around the DFE (Q^d). Thus, we have obtained a linearized matrix of the system at Q^d as shown below

$$J^d = \begin{pmatrix} -\lambda & -\frac{\beta\mu}{\lambda+\beta_1\mu} \\ 0 & (R_0-1)(\sigma+a) \end{pmatrix} \tag{2.4}$$

Now the characteristic equation of the Jacobian matrix J^d is computed as

$$q^2 - \big((R_0-1)(\sigma+a) - \lambda\big)q - \lambda(R_0-1)(\sigma+a) = 0 \tag{2.5}$$

$$\Longrightarrow q^2 + aq + b = 0$$

where $a = -\big((R_0-1)(\sigma+a) - \lambda\big)$ and $b = -\lambda(R_0-1)(\sigma+a)$

First, we will prove that the roots (q_1 and q_2) of the characteristic equation (2.5) which are given as are real

$$q_1 = \frac{-a + \sqrt{a^2 - 4\,b}}{2}$$

$$q_2 = \frac{-a - \sqrt{a^2 - 4\,b}}{2}$$

$$a^2 - 4\,b = (R_0-1)^2(\sigma+a)^2 + \lambda^2 + 2\,\lambda(R_0-1)(\sigma+a) \geq 0$$

Therefore, both the roots q_1 and q_2 are real. We now show that when $R_0 < 1$ both the roots are negative.

Sum of the roots $q_1 + q_2 = -a = (R_0-1)(\sigma+a) - \lambda$
Product of the roots $q_1 q_2 = b = -\lambda\,(R_0-1)(\sigma+a)$

Thus $a = -(R_0-1)(\sigma+a) - \lambda > 0$ (when $R_0 < 1$)
and $b = -\lambda\,(R_0-1)(\sigma+a) > 0$ (when $R_0 < 1$)

Hence, we conclude that the roots of the characteristic equation (2.5) are negative when $R_0 < 1$. Thus, alternately we can say that all the eigen values of the Jacobian matrix J^d are of negative sign when $R_0 < 1$. Consequently all the roots of the equation (2.5) have negative real parts, thus, by the fractional Routh-Hurwitz criteria (Matignon & Matignon, 1996; Otto & Day, 2019) all roots follow $|arg(q_i))| > \rho\frac{\pi}{2}$, $i = 1,2$. Figure 2.1 interprets theorem 2.2 using the values given in table 2.2.

2.4.4 EEP (Q^e) existence and study of local equilibrium

The conditions for the existence of the endemic equilibrium ($Q^e = (S^e, I^e)$) are defined here and the endemic equilibrium's local stability behavior is discussed in this section.

$$\left.\begin{aligned} \mu - \lambda S^e - \frac{\beta S^e I^e}{1+\beta_1 S^e+\beta_2 I^e} = 0 \\ \frac{\beta S^e I^e}{1+\beta_1 S^e+\beta_2 I^e} - (\lambda+\alpha+\gamma)I^e - \frac{\sigma I^e}{1+\delta I^e} = 0 \end{aligned}\right\} \quad (2.6)$$

After solving the equations (2.6) we obtain:

$$S^e = \frac{(a + a\delta I^e + \sigma)(1 + \beta_2 I^e)}{\beta(1 + \delta I^e) - \beta_1(a + a\,\delta I^e + \sigma)}$$

and I^e is the root of the following equation:

$$A_0 + A_1 I^e + A_2 I^{e^2} + A_3 I^{e^3} = 0 \quad (2.7)$$

where the coefficients A_0, A_1, A_2 *and* A_3 are given by

$$A_0 = \mu\big(\beta - \beta_1(\sigma + a)\big) - \lambda(\sigma + a) = (R_0 - 1)(\sigma + a)(\lambda + \mu\beta_1)$$

$$A_1 = \mu\,\delta(2\,\beta - 2\,\beta_1\,a - \beta_1\sigma) - \lambda\big(a\,\delta + (\sigma + a)(\delta + \beta_2)\big) - (a + \sigma)\big(\beta - \beta_1(\sigma + a)\big)$$

$$A_2 = \mu\,\delta^2(\beta - \beta_1 a) - (2a\beta_2 + a\delta + \sigma\beta_2)\lambda\delta - (2a\beta\delta - 2\,a^2\delta\beta_1 - a\delta\beta_1\sigma) - \sigma\delta(\beta - \beta_1 a)$$

$$A_3 = -\lambda a\beta_2\delta^2 - a\delta^2(\beta - a\beta_1)$$

Theorem 2.3. For $R_0 > 1$ there exist a unique endemic equilibrium (Q^e=(S^e, I^e) of model (2.2).

Proof. Let $R_0 > 1$ Considering equation (2.7) which is third degree polynomial given as $F(I^e) = A_0 + A_1 I^e + A_2 I^{e^2} + A_3 I^{e^3}$.We observe that A_3 , the coefficient of I^{e^3}, the leading coefficient, is negative. Therefore $\lim_{I^e \to \infty} F(I^e) = -\infty$, also $F(0) = A_0$ and $A_0 > 0$ for $R_0 > 1$, $F(I^e)$ is a continuous function of (I^e).

Thus, the fundamental theorem of algebra implies that there exist at most three real positive roots of $F(I^e)$. Here, we examine only the case of a particular endemic equilibrium. Assuming R_0 >1 and noting that $A_3 < 0$ and $A_0 > 0$, under the following signs of A_1 and A_2 a unique endemic equilibrium exists:

(i) $A_1 < 0, A_2 < 0$

(ii) $A_1 > 0, A_2 < 0$

(iii) $A_1 > 0, A_2 > 0$

If any of the criteria (i)-(iii) is fulfilled, then there exist a unique I^e, from which we can find the value of S^e. So, unique endemic equilibrium Q^e=(S^e, I^e) has been demonstrated for R_0 >1

The local stability of endemic equilibrium $Q^e = (S^e, I^e)$ is now examined here. To do so, we linearize the model (2.3) around endemic equilibrium Q^e and thus obtain the Jacobian matrix J^e as shown below:

$$J^e = \begin{pmatrix} -\lambda - \dfrac{\beta I^e(1+\beta_2 I^e)}{(1+\beta_1 S^e+\beta_2 I^e)^2} & -\dfrac{\beta S^e(1+\beta_1 S^e)}{(1+\beta_1 S^e+\beta_2 I^e)^2} \\ \dfrac{\beta I^e(1+\beta_2 I^e)}{(1+\beta_1 S^e+\beta_2 I^e)^2} & \dfrac{\beta S^e(1+\beta_1 S^e)}{(1+\beta_1 S^e+\beta_2 I^e)^2} - a - \dfrac{\sigma}{(1+\delta I^e)^2} \end{pmatrix}$$

The characteristic equation of J^e is given by

$$r^2 + \omega_1 r + \omega_2 = 0 \tag{2.8}$$

Where

$$\omega_1 = \lambda + \frac{\beta I^e(1+\beta_2 I)}{(1+\beta_1 S^e+\beta_2 I^e)^2} - \frac{\beta S^e(1+\beta_1 S^e)}{(1+\beta_1 S^e+\beta_2 I^e)^2} + a + \frac{\sigma}{(1+\delta I^e)^2}$$

$$\omega_2 = \left(\lambda + \frac{\beta I^e(1+\beta_2 I^e)}{(1+\beta_1 S^e+\beta_2 I^e)^2}\right)\left(a + \frac{\sigma}{(1+\delta I^e)^2}\right) - \frac{\lambda\beta S^e(1+\beta_1 S^e)}{(1+\beta_1 S^e+\beta_2 I^e)^2}$$

It can readily be seen that Jacobian matrix J^e's eigen value have negative real parts if and only if $\omega_1 > 0$ and $\omega_2 > 0$. Also, $\omega_1 > 0$ and $\omega_2 > 0$ if $\frac{\beta S^e(1+\beta_1 S^e)}{(1+\beta_1 S^e+\beta_2 I^e)^2} < a + \frac{\sigma}{(1+\delta I^e)^2}$. Hence, by fractional Routh-Hurwitz criteria (Matignon & Matignon, 1996; Otto & Day, 2019) all the roots of equation (2.8) have negative real parts and satisfy the condition $|arg(r_i))| > \rho\frac{\pi}{2}$, $i = 1,2$. This proves the following theorem.

Theorem 2.4. $Q^e=(S^e, I^e)$, the endemic equilibrium of model (2.2) is locally asymptotically stable when the Basic Reproduction number R_0 >1 and unstable otherwise.

2.4.5 Global stability analysis of DFE (Q^d) and Endemic equilibrium (Q^e)

Now we are concerned about DFE's and EE's global stability. We claim the following theorem for this and prove this:

Theorem 2.5 The disease- free equilibrium $Q^d=(S^d, I^d)$ of model (2.2) is globally asymptotically stable when $R_0 \leq 1$.

Proof. We define a Lyapunov function by

$$L_1(t) = \frac{1}{1+\beta_1 S^d}\left(S(t) - S^d - S^d ln\frac{S(t)}{S^d}\right) + I(t)$$

Now we have

$${}_0^cD_t^\rho L_1(t) = {}_0^cD_t^\rho \left(\frac{1}{1+\beta_1 S^d}\left(S(t) - S^d - S^d ln\frac{S(t)}{S^d}\right) + I(t)\right)$$

$${}_0^cD_t^\rho L_1(t) = {}_0^cD_t^\rho \ \frac{1}{1+\beta_1 S^d}\left(S(t) - S^d - S^d ln\frac{S(t)}{S^d}\right) + {}_0^cD_t^\rho I(t)$$

$${}_0^cD_t^\rho L_1(t) = \frac{1}{1+\beta_1 S^d}\,{}_0^cD_t^\rho \left(S(t) - S^d - S^d ln\frac{S(t)}{S^d}\right) + {}_0^cD_t^\rho I(t)$$

$${}_0^cD_t^\rho L_1(t) \leq \frac{1}{1+\beta_1 S^d}\left(1 - \frac{S^d}{S(t)}\right){}_0^cD_t^\rho S(t) + {}_0^cD_t^\rho I(t)$$

$${}_0^cD_t^\rho L_1(t) \leq \frac{1}{1+\beta_1 S^d}\left(1 - \frac{S^d}{S(t)}\right)\left(\mu - \lambda\, S(t) - \frac{\beta\, S(t)I(t)}{1+\beta_1 S(t) + \beta_2\, I(t)}\right) + \left(\frac{\beta\, S(t)I(t)}{1+\beta_1\, S(t) + \beta_2\, I(t)} - aI(t) - \frac{\sigma\, I(t)}{1+\delta\, I(t)}\right)$$

Using the value of $R_0\ and\ S^d = \frac{\mu}{\lambda}$ in above equation, we have

$$ {}_0^cD_t^\rho L_1(t) \le -\frac{\lambda(S(t)-S^d)^2}{S(t)(1+\beta_1 S^d)} + \left(\frac{R_0(a+\sigma)\big(1+\beta_1 S(t)\big)I(t)}{1+\beta_1 S(t)+\beta_2 I(t)}\right) - aI(t) - \frac{\sigma I(t)}{1+\delta I(t)} $$

This concludes that if $R_0 < 1$, then we have ${}_0^cD_t^\rho L_1(t) \le 0$.Furthermore, we know that ${}_0^cD_t^\rho L_1(t) = 0$, if and only if $S(t) = S^d$ and $I(t) = I^d$. Thus the largest invariant set for $\{(S,I) \in \psi : {}_0^cD_t^\rho L_1(t) = 0\}$ is the singleton set $\{Q^d\}$, where $\psi = \left\{(S,I) \in R_+^2 : 0 \le S+I \le \frac{\mu}{\lambda}, S, I \ge 0\right\}$ and also all the solutions in ψ converges to Q^d in accordance with the LaSalle's invariance principle (Diekmann et al., 2010; La Salle, 1976; Shuai & Van Den Driessche, 2013; Van Den Driessche & Watmough, 2002). So, Q^d is globally asymptotically stable when $R_0 \le 1$. Hence theorem 2.5 is verified.

Theorem 2.6. The endemic equilibrium $Q^e=(S^e, I^e)$ of model (2.2) is globally asymptotically stable when R_0 >1.

Proof. We define a Lyapunov function by

$$ L_2(t) = \left(S(t) - S^e - S^e ln\frac{S(t)}{S^e}\right) + \left(I(t) - I^e - I^e ln\frac{I(t)}{I^e}\right) $$

Now we have

$$ {}_0^cD_t^\rho L_2(t) = {}_0^cD_t^\rho \left(S(t) - S^e - S^e ln\frac{S(t)}{S^e}\right) + {}_0^cD_t^\rho \left(I(t) - I^e - I^e ln\frac{I(t)}{I^e}\right) $$

$$ {}_0^cD_t^\rho L_2(t) \le \left(1 - \frac{S^e}{S(t)}\right) {}_0^cD_t^\rho S(t) + \left(1 - \frac{I^e}{I(t)}\right) {}_0^cD_t^\rho I(t) $$

$$ {}_0^cD_t^\rho L_2(t) \le \left(1 - \frac{S^e}{S(t)}\right)\left[\mu - \lambda S(t) - \frac{\beta S(t) I(t)}{1+\beta_1 S(t)+\beta_2 I(t)}\right] + \left(1 - \frac{I^e}{I(t)}\right)\left[\frac{\beta S(t) I(t)}{1+\beta_1 S(t)+\beta_2 I(t)} - aI(t) - \frac{\sigma I(t)}{1+\delta I(t)}\right] $$

Using the endemic conditions,

$$ \mu = \lambda S^e - \frac{\beta S^e I^e}{1+\beta_1 S^e+\beta_2 I^e} $$

$$ \frac{\beta S^e I^e}{1+\beta_1 S^e+\beta_2 I^e} = aI^e - \frac{\sigma I^e}{1+\delta I^e} $$

We get

$$
\begin{aligned}
{}_0^cD_t^\rho L_2(t) \le & \left(1-\frac{S^e}{S(t)}\right)\left[\mu-\lambda\, S(t)-\frac{\beta\, S(t)I(t)}{1+\beta_1 S(t)+\beta_2\, I(t)}\right] \\
& +\left(1-\frac{I^e}{I(t)}\right)\left[\frac{\beta\, S(t)I(t)}{1+\beta_1\, S(t)+\beta_2\, I(t)}-aI(t)-\frac{\sigma\, I(t)}{1+\delta\, I(t)}\right]
\end{aligned}
$$

$$
\begin{aligned}
{}_0^cD_t^\rho L_2(t) \le & -\frac{(S(t)-S^e)^2}{S(t)}\left[\lambda+\frac{\beta\, I}{1+\beta_1 S(t)+\beta_2\, I(t)}\right] \\
& -\frac{(I(t)-I^e)^2}{I(t)}\left[a+\frac{\sigma}{1+\delta\, I(t)}\right]
\end{aligned}
$$

This implies,

$$
\begin{aligned}
{}_0^cD_t^\rho L_2(t) \le & -\frac{(S(t)-S^e)^2}{S(t)}\left[\lambda+\frac{\beta\, I}{1+\beta_1 S(t)+\beta_2\, I(t)}\right] \\
& -\frac{(I(t)-I^e)^2}{I(t)}\left[a+\frac{\sigma}{1+\delta\, I(t)}\right] \\
& \le 0,
\end{aligned}
$$

Therefore, ${}_0^cD_t^\rho L_2(t) \le 0$. Also, the largest invariant set for $\{(S,I) \in \psi: {}_0^cD_t^\rho L_2(t) = 0\}$ is the singleton set $\{Q^e\}$ and all the solutions in ψ converges to Q^e in accordance with the LaSalle's invariance principle (Diekmann et al., 2010; La Salle, 1976; Shuai & Van Den Driessche, 2013; Van Den Driessche & Watmough, 2002).Therefore, Q^e is globally asymptotically stable when R_0 >1. Hence theorem 2.6 is verified.

2.5 Numerical Simulation

In this section, to support our analytical work we performed numerical simulations using MATLAB 2012(b). The initial conditions that are used in the simulation are S (0) = 85, I (0) = 0 and R (0) = 0 (A. Kumar, 2020) and the required parameters are given in table 2.2. Parameters β_1, β_2, δ are estimated and rest are chosen from paper (A. Kumar, 2020). Using the predictor-corrector method (Diethelm et al., 2002), system (2.1) is simulated numerically by MATLAB for various values of the fractional order ρ ranging from 0.4 to 1 to observe the dynamical behavior of susceptibles, infectives, and recovered population with changed order of derivative. Figure 2.2 demonstrates the dynamic phenomena of susceptible class for various values of ρ and it is found that susceptible are significantly influenced by decreasing the fractional order value. It has been seen that the increased value of fractional order ρ is one of the reasons which held responsible for the increment in susceptible population in the community. Also, memory effect can be observed for different values of ρ, for $\rho = 1$ there is no memory effect on susceptibles and by lowering down the value of ρ the memory affect becomes visible which is the fractional order derivatives property.

Table 2.2 Model parameters with their values

S.No.	Parameters	Value
1	β	0.003
2	λ	0.05
3	μ	5
4	α	0.06
5	γ	0.002
6	β_1	0.002
7	β_2	0.001
8	σ	0.02
9	δ	0.002

Figure 2.3 indicates the pattern of infected persons for various fractional order values. From this figure it is noticed that there is a lower number of infected individulas for small order , as the order raises the number of infected individuals also increases and and then it starts decreaing as the fractional order ρ decreases after hitting the peak value of I(t) = 68 for ρ = 1. Also, we can observe the presence of memory effect because as we decrease the value of ρ, the infected people are taking more time to recover. In addition, from both the figures (Figure 2.2 and 2.3) it is seen that system converges to its steady state more rapidly as the order of fractional order derivatives decreases, which is in accordance with these papers (A. Kumar, 2020; Naik, 2020). Figure 2.4 reveals the population of people recovered for various fractional orders and it is observed that the number of those recovered people is raised as we increase the order of fractional derivatives.

Figures 2.5(i), 2.5(ii) and 2.5(iii) shows behavior of susceptible on varying preventive measures taken by susceptible for different values of fractional order and no measures of inhibition are adopted by infected individuals. It infers those preventive measures taken by susceptible will be affecting the transmission of susceptible into infected compartments. More the number of individuals following the preventive measures implies a greater number of susceptible and lesser number of infectives. Despite contact occurring between susceptible and infective individuals, if preventive measures are taken by susceptible, then the transmission from susceptible compartment to infective compartment is reduced largely.

In figure 2.5(iii) for fractional order ρ = 1, an inverted peak in the number of susceptible population can be noticed, which progressively fades as the order of derivative reduces, which is due to the memory effect or the people's encounter with the disease. For β_1= 0.001, number of susceptible peoples were 76 for ρ = 0.6 at time t = 50 days (Fig 2.5(i)), while they were 58 and 43 respectively for ρ = 0.8 (Figure 2.5(ii)) and ρ = 1 (Figure 2.5(iii)). It is indicating that for the same β_1 as the fractional

order decreases, the number of susceptible increases ultimately number of infected populations decreases which is due to the people's memory effect about the disease.

Figures 2.6(i), 2.6(ii) and 2.6(iii) shows the behavior of infected individuals by varying the level of preventive measures taken by susceptible (β_1) when no inhibitory measure is taken by infected people for different values of fractional order ρ and it is observed that on increasing the value of preventive measures by susceptibles number of infectives starts decreasing. Also, the memory effect can be seen by comparing these three graphs as the fractional order decreases the peak in the infectives gradually disappears.

Figures 2.7(a)(i,ii,iii) and 2.7(b)(i,ii,iii) show the behavior of infectives by changing the measures of inhibition taken by infectives for various values of fractional order. In figure 2.7(a)(i,ii,iii) no preventive measures are taken by susceptible while in figure 2.7(b)(i,ii,iii) susceptible take preventive measures. It is evident that at any time if enough preventive measures are taken by susceptible then number of infectives are less in comparison to when no preventative measures are taken by susceptible. Also, it is depicted that as the preventive measures taken by infectives increases, the number of infected populations starts decreasing. In figure 2.7a(ii) at time t = 50 number of infected individuals were 24 while in figure 2.7b(ii) they were 21 at same time for β_2= 0.001 which shows that if susceptible use enough preventive measures, then their chances of entering the infected compartment reduces. Initially for lower order of fractional order no peak is there but as the fractional order ρ increases, peak in the increasing infected population starts appearing which shows the effect of memory property.

Figures 2.8(a)(i,ii,iii) shows the effect of change in preventive measures taken by infectives on susceptible when no preventive measures were taken by susceptible while in figures 2.8(b)(i,ii,iii) preventive measures were taken by susceptible. First, if infected individuals would get proper and timely treatment then the rate of spreading the infection decreases due to which susceptible population also decreases. In figure 2.8a(iii) at time t = 50, number of susceptible were 51 with β_2 = 0.001 and no safety measures were used by susceptibles while in figure 2.8b(iii) at the same time susceptible population is 45, here they have used the preventive measures with same β_2. Second, when figure 2.8(a)(i,ii,iii) is compared with figure 2.8(b)(i,ii,iii) it is inferred that if susceptible population practice more preventive measures like wearing masks, keeping social distance, and maintaining sufficient hygiene, their risk of entering infected compartment decreases. When comparing graphs, the memory effect is immediately evident.

Figures 2.9(a)(i,ii,iii) shows the effect of lockdown on infected population. Because of the lockdown the rate of transmission is reduced leading in a drop of infected population. Also, it is observed that for lower order of fractional order there

is no peak but peak starts appearing as ρ increases which shows the presence of memory effect. Similar effect of lockdown can be observed for susceptible population as shown in figure 2.9(b)(i,ii,iii), because of lockdown interaction will be less and the speed of transmission will be reduced, and a smaller number of people will be infected.

Figure 2.10(i) shows the effect of immigration on infectives for different values of recruitment rate. As the pace of recruitment rate rises, so does the number of infectives; however, after reaching its peak, the number of infectives begin to decline and settles down into a steady state, likewise figure 2.10(ii) describes the effect of immigration on susceptibles and same impact can be observed on susceptibles i.e., the higher the number of immigrants, higher the number of susceptibles and after a period the number of susceptibles archives the steady state. Figure 2.11 demonstrates that when the transmission rate increases, so does the reproduction number, implying that the infected population will increase. Figure 2.12 illustrates that, the more the preventive actions like as vaccination, masking, ensuring social distance and personal hygiene are adopted by susceptible population, the lower the number of infected cases and thus reproduction number will be reduced.

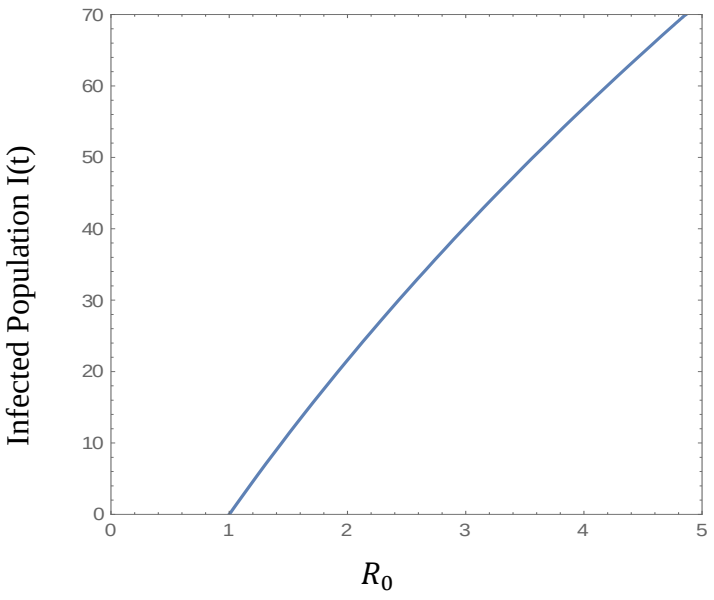

Figure 2.1. Basic Reproduction number vs Infected Population

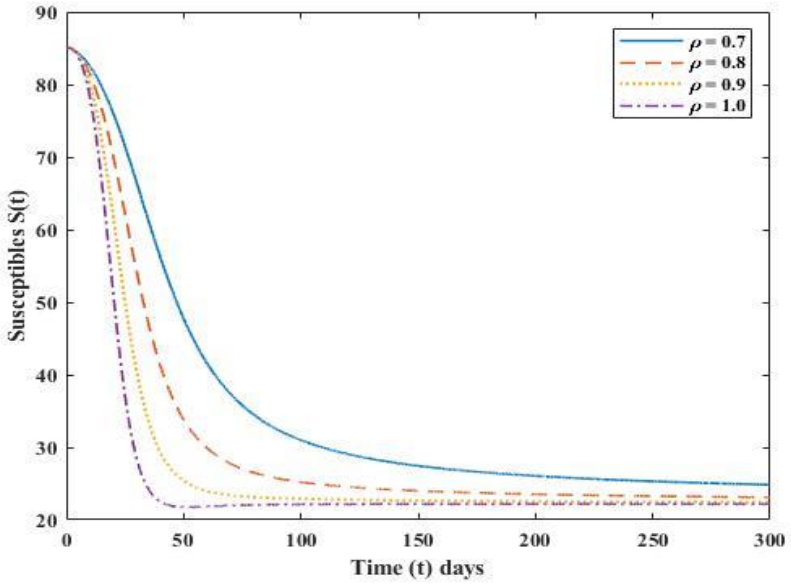

Figure 2.2 Result of varying fractional order ρ on susceptibles

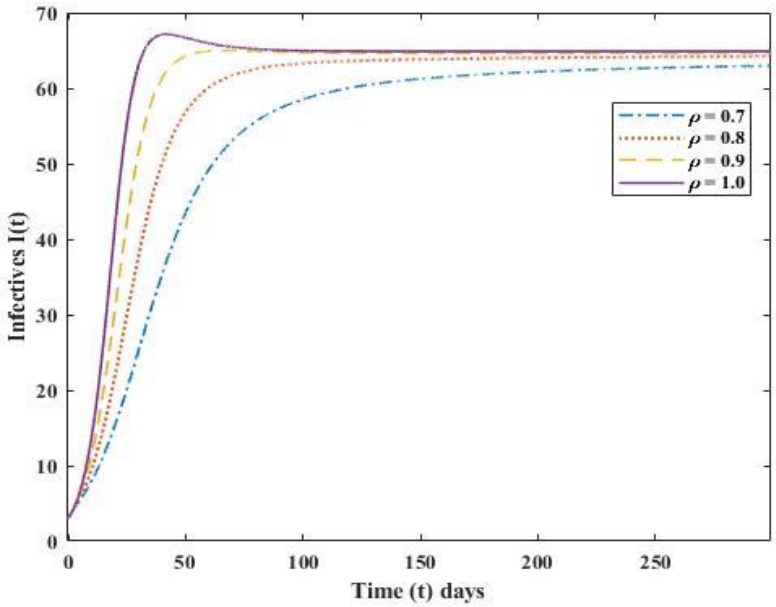

Figure 2.3 Result of varying fractional order ρ on infectives

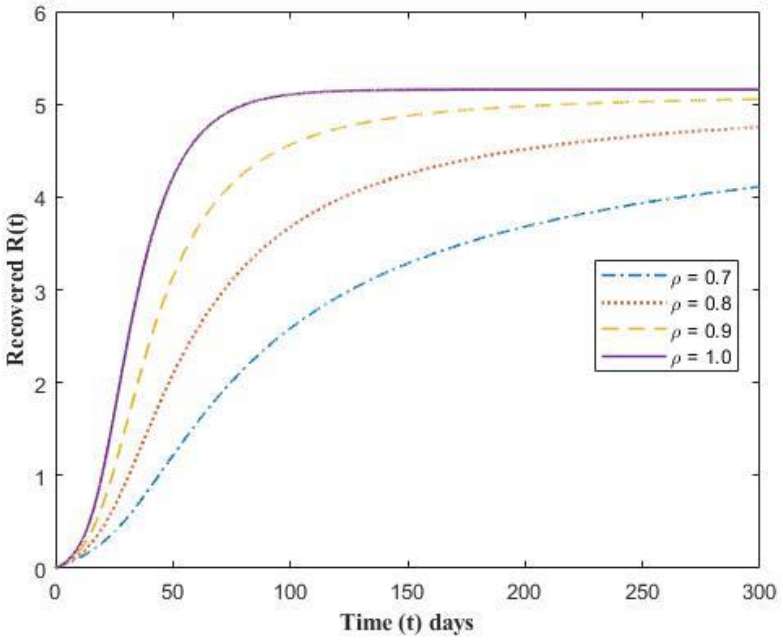

Figure 2.4 Result of varying fractional order ρ on recovered

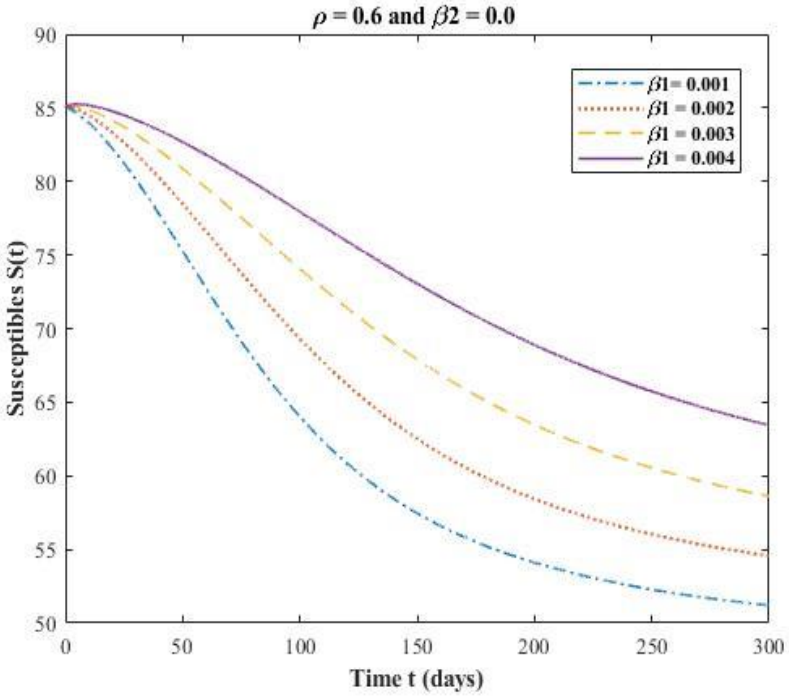

Figure 2.5 (i) Effect of varying measures taken by susceptibles on susceptibles with $\rho = 0.6$ and no measures taken by infectives

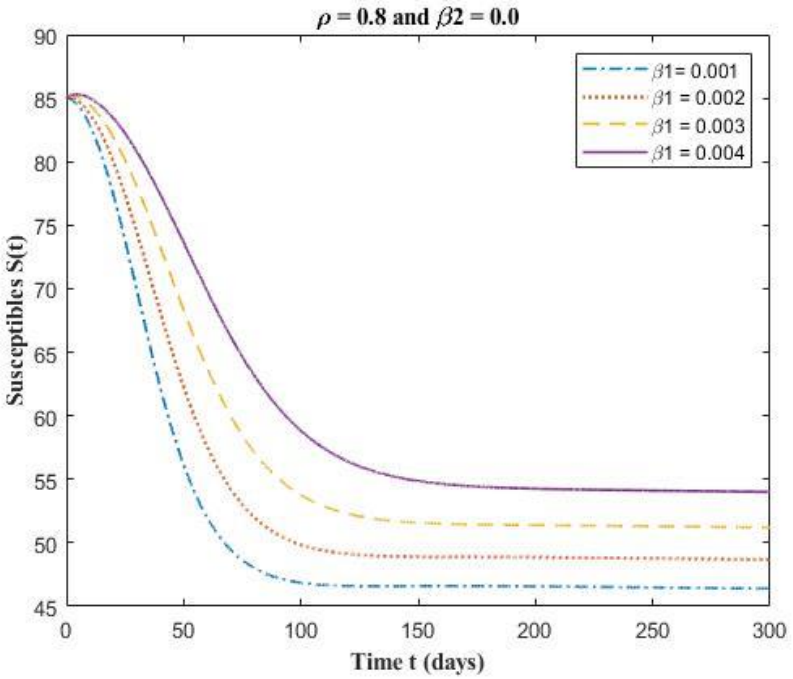

Figure 2.5(ii) Effect of varying measures taken by susceptibles on susceptibles with $\rho = 0.8$ and no measures taken by infectives

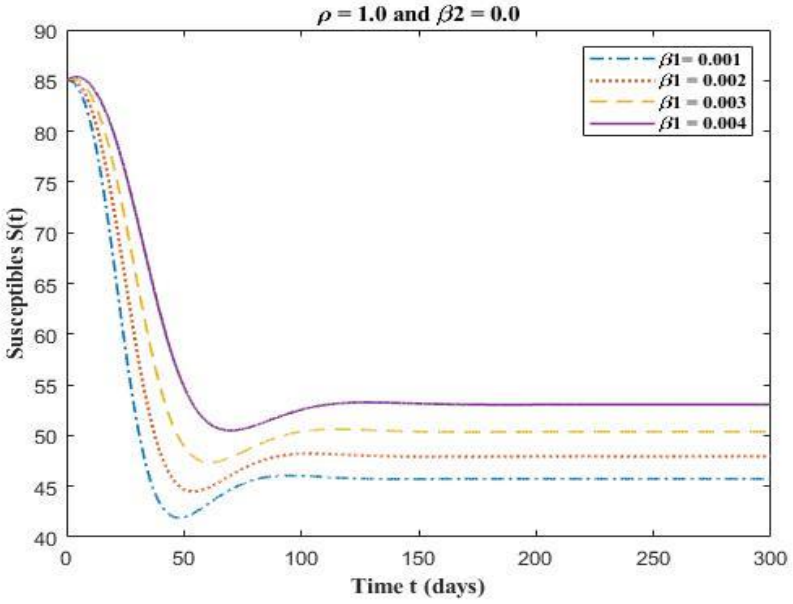

Figure 2.5(iii) Effect of varying measures taken by susceptibles on susceptibles with $\rho = 1.0$ and no measures taken by infectives

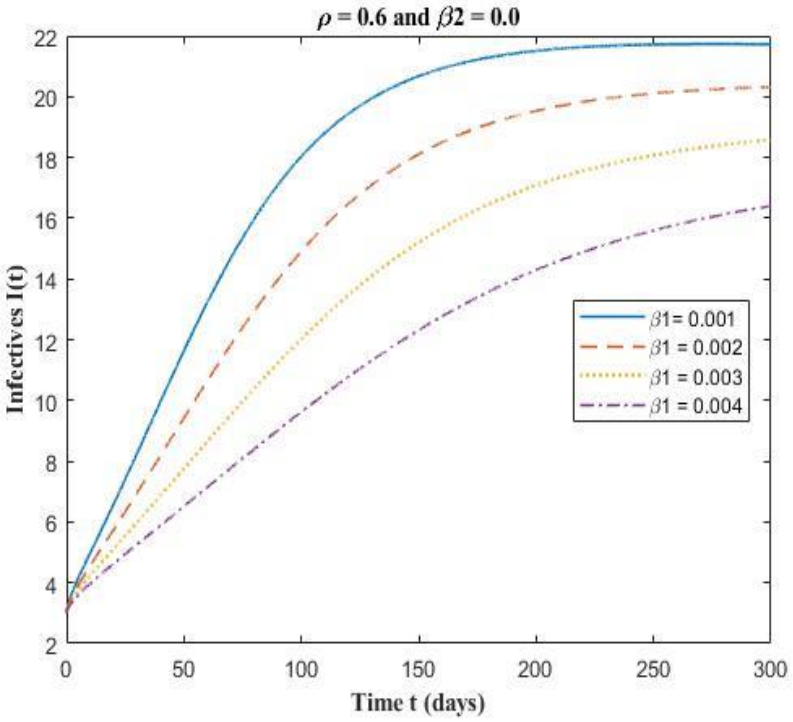

Figure 2.6(i) Effect of varying preventive measures taken by susceptibles on infectives with $\rho = 0.6$ and no measures taken by infectives

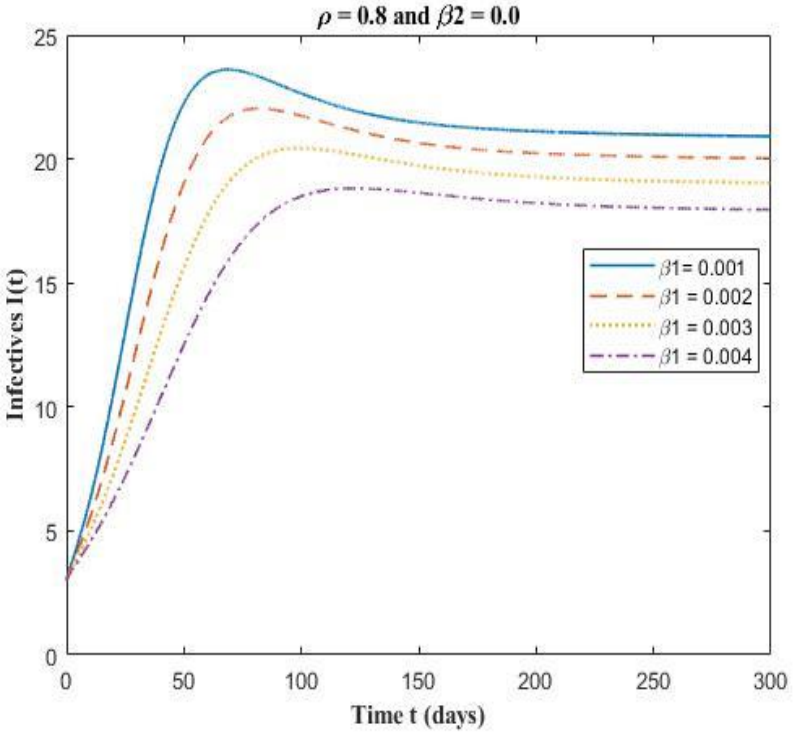

Figure 2.6 (ii) Effect of varying preventive measures taken by susceptibles on infectives with $\rho = 0.8$ and no measures taken by infectives

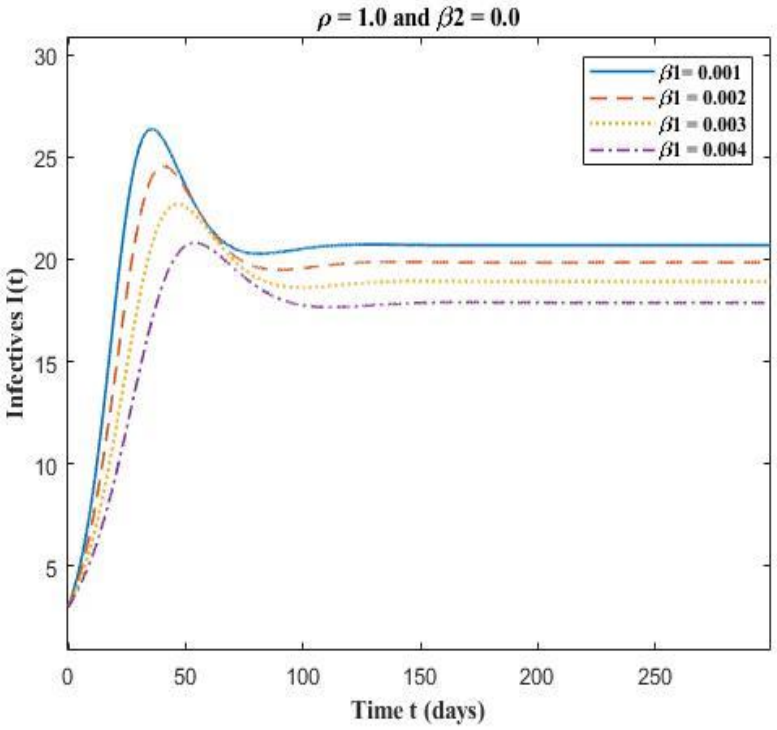

Figure 2.6 (iii) Effect of varying preventive measures taken by susceptibles on infectives with $\rho = 1.0$ and no measures taken by infectives

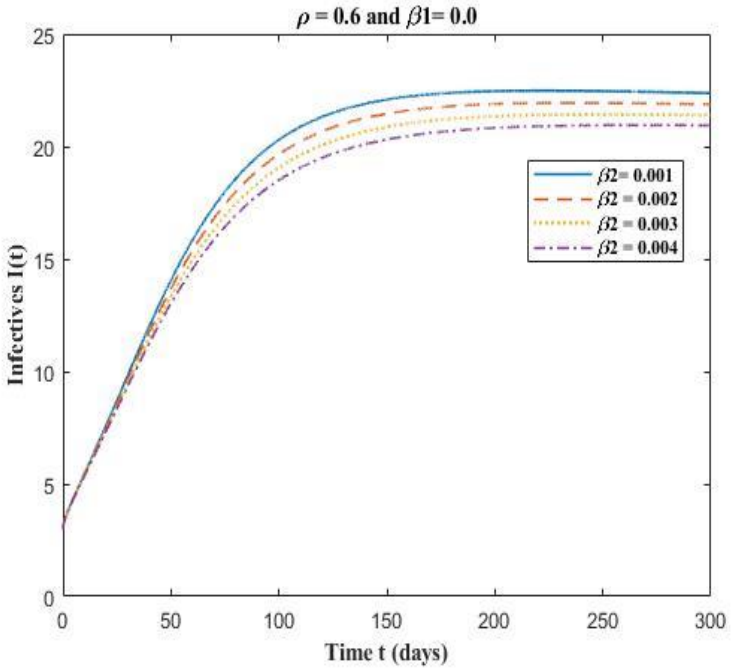

Figure 2.7a (i) Effect of varying measures taken by infectives on infectives with $\rho = 0.6$ and no measures taken by susceptibles

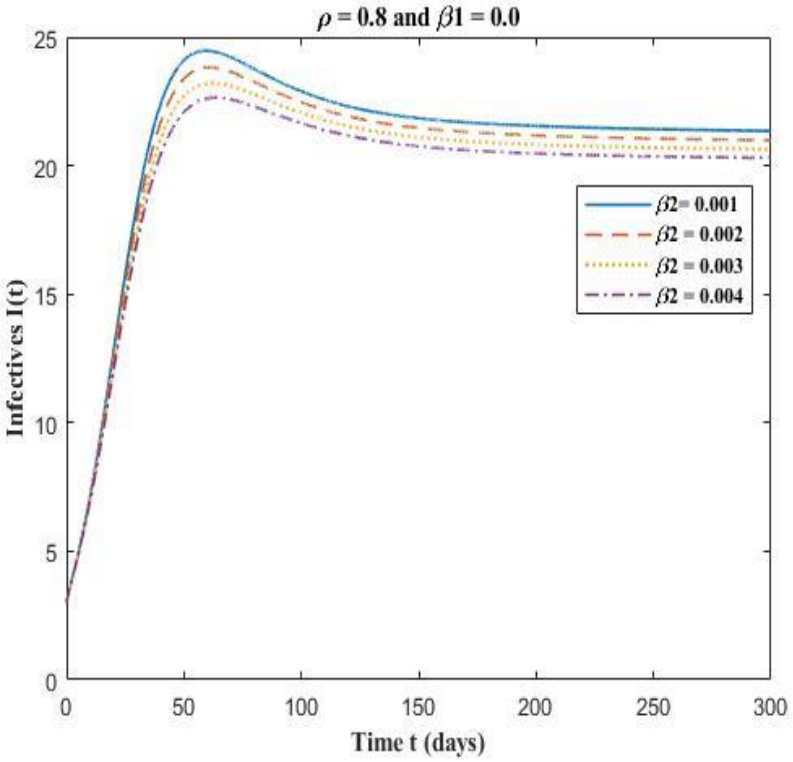

Figure 2.7a (ii) Effect of varying measures taken by infectives on infectives with $\rho = 0.8$ and no measures taken by susceptibles

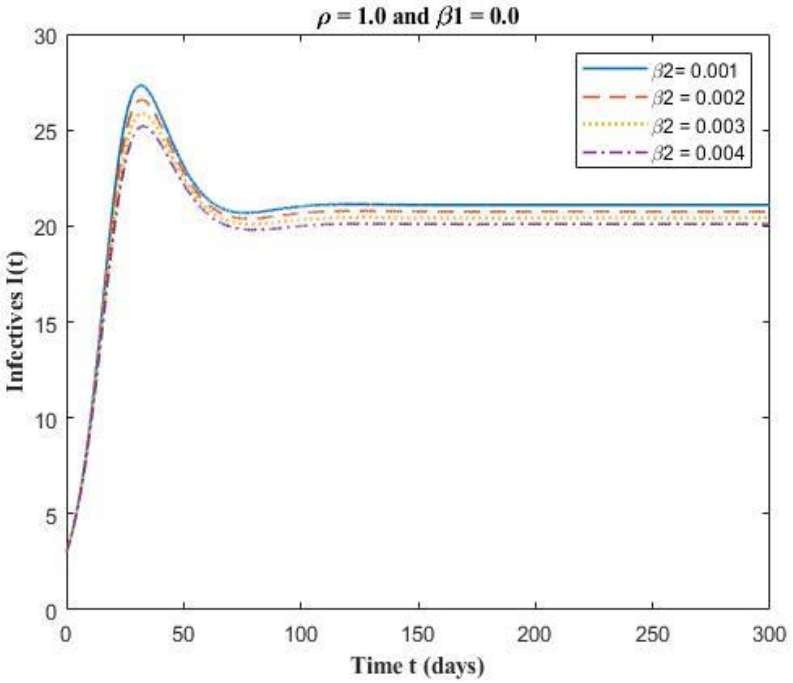

Figure 2.7a (iii) Effect of varying measures taken by infectives on infectives with $\rho = 1$ and no measures taken by susceptibles

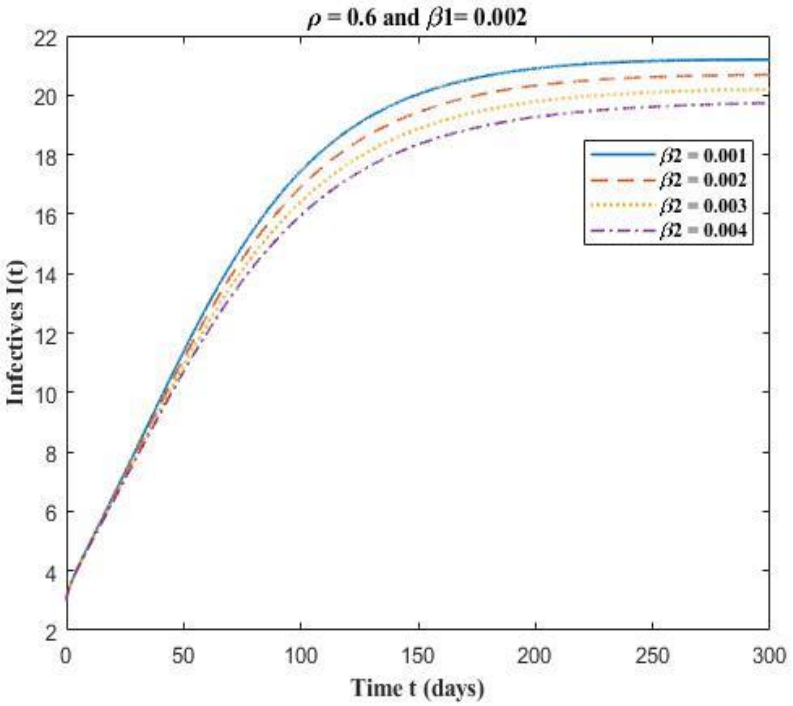

Figure 2.7b (i) Effect of varying measures taken by infectives on infectives with $\rho = 0.6$

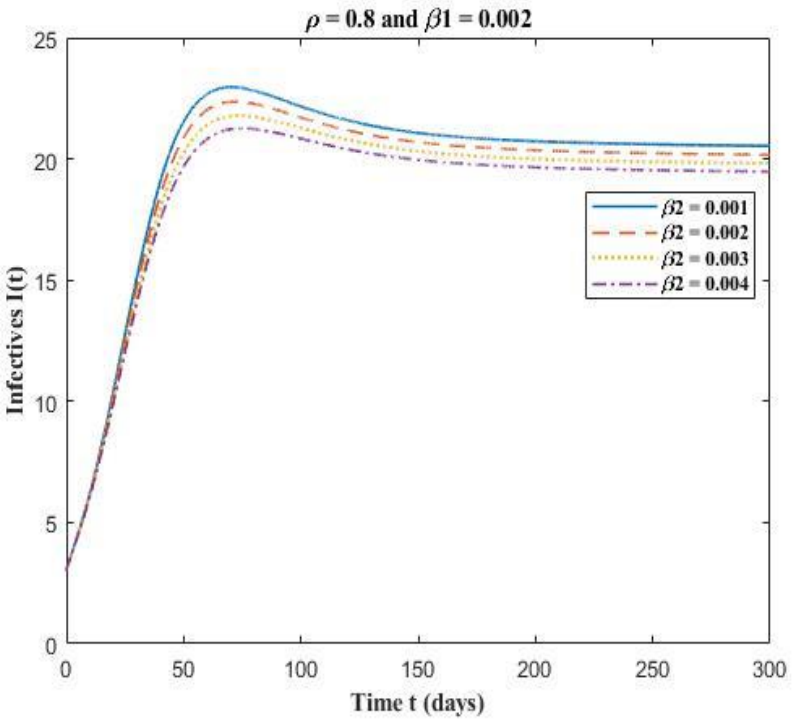

Figure 2.7b (ii) Effect of varying measures taken by infectives on infectives with $\rho = 0.8$

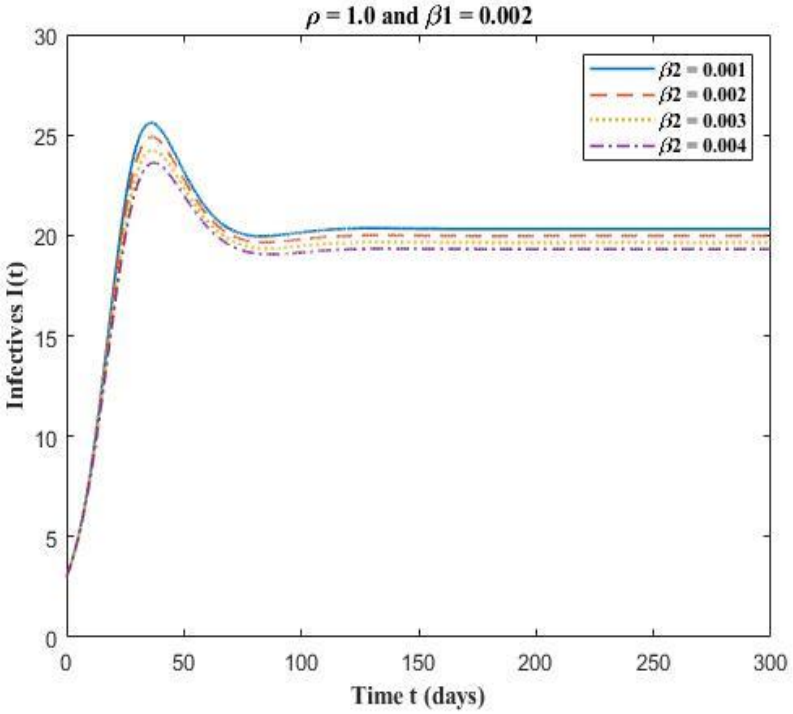

Figure 2.7b (iii) Effect of varying measures taken by infectives on infectives with $\rho = 1$

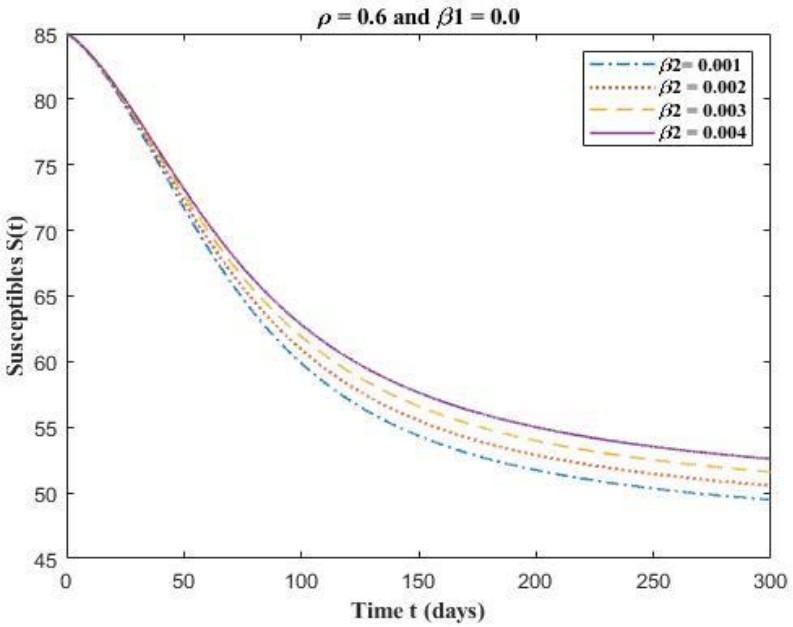

Figure 2.8a (i) Effect of varying measures taken by infectives on susceptibles with $\rho = 0.6$ and no measures taken by susceptibles

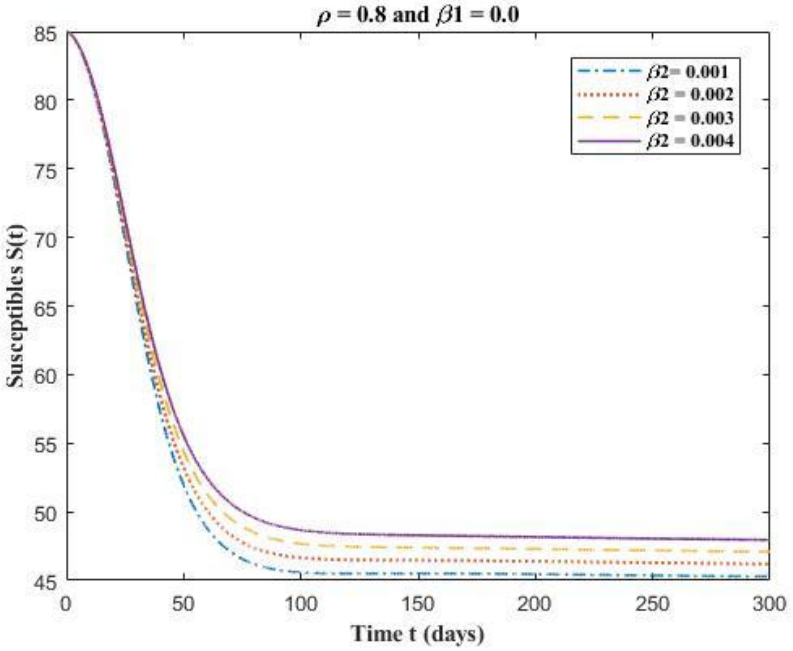

Figure 2.8a (ii) Effect of varying measures taken by infectives on susceptibles with $\rho = 0.8$ and no measures taken by susceptibles

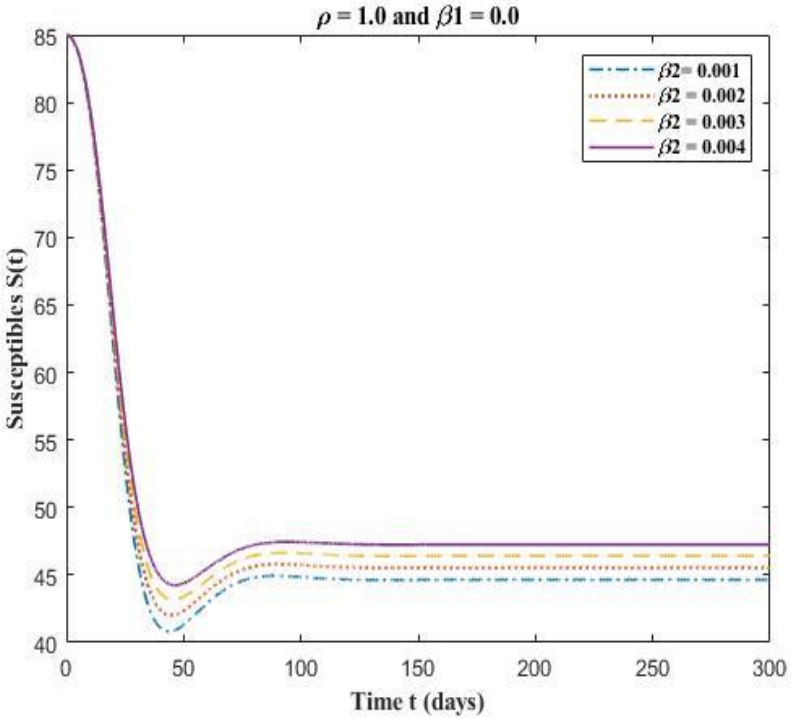

Figure 2.8a (iii) Effect of varying measures taken by infectives on susceptibles with $\rho = 1.0$ and no measures taken by susceptibles

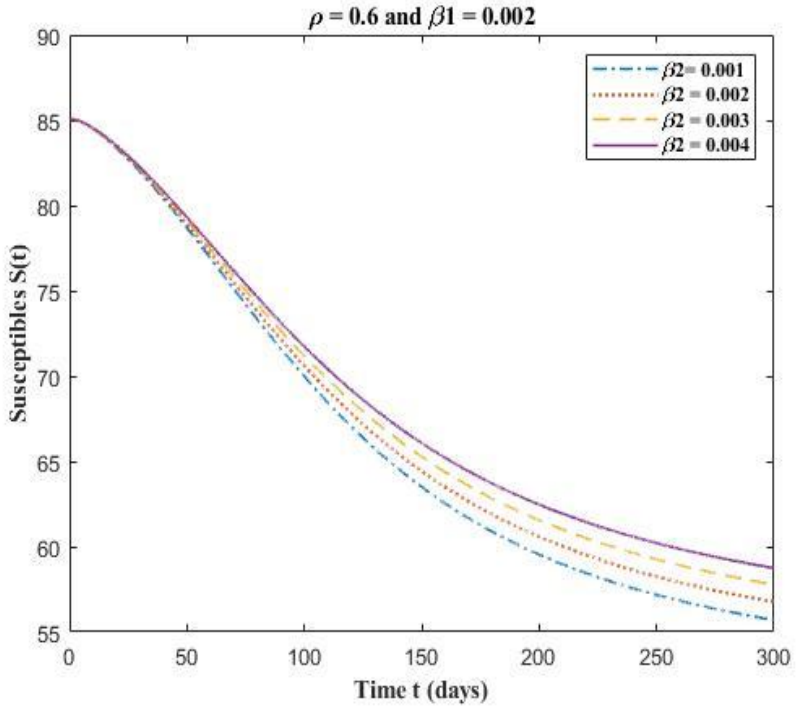

Figure 2.8b (i) Effect of varying measures taken by infectives on susceptibles with $\rho = 0.6$

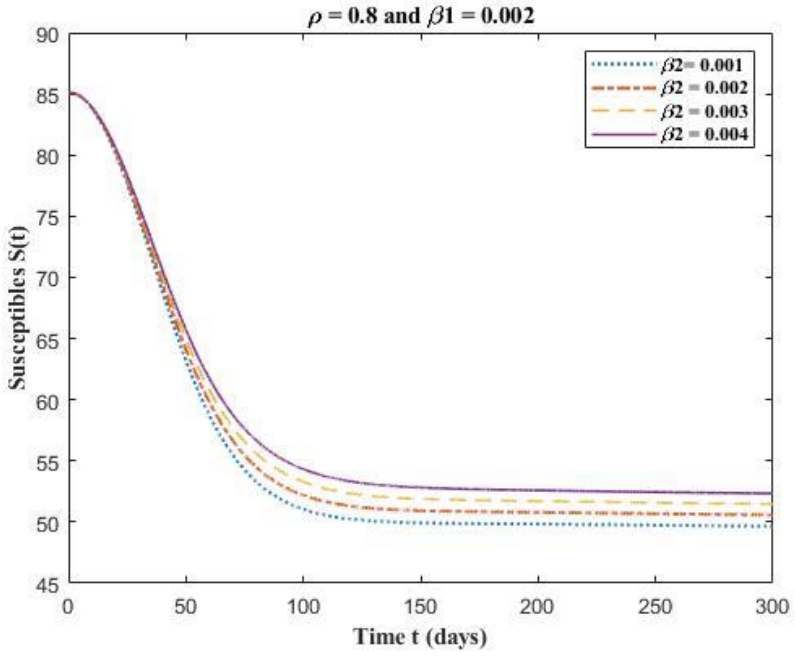

Figure 2.8b (ii) Effect of varying measures taken by infectives on susceptibles with $\rho = 0.8$

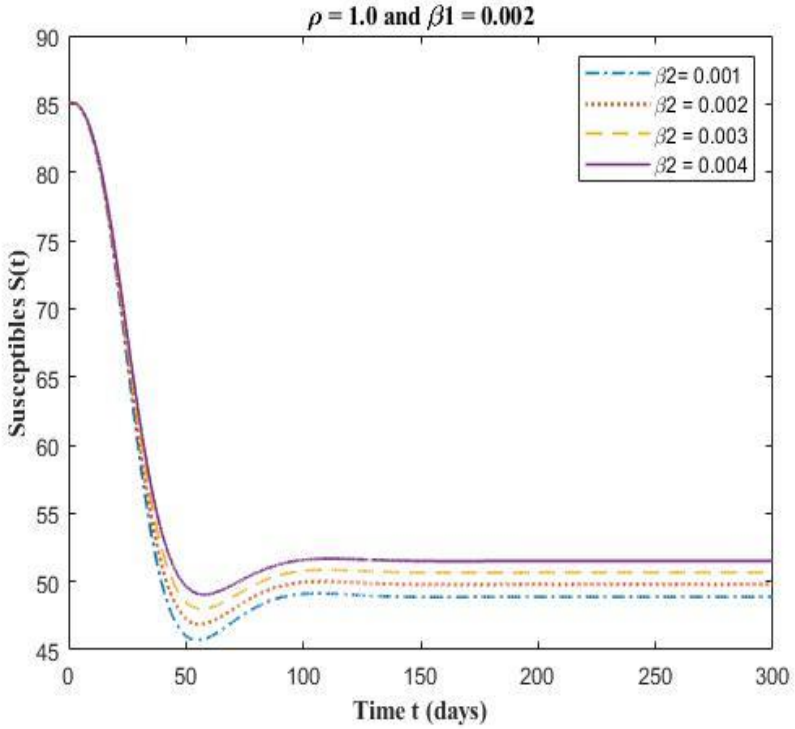

Figure 2.8b (iii) Effect of varying measures taken by infectives on susceptibles with $\rho = 1$

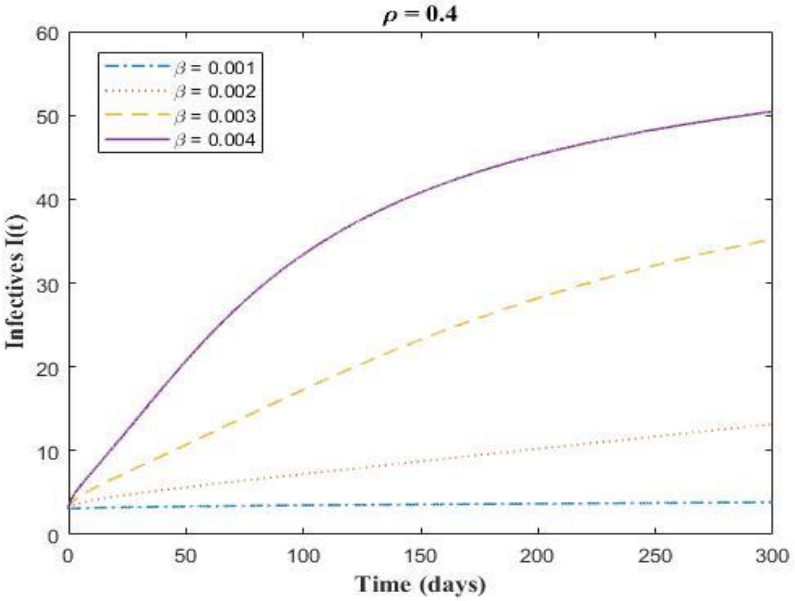

Figure 2.9a (i) Effect of lockdown on infectives with $\rho = 0.4$

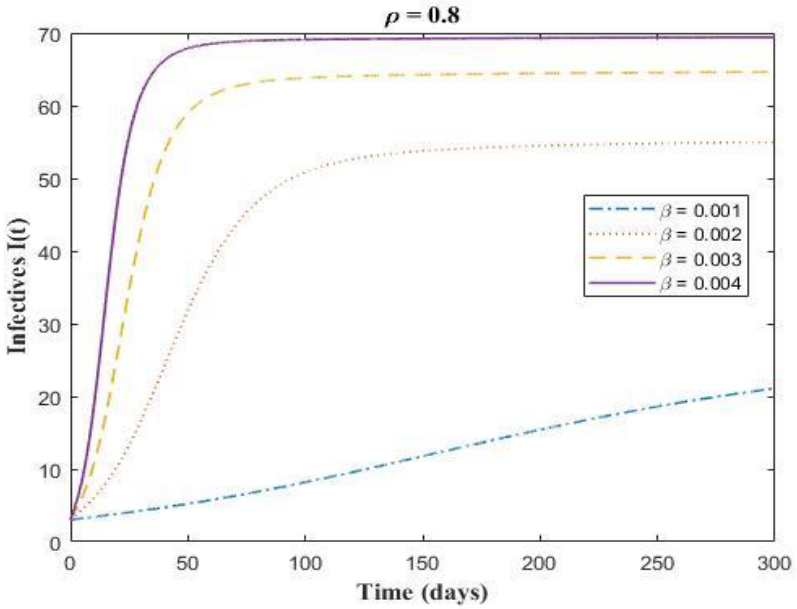

Figure 2.9a (ii) Effect of lockdown on infectives with $\rho = 0.8$

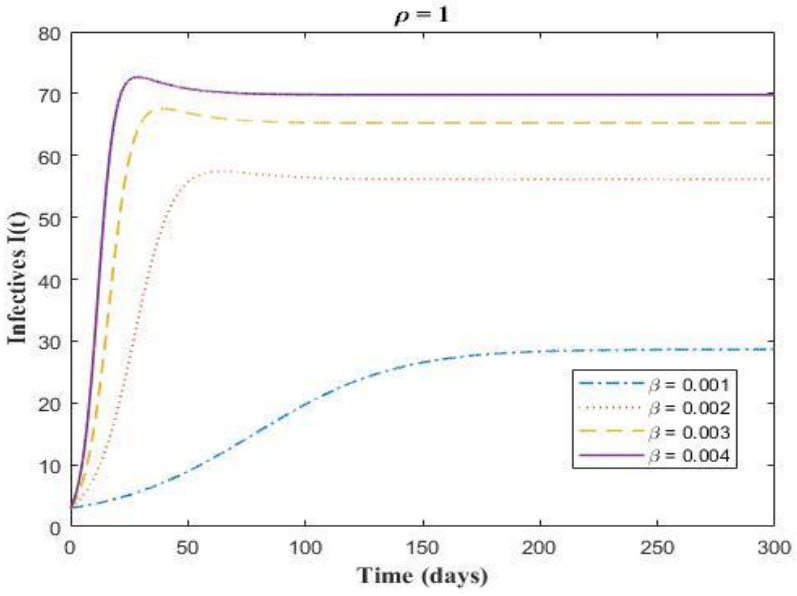

Figure 2.9a (iii) Effect of lockdown on infectives with $\rho = 1$

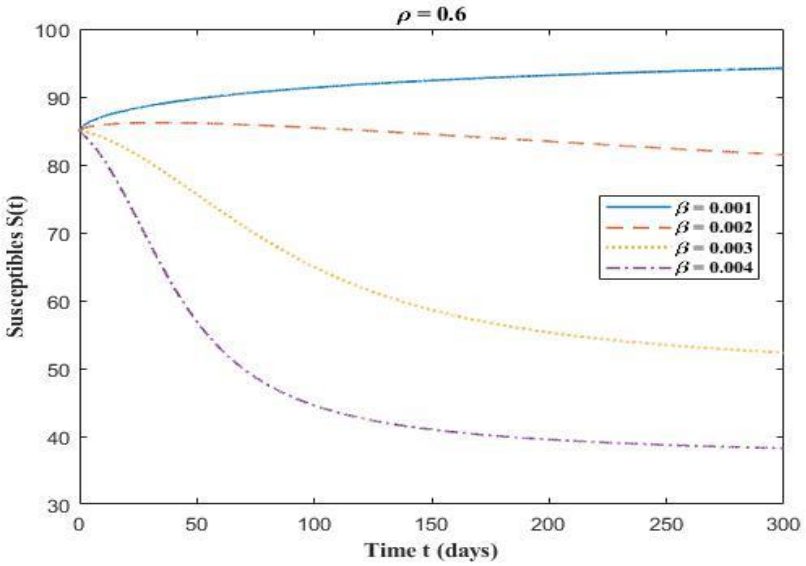

Figure 2.9b (i) Effect of lockdown on susceptibles with $\rho = 0.6$

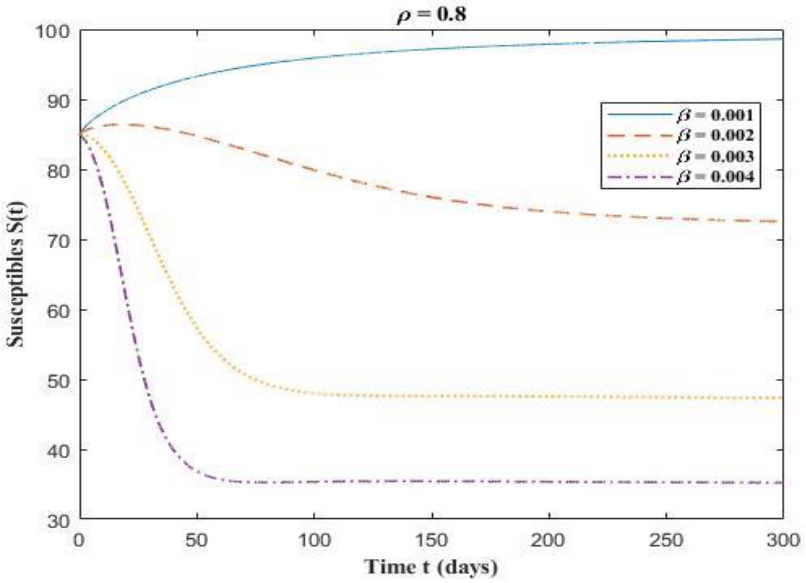

Figure 2.9b (ii) Effect of lockdown on susceptibles with $\rho = 0.8$

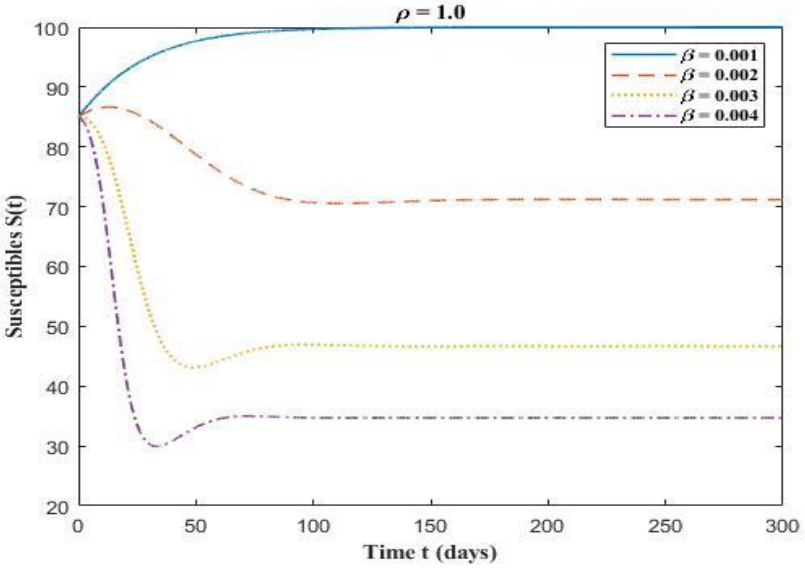

Figure 2.9b (iii) Effect of lockdown on susceptibles with $\rho = 1$

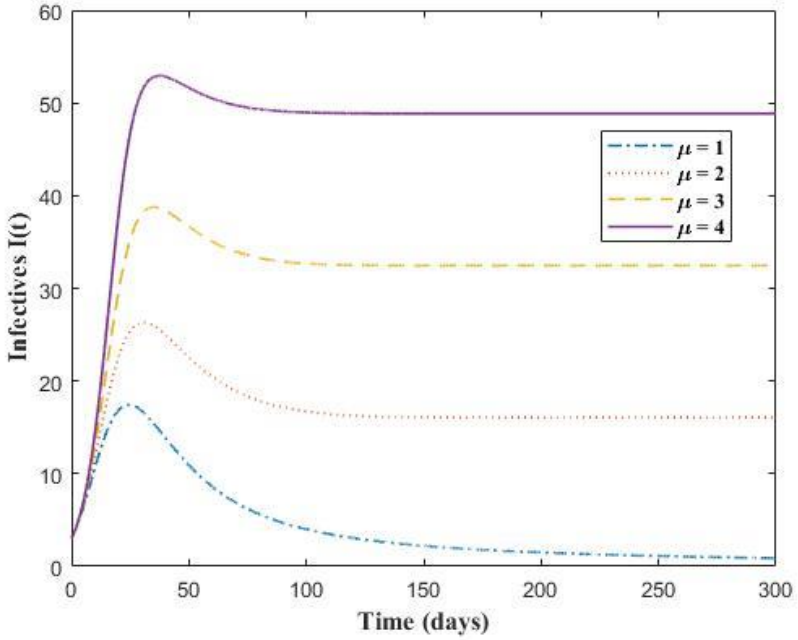

Figure 2.10 (i) Effect of immigration on infectives

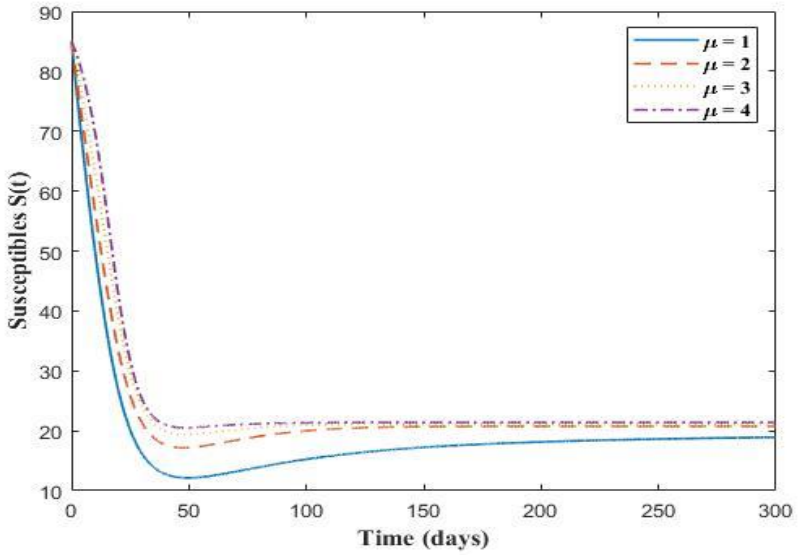

Figure 2.10 (ii) Effect of immigration on susceptibles

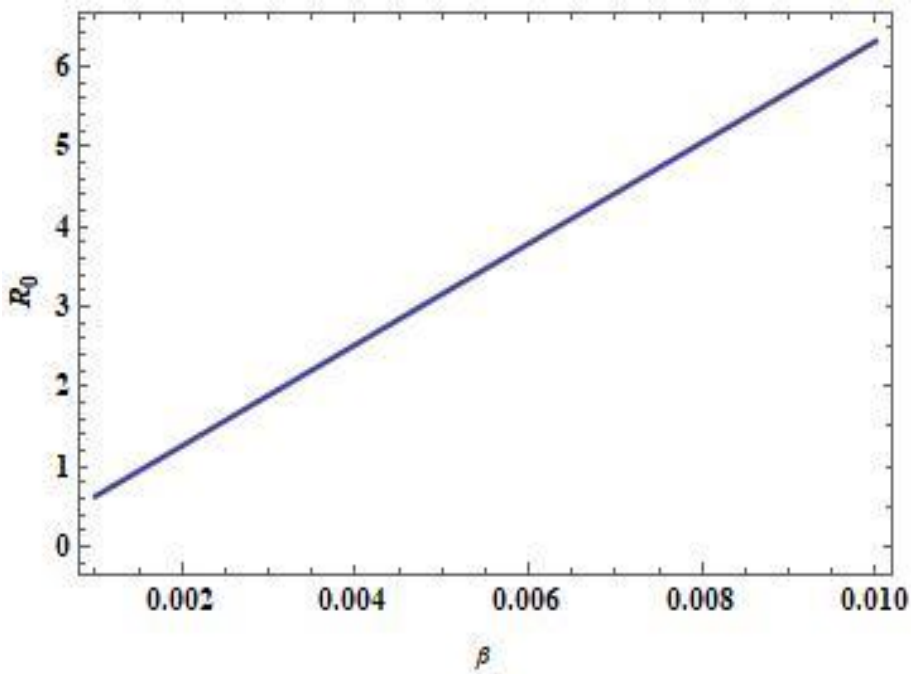

Figure 2.11 Effect of transmission of disease on basic reproduction number R_0

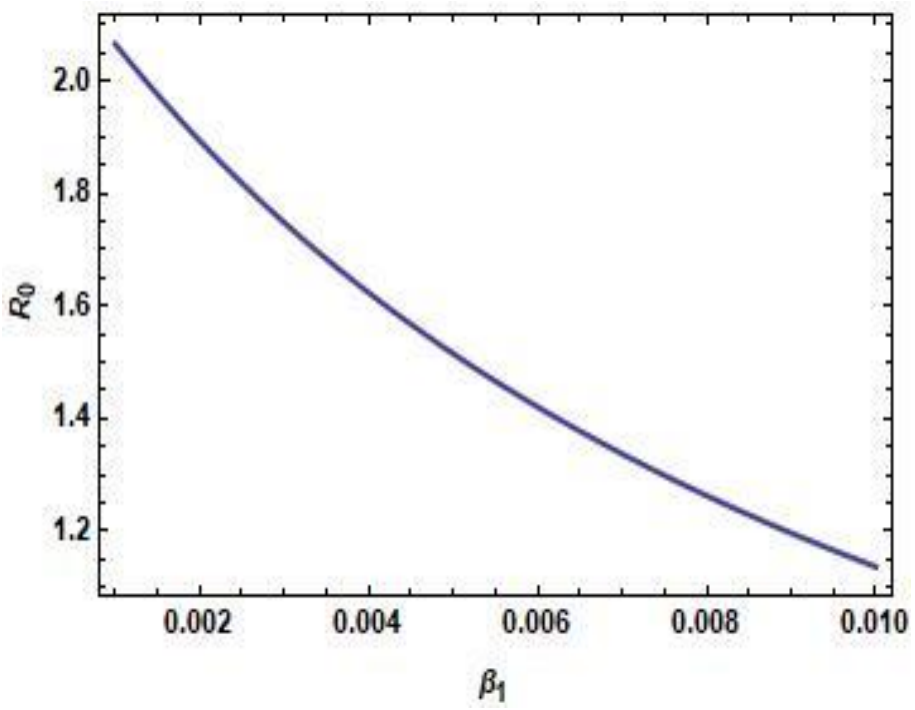

Figure 2.12 Effect of measures taken by susceptibles on basic reproduction number R_0

2.6 Conclusion

This chapter introduces and discusses a novel Caputo-fractional SIR model with Beddington-De Angelis incidence rate for COVID-19 and Holling type II type saturated treatment rate. The system (2.1) experience two equilibriums: disease-free equilibrium Q^d and endemic equilibrium Q^e. The R_0, basic reproduction number studied the analysis of local stability for both the equilibria. The equilibrium of disease-free state has proven to be stable for $R_0 < 1$ i.e., disease diminishes and for $R_0 > 1$, the disease-free equilibrium Q^d becomes unstable and the endemic equilibrium Q^e becomes stable under some conditions. Further, the global stability behavior of both the disease-free equilibria and the endemic equilibria is analysed and it is found that DFE is globally asymptotically stable when $R_0 \leq 1$ and the endemic equilibrium is globally asymptotically stable when $R_0 > 1$.

Moreover, numerical results for the favour of the analytical work are obtained. It is noted that the variation in the values of non-integer order derivatives ρ does not impact the equilibrium stability of the system but the time to achieve steady conditions or endemic equilibrium decreases i.e., better convergence can be accomplished by reducing the order of fractional derivatives or greater the values of

ρ slower is the convergence thus, the utility of the non-integer order derivative rather than the integer order model has been investigated. The rate of disease transmission will decrease if there is less contact between susceptibles and infectives, which could be achieved by taking adequate safety precautions both by susceptibles and infectives, as well as imposing lockdown. Moreover, if disease transmission is reduced, R_0, the basic reproduction number declines. With this fractional order model and taking the authentic data of COVID-19, the dynamics of COVID-19 can be predicted.

CHAPTER 3

FRACTIONAL ORDER MODEL USING CAPUTO FRACTIONAL DERIVATIVE TO ANALYSE THE EFFECTS OF SOCIAL MEDIA ON MENTAL HEALTH DURING COVID-19

During COVID-19 outbreak, the large population was exposed to social media. Since it was a new virus and no specific information was available about its dynamics, therefore people were dependent on social media to gather more and more information. Social media has its pros and cons, which have an impact on the life of human being which was more in case of COVID-19 due to restricted interaction during the period of pandemic. In this chapter the effects of social media on the mental health of people have been investigated with the help of Holling type II and Monod Haldane rates in the form of incidence and treatment rates, respectively. The model exhibits two types of equilibria viz. disease-free equilibrium (DFE) and endemic equilibrium (EE), which has been confirmed by the Fractional Routh-Hurwitz criterion. Further stability behavior has been also analyzed under certain sufficient conditions that depends on R_0, a Basic Reproduction number, which is determined by the method of next generation matrix. The findings indicate that the fractional derivative order has a considerable influence on the dynamic process. The difference between fractional and integer order derivatives is illustrated by the memory effect. Finally, numerical simulations have been performed to examine the effect of various parameters on the dynamics of social media on mental health.

3.1 Introduction

Severe Acute Respiratory Syndrome CoronaVirus-2 (SARS CoV-2), 2019-nCoV a new coronavirus capable of causing coronavirus disease, a severe respiratory illness similar to SARS and MERS, originally first identified in Wuhan, China, in December 2019. The World Health Organization first declared the COVID-19 breakout as Concern of International Public Health Emergency and then as pandemic. As a result of the breakout, rigorous laws prohibiting massive gatherings and social activities have been implemented across the world. Because of the stringent social distancing restrictions, people were heavily relying on media, particularly social media, for up-to-date information regarding the outbreak and to maintain connectivity. Among the most widely utilized resources of information is social media networks; they are one of the simplest and most effective techniques of transmitting information. The World Health Organization has revealed that they are currently fighting not only with a global pandemic, but also with a social media infodemic, with some media organizations claiming that the coronavirus is the first true social media infodemic because it has exacerbated information and misinformation globally, causing panic and confusion among people (Hao & Basu, 2020).The term infodemic (Zarocostas, 2020) has been coined to outline the perils of misinformation phenomena during the management of disease outbreaks, since it could even speed up the epidemic process by influencing and fragmenting social response(Kimid et al., 2019).

Indeed, Li et al. (Z. Li et al., 2020) found that the public reported even higher levels of vicarious traumatization than front-line nurses fighting COVID-19. According to an ABC News poll, anxiety due to the coronavirus spreads faster on social media than the virus itself, triggering mass chaos (Joan Muwahed, 2020). Compared with traditional media, social media has played a multitude of positive roles in information exchange during the COVID-19 crisis, including disseminating health-related recommendations, enabling connectivity and psychological first aid (Merchant & Lurie, 2020). On the other hand, social media has also fuelled the rapid spread of misinformation and rumours, which can create a sense of panic and confusion among the public (Garfin et al., 2020). In China, the peak of information searches on the Internet and social media platforms came 10-14 days before the peak of COVID-19 cases, suggesting that searches on the Internet and social media networks are linked to disease occurrence (C. Li et al., 2020).

Social media networks have shown to be effective in keeping people in touch with friends and family, preventing solitude and monotony, which have been associated with stress and long-term misery, and have thus emerged as a viable alternative for minimizing isolation at home. Social media may lead to (mis)information overload (Bontcheva et al., 2013; Roth & Brönnimann, 2014), which in turn may cause mental health problems such as stress, anxiety, depressive symptoms, insomnia, denial, anger, and fear etc.

Public awareness is crucial for controlling the infectious diseases and prevention from COVID-19, inadequate understanding of infectious illnesses brings about less identification rates. Therefore, to stop the spread of COVID-19 infection in Jordan, the Jordanian Ministry of Health launched specific national disease control measures, using several media campaigns (Ministry of Health, 2021), posters, and advertisements on television and printed media along with other methods to improve the awareness of this pandemic among the general population. The assessment of government websites and social media platforms for public awareness is important because it helps determine the impact of governmental prevention efforts and measures and gauges the need for intervention (Allgaier & Svalastog, 2015). Researchers have proposed numerous mathematical compartmental models for predicting and understanding the time-evolution of infectious disease epidemics (Dubey et al., 2013; Goel et al., 2020; A. Kumar, Kumar, et al., 2020). Because of its ability to provide a convincing analysis of certain nonlinear dynamics, infectious simulation research has recently been diverted to fractional differential research(Awais et al., 2020; Debasis Mukherjee & Maji, 2020; A. Kumar, 2020; Swati & Nilam, 2022).

Whenever we see, read, or hear something, its good, or bad effect remains in our memory and therefore fractional or non-integer differential equations are better for modeling the effects of having memory of things on social media regarding COVID-19. In this chapter, we have formulated a non-integer i.e., fractional order SIR model to analyze the effect of social media during COVID-19 on public mental health with the Holling type II incidence and Monod-Haldane treatment rate. Caputo form of fractional order has been considered here to capture the memory property which exists in most biological scenarios. The reason behind choosing the Holling type II incidence rate is to investigate the effects of infectives induced inhibitory measures such as awareness about consequences of overusing social media, switching to traditional media use (television, radio, newspaper etc.), focusing on exercise, yoga meditation etc. Monod-Haldane treatment rate has been chosen here to represent the constraints in treatment availability for huge number affected people.

3.2 Formulation of Fractional order Mathematical Model

In this section a non-integer fractional order mathematical model is formulated to observe the effect of social media on mental health during COVID time. The whole population N(t) is categorized into three classes viz. Susceptibles S(t), Infectives I(t) and Recovered R(t). Holling type II incidence rate and Monod-Haldane treatment rate have been used to derive the model using Caputo form of fractional derivative. The Caputo derivative is described in definition 1in Appendix. The model is as follows:

$$\left.\begin{aligned} {}_0^cD_t^{\rho}\, S(t) &= \mu - \lambda\, S(t) - \frac{\beta\, S(t)I(t)}{1+\alpha\, I(t)} \\ {}_0^cD_t^{\rho} I(t) &= \frac{\beta\, S(t)I(t)}{1+\alpha\, I(t)} - (\lambda+\delta+\sigma)I(t) - \frac{a\, I(t)}{1+b\,\left(I(t)\right)^2} \\ {}_0^cD_t^{\rho} R(t) &= \frac{a\, I(t)}{1+b\,\left(I(t)\right)^2} + \sigma\, I(t) - \lambda\, R(t) \end{aligned}\right\} \quad (3.1)$$

$S(0) = S_0 \geq 0, I(0) = I_0 \geq 0$ and $R(0) = R_0 \geq 0$ are the positive initial conditions.

S(t) : Number of people using social media at time t

I(t) : Number of people suffering from mental health problem because of using social media

R(t) : Number of people recovered from mental health problems

μ : Recruitment rate

λ : Rate at which individuals leave their respective compartments.

β : Transmission rate

α : Inhibition rate by infectives such as awareness about consequences of overusing social media, switching to traditional media (TV, radio, newspaper etc), getting involved into exercise, yoga, meditation, self-induced restricted use of social media, etc.

δ : Disease induced mortality rate

σ : Recovery rate

a : Cure rate

b : Limitation in treatment availability

3.3 Basic Properties of the Model

Let $\mathbb{R}^3_+ := \{X \epsilon\, \mathbb{R}^3 : X \geq 0\}$ and $X(t) = \left(S(t), I(t), R(t)\right)^T$ on non-negative solutions, the lemmas needed to prove the theorem are mentioned in Appendix.

Theorem 3.1 The region of attractor of solution, which remains positive, corresponding to system (3.1) is $\Omega = \left\{(S, I, R) \in R^3_+ : 0 < S + I + R = N \leq C_E \frac{\mu}{\lambda}\right\}$ for $t \geq 0$, where C_E is defined in Lemma 4.

Proof. To prove the positiveness of each solution with corresponding initial conditions of the model (3.1), assume that at t = 0, $S(0) > 0$. Now we prove that $S(t) \geq 0 \; \forall \; t \; \geq 0$. We will demonstrate this using a contradiction, let $S(t) \leq 0 \; \forall \; t \; \geq 0$. After that, there is a $\omega_1 > 0$ as a result $S(t) > 0$ for that $0 \leq t < \omega_1$, $S(t) = 0$ at $t = \; \omega_1$, and $S(t) < 0$ for $\omega_1 < t < \omega_1 + \epsilon_1$ with sufficiently small $\epsilon_1 > 0$. So, if we take the first equation in model (3.1), we get ${}_0^c D^\rho \; S(t)|_{t=\omega_1} = \mu > 0$. From Lemma 2, for any $0 < \epsilon_1 \ll 1$, we have $S(\omega_1 + \epsilon_1) = S(\omega_1) + \frac{1}{\Gamma(\alpha)} D^\rho S(\xi) \; (\epsilon_1)^\rho$. Thus, we get $S(\omega_1 + \epsilon_1) \geq 0$, which is in contradiction to the fact that $S(t) < 0$ for $\omega_1 < t < \omega_1 + \epsilon_1$. As a result, we obtain $S(t) \geq 0 \; \forall \; t \; \geq 0$. Then we show that $I(t) \geq 0 \; \forall \; \; t \; \geq 0$. Again, we accomplish this through contradiction by, assuming that $I(t) \geq 0$ is not true, then $\exists$ a $\omega_2 > 0$ as a result $I(t) > 0$ for that $0 \leq t < \omega_2$, $I(t) = 0$ at $t = \; \omega_2$, and $I(t) < 0$ for $\omega_2 < t < \omega_2 + \epsilon_2$ with sufficiently small $\epsilon_2 > 0$. Then we obtain

$$ {}_0^c D^\rho \; I(t)|_{t=\omega_2} = 0 $$

From Lemma 2, for any $0 < \epsilon_2 \ll 1$, we have $I(\omega_2 + \epsilon_2) = I(\omega_2) + \frac{1}{\Gamma(\alpha)} D^\rho I(\xi) \; (\epsilon_2)^\rho$. Thus, we get $I(\omega_2 + \epsilon_2) \geq 0$, despite the fact that $I(t) < 0$ for $\omega_2 < t < \omega_2 + \epsilon_2$. Thus, we have $I(t) \geq 0$ for all $\; t \; \geq 0$. Likewise, we can establish that $R(t) \geq 0$ for all $\; t \; \geq 0$.

Therefore, each solution of model (3.1) considering initial conditions is nonnegative. We will now illustrate that solutions are bounded. When all the three equations of model (3.1) are added together, we get:

$$ D_t^\rho N = \; \mu - \lambda N - \delta I $$

Where $N = S + I + R$. As $\; I(t) \geq 0$, we have

$$ D_t^\rho N \leq \; \mu - \lambda N. $$

Consider the initial value problem $D_t^\rho \overline{N} = \; \mu - \lambda \overline{N}$, $\overline{N}(0) = \overline{N}_0$. Using comparison principle (Lu & Zhu, 2018), we obtain the following inequality:
$N(t) \leq \overline{N}(t)$ for all $t \geq 0$. The initial value problem has been solved using Laplace transform

$$ s^\rho L[\overline{N}(t)] - s^{\rho-1} \overline{N}_0 = \frac{\mu^\rho}{s} - \lambda L[\overline{N}(t)] $$

$$ \Rightarrow L[\overline{N}(t)] = \frac{s^{\rho-1} \overline{N}_0}{s^\rho + \lambda} + \frac{\mu^\rho s^{-1}}{s^\rho + \lambda} $$

Using Lemma 3, we obtain

$$L\left[E_{\rho,1}(-\lambda t^{\rho})\right] = \frac{s^{\rho-1}}{s^{\rho}+\lambda}$$

$$L\left[t^{\rho}E_{\rho,\rho+1}(-\lambda t^{\rho})\right] = \frac{s^{-1}}{s^{\rho}+\lambda}$$

The above two equations reduced into the following form by applying the inverse Laplace transform,

$\bar{N}(t) = \bar{N}_0 E_{\rho,1}(-\lambda t^{\rho}) + \mu t^{\rho} E_{\rho,\rho+1}(-\lambda t^{\rho})$, using $D_t^{\rho} N \leq \mu - \lambda N$,

we have

$$N(t) \leq N_0 E_{\rho,1}(-\lambda t^{\rho}) + \mu t^{\rho} E_{\rho,\rho+1}(-\lambda t^{\rho}),$$

By Lemma 3.4, we obtain

$$|N(t)| \leq \frac{N_0 C_E}{1+\lambda t^{\rho}} + \frac{\mu t^{\rho} C_E}{1+\lambda t^{\rho}}$$

C_E is a constant term stated in the Lemma 4. Thus, for time t tending towards infinity, we see $N(t) \leq \bar{N}$ with $\bar{N} \geq C_E \frac{\mu}{\lambda}$. For $t \geq 0$, solution remain in region Ω which is bounded also.

3.4 Mathematical analysis of the model

This section performs stability analysis of the disease free equilibrium point and the endemic equilibrium point.

3.4.1 Equilibria and their Stability

Since the third equation is independent of two initial equations, hence we simply consider first two equations of the system for stability analysis.

$$\left.\begin{aligned} {}_0^cD_t^\rho\, S(t) &= \mu - \lambda\, S(t) - \frac{\beta\, S(t)I(t)}{1+\alpha\, I(t)} \\ {}_0^cD_t^\rho I(t) &= \frac{\beta\, S(t)I(t)}{1+\alpha\, I(t)} - (\lambda+\delta+\sigma)I(t) - \frac{a\, I(t)}{1+b\left(I(t)\right)^2} \end{aligned}\right\} \tag{3.2}$$

Let $c = \lambda + \delta + \sigma$

$$\left.\begin{aligned} {}_0^cD_t^\rho\, S(t) &= \mu - \lambda\, S(t) - \frac{\beta\, S(t)I(t)}{1+\alpha\, I(t)} \\ {}_0^cD_t^\rho I(t) &= \frac{\beta\, S(t)I(t)}{1+\alpha\, I(t)} - (\lambda+\delta+\sigma)I(t) - \frac{a\, I(t)}{1+b\left(I(t)\right)^2} \end{aligned}\right\} \tag{3.3}$$

For equilibrium points, setting right hand side of (3.3) to zero:

$$\left.\begin{aligned} \mu - \lambda\, S(t) - \frac{\beta\, S(t)I(t)}{1+\alpha\, I(t)} &= 0 \\ \frac{\beta\, S(t)I(t)}{1+\alpha\, I(t)} - (\lambda+\delta+\sigma)I(t) - \frac{a\, I(t)}{1+b\left(I(t)\right)^2} &= 0 \end{aligned}\right\} \tag{3.4}$$

3.4.2 Disease free equilibria (DFE):

There is no epidemic i.e., no infectives in the community ($I = 0$)

$$D^f = (S^f, I^f) = \left(\frac{\mu}{\lambda}, 0\right)$$

3.4.3 Endemic equilibria (EE):

$$\left.\begin{aligned} \mu - \lambda\, S^*(t) - \frac{\beta\, S^*(t)I^*(t)}{1+\alpha\, I^*(t)} &= 0 \\ \frac{\beta\, S(t)I(t)}{1+\alpha\, I(t)} - (\lambda+\delta+\sigma)I(t) - \frac{a\, I(t)}{1+b\left(I(t)\right)^2} &= 0 \end{aligned}\right\} \tag{3.5}$$

From equation (3.4) we obtain

$$S^* = \frac{\left(a+c+b\, c\, (I^*(t))^2\right)\left(1+\alpha\, I^*(t)\right)}{(1+b\, I^*(t)^2)\beta} \tag{3.6}$$

Now adding (3.3) and (3.4), and using (3.5) we get

$$J_0 + J_1 I^*(t) + J_2\left(I^*(t)\right)^2 + J_3\left(I^*(t)\right)^3 = 0 \tag{3.7}$$

Where these coefficients are given by:

$$\left.\begin{aligned} J_0 &= \mu\beta - \lambda(a+c) \\ J_1 &= -(a+c)(\alpha\lambda + \beta) \\ J_2 &= b(\mu\beta - \lambda c) \\ J_3 &= -b\,c\,(\alpha\lambda + \beta) \end{aligned}\right\} \tag{3.8}$$

3.4.4 Computation of Basic Reproduction Number

The Basic Reproduction number R_0 is determined using the next generation matrix method as discussed in (Diekmann et al., 2010; La Salle, 1976; Shuai & Van Den Driessche, 2013; Van Den Driessche & Watmough, 2002). We assume that

$$D_t^{\rho} x = P(x) - S(x)$$

Where $x = (S, I)^T$, $P(x)$ denotes the matrix of new infections arriving, and $S(x)$ denotes the matrix of people entering and exiting the compartments. $P(x)$ and $S(x)$ Jacobian matrices are calculated at the disease free equilibrium point D^f and are given by

$$P = \begin{pmatrix} \frac{\beta\mu}{\lambda} & 0 \\ 0 & 0 \end{pmatrix}$$

$$S = \begin{pmatrix} c+a & 0 \\ \frac{\beta\mu}{\lambda} & \lambda \end{pmatrix}$$

Now we need to compute PS^{-1} :

$$PS^{-1} = \begin{pmatrix} \frac{\beta\mu}{\lambda(c+a)} & 0 \\ 0 & 0 \end{pmatrix}$$

This matrix PS^{-1} is referred as next generation matrix and the spectral radius of the matrix PS^{-1} is equal to the basic reproduction number R_0. Thus, R_0 for our model is

$$R_0 = \frac{\beta\mu}{\lambda(c+a)}$$

3.4.5 Local stability analysis of DFE (D^f) and EEP (D^e)

We prove a theorem for the local stability of disease-free equilibrium point (DFE D^f**)**.

Theorem 3.2. When the Basic Reproduction number $R_0 < 1$, the model's disease-free equilibrium D^f is locally asymptotically stable, otherwise unstable.

Proof. We analyse the local stability behaviour of the disease free equilibrium point of the non-linear system (3.4) by linearizing the system around the DFE (D^f), as a result, at D^f, on linearizing the matrix of the system, we get

$$J^f = \begin{pmatrix} -\lambda & -\frac{\beta\mu}{\lambda} \\ 0 & (R_0 - 1)(c + a) \end{pmatrix} \tag{3.9}$$

The Jacobian matrix J^f has the following characteristic equation

$$d^2 - \big((R_0 - 1)(c + a) - \lambda\big)d - \lambda(R_0 - 1)(c + a) = 0 \tag{3.10}$$

$$\Rightarrow d^2 + r_1 d + r_2 = 0$$

where $r_1 = -\big((R_0 - 1)(c + a) - \lambda\big)$ and $r_2 = -\lambda(R_0 - 1)(c + a)$

First, we will prove that the roots (d_1 and d_2) of (3.10) are real.

$$d_1 = \frac{-r_1 + \sqrt{r_1^2 - 4\,r_2}}{2} \qquad and \qquad d_2 = \frac{-r_1 - \sqrt{r_1^2 - 4\,r_2}}{2}$$

$$r_1^2 - 4r_2 = (R_0 - 1)^2(c + a)^2 + \lambda^2 + 2\,\lambda(R_0 - 1)(c + a) \geq 0$$

Thus, both the roots d_1 and d_2 are real. We now show that both the roots are negative in nature when $R_0 < 1$.

Sum of the roots $d_1 + d_2 = -r_1 = (R_0 - 1)(c + a) - \lambda$

Product of the roots $d_1 d_2 = r_2 = -\lambda\,(R_0 - 1)(c + a)$

Thus $r_1 = -\big((R_0 - 1)(c + a) - \lambda\big) > 0$

and $r_2 = -\lambda\,(R_0 - 1)(\sigma + a) > 0$

Thus, when $R_0 < 1$, we concluded that every eigenvalue of the Jacobian matrix J^f have negative sign. Consequently, both the roots of the equation (3.10) have negative real parts, thus, by the fractional Routh-Hurwitz criteria (Matignon & Matignon, 1996; Otto & Day, 2019) all roots follow $|arg(d_i))| > \rho\frac{\pi}{2}$, $i = 1,2$

Theorem 3.3. $D^e=(S^*, I^*)$, the unique endemic-equilibrium point of the model (3.1) is locally asymptotically stable for the Basic Reproduction number R_0 >1, otherwise unstable.

Proof. Let R_0 >1, considering equation (3.7)
$J(I^*) = J_0 + J_1 I^*(t) + J_2\left(I^*(t)\right)^2 + J_3\left(I^*(t)\right)^3 = 0$ We observe that J_3, the leading coefficient, is negative. Therefore $\lim_{I^*\to\infty} J(I^*) \to -\infty$, also $J(0) = J_0$ and $J_0 > 0$ for R_0 >1, $J(I^*)$ is a continuous function of (I^*).

According to the fundamental theorem of algebra, $J(I^*)$ has no more than three real positive roots. Only case of specific endemic equilibrium is examined in this paper. Assuming R_0 >1 and considering that $J_3 < 0$ and $J_0 > 0$, a unique endemic equilibrium exists under the following J_1 and J_2 signs.:

(i) $J_1 < 0,\ J_2 < 0$
(ii) $J_1 > 0,\ J_2 < 0$
(iii) $J_1 > 0,\ J_2 > 0$

If any of the conditions (i)-(iii) is satisfied, then there exists a unique I^* from which the value of R can be calculated. For R_0 >1, a unique endemic equilibrium $D^e=(S^*, I^*)$ has been shown. This paper investigates the local stability of the endemic equilibrium $D^e = (S^*, I^*)$. Now, linearizing the model equations (3.4) about the endemic-equilibrium D^e, resulting in the Jacobian matrix J^*, as shown below.

$$J^e = \begin{pmatrix} -\lambda - \dfrac{\beta I^*}{(1+\alpha I^*)} & -\dfrac{\beta S^*}{(1+\alpha I^*)^2} \\ \dfrac{\beta I^*}{(1+\alpha I^*)} & \dfrac{\beta S^*}{(1+\alpha I^*)^2} - c - \dfrac{a(1-bI^{*2})}{(1+bI^{*2})^2} \end{pmatrix}$$

The characteristic equation of J^* is given by

$$s^2 + \nabla_1 s + \nabla_2 = 0 \tag{3.11}$$

where

$$\nabla_1 = \lambda + \frac{\beta I^*}{(1+\alpha I^*)} - \frac{\beta S^*}{(1+\alpha I^*)^2} + c + \frac{a(1-bI^{*2})}{(1+bI^{*2})^2}$$

$$\nabla_2 = \left(\lambda + \frac{\beta I^*}{(1+\alpha I^*)}\right)\left(c + \frac{a(1-bI^{*2})}{(1+bI^{*2})^2}\right) - \frac{\lambda\beta S^*}{(1+\alpha I^*)^2}$$

It is clear that the eigen value of Jacobian matrix J^*'s has negative real components if and only if $\nabla_1 > 0$ and $\nabla_2 > 0$. Also, $\nabla_1 > 0$ and $\nabla_2 > 0$ if $\left(\lambda + \frac{\beta I^*}{(1+\alpha I^*)}\right)\left(c + \frac{a(1-bI^{*2})}{(1+bI^{*2})^2}\right) < \frac{\lambda\beta S^*}{(1+\alpha I^*)^2}$. Hence, by fractional Routh-Hurwitz criteria all the roots of equation (3.9) have negative real parts and satisfy the condition $|arg(s_i))| > \rho\frac{\pi}{2}$, $i = 1,2$.

3.4.6 Global stability analysis of DFE (D^f) and EEP (D^e)

Theorem 3.4 The disease- free equilibrium D^f of model (3.3) is globally-asymptotically stable for $R_0 \leq 1$.

Proof. Defining a Lyapunov function as

$$F_1(t) = \left(S(t) - S^f(t) - S^f(t) ln\frac{S^f(t)}{S(t)}\right) + \left(I(t) - I^f(t) - I^f(t) ln\frac{I^f(t)}{I(t)}\right)$$

Differentiating $F_1(t)$ along with the solution of system (3.3) gives

$${}_0^cD_t^\rho F_1(t) = \left(1 - \frac{S^f(t)}{S(t)}\right){}_0^cD_t^\rho S(t) + \left(1 - \frac{I^f(t)}{I(t)}\right){}_0^cD_t^\rho I(t)$$

$${}_0^cD_t^\rho F_1(t) = \left(1 - \frac{S^f(t)}{S(t)}\right)\left(\mu - \lambda\, S(t) - \frac{\beta\, S(t)I(t)}{1+\alpha I(t)}\right) + \left(1 - \frac{I^f(t)}{I(t)}\right)\left(\frac{\beta\, S(t)I(t)}{1+\alpha I(t)} - c\, I(t) - \frac{a\, I(t)}{1 + b\left(I(t)\right)^2}\right)$$

Using the value of $R_0\, and\ S^f = \frac{\mu}{\lambda}$ in above equation, we have

$${}_0^cD_t^\rho F_1(t) \leq -\frac{\lambda(S(t)-S^f)^2}{S(t)} + \left(\frac{R_0(c+a)I(t)}{1+\alpha I(t)}\right) - c\, I(t) - \frac{a\, I(t)}{1 + b\left(I(t)\right)^2}$$

This draws the inference that if $R_0 < 1$, then we have ${}_0^cD_t^\rho F_1(t) \leq 0$. Furthermore, we know that ${}_0^cD_t^\rho F_1(t) = 0$, if and only if $S(t) = S^f(t)$ and $I(t) = I^f(t)$. Thus the largest invariant set for $\{(S,I) \in \psi: {}_0^cD_t^\rho F_1(t) = 0\}$ is the singleton set $\{D^f\}$, where $\psi = \left\{(S,I) \in R_+^2: 0 \leq S + I \leq \frac{\mu}{\lambda}, S, I \geq 0\right\}$ and also all the solutions in ψ converges to D^f in accordance with the LaSalle's invariance principle (Diekmann et al., 2010; La Salle, 1976; Shuai & Van Den Driessche, 2013; Van Den Driessche & Watmough, 2002). So, D^f is globally asymptotically stable for $R_0 \leq 1$.

Theorem 5. The endemic equilibrium D^e=(S^*, I^*) of model (3.3) is globally asymptotically stable for R_0 >1.

Proof. Let a Lyapunov function be defined as

$$F_2(t) = \left(S(t) - S^*(t) - S^*(t) ln \frac{S^*(t)}{S(t)}\right) + \left(I(t) - I^*(t) - I^*(t) ln \frac{I^*(t)}{I(t)}\right)$$

Differentiating $F_2(t)$ along with the solution of system (3.3)

$${}_0^cD_t^\rho F_2(t) = {}_0^cD_t^\rho \left(S(t) - S^*(t) - S^*(t) ln \frac{S^*(t)}{S(t)}\right) + {}_0^cD_t^\rho \left(I(t) - I^*(t) - I^*(t) ln \frac{I^*(t)}{I(t)}\right)$$

$${}_0^cD_t^\rho F_2(t) = \left(1 - \frac{S^*(t)}{S(t)}\right) {}_0^cD_t^\rho S(t) + \left(1 - \frac{I^*(t)}{I(t)}\right) {}_0^cD_t^\rho I(t)$$

$${}_0^cD_t^\rho F_2(t) = \left(1 - \frac{S^*(t)}{S(t)}\right)\left(\mu - \lambda\, S(t) - \frac{\beta\, S(t) I(t)}{1 + \alpha I(t)}\right) + \left(1 - \frac{I^*(t)}{I(t)}\right)\left(\frac{\beta\, S(t) I(t)}{1 + \alpha I(t)} - c\, I(t) - \frac{a\, I(t)}{1 + b\left(I(t)\right)^2}\right)$$

Using the Endemic Conditions:

$$\mu = \lambda\, S^*(t) - \frac{\beta\, S^*(t) I^*(t)}{1 + \alpha I^*(t)}$$

$$\frac{\beta\, S^*(t) I^*(t)}{1 + \alpha I^*(t)} = c\, I^*(t) - \frac{a\, I^*(t)}{1 + b\left(I^*(t)\right)^2}$$

$$
\begin{aligned}
{}_0^cD_t^\rho F_2(t) \leq & -\left(\frac{(S(t)-S^*(t))^2}{S(t)}\right)\left(\lambda+\frac{\beta\, I(t)}{1+\alpha I(t)}\right) \\
& -\left(\frac{(I(t)-I^*(t))^2}{I(t)}\right)\left(\frac{\beta\, S(t)I(t)}{1+\alpha I(t)}-c\, I(t)-\frac{a\, I(t)}{1+b\left(I(t)\right)^2}\right)
\end{aligned}
$$

Thus, ${}_0^cD_t^\rho F_2(t) \leq 0$. Therefore, ${}_0^cD_t^\rho F_2(t) \leq 0$. In addition, the largest invariant set for $\{(S,I) \in \psi: {}_0^cD_t^\rho F_2(t) = 0\}$ is the singleton set $\{D^e\}$ and all the solutions in ψ converges to D^e in accordance with the LaSalle's invariance principle. Therefore, Endemic equilibrium D^e is globally asymptotically stable for R_0 >1.

3.5 Numerical Simulations

In this section, using MATLAB 2012(b) and the predictor-corrector method (Diethelm et al., 2002), numerical simulations are presented for different fractional orders to observe the dynamical behavior of susceptibles, infectives, and recovered population.

The initial values of the subpopulations are S (0) = 85, R (0) = 0 and I (0) = 3. The set of tested values of parameters have been chosen from (A. Kumar & Nilam, 2019).

Table 3.1 Model parameters with their values

S.No.	Parameters	Value
1	β	0.004 per person- per day
2	λ	0.05 per day
3	μ	5 person- per day
4	α	0.002 per person- per day
5	a	0.2 per day
6	b	0.004 per person- per day
7	σ	0.002 per day
8	δ	0.001 per day

Figures 3.1 and 3.2 depicts the effect of memory about the social media's influence on mental health of susceptibles and infectives respectively. In figure 3.1,

for $\rho = 1.0$, after 50 days there is no change in number of susceptibles, it is because single search with no memory has less effect on mental health and therefore susceptibles decreases as memory decreases.

From figure 3.2, it is inferred that as the fractional order ρ decreases, i.e., memory about the disease increases in the society, number of infectives start reducing significantly. Incidence rate and treatment rate takes care of preventive measures to use social media and treatment of the people suffering from mental health problem majorly due to overuse of social media.

Figure 3.3 and 3.4 shows that as the limitation on available resources increases for fractional order ρ = 0.50 and ρ = 1.0 respectively, the number of infectives also increases, because due to limited resources, the treatment will not be available to all infected individuals resulting in an increment in the population of infectives. The difference in the infected population is significantly large between b = 0.002 and b = 0.004 in both the figures. It illustrates the situation of availability of ample resources for the infected population.

Figures 3.5, 3.6 and 3.7 shows the effect of varying cure rates on infectives with various fractional orders ρ = 0.60, 0.80 and 1.0 respectively. It has been noted that the number of infectives reduces remarkably on increasing the cure rates. Also, on comparing these figures it can be stated that as the memory about the disease in the society increases, number of infectives also starts decreases with time.

Figures 3.8, 3.9 and 3.10 presents the effect of varying inhibition rate due to infection on infected people with ρ = 1, 0.80 and 0.60 respectively. This has been observed that more the inhibitory procedures taken by infected individuals, lower will be the number of infective populations. Also, if fractional order decreases, then number of infectives starts decreasing.

The phase portraits depict that all the trajectories beginning from different starting points are converging to its equilibrium point as shown in figures 3.11 and 3.12 for fractional order ρ = 0.90 and ρ = 0.70 respectively.

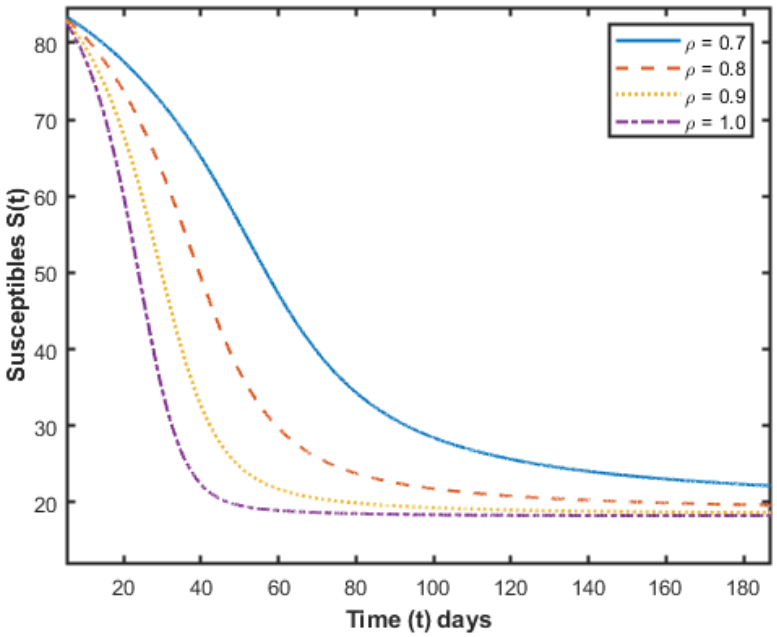

Figure 3.1 Effect of memory on susceptibles

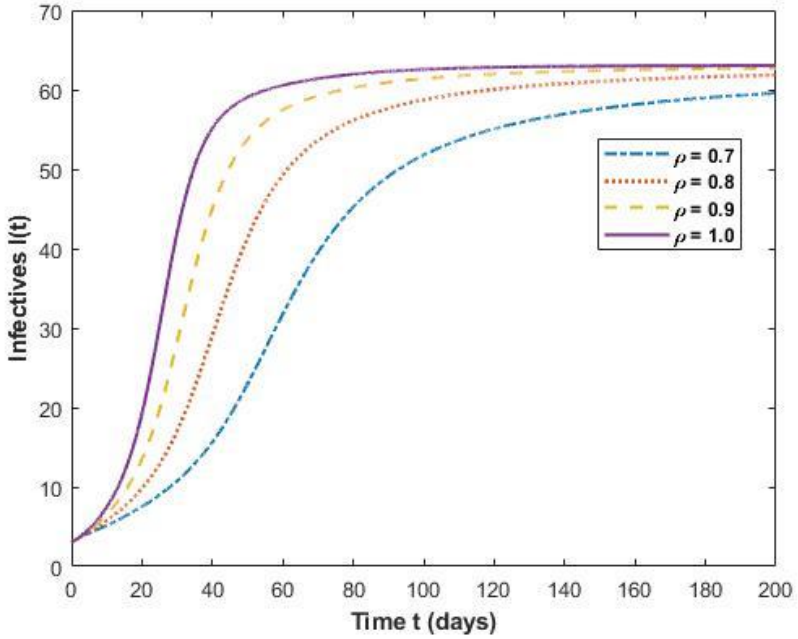

Figure 3.2 Effect of memory on infectives

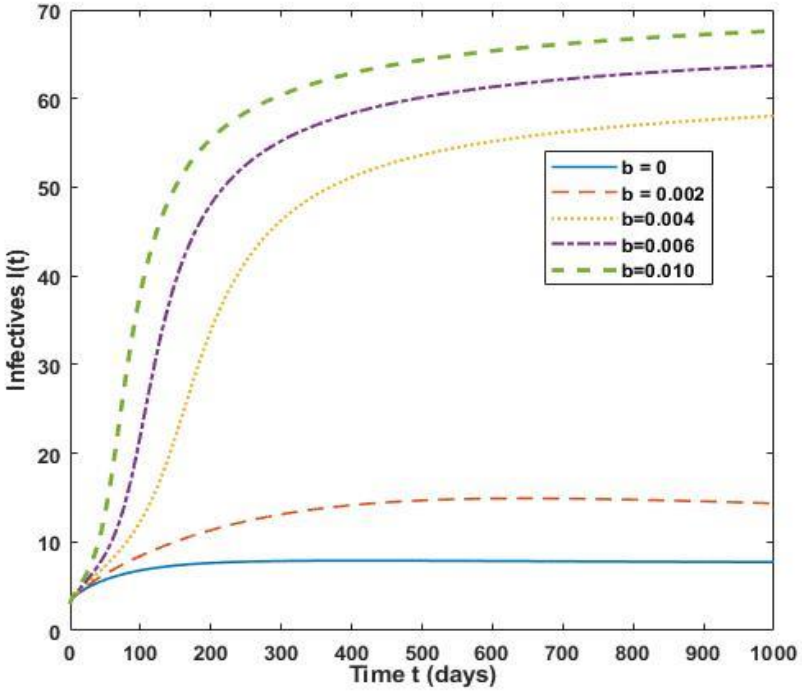

Figure 3.3 Effect of limitation in treatment availability on infectives for fractional order $\rho = 0.50$

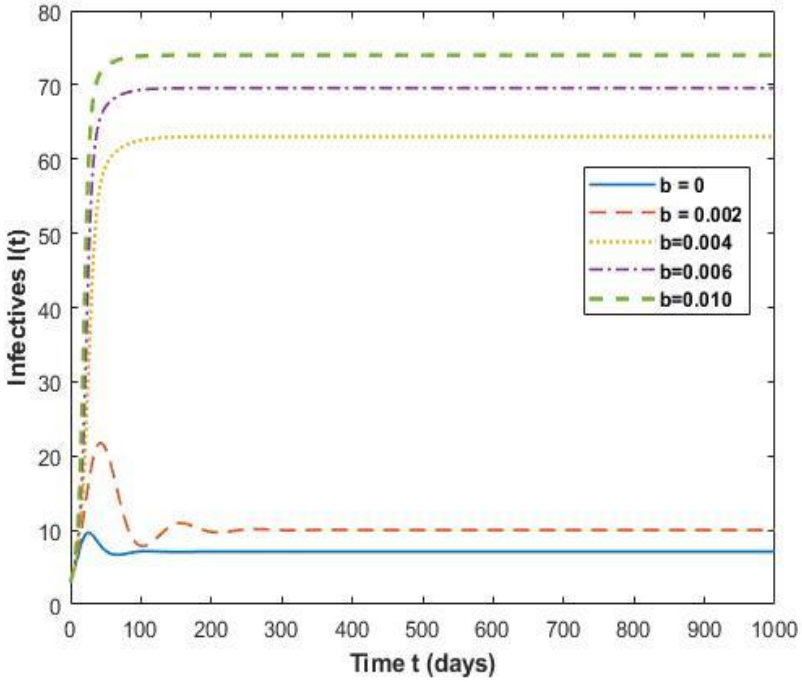

Figure 3.4 Effect of limitation in treatment availability on infectives for fractional order $\rho = 1.0$

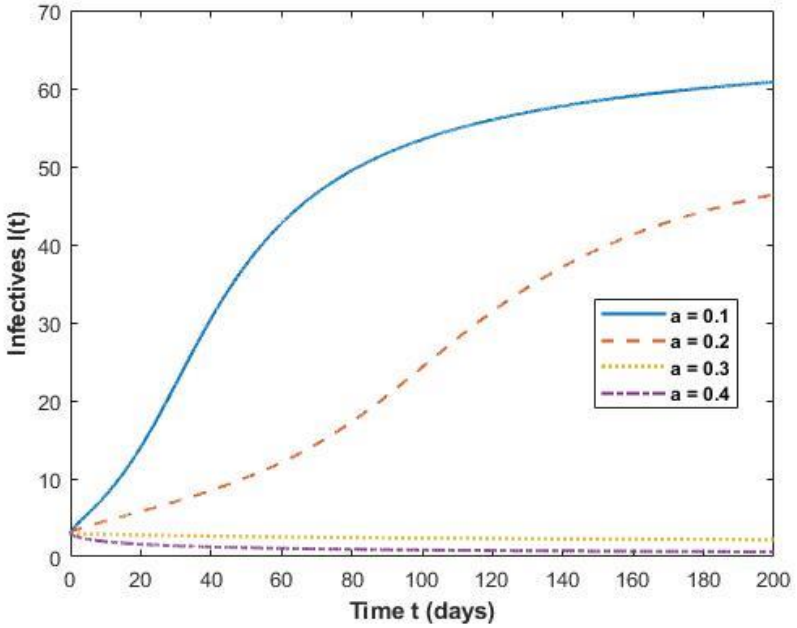

Figure 3.5 Effect of varying cure rates on infectives for $\rho = 0.60$

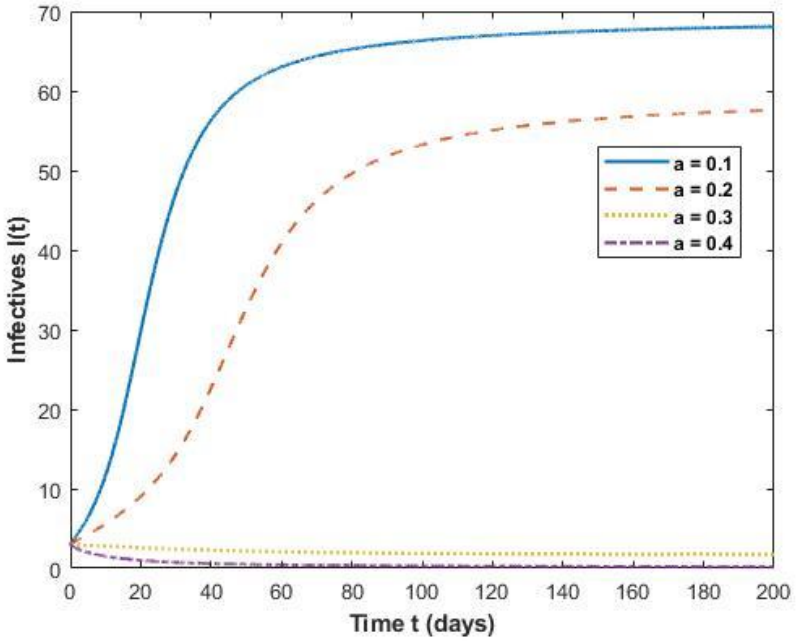

Figure 3.6 Effect of varying cure rates on infectives for $\rho = 0.80$

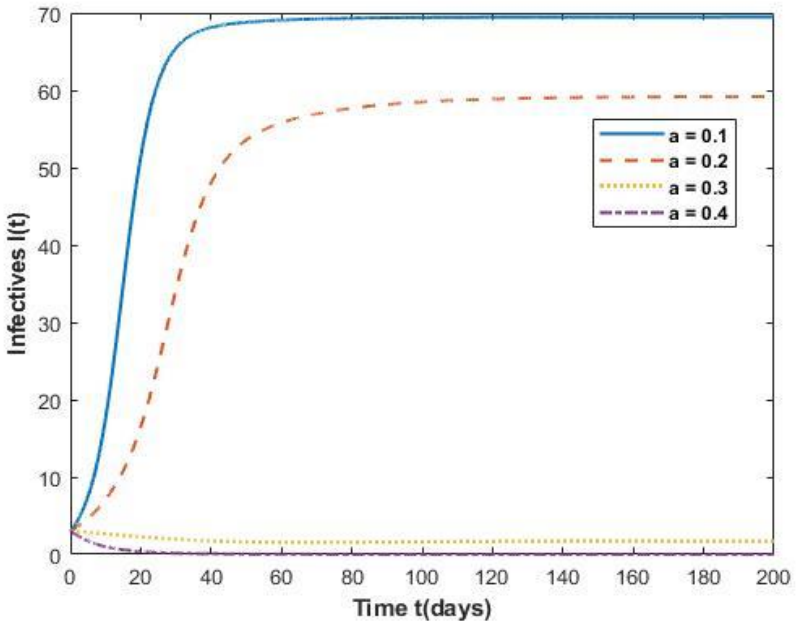

Figure 3.7 Effect of varying cure rates on infectives for $\rho = 1$

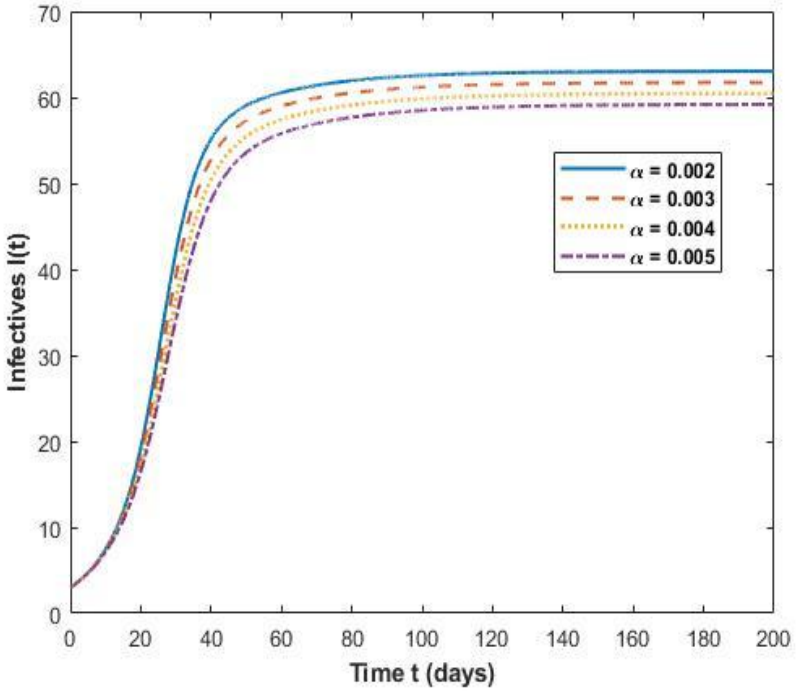

Figure 3.8 Effect of varying inhibition rate due to infection on infectives for $\rho = 1$

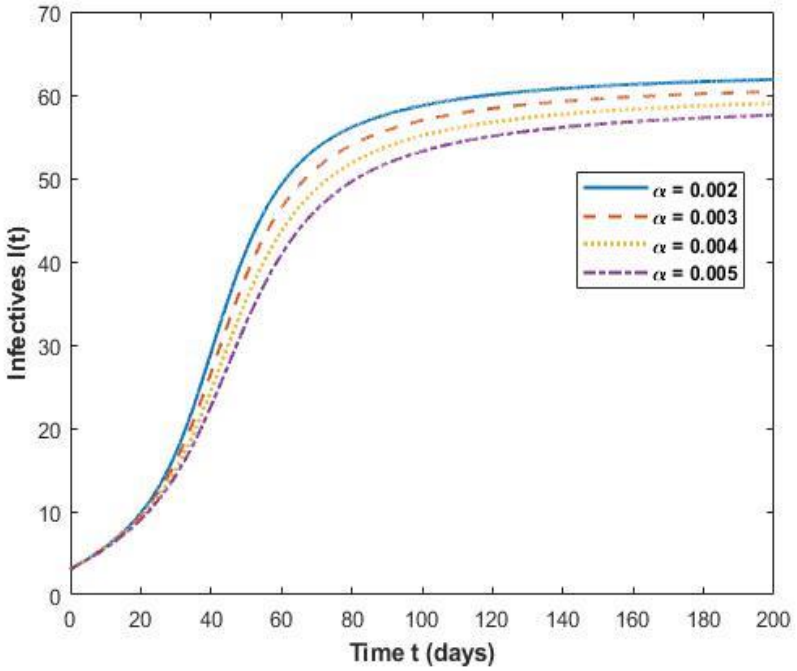

Figure 3.9 Effect of varying inhibition rate due to infection on infectives for $\rho = 0.80$

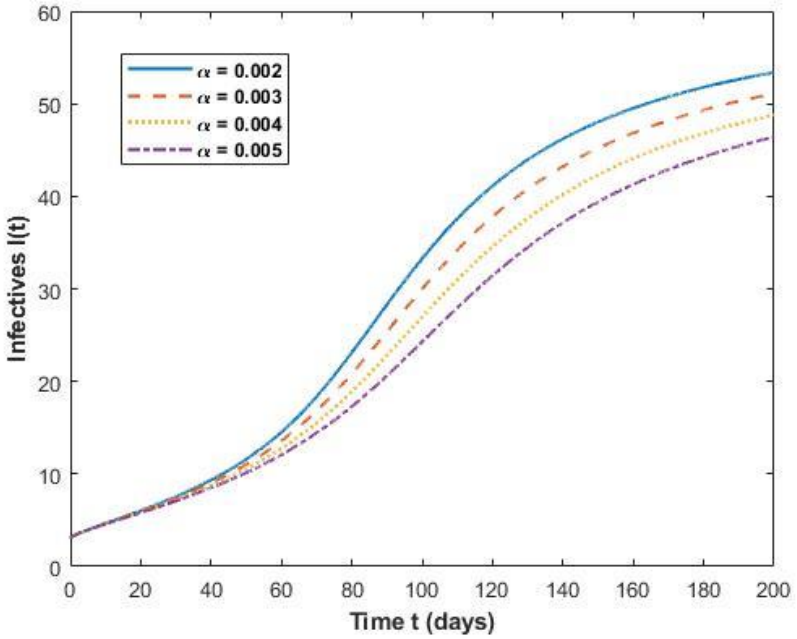

Figure 3.10 Effect of varying inhibition rate due to infection on infectives for $\rho = 0.60$

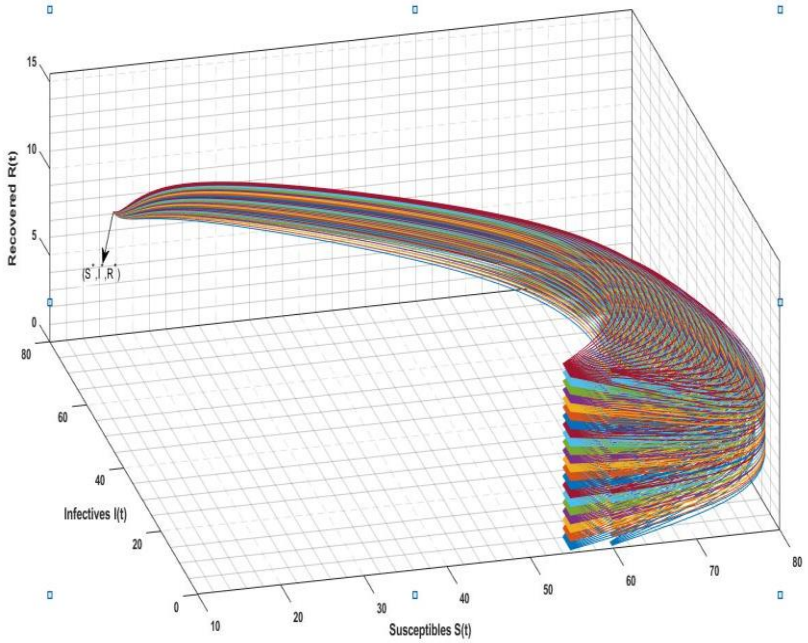

Figure 3.11 Phase portrait of the system for fractional order $\rho = 0.90$

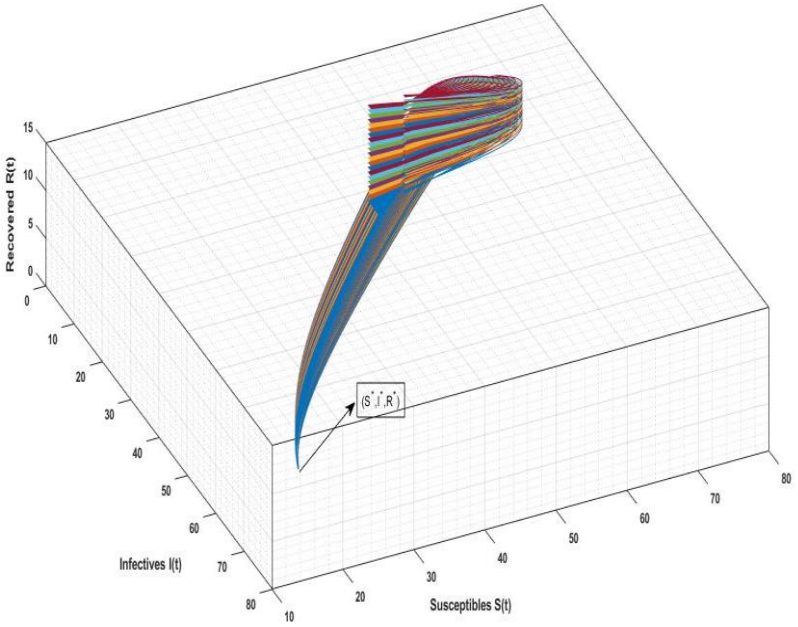

Figure 3.12 Phase portrait of the system for fractional order $\rho = 0.70$

3.6 Conclusion

A fractional order model has been presented and examined here aiming to include the effect of social media on mental health due to corona using Caputo-fractional order derivative, by taking Holling type- II functional as incidence rate and Monod-Haldane functional as treatment rate. For the basic reproduction number R_0 less than one, the disease-free equilibrium point is locally asymptotically stable, but when R_0 is more than one, it is unstable. The presence of a unique positive endemic-equilibrium is also established, and the stability of endemic equilibrium point is examined. When R_0 is more than one and the condition specified in theorem-3 holds, the endemic-equilibrium point is found to be locally asymptotically stable. Also, for some conditions, the global stability behaviour of both disease-free equilibrium and endemic equilibrium is explored, and it is established that DFE is globally asymptotically stable for $R_0 \leq 1$ and EE is globally asymptotically stable if $R_0 > 1$, as demonstrated in theorems 3.4 and 3.5.

We can see through simulation that as the fractional order reduces or the memory rises, the population of susceptible increases because, in the case of having a memory from social media use, individuals explore and respond for it, resulting in an increase in the number of susceptible. On reducing the fractional order, number of infectives decreases. Also, number of infectives decreases by optimum and control use of social media in case of any situation like COVID-19 where the possibility of panic is very high. From this work we suggest that as the infected individuals take more precautions such as switching to traditional media use, reducing online time, practicing yoga, exercise and meditation, appropriate use of social media etc, number of infectives decreases.

CHAPTER 4

CAPUTO FRACTIONAL DERIVATIVE MODEL FOR IMPACT OF AWARENESS ON INFECTIOUS DISEASE

During times of crisis, mass-media coverage is amongst the most widely used government strategies to influence public opinion. The use of awareness campaigns during epidemics and pandemics is a very effective method of promoting healthy behavioral practices among individuals. An important tool in analyzing the effects of media awareness on infectious disease spread is mathematical modeling. This chapter examines an infectious disease non integer SIR-type mathematical model that considers the behavioural changes in people spurred on by the concurrent spread of public awareness. The behavior of a human population in response to an outbreak of disease can alter the spread of the disease. Therefore, a nonlinear, non-integer model has been formulated here by considering Caputo derivative, Holling type III treatment rate and Monod-Haldane incidence rate. Solutions with positive initial values are tested for nonnegativity and boundedness, indicating that the model is well-posed. To compute the basic reproduction number R_0, the next generation matrix approach is used. A local stability analysis has been performed after determining the existence and stability of disease free and endemic equilibrium points using Routh Hurwitz's criteria. Based on Lyapunov-stability LaSalle's theorem, the global stability analysis of both the equilibrium points is examined by building appropriate Lyapunov functions. To demonstrate consistency with the theoretical analysis, numerical simulations have been conducted. It has been observed that the stability of the equilibrium points is not affected by the long-term memory. However, when the fractional derivative order parameter is increased each solution attains equilibrium more rapidly. Further, it has been discovered that increasing media awareness decreases the number of infected individuals and consequently reduces the peak of the epidemic.

4.1 Introduction

An epidemic outbreak is typically spread by a transmissible infection, which can be spread from animal to human, animal to animal, or person to person, or direct contact with potentially infected environments (van Seventer & Hochberg, 2016). Several large-scale epidemic outbreaks such as Ebola, SARS, Zika virus, and swine flu have affected the socioeconomic status of the population and inadequate healthcare access over the last two decades (Fauci & Morens, 2012). Information about these outbreaks is disseminated swiftly because of globalized travel and significant advancements in social media, which can have a considerable impact on the dynamics of the epidemic itself (Jones & Salathé, 2009; Pruyt et al., 2015). It is important for every individual to be aware about the identification of such diseases and the preventive measures to be followed. Awareness is the understanding of an issue or problem, recognizing that it exists and knowing what actions are necessary in response. The more aware we are about the dynamics of a disease, the better equipped we are to prevent it from spreading up to certain extent. It is important for people to be aware of their surroundings and recognize when someone might have an illness that could potentially be contagious. It is indeed interesting to note that raising awareness can impact the dynamics of disease propagation in extremely intricate and perhaps surprising ways. The awareness about infectious diseases can be carried out in many ways like by public education campaigns, media coverage, social media posts etc. Traditional models of infectious illnesses consider the interactions between susceptibles and infectives. The transmission of infectious diseases is nevertheless also influenced by other factors, like media exposure, immunization, people's mobility, awareness programs, etc. In particular, the awareness programs have a significant impact on how people respond to diseases and how the government intervenes in wellness programs to stop the spread of such diseases. By educating the public about the disease and the steps that may be taken to lessen their risk of getting infected with it, such as wearing protective masks, getting vaccinated etc, the awareness programs have been essential in the spread of the disease. Consequently, the impact of the awareness programs must be considered during the modelling process in order to anticipate the effects of infectious disease. The disease transmission may be minimized by a variety of disease control techniques, such as the use of face masks, sanitizers, or other equipment designed to prevent the spread of a particular disease along with immunizations and even quarantine have a significantly positive impact.

In the presence of awareness, behavioral changes in the population become more complicated, and this behavior have influences on disease dynamics. To examine how knowledge and awareness affect epidemic spread, several mathematical models have been proposed (Al-Dmour et al., 2020; Funk et al., 2009; Goel et al., 2020; A. Kumar et al., 2019; Manzoni et al., 2021; Misra et al., 2011; Naik, 2020). A statistical analysis of AIDS awareness campaigns reveals that raising public awareness can significantly contribute to reducing the AIDS epidemic (Misra et al., 2011). There have been some compartmental models created with the presumption that the media will decrease the possibility of interaction between susceptibles with infectives (J. Cui et

al., 2008; J. A. Cui et al., 2008; Y. Liu & Cui, 2012). Recently, however, many researchers have applied fractional extensions to mathematical models to study the dynamics of epidemics (Akdim et al., 2022; Mandal et al., 2020; Naik, 2020; Rostamy & Mottaghi, 2016) because biological systems involve dynamical processes with memory effects, which can be captured properly by fractional-order differential equations. A decline in infections or diseases may be observed during epidemics because of population experiences and memory effects, which can't be modeled by natural derivatives alone. Because of this, fractional models are more accurate than models based on ordinary differential equations. Numerous fractional SIR-type models involving the Caputo fractional derivative have been developed and studied in recent years (Naik, 2020; Swati & Nilam, 2022). In their study, the authors found that memory effects influence the dynamics of epidemics, which is governed by the order of fractional derivatives. Recent research has explored the dynamics of the COVID-19 pandemic using fractional-order mathematical models (Boudaoui et al. 2021; Kozioł, Stanisławski, and Bialic 2020; Yadav et al. 2021). To slow down the spread of an epidemic, public health departments have used awareness campaigns as their most reliable non-pharmaceutical method. The media has shown a significant amount of interest in the present COVID-19 pandemic problem as a way of health education through the spread of awareness programmes and preventive actions. Health awareness programmes have had a significant impact on how individuals behave, which has helped to reduce the severity of the infection (Musa et al. 2021).

In this chapter, we focus on the question of how much awareness through various media and information campaigns is enough to control the disease significantly from the society using a non-integer model with Caputo derivative, Monod-Haldane incidence rate and Holling type III treatment rate. Choosing Monod-Haldane incidence rate is a rational choice as it takes into consideration psychological effects of behavioral changes in susceptible individuals, whereas Holling type III treatment rate is based on a known disease that has resurfaced and has treatment options available. As infectives increase, removal rates initially grow very fast, slowly grow till they finally settle down to maximum saturated levels. The Caputo derivative is a generalization of the Taylor series, and it is used to model various phenomena in physics, engineering, and economics which has been found to be more accurate than other types of derivatives. This is because it does not have any singularity points and has memory property, which makes it easier for it to accurately simulate the spread of an epidemic.

Awareness Strategy

In this work, to introduce the concept of awareness for reducing the infected population, we have considered the fractional order σ as σ =1- u, where u is the percentage awareness in the entire population. Also, we have supposed that u less than 20% means there is hardly any awareness in the society and u greater than 80% means

that almost population has awareness about the disease. Higher the value of u, more the memory of the past things and people will be more alert for the upcoming incidents.

4.2 Formulation of Fractional order Mathematical Model

The first step in modeling an epidemic with a fractional-order differential equation (FODE) is to create a differential equation that represents the population in each state. The most important equation in the fractional order model is the Susceptible-Infective-Recovered (SIR) equation, which describes how an infection spreads through a population. Population $N(t)$ can be divided into three types - susceptible $S(t)$, infectious $I(t)$and recovered $R(t)$. Our assumption is that recovered individuals cannot become infected again, nor can they infect the susceptible population again. The Caputo derivative is described in definition 1in Appendix. This assumption led to a Caputo-fractional order SIR model expressed as the following non-linear differential equations:

$$\left.\begin{aligned} {}_0^cD_t^{\sigma}\, S(t) &= \theta - \varphi\, S(t) - \frac{\beta\, S(t)I(t)}{1+\gamma\left(I(t)\right)^2} \\ {}_0^cD_t^{\sigma}\, I(t) &= \frac{\beta\, S(t)I(t)}{1+\gamma\left(I(t)\right)^2} - (\varphi+\alpha+\delta)I(t) - \frac{\mu\left(I(t)\right)^2}{1+\rho\left(I(t)\right)^2} \\ {}_0^cD_t^{\sigma}\, R(t) &= \frac{\mu\left(I(t)\right)^2}{1+\rho\left(I(t)\right)^2} - \varphi R(t) + \alpha I(t) \end{aligned}\right\} \tag{4.1}$$

with non-negative initial conditions: $S(0) = S_0 \geq 0, I(0) = I_0 \geq 0$ and $R(0) = R_0 \geq 0$, where the different model parameters are defined below:

Table 4.1 The parameters and their Illustrations

The Parameter	Illustration	Unit
β	Transmission coefficient between susceptibles S and infected persons I	per person - per day
φ	The rate of natural mortality for each class of people	per day
θ	Immigrant's constant recruitment rate	person - per day
δ	Death rate from infection among infected individuals	per day
α	Infection recovery rate	per day
γ	Inhibition by infected individuals	per person - per day

μ	Disease cure rate	per day
ρ	The rate at which access to treatment is limited	per person - per day

4.3 Basic Properties of the Model

Let $\mathbb{R}^3_+ := \{X \epsilon \mathbb{R}^3 : X \geq 0\}$ and $X(t) = \big(S(t), I(t), R(t)\big)^T$ on non-negative solutions, the lemmas needed to prove the theorem are mentioned in Appendix.

Theorem 4.1. For the fractional differential equation represented by system (4.2) for $t \geq 0$, there is only one non-negative solution that exists, and that solution will remain in the region $M = \left\{(S, I, R) \in R^3_+ : 0 < S + I + R \leq \overline{D}\ , \overline{D}\ \geq C_E \frac{\mu}{\lambda}\right\}$ for $t \geq 0$.

Proof. We first verify that all the model (4.1) solutions under its initial conditions are positive. Considering $S(0) > 0$ for $t = 0$. For all $t \geq 0$ we demonstrate that $S(t) \geq 0$. This will be established by contradiction, let $S(t) \leq 0$ for each $t \geq 0$. Consequently, there is a $\vartheta_1 > 0$ such that $S(t) > 0$ for that $0 \leq t < \vartheta_1$, $S(t) = 0$ at $t = \vartheta_1$, and $S(t) < 0$ for $\vartheta_1 < t < \vartheta_1 + \varepsilon_1$ with sufficiently small $\varepsilon_1 > 0$. Taking the model's (4.1) first, We achieve ${}_0^c D^\rho\ S(t)|_{t=\vartheta_1} = \mu > 0$. From Lemma 2, for any $0 < \varepsilon_1 \ll 1$, we have $S(\vartheta_1 + \varepsilon_1) = S(\vartheta_1) + \frac{1}{\Gamma(\alpha)} D^\rho S(\xi)\ (\varepsilon_1)^\rho$. Thus, we get $S(\vartheta_1 + \varepsilon_1) \geq 0$, which is in contradiction to the fact that $S(t) < 0$ for $\vartheta_1 < t < \vartheta_1 + \varepsilon_1$. As a result, we obtain $S(t) \geq 0$ for all $t \geq 0$.

Thereafter, we demonstrate that $I(t) \geq 0$ for every $t \geq 0$. We accomplish it once more through contradiction. Assuming, $I(t) \geq 0$ is not true, then there exists a $\vartheta_2 > 0$ such that $I(t) > 0$ for that $0 \leq t < \vartheta_2$, $I(t) = 0$ at $t = \vartheta_2$, and $I(t) < 0$ for $\vartheta_2 < t < \vartheta_2 + \varepsilon_2$ with sufficiently small $\varepsilon_2 > 0$. Then we obtain

$$ {}_0^c D^\rho\ I(t)|_{t=\vartheta_2} = 0. $$

From Lemma 2, for any $0 < \varepsilon_2 \ll 1$, we have $I(\vartheta_2 + \varepsilon_2) = I(\vartheta_2) + \frac{1}{\Gamma(\alpha)} D^\rho I(\xi)\ (\varepsilon_2)^\rho$. Thus, we get $I(\vartheta_2 + \varepsilon_2) \geq 0$, which is in contradiction to the fact that $I(t) < 0$ for $\vartheta_2 < t < \vartheta_2 + \varepsilon_2$. Hence, we have $I(t) \geq 0$ for all $t \geq 0$. In a similar manner, we can demonstrate that $R(t) \geq 0$ for any $t \geq 0$.

As a result, it can be said that all of model (4.1)'s solutions under the initial conditions are positive. We now demonstrate the solutions' boundness. When all the model's (4.1) equations are added together, we get:

$$D_t^{\rho} N = \theta - \varphi\, N - \delta I$$

Where

$$N = S + I + R.$$

As $I(t) \geq 0$, we have

$$D_t^{\rho} N \leq \theta - \varphi\, N$$

Now consider the initial value problem

$$D_t^{\rho} \bar{N} = \theta - \varphi\, N, \bar{N}(0) = \bar{N}_0.$$

Using comparison principle (Lu and Zhu 2018), we obtain the following inequality:

$$N(t) \leq \bar{N}(t) \text{ for all } t \geq 0.$$

Implementing the Laplace transform to the initial value problem, we now get the following:

$$s^{\rho} L[\bar{N}(t)] - s^{\rho-1}\bar{N}_0 = \frac{\theta^{\rho}}{s} - \varphi L[\bar{N}(t)]$$

$$\Rightarrow L[\bar{N}(t)] = \frac{s^{\rho-1}\bar{N}_0}{s^{\rho} + \varphi} + \frac{\theta^{\rho} s^{-1}}{s^{\rho} + \varphi}$$

Using Lemma 3, we obtain

$$L\left[E_{\rho,1}(-\varphi t^{\rho})\right] = \frac{s^{\rho-1}}{s^{\rho} + \varphi}$$

$$L\left[t^{\rho} E_{\rho,\rho+1}(-\varphi t^{\rho})\right] = \frac{s^{-1}}{s^{\rho} + \varphi}$$

When we use the inverse Laplace transform on the two equations above, we get

$$\bar{N}(t) = \bar{N}_0 E_{\rho,1}(-\varphi t^{\rho}) + \theta t^{\rho} E_{\rho,\rho+1}(-\varphi t^{\rho})$$

using $D_t^{\rho} N \leq \theta - \varphi N$ we have

$$N(t) \leq N_0 E_{\rho,1}(-\varphi t^{\rho}) + \theta t^{\rho} E_{\rho,\rho+1}(-\varphi t^{\rho})$$

By Lemma 4, we obtain

$$|N(t)| \leq \frac{N_0 C_E}{1+\varphi t^{\rho}} + \frac{\theta t^{\rho} C_E}{1+\varphi t^{\rho}}$$

Where C_E is constant given in Lemma 4. Hence, as $t \to \infty$, we have $N(t) \leq \overline{D}$ with $\overline{D} \geq C_E \frac{\theta}{\varphi}$. The solutions are therefore bounded and will remain in domain M for $t \geq 0$.. As a result, Theorem 4.1 is established, and $\mathbb{R}_+^3$ still holds the solutions.

4.4 Mathematical analysis of the model

This section begins by identifying disease-free equilibrium and endemic equilibrium, and then observes stability results for both equilibrium types. A next-generation matrix is then used to determine the Basic Reproduction number, which involves persistence and eradication of the disease. Lastly, we discussed the existence and stability of equilibrium points as well as their local stability.

4.4.1 Equilibria and their stability

In the non-linear model above, the first two equations are independent of the third equation, therefore stability is only determined by the first two. The model is therefore reduced to:

$$\left.\begin{aligned} {}_0^c D_t^{\sigma} S(t) &= \theta - \varphi S(t) - \frac{\beta S(t) I(t)}{1+\gamma\left(I(t)\right)^2} \\ {}_0^c D_t^{\sigma} I(t) &= \frac{\beta S(t) I(t)}{1+\gamma\left(I(t)\right)^2} - (\varphi + \alpha + \delta) I(t) - \frac{\mu\left(I(t)\right)^2}{1+\rho\left(I(t)\right)^2} \end{aligned}\right\} \tag{4.2}$$

To find the equilibrium points, set the right side of the system (4.2) to zero, we get

$$\left.\begin{aligned} \theta - \varphi S(t) - \frac{\beta S(t) I(t)}{1+\gamma\left(I(t)\right)^2} &= 0 \\ \frac{\beta S(t) I(t)}{1+\gamma\left(I(t)\right)^2} - (\varphi + \alpha + \delta) I(t) - \frac{\mu\left(I(t)\right)^2}{1+\rho\left(I(t)\right)^2} &= 0 \end{aligned}\right\} \tag{4.3}$$

As a result of solving the above system, we obtain the two equilibrium points, disease free equilibrium point (DFE) and endemic equilibrium point (EEP), which are specified as follows:

(i) DFE: $B^0 = (S^0, I^0) = \left(\frac{\theta}{\varphi}, 0\right)$. There is no illness in the environment, and all people are only susceptible.

(ii) EEP: $B^* = (S^*, I^*)$. A description of this can be found in the following sections.

Now, to obtain the behaviour of stability of these two equilibria, basic reproduction number R_0 is required to be computed (Van Den Driessche and Watmough 2002).

4.4.2 Determination of Basic Reproduction Number

Next generation matrix method calculates the basic reproduction number as follows:

$$D_t^{\alpha} x = R(x) - S(x)$$

Where $x = (S, I)^T$, matrix $R(x)$ represents the matrix of new infections coming in, while matrix $S(x)$ represents the transfer of individuals leaving and entering compartments. A Jacobian matrix of $R(x)$ and $S(x)$ is evaluated at disease free equilibrium point and is expressed as follows:

$$R = \begin{pmatrix} \frac{\beta\theta}{\varphi} & 0 \\ 0 & 0 \end{pmatrix}$$

$$S = \begin{pmatrix} \varphi + \delta + \alpha & 0 \\ \frac{\beta\theta}{\varphi} & \varphi \end{pmatrix}$$

Now we need to compute the inverse of R and then RS^{-1} given by

$$RS^{-1} = \begin{pmatrix} \frac{\beta\theta}{\varphi(\varphi + \delta + \alpha)} & 0 \\ 0 & 0 \end{pmatrix}$$

This matrix RS^{-1} is known as next generation matrix and the spectral radius of this matrix is the basic reproduction number R_0 for our model is

$$R_0 = \rho(RS^{-1}) = \frac{\beta\theta}{\varphi(\varphi + \delta + \alpha)}$$

4.4.3 Analysis of local stability behavior

A study of local stability behavior of both DFE and EEP is presented in this section.

4.4.3.1 Local stability analysis of DFE (B^0)

We are now interested in finding out if the disease-free equilibrium point. Is stable locally (DFE B^0**)**. We claim the following theorem for this:

Theorem 4.2 $B^0 = (S^0, I^0) = \left(\frac{\theta}{\varphi}, 0\right)$, the disease- free equilibrium of model (4.2) is locally asymptotically stable when the Basic Reproduction number $R_0 < 1$ and unstable otherwise.

Proof. By linearizing the system around the disease-free equilibrium point DFE (B^0) of the non-linear system (4.3), we can calculate its local stability behavior. We have thus obtained the linearized matrix of the system shown below

$$J^0 = \begin{pmatrix} -\varphi & -\frac{\beta\theta}{\varphi} \\ 0 & (R_0 - 1)(\varphi + \delta + \alpha) \end{pmatrix} \tag{4.4}$$

Therefore, we have seen that one eigenvalue is negative i.e., $-\varphi$, at disease-free equilibrium B^0 and the other eigen value is $(R_0 - 1)(\varphi + \delta + \alpha)$ is negative if $R_0 < 1$. Therefore, by the Routh-Hurwitz stability conditions for fractional order systems (Matignon 1996) describes that the necessary and sufficient condition $\left|\arg\left(eig(J^0)\right)\right| > \sigma\frac{\pi}{2}$ for various fractional order models. The eigenvalues of both equations meet the above condition. Hence, as long as R_0 is less than one, the disease-free equilibrium in the system (4.1) is locally asymptotically stable.

4.4.3.2 EEP (B^*) existence and study of local equilibrium

This section discusses the conditions for endemic equilibrium $B^* = (S^*, I^*)$ to form and the local stability behavior of the equilibrium.

$$\left.\begin{array}{c} \theta - \varphi\, S^*(t) - \frac{\beta\, S^*(t)I^*(t)}{1+\gamma\left(I^*(t)\right)^2} = 0 \\ \frac{\beta\, S^*(t)I^*(t)}{1+\gamma\left(I^*(t)\right)^2} - (\varphi+\alpha+\delta)I^*(t) - \frac{\mu\left(I^*(t)\right)^2}{1+\rho\left(I^*(t)\right)^2} = 0 \end{array}\right\} \tag{4.5}$$

After solving the equations (4.5) we obtain:

$$S^* = \frac{\left((\varphi+\alpha+\delta)\left(1+\rho\left(I^*(t)\right)^2\right)+\mu I^*(t)\right)\left(1+\gamma\left(I^*(t)\right)^2\right)}{\beta\left(1+\rho\left(I^*(t)\right)^2\right)}$$

and I^* is the root of the following equation:

$$a_5 + a_4 I^*(t) + a_3\left(I^*(t)\right)^2 + a_2\left(I^*(t)\right)^3 + a_1\left(I^*(t)\right)^4 = 0 \tag{4.6}$$

where the coefficients $a_5,\ a_4\ , a_3,\ a_2$ and a_1 are given by

$$\left.\begin{array}{c} a_5 = \theta\beta - \varphi(\varphi+\alpha+\delta) = (R_0-1)\varphi(\varphi+\alpha+\delta) \\ a_4 = -\beta(\varphi+\alpha+\delta) - \varphi\mu \\ a_3 = \theta\beta\rho - \mu\beta - \varphi\rho(\varphi+\alpha+\delta) - \varphi\gamma(\varphi+\alpha+\delta) \\ a_2 = -\mu\varphi\gamma - \beta\rho(\varphi+\alpha+\delta) \\ a_1 = -\varphi\rho\gamma(\varphi+\alpha+\delta) \end{array}\right\} \tag{4.7}$$

Theorem 4.3. For R_0 >1 and under the condition that $\theta\rho < \mu$ there exist a unique endemic equilibrium $B^* = (S^*, I^*)$ of model (4.2).

Proof. Let R_0 >1, In equation (4.7), we have a fourth-degree polynomial given as $H\left(I^*(t)\right) = a_5 + a_4 I^*(t) + a_3\left(I^*(t)\right)^2 + a_2\left(I^*(t)\right)^3 + a_1\left(I^*(t)\right)^4$. It is noted that a_1, the leading coefficient of $\left(I^*(t)\right)^4$, is negative.Therefore $\lim_{I^*\to\infty} H(I^*) = -\infty$, also $H(0) = a_5$ and $a_5 > 0$ for R_0 >1, $H(I^*)$ is a continuous function of I^*.

Thus, the fundamental theorem of algebra implies that there exists a unique endemic equilibrium point under the condition that R_0 >1 and for $\theta\rho < \mu$. Thus, there exist a unique $I^*(t)$, from which we can find the value of $S^*(t)$. So, unique endemic equilibrium $B^* = (S^*, I^*)$ has been demonstrated for R_0 >1. Here, we examine local stability of endemic equilibrium $B^* = (S^*, I^*)$. As shown below, by linearizing the model (4.3) around equilibrium, we obtain the Jacobian matrix.

$$J^* = \begin{pmatrix} -\varphi - \dfrac{\beta I^*(t)}{1+\gamma\left(I^*(t)\right)^2} & -\dfrac{\beta S^*(t)\left(1-\gamma\left(I^*(t)\right)^2\right)}{\left(1+\gamma\left(I^*(t)\right)^2\right)^2} \\ \dfrac{\beta I^*(t)}{1+\gamma\left(I^*(t)\right)^2} & \dfrac{\beta S^*(t)\left(1-\gamma\left(I^*(t)\right)^2\right)}{\left(1+\gamma\left(I^*(t)\right)^2\right)^2} - (\varphi+\alpha+\delta) - \dfrac{2\mu I^*(t)}{\left(1+\rho\left(I^*(t)\right)^2\right)^2} \end{pmatrix}$$

The characteristic equation of J^* is given by

$$l^2 + \tau_1 l + \tau_2 = 0 \tag{4.8}$$

Where

$$\tau_1 = \varphi + \frac{\beta I^*(t)}{1+\gamma\left(I^*(t)\right)^2} - \frac{\beta S^*(t)\left(1-\gamma\left(I^*(t)\right)^2\right)}{\left(1+\gamma\left(I^*(t)\right)^2\right)^2} + (\varphi+\alpha+\delta) + \frac{2\mu I^*(t)}{\left(1+\rho\left(I^*(t)\right)^2\right)^2}$$

$$\tau_2 = \varphi + \frac{\beta I^*(t)}{1+\gamma\left(I^*(t)\right)^2}\left((\varphi+\alpha+\delta) + \frac{2\mu I^*(t)}{\left(1+\rho\left(I^*(t)\right)^2\right)^2}\right) - \frac{\varphi\beta S^*(t)\left(1-\gamma\left(I^*(t)\right)^2\right)}{\left(1+\gamma\left(I^*(t)\right)^2\right)^2}$$

Eigen values with negative real parts are readily apparent if and only $\tau_1 > 0$ and $\tau_2 > 0$. Also, $\tau_1 > 0$ and $\tau_2 > 0$ if $(\varphi+\alpha+\delta) + \frac{2\mu I^*(t)}{\left(1+\rho\left(I^*(t)\right)^2\right)^2} > \frac{\beta S^*(t)\left(1-\gamma\left(I^*(t)\right)^2\right)}{\left(1+\gamma\left(I^*(t)\right)^2\right)^2}$. Hence, by fractional Routh-Hurwitz criteria (Matignon and Matignon 1996; Otto and Day 2019) both the roots of equation (4.8) have negative real parts and satisfy the condition $|arg(l_i)| > \alpha\frac{\pi}{2}$, $i = 1,2$. This proves the following theorem.

Theorem 4.4 $B^* = (S^*, I^*)$, the endemic equilibrium of model (4.2) is locally asymptotically stable when the Basic Reproduction number R_0 > 1 and unstable otherwise.

4.4.4 Global Stability Analysis of Disease free equilibrium (B^0) and Endemic equilibrium point (B^*)

We now concern about the global stability of the DFE and EE. To support our assertion, we provide the following theorem:

Theorem 4.5 The model's (4.2) disease- free equilibrium $B^0 = (S^0, I^0)$ is globally asymptotically stable when $R_0 < 1$ and unstable if $R_0 > 1$.

Proof. To prove this, we define a Lyapunov function by

$\mathcal{H}_1(t) : \mathbb{R}^2_+ \longrightarrow \mathbb{R}^2_+$ given by

$$\mathcal{H}_1(t) = \left(S(t) - S^0 - S^0 ln\frac{S(t)}{S^0}\right) + I(t)$$

This function is defined, continuous and positive definite for all $t \geq 0$. It can be verified that the equality holds if and only if $S(t) = S^0$ and $I(t) = I^0$. Now we have

$${}_0^C D_t^\sigma \mathcal{H}_1(t) = {}_0^C D_t^\sigma \left(\left(S(t) - S^0 - S^0 ln\frac{S(t)}{S^0}\right) + I(t)\right)$$

$${}_0^C D_t^\sigma \mathcal{H}_1(t) = {}_0^C D_t^\sigma \left(S(t) - S^0 - S^0 ln\frac{S(t)}{S^0}\right) + {}_0^C D_t^\sigma I(t)$$

Now using Lemma 4.8 (Mandal et al. 2020), we have

$${}_0^C D_t^\sigma \mathcal{H}_1(t) \leq \left(1 - \frac{S^0}{S(t)}\right) {}_0^C D_t^\sigma S(t) + {}_0^C D_t^\sigma I(t)$$

$${}_0^C D_t^\sigma \mathcal{H}_1(t) \leq \left(1 - \frac{S^0}{S(t)}\right)\left(\theta - \varphi\, S(t) - \frac{\beta\, S(t)I(t)}{1+\gamma\left(I(t)\right)^2}\right) + \left(\frac{\beta\, S(t)I(t)}{1+\gamma\left(I(t)\right)^2} - (\varphi + \alpha + \delta)I(t) - \frac{\mu\left(I(t)\right)^2}{1+\rho\left(I(t)\right)^2}\right)$$

Using the value of $R_0\, and\ S^0 = \frac{\theta}{\varphi}$ in above equation, we have

$${}_0^C D_t^\sigma \mathcal{H}_1(t) \leq -\frac{\varphi\left(S(t)-S^0\right)^2}{S(t)} + \left(\frac{R_0(\varphi+\alpha+\delta)I(t)}{1+\gamma\left(I(t)\right)^2}\right) - (\varphi + \alpha + \delta)I(t) - \frac{\mu\left(I(t)\right)^2}{1+\rho\left(I(t)\right)^2}$$

This concludes that if $R_0 < 1$, then we have ${}_0^C D_t^\sigma \mathcal{H}_1(t) \leq 0$.Furthermore, we know that ${}_0^C D_t^\sigma \mathcal{H}_1(t) = 0$, if and only if $S(t) = S^0$ and $I(t) = I^0$. Thus the largest invariant set for $\{(S, I) \in X: {}_0^C D_t^\sigma \mathcal{H}_1(t) = 0\}$ is the singleton set $\{B^0\}$, where $X =$

$\left\{(S,I) \in \mathbb{R}_+^2 : 0 \leq S+I \leq \frac{\theta}{\varphi}, S, I \geq 0\right\}$ and also all the solutions in X converges to B^0 in accordance with the LaSalle's invariance principle (Diekmann, Heesterbeek, and Roberts 2010; Van Den Driessche and Watmough 2002; Shuai and Van Den Driessche 2013). So, B^0 is globally asymptotically stable when $R_0 \leq 1$. Hence theorem 4.5 is verified.

Theorem 4.6. The endemic equilibrium $B^* = (S^*, I^*)$ of model (4.2) is globally asymptotically stable when R_0 >1.

Proof. We define a Lyapunov function by

$\mathcal{H}_2(t) : \mathbb{R}_+^2 \longrightarrow \mathbb{R}_+^2$ given by

$$L_2(t) = \left(S(t) - S^* - S^* ln \frac{S(t)}{S^*}\right) + \left(I(t) - I^* - I^* ln \frac{I(t)}{I^*}\right)$$

This function is defined, continuous and positive definite for all $t \geq 0$. It can be verified that the equality holds if and only if $S(t) = S^0$ and $I(t) = I^0$
Now we have

$${}_0^c D_t^\sigma \mathcal{H}_2(t) = {}_0^c D_t^\sigma \left(S(t) - S^* - S^* ln \frac{S(t)}{S^*}\right) + {}_0^c D_t^\rho \left(I(t) - I^* - I^* ln \frac{I(t)}{I^*}\right)$$

Again, using Lemma 4.8 (Mandal et al. 2020) we have

$${}_0^c D_t^\sigma \mathcal{H}_2(t) \leq \left(1 - \frac{S^*}{S(t)}\right) {}_0^c D_t^\sigma S(t) + \left(1 - \frac{I^*}{I(t)}\right) {}_0^c D_t^\sigma I(t)$$

$$\begin{aligned} {}_0^c D_t^\sigma \mathcal{H}_2(t) \leq & \left(1 - \frac{S^*}{S(t)}\right)\left[\theta - \varphi\, S(t) \right. \\ & \left. - \frac{\beta\, S(t) I(t)}{1 + \gamma\left(I(t)\right)^2}\right] \\ & + \left(1 - \frac{I^*}{I(t)}\right)\left[\frac{\beta\, S(t) I(t)}{1 + \gamma\left(I(t)\right)^2} - (\varphi + \alpha + \delta) I(t) - \frac{\mu\left(I(t)\right)^2}{1 + \rho\left(I(t)\right)^2}\right] \end{aligned}$$

Using the endemic conditions,

$$\theta = \varphi\, S^*(t) + \frac{\beta\, S^*(t)\, I^*(t)}{1 + \gamma\left(I^*(t)\right)^2}$$

$$\frac{\beta\, S^*(t)\, I^*(t)}{1 + \gamma\left(I^*(t)\right)^2} = (\varphi + \alpha + \delta)\, I^*(t) + \frac{\mu\left(I^*(t)\right)^2}{1 + \rho\left(I^*(t)\right)^2}$$

$$ {}_0^C D_t^{\rho} \mathcal{H}_2(t) \leq -\frac{(S(t)-S^*)^2}{S(t)}\left[\varphi + \frac{\beta\ I(t)}{1+\gamma\left(I(t)\right)^2}\right] - \frac{(I(t)-I^*)^2}{I(t)}\left[(\varphi+\alpha+\delta) + \frac{\mu\, I(t)}{1+\rho\left(I^*(t)\right)^2}\right] $$

This implies,

${}_0^C D_t^{\rho} \mathcal{H}_2(t) \leq 0$ for all $t \geq 0$.

Therefore $\mathcal{H}_2(t)$ is bounded and non-increasing. Further, the limit of $\mathcal{H}_2(t)$ exist as $t \to \infty$. In addition, we know that ${}_0^C D_t^{\rho} \mathcal{H}_2(t)|_6 = 0$, if and only if $S(t) = S^*$ and $I(t) = I^*$. Therefore, the maximum invariant set for $\{(S, I) \in X: {}_0^C D_t^{\sigma} \mathcal{H}_2(t)|_6 = 0\}$ is the singleton set $\{ B^*\}$. According to the with the LaSalle's invariance principle, we know that all solutions in X converge to B^*, Therefore, the endemic equilibrium of model (4.5) is globally asymptotically stable when R_0 >1. Hence the theorem 4.6.

4.5 Numerical Simulation

In this section, using MATLAB 2012(b) and the predictor-corrector method (Diethelm et al. 2002), numerical simulations are presented for different fractional orders to observe the dynamical behavior of susceptible, infectives, and recovered population. The initial values of the subpopulations are S (0) = 100, I (0) = 5 and R (0) = 0 and from the literature (Kumar and Nilam 2019), we chose the following set of tested parameter values given in Table 4.2.

Table 4.2 Model parameters with their values

S.No.	Parameters	Value
1	β	0.05 per person- per day
2	φ	0.05 per day
3	μ	0.02 person-per day
4	α	0.002 per person-per day
5	θ	12 persons per day
6	δ	0.01 per person- per day
7	γ	0.001 per person-per day
8	ρ	0.002 per person-per day

Figures 4.1, 4.2 and 4.3 depicts the effect of varying awareness about the disease among the infected population and from the graphs it is inferred that as the awareness about the disease increases in the society, number of infectives start reducing significantly. Similar effect can be seen for susceptible population that if we increase the awareness about consequences of using social media then, number of susceptible populations starts increasing as shown in figures 4.4, 4.5 and 4.6. Figure 4.7 illustrates the considerable decrease in percentage of infected population for different values of u, u = 25%, 50%, 75%. For u = 25% in 38.59 days there is a decrease

of 34% in infected population after that infection starts increasing specifying that there will be no use of spreading awareness after 38.59 days. In the same way for u = 50%, due to the awareness programs there is a decrement of 52% in 59.9 days and for u = 75%, 57.85% in 84 days. It is clear from the graph that as the awareness about the mental illness caused due to social media increases, infected population starts declining.

Figure 4.8 shows the increase in percentage in susceptible population with increasing values of u, u = 25%, u = 50% and u = 75%. For u = 25%, the susceptible population increases till 38 days to 39% after that it starts decreasing, which means that there will be no of use awareness programs after 38 days. Similarly for u = 50% and u= 75%, infected population increases to 58.18% and 64.42% in 51 days and 57 days respectively and then starts declining indicating that organizing awareness programs will no longer be helpful after that. This means that as the awareness percentage increases in the society there will be more susceptibles and less infectives. Figures 4.9, 4.10 and 4.11 shows the effect of varying treatment rates on infectives with u = 40%, 20% and 0% respectively. It is observed that as the treatment rate increases the number of infectives decreases. Also, on comparing these figures, it can be stated that as the awareness in the society increases, number of infectives also starts decreases with time. Figures 4.12, 4.13 and 4.14 presents the effect of varying inhibition rate due to infection on infectives with awareness percentage u = 0, 20% and 30% respectively. It is observed that more the preventive measures taken by infectives, lower will be the number of infectives. Also, along with the preventive measures if we increase the awareness then also number of infectives starts decreasing.

Figures 4.15, 4.16 and 4.17 shows the effect of varying inhibition rate due to infection on susceptibles with awareness percentage u = 0, 20% and 40% respectively. It is inferred that more the preventive measures taken by infectives lesser number of susceptible people will get infected, thus the susceptible population rises. Figures 4.18, 4.19 and 4.20 shows the phase portraits of the system for different fractional orders 0.8, 0.9 and 1.0 respectively. All the trajectories starting from different initial conditions are converging to its equilibrium point.

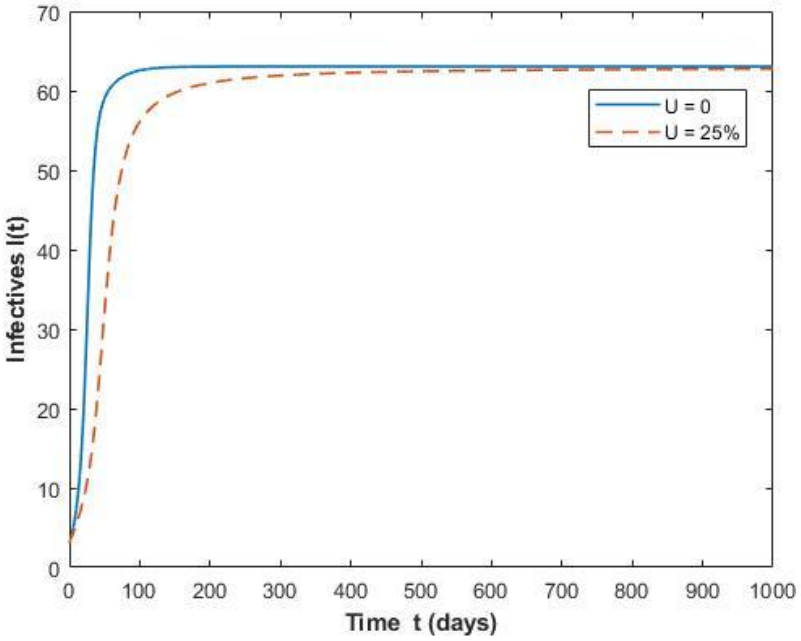

Figure 4.1 Effect of awareness on infectives for u = 0 and u = 25%

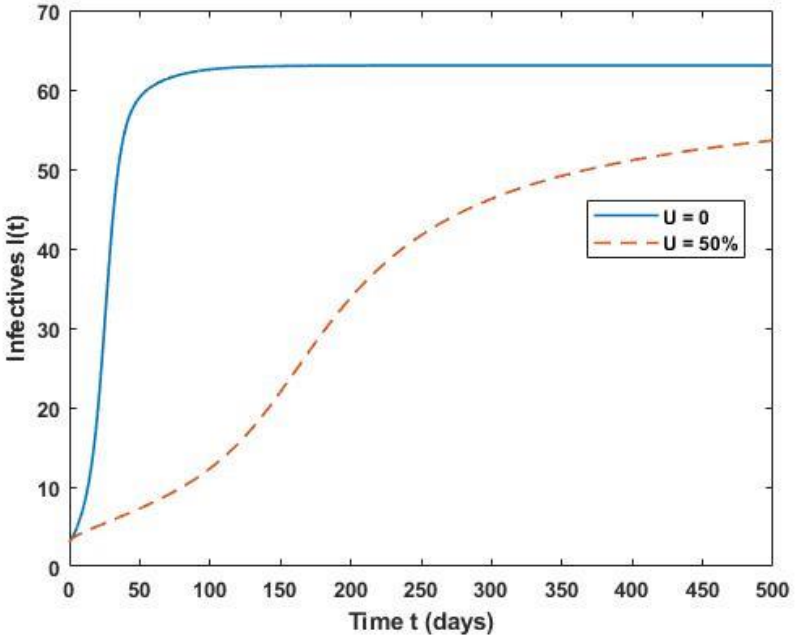

Figure 4.2 Effect of awareness on infectives for u = 0 and u = 50 %

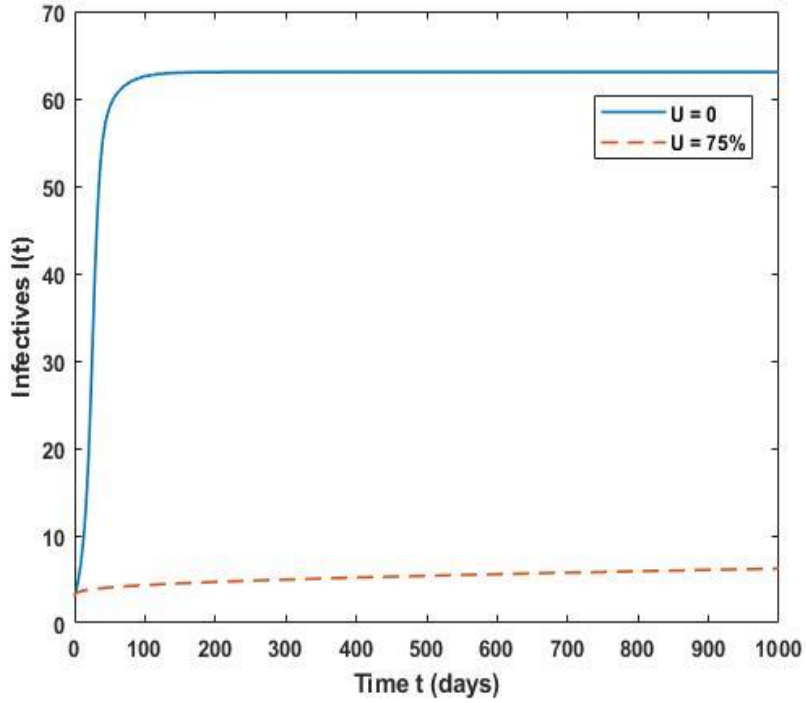

Figure 4.3 Effect of awareness on Infectives for u = 0 and u = 75%

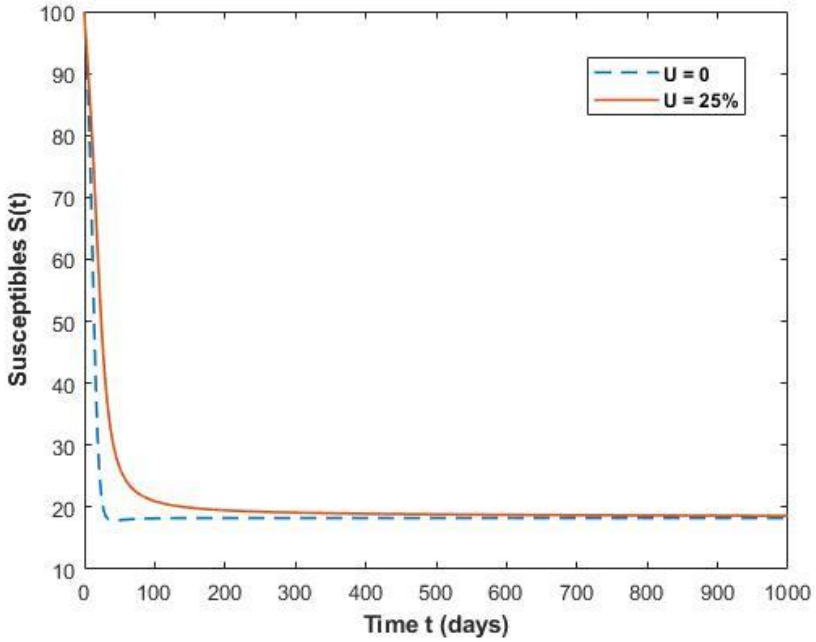

Figure 4.4 Effect of awareness on susceptibles for u = 0 and u = 25%

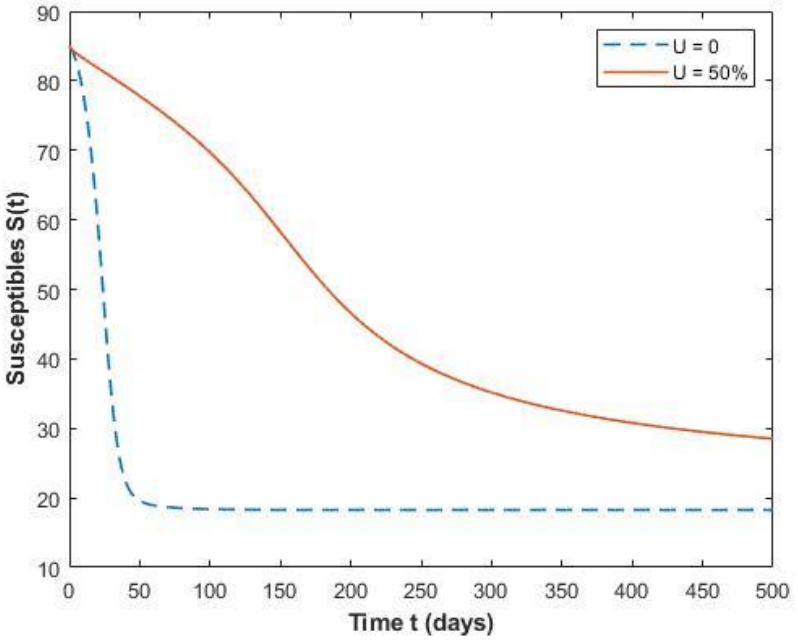

Figure 4.5 Effect of awareness on susceptibles for u = 0 and u = 50%

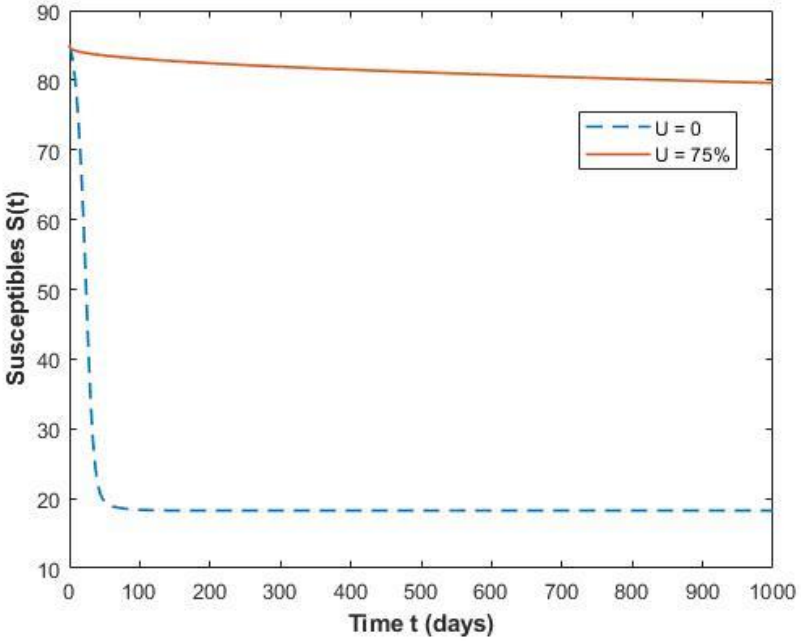

Figure 4.6 Effect of awareness on susceptibles for u = 0 and u = 75%

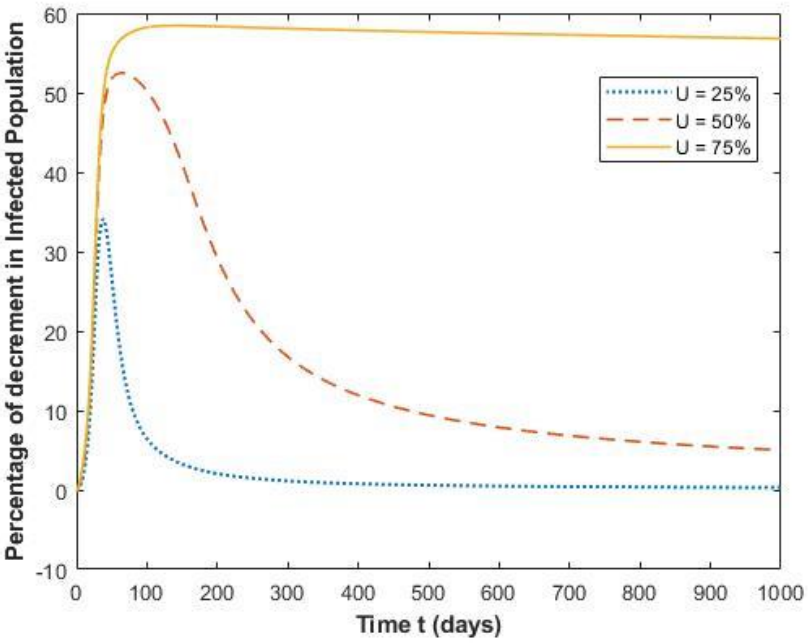

Figure 4.7 Percentage of decrement in infected population for different u

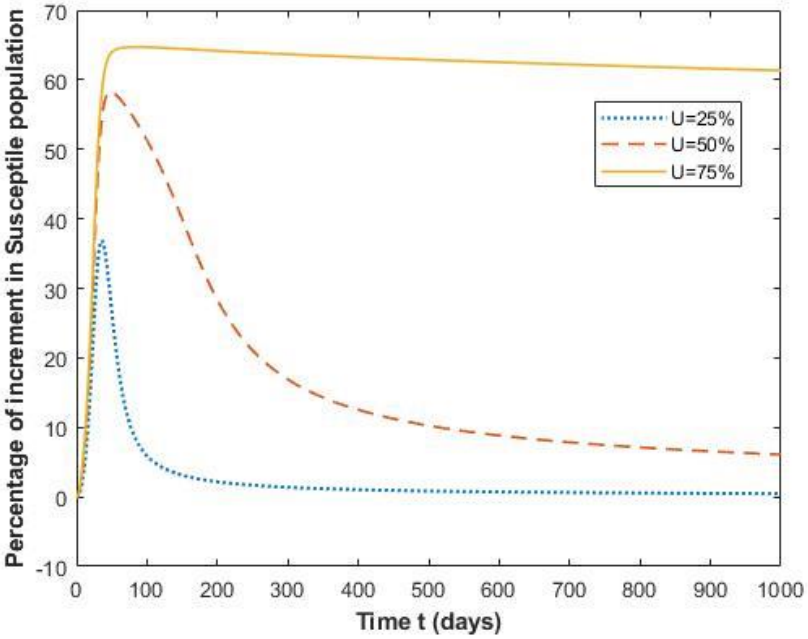

Figure 4.8 Percentage of increment in susceptible population for different u

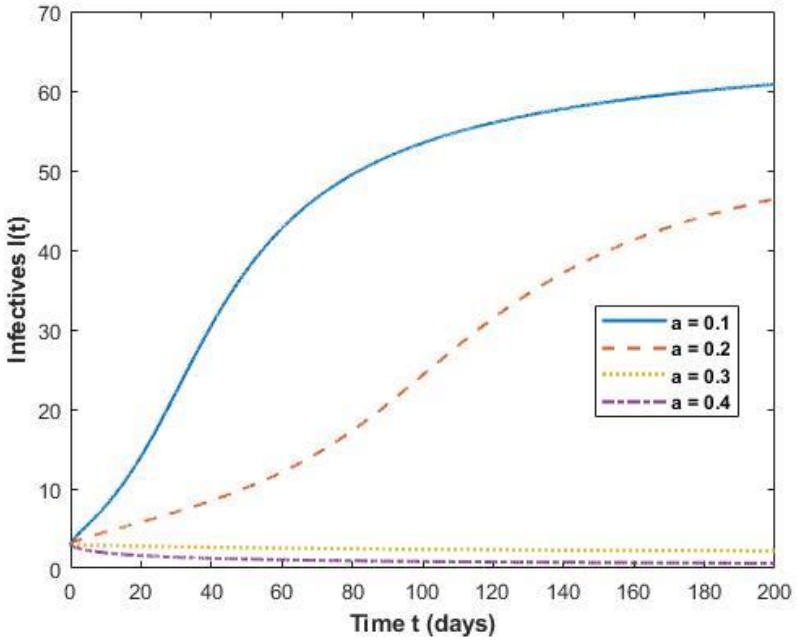

Figure 4.9 Effect of varying treatment rates on infectives with u = 40%

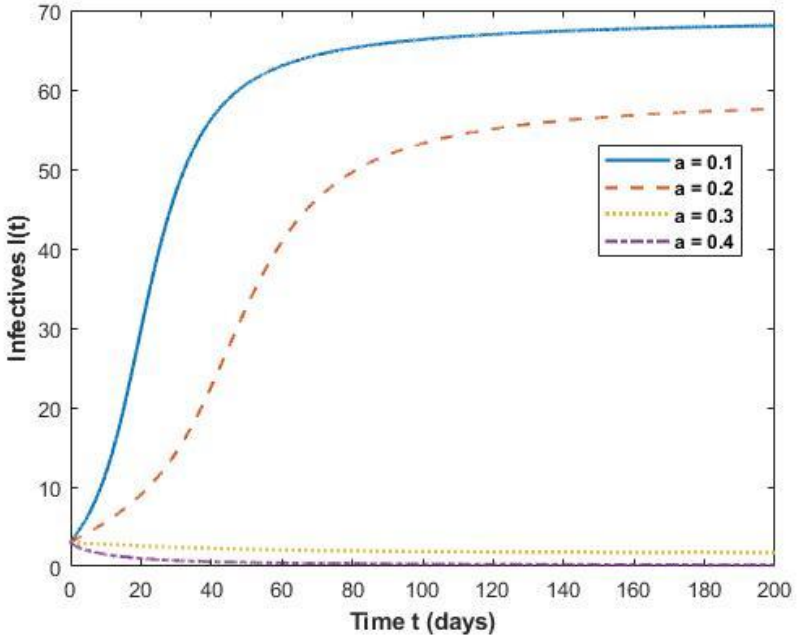

Figure 4.10 Effect of varying treatment rates on infectives with u =20%

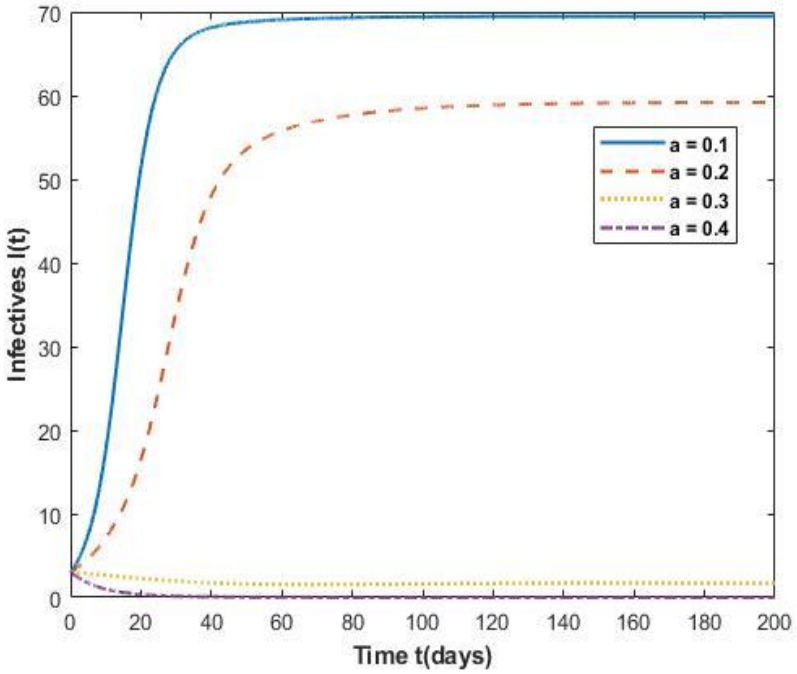

Figure 4.11 Effect of varying treatment rates on infectives with u = 0

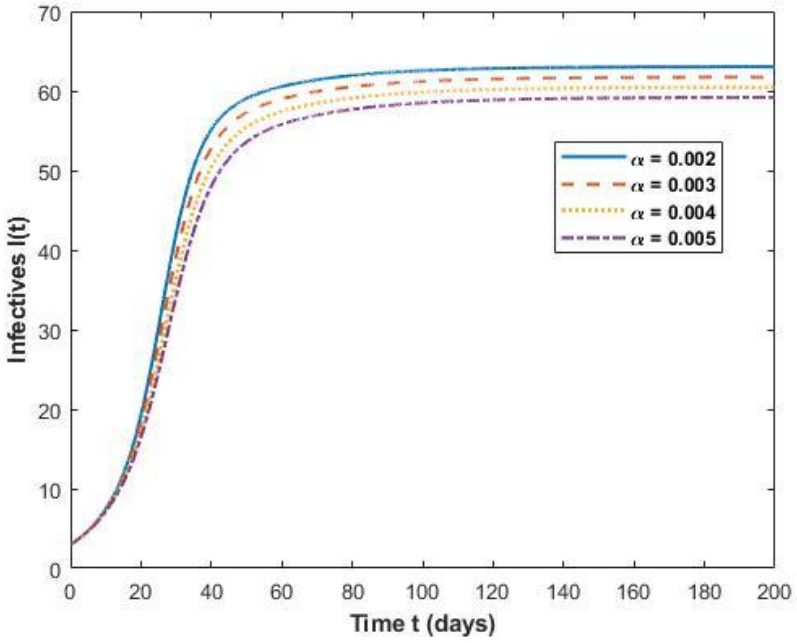

Figure 4.12 Effect of varying inhibition rate due to infection on infectives with u = 0

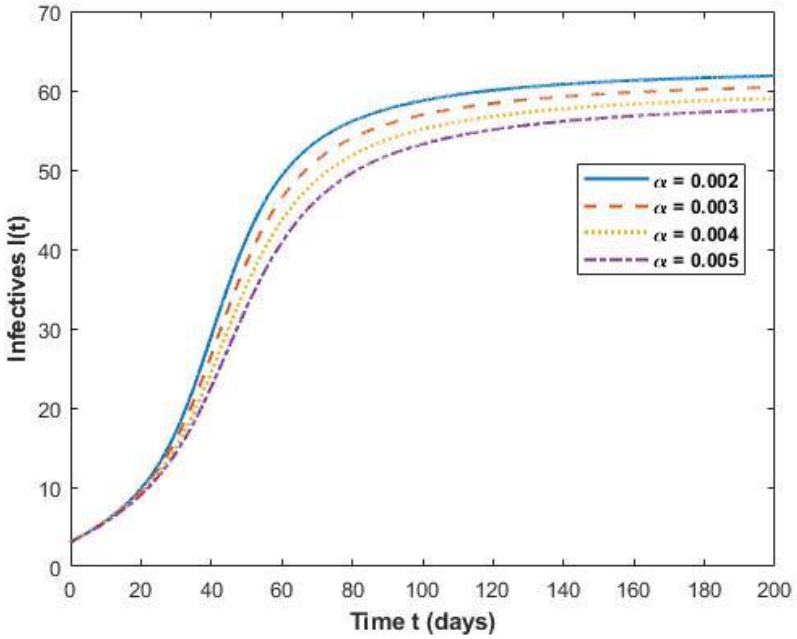

Figure 4.13 Effect of varying inhibition rate due to infection on infectives with u = 20%

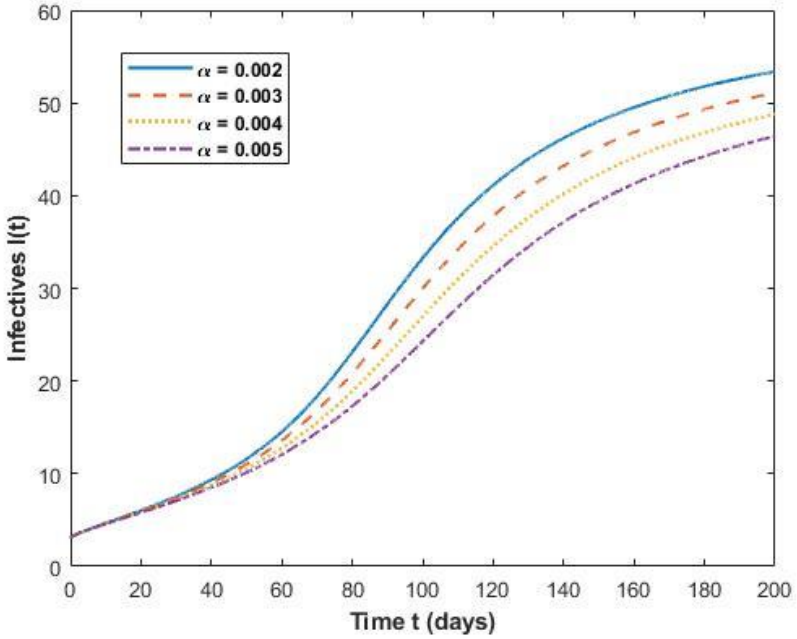

Figure 4.14 Effect of varying inhibition rate due to infection on infectives with u = 40%

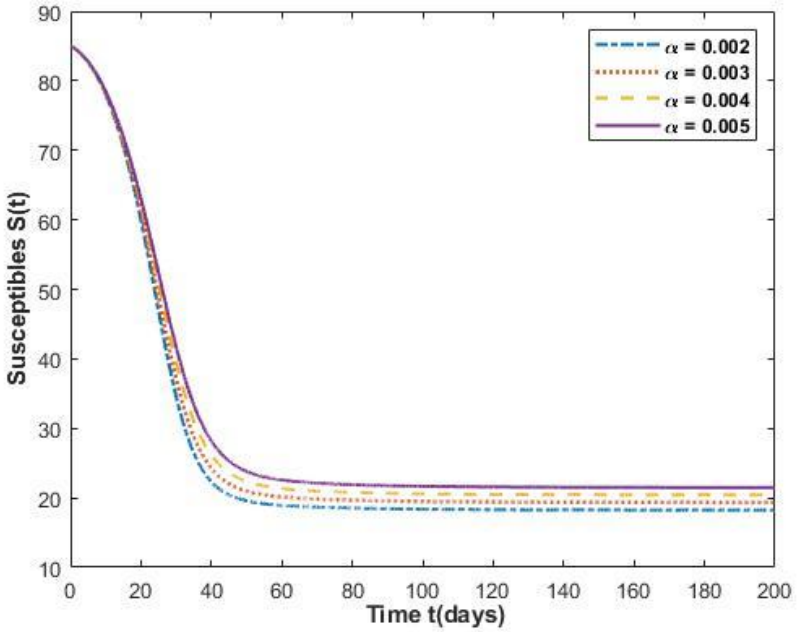

Figure 4.15 Effect of varying inhibition rate due to infection on susceptibles with u = 0

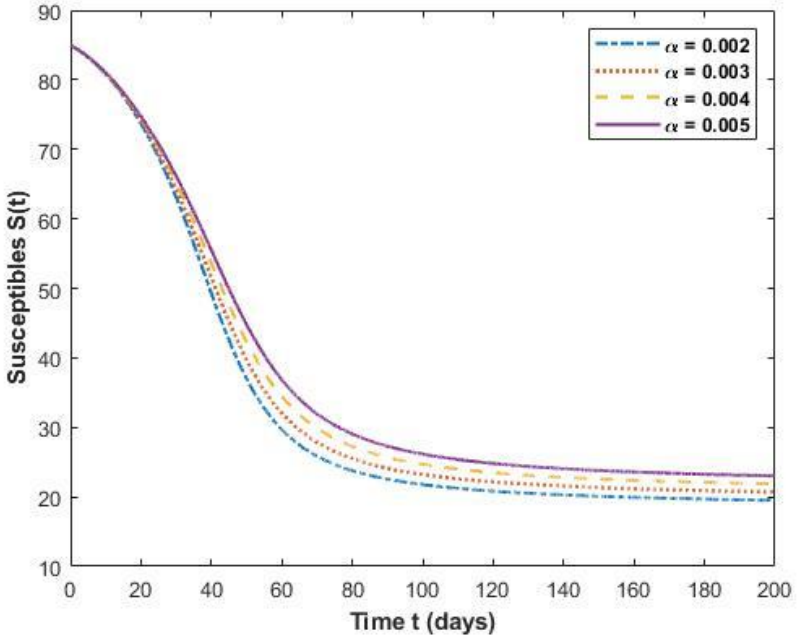

Figure 4.16 Effect of varying inhibition rate due to infection on susceptibles with u = 20%

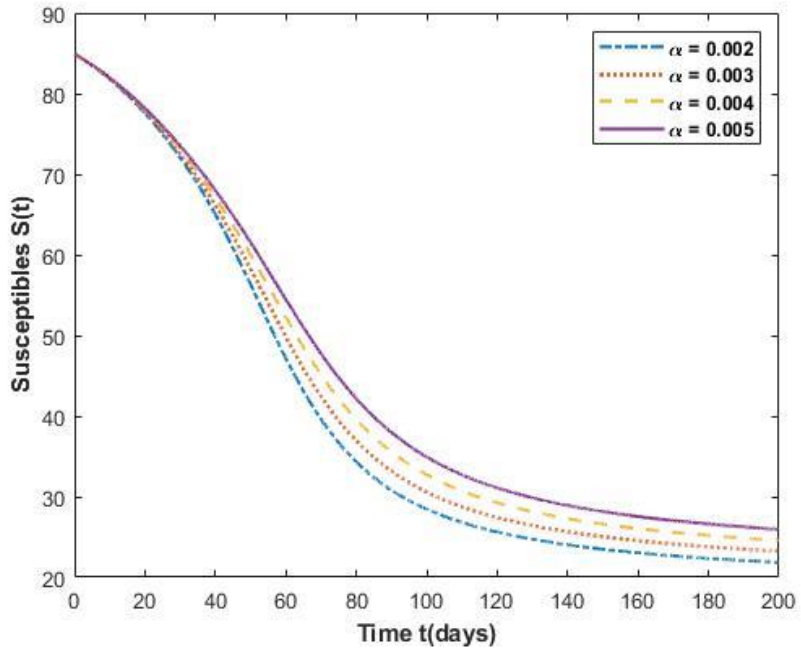

Figure 4.17 Effect of varying inhibition rate due to infection on susceptibles with u = 30%

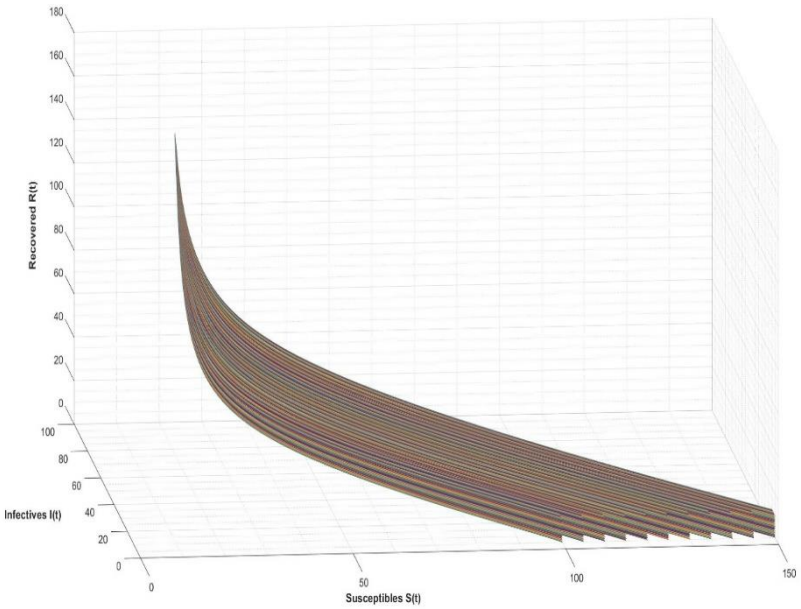

Figure 4.18 Phase Portrait for fractional order 0.8

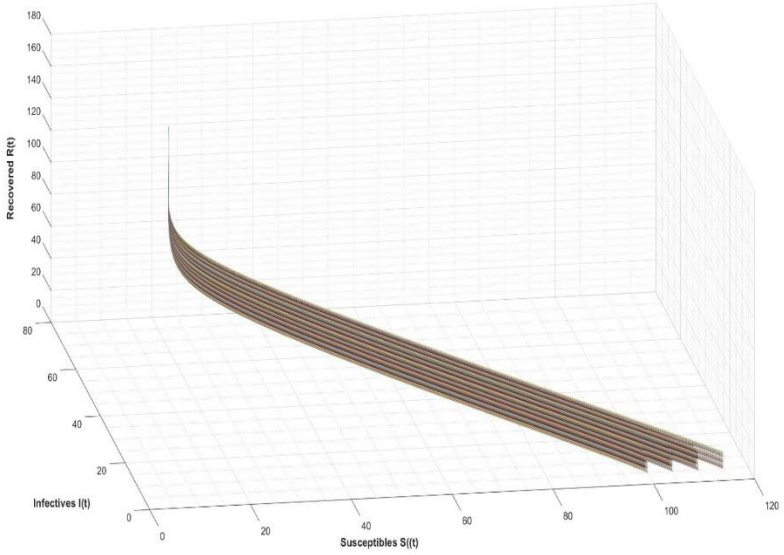

Figure 4.19 Phase Portrait for fractional order 0.9

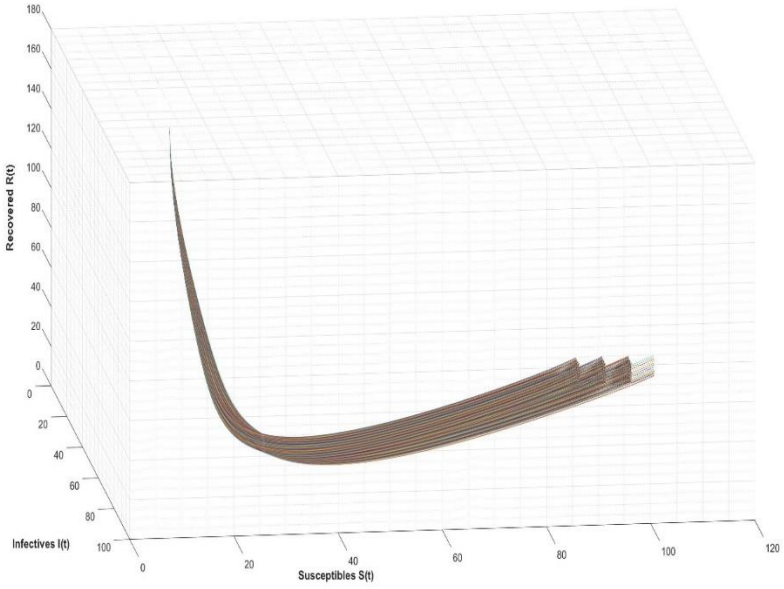

Figure 4.20 Phase Portrait for Integer order system with order 1.0

4.6 Conclusion

The goal of this chapter was to incorporate the impact of awareness on susceptible populations into a fractional-order SIR epidemic model using the Caputo-fractional order derivative since awareness can play a vital role in controlling the spread of an infectious disease especially in case of newly emerging diseases when either the treatment strategy is unknown or very limited. A Monod-Haldane functional was used as an incidence rate and a Holling Type III functional as a treatment rate in the study. The disease-free equilibrium point is locally asymptotically stable when the basic reproduction number R_0 is less than one, but it is unstable when R_0 is more than one, as shown in theorem 4.2. The presence of a unique positive endemic- equilibrium is also established in theorem 4.3, and the stability of endemic equilibrium point is examined. The endemic-equilibrium point is discovered to be locally asymptotically stable if R_0 is greater than 1, otherwise unstable as stated in theorem 4.4. Also, for some condition, the global stability behaviour of both disease-free equilibrium and endemic equilibrium is explored, and it is established that DFE is globally asymptotically stable for $R_0 \leq 1$ and EE is globally asymptotically stable if $R_0 > 1$, as demonstrated in theorems 4.5 and 4.6.

It is observed through simulation that as the fractional order reduces or the awareness increases, the population of susceptible increases because, in case of having awareness from different means, individuals explore and respond for it, resulting in an increase in the number of susceptibles. On the other hand, the number of infectives decreases on reducing the fractional order meaning hereby spreading optimal awareness as in case of any situation like COVID-19. This is possible because of adopting various preventive measures and other strategies which have been made popular through awareness programmes. It is also inferred that spreading awareness about a disease is effective only for a certain period after which, it is no longer necessary since people have sufficient information about the disease or might take it for granted if repeated information is provided. It is stated that as the treatment rate increases the number of infectives decreases, also, as the awareness in the society increases, number of infectives start reducing with time. From this work we suggest that along with inhibitory measures if proper awareness for a sufficient time period is spread among the population, then the number of susceptibles increases due to prior knowledge about the disease due to awareness programmes but number of infectives decreases in a more significant way.

CHAPTER 5

THE BEHAVIOR OF THE FRACTIONAL ORDER DELAY DIFFERENTIAL SIR EPIDEMIC MODEL WITH HOLLING TYPE II TREATMENT RATE AND CROWLEY-MARTIN RATE OF INCIDENCE

Time delays and fractional order are critical components of biological memory systems. Non-integer order enhances the model's behaviour; however, time lag has major implication on the occurrence of Hopf bifurcation and system stability. The present chapter examines the dynamics of fractionally ordered delay differential Susceptibles-Infectives-Recovered epidemiological model with Holling functional type II treatment rate and Crowley-Martin (CM) functional type incidence. To acquire a more practical understanding of the epidemic's dynamics, the incidence rate was delayed by the latency time. We have examined the sufficient requirements for steady-state stability and Hopf bifurcation in the presence of time delay. The model exhibits a Hopf bifurcation at the threshold parameters. When time delays exceed critical values, the model goes through Hopf bifurcation. Numerical simulations have been offered to support the theoretical findings. Numerical studies demonstrate that combining fractional order with time delays in the epidemic model affects the behavior and improves the model's stability.

5.1 Introduction

Spreading infectious diseases continue to pose a serious threat to world health, impacting populations and economies worldwide. Mathematical models have proven invaluable in understanding the spread and control of such diseases, providing insights into transmission dynamics and informing public health interventions. In epidemic modeling literature a number of mathematical models such as SIS (J. A. Cui et al., 2008; J. Liu et al., 2018; Y. Wang et al., 2012; Wu & Fu, 2011), SIR(Gomez Alcaraz & Vargas-De-Leon, 2012; Hattaf, Lashari, et al., 2013; Hattaf, Lashari, Louartassi, et al., 2013; A. Kumar, Goel, et al., 2020; M. Li & Liu, 2014; Shulgin et al., 1998; Zhonghua & Yaohong, 2010; Zhou & Fan, 2012) , SEIR (Aghdaoui et al., 2021; S. Kumar et al., 2023; M. Y. Li et al., 1999; Mammeri, 2020; Tipsri & Chinviriyasit, 2014), SIRS (C. H. Li et al., 2014), and many more have been proposed to control the spread of disease. Furthermore, in epidemiology, measures like as medical care, immunization, isolation, and many more are crucial in limiting the spread of the illness. Traditional SIR models, however, often use integer-order derivatives and may not fully capture the intricacies of disease dynamics such as memory effects, time delays etc.

Extensive research has been conducted to understand infectious disease dynamics and generalize epidemic models in the literature. Real-world application challenges necessitate the use of fractional-order differential equations (FODE). Several well-known mathematicians, including Abel, Fourier, Riemann, and Liouville, contributed to the Theory of Fractional Calculus. With fractional-order derivatives describing the entire space and integer-order derivatives providing information about only the local characteristics of a state, FODE models are preferable than classical ODE and/or delay differential equation models (Podlubny, I. (1999)). To explain it simply, the FODE models assume that a physical phenomenon's next certain location depends on all past states in addition to its current condition. Therefore, fractional-order models expand the stability zone of the states and provide more realistic biological models requiring memory. Several fields in science, engineering, applied mathematics, economics, and bioengineering have used fractional-order models in the past few decades (Baleanu et al., 2019; Hilfer, 2000). Unlike integer-order models, which either don't account for these effects or make them impractical to take into consideration, fractional-order differential equations offer a strong tool for incorporating memory and hereditary features of the systems. Furthermore, the fractional models have one extra degree of freedom when fitting data compared to the integer-order model (Rihan et al., 2017). Several researchers have established intriguing applications to study the dynamics of such fractional order models with memory systems based on these advantages (Chen, 2008; El-Sayed et al., 2007; Hoan et al., 2020; S. Liu et al., 2020; Naik, 2020; Owoyemi et al., 2020; Rostamy & Mottaghi, 2016; Sene, 2021)

Time delay is a common and natural feature in population dynamics models, especially in macroscopic models of the immune response. Time delay affects biological systems' dynamical behaviors in several ways. Time delays must therefore be considered when studying biological systems from both a theoretical and a practical standpoint. There is a latent period before an infected person becomes contagious, according to the assumptions made in infectious disease modeling. Stated alternatively, the transmission of an infection from one susceptible host to another occurs gradually. As a result, it is crucial to analyse the dynamical characteristics of systems with time delays (Deng et al., 2007; Goel & Nilam, 2019; Hattaf, Lashari, et al., 2013; Hattaf, Lashari, Louartassi, et al., 2013; A. Kumar & Nilam, 2019; M. Li & Liu, 2014; Tipsri & Chinviriyasit, 2014). In (Rakkiyappan et al., 2019), a system of nonlinear differential equations with multiple time delays is used to evaluate zika virus infection. The authors of (Wei et al., 2008) took into account the vector borne epidemic model with time delay. Influence of time lag on the transmission term between the host and the vector, which has the potential to destabilize the system, was extensively covered by the authors. Hopf bifurcation is another method for raising periodic solutions.

Recently, there has been a growing fascination with epidemic models that incorporate fractional-order derivatives and time delays (Chinnathambi & Rihan, 2018; Deng et al., 2007a; S. Liu et al., 2020). Naturally, memory or time delay play an inevitable role in the dynamics of most real-world phenomena. The authors of (Naim et al., 2022) examined the impact of dual time delay and Caputo fractional derivative on the long-run behavior of a viral system with the non-cytolytic immune hypothesis and they found that the combination of fractional order can significantly improve the dynamics and strengthen the infection model's stability condition. Authors in (S. Liu et al., 2020) studies the bifurcation analysis of a fractional order SIQR model with double delay.

5.2 Formulation of Fractional order Mathematical Model

The literature indicates that most mathematical modeling of biological systems relies on fractional-order differential equations without delays or delay differential equations (DDEs) with integer orders. However, non-integer-order calculus is more appropriate than integer-order calculus for simulating systems of biological world with complex memory and long-range interactions, especially mechanisms of epidemic evolution. Compared to conventional integer-order mathematical modeling, which disregards the effects of memory or long-range interactions, fractional-order differential equation modeling of such systems offers more advantages. Indeed, memory effects are critical in the transmission of diseases. Memory effects in epidemic models of susceptible-infected-recovered (SIR) appear to be an appropriate fit for this type of analysis. We study the impact of incorporating time delays and fractional order in an epidemic model.

The disease transmission model splits up the population into three groups: susceptible (S), infected (I), and recovered (R). Individuals that are susceptible to the disease but not yet afflicted at time t are denoted by $S(t)$. The term $I(t)$ refers to infected persons who can spread the infection to others. $R(t)$ refers to individuals who have been infected, removed from the risk of infection, and entered the recovered compartment due to the body's autoimmune reaction and medical treatment.
We suppose that individuals who are susceptible are recruited at rate σ. The Crowley-Martin incidence rate governs the movement from the susceptible compartment to the infective compartment, taking into account the effect of inhibition among infectives even in cases of high susceptible population density, which is ignored by other incidence rates.

$$\frac{\beta S(t-\tau)I(t-\tau)}{\big(1+\alpha_1 S(t-\tau)\big)\big(1+\alpha_2 I(t-\tau)\big)}$$

The delay due to the latency period is $\tau > 0$, and the infected vector can only infect a susceptible individual after this time. The transmission rate is represented by β, whereas susceptible adopt α_1 and infectives adopt α_2 measures of inhibition.

The term $\frac{\gamma_1 I(t)}{1+\gamma_2 I(t)}$ defines the Holling type II treatment rate where γ_1 represents the treatment rate and γ_2 indicates the limiting rate in resource availability. The parameters δ_1, δ_2, and δ_3 refers the rates for natural mortality, disease-induced, and recovery. ρ is the Caputo fractional derivative with a range of (0,1]. The Caputo derivative is described in definition 1in Appendix. Based on these assumptions, changes in $S(t), I(t)$ and $R(t)$ with respect to time t are described by the nonlinear system of delay differential equations that follows:

$$\left.\begin{aligned} {}_0^C D_t^\rho S(t) &= \sigma - \delta_1 S - \frac{\beta S(t-\tau)I(t-\tau)}{\big(1+\alpha_1 S(t-\tau)\big)\big(1+\alpha_2 I(t-\tau)\big)} \\ {}_0^C D_t^\rho I(t) &= \frac{\beta S(t-\tau)I(t-\tau)}{\big(1+\alpha_1 S(t-\tau)\big)\big(1+\alpha_2 I(t-\tau)\big)} - (\delta_1+\delta_2+\delta_3)I(t) - \frac{\gamma_1 I(t)}{1+\gamma_2 I(t)} \\ {}_0^C D_t^\rho R(t) &= \frac{\gamma_1 I(t)}{1+\gamma_2 I(t)} + \delta_3\, I(t) - \delta_1 R(t) \end{aligned}\right\} \quad (5.1)$$

The initial conditions of the model (5.1) are provided by

$$S(t) = \varphi_1(t), I(t) = \varphi_2(t)\ , R(t) = \varphi_3(t), \varphi_i(t) \geq 0, t \in [-\tau, 0] \quad (5.2)$$

5.3 Basic Properties of the Model

The model describes the dynamics of the human population; hence the system has non-negative solutions. Furthermore, the model's state variables are non-negative and bounded for all (t $\geq$ 0). Let $\mathbb{R}^3_+ := \{X \epsilon \mathbb{R}^3 : X \geq 0\}$ and $X(t) = \big(S(t), I(t), R(t)\big)^T$ on non-negative solutions, the lemmas needed to prove the theorem are mentioned in Appendix.

Theorem 5.1 All the solutions of the system (5.1) satisfying the initial conditions (5.2) are non-negative and the solution will persists in region $E = \{(S, I, R) \in R^3_+ : 0 < S + I + R \leq \bar{Q}\ , \bar{Q}\ \geq C_E \frac{\sigma}{\delta_1}\}$ for $t \geq 0$.

Proof. In order to prove the non-negativity of the system it is assumed that there exist a $t_* > t_0$ such that $S(t_*) = 0$ and $S(t) < 0$ for $t \in (t_*, t_1]$ where t_1 is sufficiently close to t_*. If $S(t) = 0$, $D_t^\rho S(t_*) = \sigma$, thus one obtains, $D_t^\rho S(t) > 0$ for all $t \in [t_*, t_1]$ and $D_t^\rho S(t) > \epsilon\, S(t)$ where $\epsilon > 0$. Hence one derives $S(t) > S(t_*) E_\rho(\epsilon(t - t_*)^\rho), t \in [t_*, t_1]$ where $E_\rho(z) = \sum_{k=0}^{\infty} \frac{z^k}{\Gamma(\rho k+1)}$ is the Mittag Leffler function, this contradicts our assumption. Hence $S(t) > 0$ for any $t > t_0$. In the same manner $I(t)$ and $R(t)$ are non-negative. The boundedness of the solutions is now proved. By adding together each equation in model (5.1), we get:

$$D_t^\rho N(t) = \sigma - \delta_1 N(t) - \delta_2 I(t)$$

Where $N(t) = S(t) + I(t) + R(t)$. As $I(t) \geq 0$, we have

$$D_t^\rho N \leq \sigma - \delta_1 N(t)$$

Now consider the initial value problem $D_t^\rho \bar{N} = \sigma - \delta_1 \bar{N}$, $\bar{N}(0) = \bar{N}_0$. Using comparison principle (Lu & Zhu, 2018), we obtain the following inequality:

$N(t) \leq \bar{N}(t)$ for all $t \geq 0$. By using the Laplace transform on the initial value problem, we can now obtain

$$s^\rho L[\bar{N}(t)] - s^{\rho-1}\bar{N}_0 = \frac{\sigma^\rho}{s} - \delta_1 L[\bar{N}(t)]$$

$$\Rightarrow L[\bar{N}(t)] = \frac{s^{\rho-1}\bar{N}_0}{s^\rho + \delta_1} + \frac{\sigma^\rho s^{-1}}{s^\rho + \delta_1}$$

Using Lemma 3, we obtain

$$L\left[E_{\rho,1}(-\delta_1 t^{\rho})\right] = \frac{s^{\rho-1}}{s^{\rho}+\delta_1}$$

$$L\left[t^{\rho}E_{\rho,\rho+1}(-\delta_1 t^{\rho})\right] = \frac{s^{-1}}{s^{\rho}+\delta_1}$$

Using the inverse Laplace transform on the two equations above, we obtain

$$\bar{N}(t) = \bar{N}_0 E_{\rho,1}(-\delta_1 t^{\rho}) + \sigma t^{\rho} E_{\rho,\rho+1}(-\delta_1 t^{\rho}),$$

using $D_t^{\rho} N \leq \sigma - \delta_1 N$ we have

$$N(t) \leq N_0 E_{\rho,1}(-\delta_1 t^{\rho}) + \sigma t^{\rho} E_{\rho,\rho+1}(-\delta_1 t^{\rho}),$$

By Lemma 4, we obtain

$$|N(t)| \leq \frac{N_0 C_E}{1+\delta_1 t^{\rho}} + \frac{\sigma t^{\rho} C_E}{1+\delta_1 t^{\rho}}$$

where C_E is constant given in Lemma 4. Hence, as $t \to \infty$, we have $N(t) \leq \bar{L}$ with $\bar{L} \geq C_E \frac{\sigma}{\delta_1}$. Thus, the solutions are bounded and will remain in region E for $t \geq 0$. Therefore, theorem 1 is proved and solution remains in R_+^3. Therefore, for $t \geq 0$, the solutions are bounded and continue to exist in region E. Thus, the solution is still in R_+^3, and theorem 5.1 is validated.

5.4 Mathematical analysis of the model

This section performs stability analyses of the disease free equilibrium point and the endemic equilibrium point.

5.4.1 Disease Free Equilibria and Stability Analysis

In this section we study the stability analysis of disease-free equilibrium points, basic reproduction number and endemic equilibrium points and its stability analysis.

We are examining the following reduced system for analysis because the first two equations of the model (5.1) are not affected by R:

$$\left.\begin{aligned} {}_0^C D_t^\rho S(t) &= \sigma - \delta_1 S - \frac{\beta S(t-\tau) I(t-\tau)}{(1+\alpha_1 S(t-\tau))(1+\alpha_2 I(t-\tau))} \\ {}_0^C D_t^\rho I(t) &= \frac{\beta S(t-\tau) I(t-\tau)}{(1+\alpha_1 S(t-\tau))(1+\alpha_2 I(t-\tau))} - (\delta_1+\delta_2+\delta_3) I(t) - \frac{\gamma_1 I(t)}{1+\gamma_2 I(t)} \end{aligned}\right\} \quad (5.3)$$

$$S(t) = \varphi_1(t), I(t) = \varphi_2(t)\ , \varphi_i(t) \geq 0, t \in [-\tau, 0] \quad (5.4)$$

The system's (5.3) right side is brought to zero to solve the equilibria. Evidently, system (5.3) consistently maintains disease free equilibrium $Y_1 = \left(\frac{\sigma}{\delta_1}, 0\right)$. Using the next-generation matrix approach (Van Den Driessche & Watmough, 2002), the basic reproduction number is given by

$$R_0 = \frac{\beta\sigma}{(\delta_1+\alpha_1\sigma)(\delta_1+\delta_2+\delta_3+\gamma_1)}$$

which represents the expected number of secondary cases generated by a single infectious case in a susceptible population. We are now investigating local stability of disease free equilibrium point. The matrix of characteristics associated to system (5.6) is provided by:

$$\Delta(\lambda) = \begin{bmatrix} -\delta_1 - \lambda^\rho & -\frac{\beta\sigma\, e^{-\lambda\tau}}{(\delta_1+\alpha_1\sigma)} \\ 0 & \frac{\beta\sigma\, e^{-\lambda\tau}}{(\delta_1+\alpha_1\sigma)} - (\delta_1+\delta_2+\delta_3) - \gamma_1 - \lambda^\rho \end{bmatrix}$$

The corresponding characteristic polynomial at disease -free equilibrium $Y_1 = \left(\frac{\sigma}{\delta_1}, 0\right)$ is

$$(\delta_1+\lambda^\rho)\left(-\frac{\beta\sigma\, e^{-\lambda\tau}}{(\delta_1+\alpha_1\sigma)} + (\delta_1+\delta_2+\delta_3) + \gamma_1 + \lambda^\rho\right) = 0 \quad (5.5)$$

Case 5.4.1.1 When $\tau = 0$, equation (5.5) can be written as

$$(\delta_1+\lambda^\rho)\left(-\frac{\beta\sigma}{(\delta_1+\alpha_1\sigma)} + (\delta_1+\delta_2+\delta_3) + \gamma_1 + \lambda^\rho\right) = 0$$

$$(\delta_1+\lambda^\rho)((\delta_1+\delta_2+\delta_3+\gamma_1)(1-R_0) + \lambda^\rho) = 0 \quad (5.6)$$

It is evident that if $R_0 < 1$, then every root of equation (5.6) would have negative real components. If $R_0 < 1$, Y_1 is then locally asymptotically stable.

Case 5.4.1.2 When $\tau \neq 0$, equation (5.5) can be deduced as the following equation

$$-\frac{\beta\sigma}{(\delta_1+\alpha_1\sigma)}e^{-\lambda\tau}+(\delta_1+\delta_2+\delta_3)+\gamma_1+\lambda^\rho=0 \quad (5.7)$$

Suppose the above equation has purely imaginary roots $\lambda = i\omega, \omega > 0$, then ω satisfy

$$(i\omega)^\rho+(\delta_1+\delta_2+\delta_3+\gamma_1)-\frac{\beta\sigma}{(\delta_1+\alpha_1\sigma)}e^{-(i\omega)\tau}=0$$

$$\omega^\rho\left(\cos\frac{\rho\pi}{2}+i\sin\frac{\rho\pi}{2}\right)+(\delta_1+\delta_2+\delta_3+\gamma_1)-\frac{\beta\sigma}{(\delta_1+\alpha_1\sigma)}(\cos\omega\tau-i\sin\omega\tau)=0$$

Separating the real and imaginary parts of the above equation

$$\omega^\rho\cos\frac{\rho\pi}{2}+(\delta_1+\delta_2+\delta_3+\gamma_1)=\frac{\beta\sigma}{(\delta_1+\alpha_1\sigma)}\cos\omega\tau$$

$$\omega^\rho\sin\frac{\rho\pi}{2}=-\frac{\beta\sigma}{(\delta_1+\alpha_1\sigma)}\sin\omega\tau$$

Squaring and adding both sides, we get

$$\omega^{2\rho}+2(\delta_1+\delta_2+\delta_3+\gamma_1)\cos\frac{\rho\pi}{2}\omega^\rho+(\delta_1+\delta_2+\delta_3+\gamma_1)^2(1-R_0^2)=0 \quad (5.8)$$

It is evident that equation (5.8) has no positive root if $R_0 < 1$, however equation (5.8) has a positive root for $R_0 > 1$. Hence equation (5.7) has no purely imaginary roots for $R_0 < 1$ and $\tau > 0$. From Lemma 5, the disease-free equilibrium point is asymptotically stable for $\tau \geq 0$.

Theorem 5.2 If $R_0 < 1$ and $\tau \geq 0$ then the disease free equilibrium of system (5.3) $Y_1\left(\frac{\sigma}{\delta_1}, 0\right)$ is locally asymptotically stable and if $R_0 > 1$ then Y_1 is unstable.

5.4.2 Existence and stability analysis of endemic equilibrium

After rearranging system (5.3) to obtain S^* and I^*, we may determine the presence of an endemic equilibrium $Y_2(S^*, I^*)$.

$$S^*=\frac{\sigma+(\sigma\vartheta_2-\delta_1-\delta_2-\delta_3-\gamma_1)I^*-\gamma_2(\delta_1+\delta_2+\delta_3){I^*}^2}{\delta_1(1+\gamma_2 I^*)}$$

and the following equation yields I^*:

$$D_1{I^*}^4+D_2{I^*}^3+D_3{I^*}^2+D_4I^*+D_5=0 \quad (5.9)$$

$$D_1=\alpha_2\gamma_2^2\alpha_1(\delta_1+\delta_2+\delta_3)^2$$

$$D_2 = (\alpha_2\gamma_2\alpha_1(\delta_1+\delta_2+\delta_3)(\delta_1+\delta_2+\delta_3+\gamma_1) + \gamma_2(\delta_1+\delta_2+\delta_3)\big(-\alpha_1\gamma_2(\delta_1+\delta_2+\delta_3)+\alpha_2\delta_1\gamma_2 + \alpha_2\alpha_1(\sigma\gamma_2-\delta_1-\delta_2-\delta_3-\gamma_1)\big)+\beta\gamma_2^2(\delta_1+\delta_2+\delta_3))$$

$$D_3 = ((\delta_1+\delta_2+\delta_3+\gamma_1)(-\alpha_1\gamma_2(\delta_1+\delta_2+\delta_3)+\alpha_2\delta_1\gamma_2+\alpha_2\alpha_1(\sigma\gamma_2-\delta_1-\delta_2-\delta_3-\gamma_1))+\gamma_2(\delta_1+\delta_2+\delta_3)(\delta_1\gamma_2+\alpha_1(\sigma\gamma_2-\delta_1-\delta_2-\delta_3-\gamma_1)+\alpha_2\delta_1+\alpha_2\alpha_1\sigma)-\beta\gamma_2(\sigma\gamma_2-2\delta_1-2\delta_2-2\delta_3-\gamma_1))$$

$$D_4 = ((\delta_1+\delta_2+\delta_3+\gamma_1)(\delta_1\gamma_2+\alpha_1(\sigma\gamma_2-\delta_1-\delta_2-\delta_3-\gamma_1)+\alpha_2\delta_1+\alpha_2\alpha_1\sigma) + \gamma_2(\delta_1+\delta_2+\delta_3)(\delta_1+\alpha_1\sigma)-\beta(2\sigma\gamma_2-\delta_1-\delta_2-\delta_3-\gamma_1))$$

$$D_5 = ((\delta_1+\delta_2+\delta_3+\gamma_1)(\delta_1+\alpha_1\sigma)-\beta\sigma) = (\delta_1+\delta_2+\delta_3+\gamma_1)(\delta_1+\alpha_1\sigma)(1-R_0)$$

According to Descarte's Rule of signs, the biquadratic equation (5.9) has a unique positive real I^* if any of the following conditions are fulfilled:

i. $D_1 > 0, D_2 < 0, D_3 < 0, D_4 < 0$ and $D_5 < 0$
ii. $D_1 > 0, D_2 > 0, D_3 < 0, D_4 < 0$ and $D_5 < 0$
iii. $D_1 > 0, D_2 > 0, D_3 > 0, D_4 < 0$ and $D_5 < 0$
iv. $D_1 > 0, D_2 > 0, D_3 > 0, D_4 > 0$ and $D_5 < 0$

If any of the aforementioned conditions are fulfilled, there will be a unique $I^* > 0$ that can be used to calculate the value of S^*. This means that there exists a unique endemic equilibrium $Y_2(S^*, I^*)$. Now, we analyse the local stability of Y_2. Now linearizing the matrix at $Y_2(S^*, I^*)$, we get the following Jacobian matrix

$$J(Y_2) = \begin{pmatrix} -a_1 - a_2e^{-\lambda\tau} & -a_3e^{-\lambda\tau} \\ a_2e^{-\lambda\tau} & a_3e^{-\lambda\tau} - a_4 - a_5 \end{pmatrix}$$

Where

$a_1 = \delta_1$, $a_2 = \frac{\beta I^*}{(1+\alpha_2 I^*)(1+\alpha_1 S^*)^2}$, $a_3 = \frac{\beta S^*}{(1+\alpha_1 S^*)(1+\alpha_2 I^*)^2}$, $a_4 = \delta_1+\delta_2+\delta_3$ and $a_5 = \frac{\gamma_1}{(1+\gamma_2 I^*)^2}$

Thus, we get the characteristic equation as

$$\lambda^{2\rho} + \lambda^{\rho}(a_1+a_4+a_5) + a_1(a_4+a_5) + \lambda^{\rho}e^{-\lambda\tau}(-a_3+a_2) + e^{-\lambda\tau}\big(-a_1a_3 + a_2(a_4+a_5)\big) = 0 \quad (5.10)$$

Case 5.4.2.1 Suppose $\tau = 0$, then equation (5.10) becomes

$$\lambda^{2\rho} + \lambda^{\rho}(B_1 + B_3) + (B_2 + B_4) = 0 \tag{5.11}$$

Where $B_1 = a_1 + a_4 + a_5$, $B_3 = -a_3 + a_2$, $B_2 = a_1(a_4 + a_5)$, $B_4 = -a_1a_3 + a_2(a_4 + a_5)$

Assume that

$$(G_1)\colon (B_1 + B_3) > 0, (B_2 + B_4) > 0,$$

Using the Routh-Hurwitz Criterion, we have established-

Proposition 5.1 For $\tau = 0$, if $R_0 > 1$ and assumption (G_1) is satisfied then the roots of (5.11) are real and negative. As a result, the endemic equilibrium $Y_2(S^*, I^*)$ is locally asymptotically stable.

Case 5.4.2.2 Suppose $\tau > 0$ and $R_0 > 1$ then equation (5.10) becomes

$$\lambda^{2\rho} + B_1\lambda^{\rho} + B_2 + B_3\lambda^{\rho}e^{-\lambda\tau} + B_4e^{-\lambda\tau} = 0 \tag{5.12}$$

Let $\lambda = i\omega$ $(\omega > 0)$ be a root of (5.12), then we have

$$\omega^{2\rho}(\cos\rho\pi + i\sin\rho\pi) + B_1\omega^{\rho}\left(\cos\frac{\rho\pi}{2} + i\sin\frac{\rho\pi}{2}\right) + B_2 + B_4(\cos\omega\tau - i\sin\omega\tau)$$
$$+ B_3\omega^{\rho}(\cos\omega\tau - i\sin\omega\tau)\left(\cos\frac{\rho\pi}{2} + i\sin\frac{\rho\pi}{2}\right) = 0$$

Separating the real and imaginary parts, we get

$$\left.\begin{aligned} C_1\cos\omega\tau + C_2\sin\omega\tau &= -C_3 \\ C_2\cos\omega\tau - C_1\sin\omega\tau &= -C_4 \end{aligned}\right\} \tag{5.13}$$

where

$$C_1 = B_3\omega^{\rho}\cos\frac{\rho\pi}{2} + B_4$$
$$C_2 = B_3\omega^{\rho}\sin\frac{\rho\pi}{2}$$
$$C_3 = \omega^{2\rho}\cos\rho\pi + B_1\omega^{\rho}\cos\frac{\rho\pi}{2} + B_2$$

$$C_4 = \omega^{2\rho} \sin \rho\pi + B_1 \omega^{\rho} \sin \frac{\rho\pi}{2}$$

It follows from (5.13) that

$$\sin \omega\tau = \frac{C_1 C_4 - C_2 C_3}{C_1^2 + C_2^2}$$

$$\cos \omega\tau = -\frac{C_1 C_3 + C_2 C_4}{C_1^2 + C_2^2}$$

By $\sin^2 \omega\tau + \cos^2 \omega\tau = 1$,

we get

$$C_3^2 + C_4^2 = C_1^2 + C_2^2.$$

By calculation we deduce that

$$\lambda^4 + N_1 \lambda^3 + N_2 \lambda^2 + N_3 \lambda + N_4 = 0$$

Where

$\lambda = \omega^{\rho}$, $N_1 = 2\, B_1 \cos \frac{\rho\pi}{2}$, $N_2 = B_1^2 + 2\, B_2 \cos \rho\pi - B_3^2$, $N_3 = 2(B_1 B_2 - B_3 B_4) \cos \frac{\rho\pi}{2}$, $N_4 = B_2^2 - B_4^2$.

Assume that

$$(G_2): \quad N_4 < 0$$

then equation (5.12) has at least one positive real root ω_0. Denote

$$\tau^{(i)} = \frac{1}{\omega_0} \left[\arccos \frac{C_1 C_3 + C_2 C_4}{C_1^2 + C_2^2} + 2\, i\pi \right] \quad i = 1, 2, 3\ldots$$

Define $\tau^0 = \min\{\tau^{(i)}\}$ $\quad i = 1, 2, 3\ldots$

To deduce the conditions for the occurrence of Hopf bifurcation, we propose the following hypothesis:

$$(G_3): \frac{\xi_1 \zeta_1 + \xi_2 \zeta_2}{\zeta_1^2 + \zeta_2^2} \neq 0,$$

where $\xi_1,\ \xi_2,\ \zeta_1, \zeta_2$ are defined as

$$\xi_1 = B_4\omega_0 \sin\omega_0\,\tau^0 + B_3\omega_0^{\rho+1} \sin\,(\omega_0\tau^0 - \frac{\rho\pi}{2})$$

$$\xi_2 = B_4\omega_0 \cos\omega_0\,\tau^0 + B_3\omega_0^{\rho+1} \cos\,(\omega_0\tau^0 - \frac{\rho\pi}{2})$$

$$\begin{aligned}\zeta_1 = {} & 2\,\rho\omega_0^{2\rho-1} \sin\rho\pi + \rho B_1\omega_0^{\rho-1} \sin\frac{\rho\pi}{2} \\ & + \rho\, B_3\omega_0^{\rho-1} \sin\left(\frac{\rho\pi}{2} - \omega_0\tau^0\right) \\ & - B_3\tau^0\omega_0^{\rho} \cos\left(\frac{\rho\pi}{2} - \omega_0\tau^0\right) - B_4\,\tau^0 \cos\omega_0\tau^0\end{aligned}$$

$$\begin{aligned}\zeta_2 = -\Big(2\,\rho\omega_0^{2\rho-1} \cos\rho\pi + \rho B_1\omega_0^{\rho-1} \cos\frac{\rho\pi}{2} \\ + \rho\, B_3\omega_0^{\rho-1} \cos\left(\frac{\rho\pi}{2} - \omega_0\tau^0\right) \\ + B_3\tau^0\omega_0^{\rho} \sin\left(\frac{\rho\pi}{2} - \omega_0\tau^0\right) - B_4\,\tau^0 \sin\omega_0\tau^0\Big)\end{aligned}$$

Lemma 5.1 Let $\lambda(\tau) = \varphi(\tau) + i\,\omega(\tau)$ be a root of the characteristic equation (5.12) near $\tau = \tau^i$ meeting $\varphi(\tau^i) = 0,\ \omega(\tau^i) = \omega_0$, then the transversality condition $Re\left[\frac{d\lambda}{d\tau}\right]\Big|_{(\tau=\tau^0,\omega=\omega_0)} \neq 0$ holds.

Proof. Differentiating both sides of (5.15) with respect to τ, we get

$$\frac{d\lambda}{d\tau} = \frac{(B_3\lambda^{\rho}+B_4)\lambda e^{-\lambda\tau}}{2\rho\lambda^{2\rho-1}+\rho B_1\lambda^{\rho-1}+\rho\, B_3\lambda^{\rho-1}e^{-\lambda\tau}-B_3\tau\lambda^{\rho}e^{-\lambda\tau}-B_4\tau e^{-\lambda\tau}} = \frac{\xi(\lambda)}{\zeta(\lambda)} \tag{5.14}$$

and

$$\left.\begin{aligned}\xi(\omega_0 i)|_{\tau=\tau^0} &= \xi_1 + i\xi_2 \\ \zeta(\omega_0 i)|_{\tau=\tau^0} &= \zeta_1 + i\zeta_2\end{aligned}\right\} \tag{5.15}$$

By computation, it can be derived from (5.14) that

$$Re\left[\frac{d\lambda}{d\tau}\right]\Big|_{(\tau=\tau^0,\omega=\omega_0)} = \frac{\xi_1\zeta_1 + \xi_2\zeta_2}{\zeta_1^2 + \zeta_2^2} \neq 0$$

This completes the proof.

Theorem 5.3 If assumptions (G_1)- (G_3) hold then the endemic equilibrium Y_2 of the system (5.3) is locally asymptotically stable for $\tau \in [0, \tau_0)$ and it undergoes Hopf bifurcation at Y_2 when $\tau = \tau_0$.

5.5 Numerical Simulations

To confirm the viability of the theoretical analysis on system stability and bifurcation, we investigate the system with the parameters used in (A. Kumar & Nilam, 2019), $\sigma = 11, \alpha_1 = 0.005, \alpha_2 = 0.005, \beta = 0.003, \delta_1 = 0.03, \delta_2 = 0.04, \delta_3 = 0.001, \gamma_1 = 0.02, \gamma_2 = 0.02,$ we get the unique endemic equilibrium Y_2 = (82.0164, 110.576) and the basic reproduction number R_0 = 4.266.

We now analyse the stability and Hopf bifurcation outcomes. First, we observe the effect of different fractional orders on the endemic equilibrium point of the system when there is no impact of latency delay i.e. $\tau = 0$. Figures 5.1 and 5.2 clearly show that the as the order of the fractional derivative decreases, the system accelerates its convergence to a steady state. Figure 5.3 demonstrates the influence of cure rate on infectives; as the cure rate grows, the number of infectives decreases significantly until it reaches a stable state. Figure 5.4 shows that as the constraint in treatment availability increases, so do infections, which is due to society's restricted resource availability.

Next, we investigate how the latency period delay (τ) affects the system's dynamical characteristics. Here we fix the fractional order $\rho = 0.85$. We obtain the critical values ω_0= 0.259347 and $\tau_0 = 4.3$. Figure 5.5 and 5.6 shows that the endemic equilibrium Y_2 is asymptotically stable when $\tau = 3.5 < \tau_0$, which agrees with the theorem 5.1. Figure 5.7 and 5.8 shows that the endemic equilibrium Y_2 is unstable when $\tau = 4.5 > \tau_0$ and a Hopf bifurcation occurs.

We also assess the effect of the fractional order ρ on the system dynamics. While selecting, $\tau = 3.7$, it can be seen from figures 5.9 and 5.10 that with the decrease of the fractional order ρ, the rate of convergence of the system speeds up. Setting, $\tau = 4.0$, system demonstrates an unstable behavior when fractional order $\rho = 1$ and hopf bifurcation occurs, however the endemic equilibrium of the system is locally stable when ρ = 0.8 or 0.9 (see Figure 5.11 and 5.12). This suggests that in a fractional order system, the unstable equilibrium of an integer order system could become stable. Figure 5.13 and 5.14 shows the effect of cure rate (γ_1) and limitation rate (γ_2) in treatment availability on infected population with various values of γ_1 and γ_2 at $\tau = 3.3$. Figure 5.13 depicts the decline in the number of infected population as the cure rate rises, and it is seen that the higher the cure rate, the less time it takes to achieve the steady state. Figure 5.14 depicts that the system undergoes bifurcation and could

not achieve its steady state as the limitation in treatment raises, which is due to the restricted resources in society.

Figure 5.15 shows that for fractional orders ρ = 0.8 and $\tau = 3.3$, when susceptibles adopt fewer preventive actions, the time to achieve steady state raises. The greater the number of people who take preventative measures, the more susceptible individuals are and lesser the infectives.

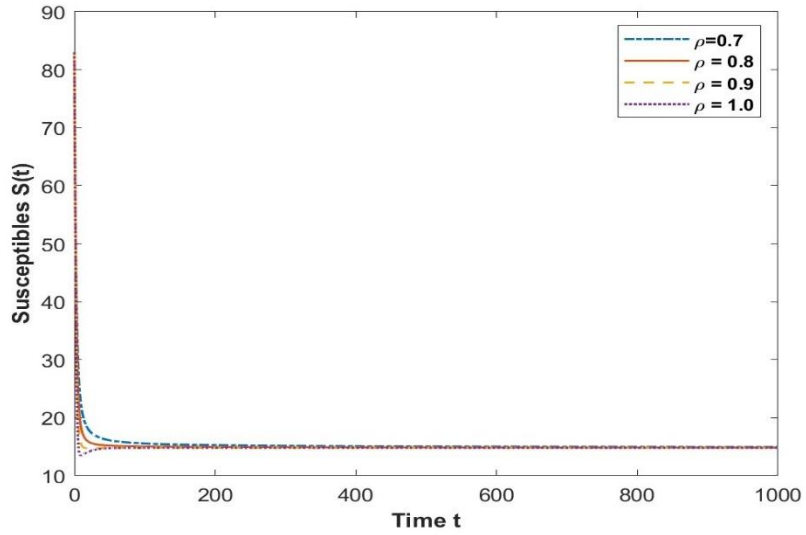

Figure 5.1 Effect of varying fractional orders on susceptibles

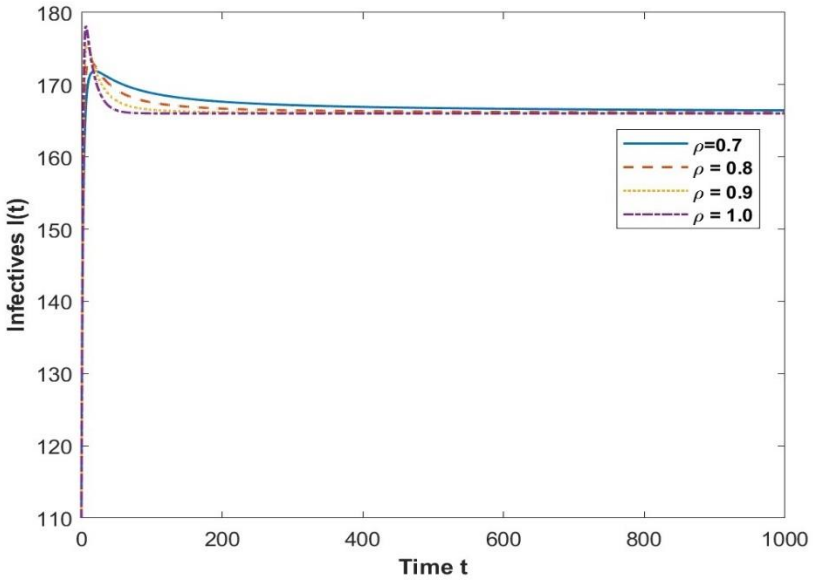

Figure 5.2 Effect of varying fractional orders on infectives

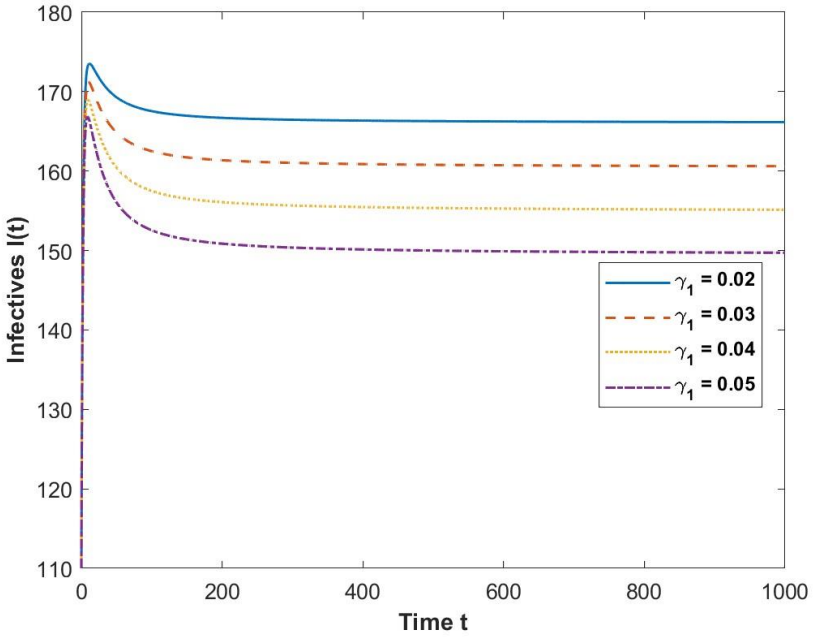

Figure 5.3 Effect of varying γ_1 on infectives when fractional order ρ = 0.85

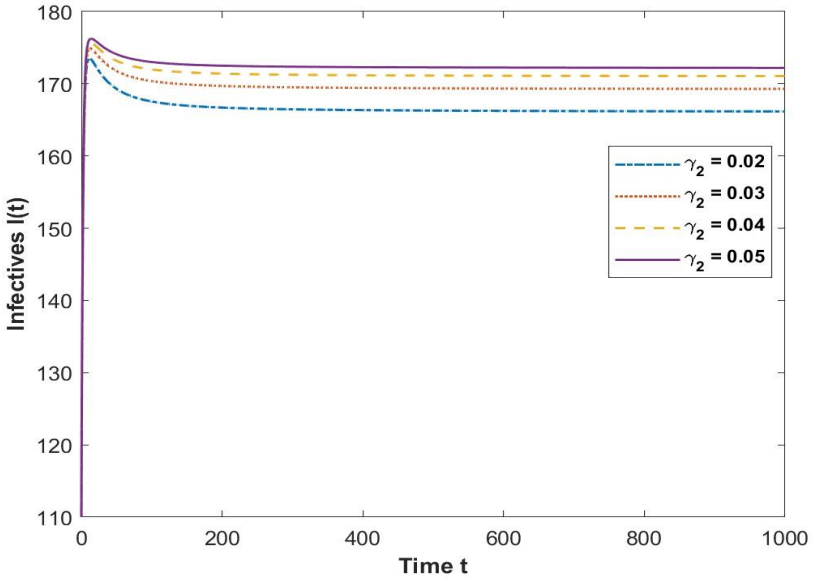

Figure 5.4 Effect of varying γ_2 on infectives when fractional order ρ = 0.85

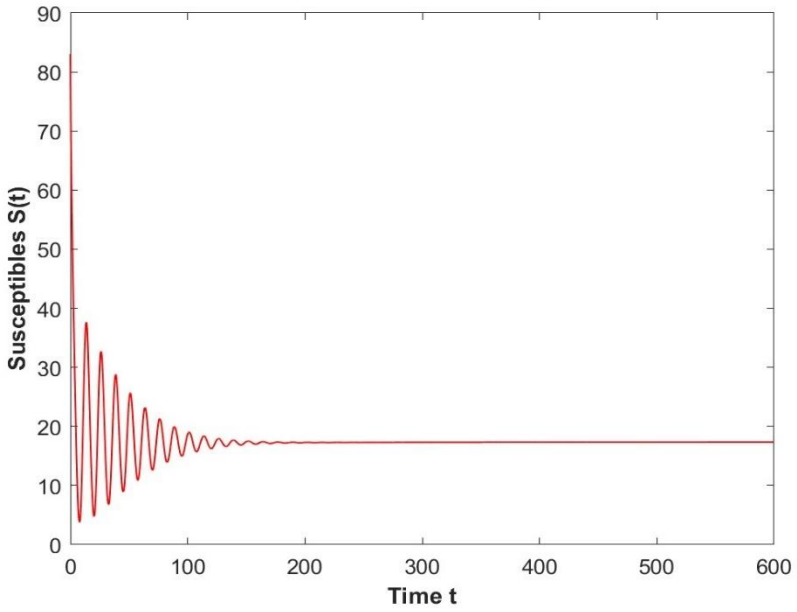

Figure 5.5 Time series for susceptible population when $\rho = 0.85, \tau = 4.1 < \tau_0$

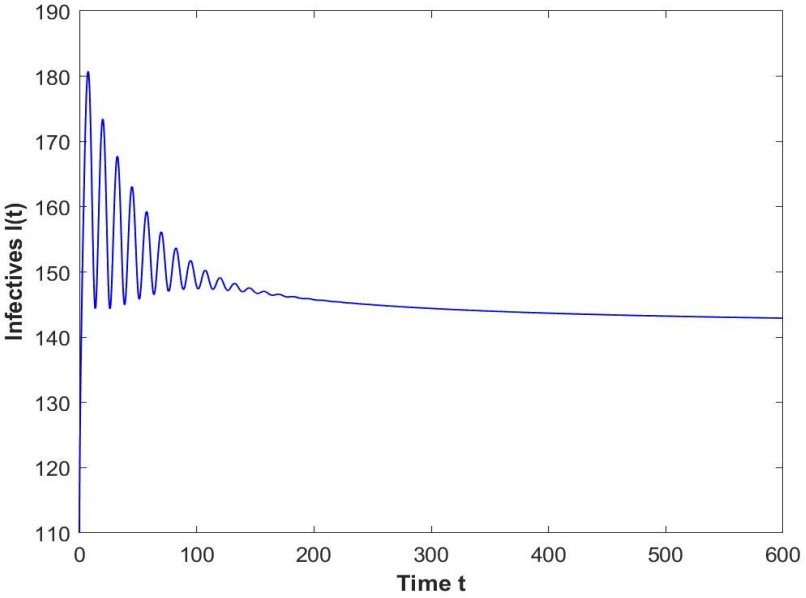

Figure 5.6 Time series for infected population when $\rho = 0.85, \tau = 4.1 < \tau_0$

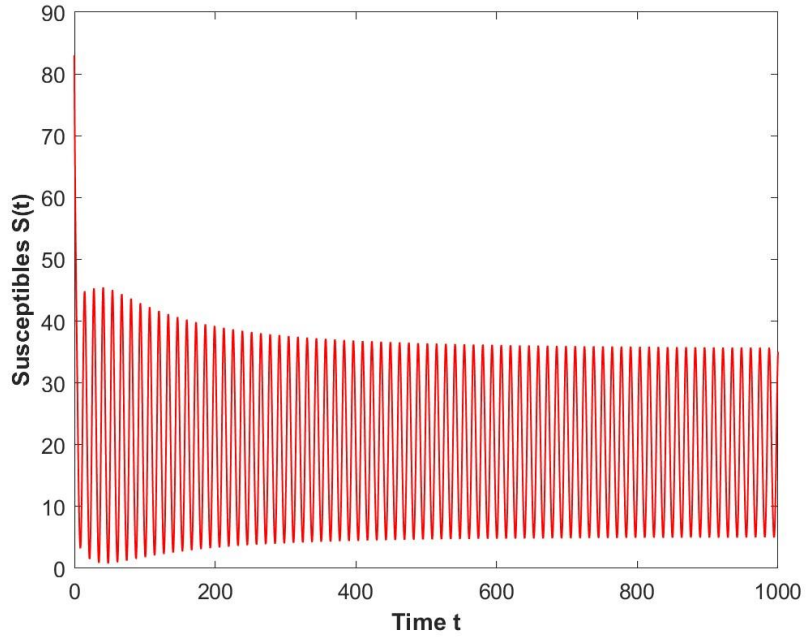

Figure 5.7 Time series for susceptible population when $\rho = 0.85, \tau = 4.5 > \tau_0$

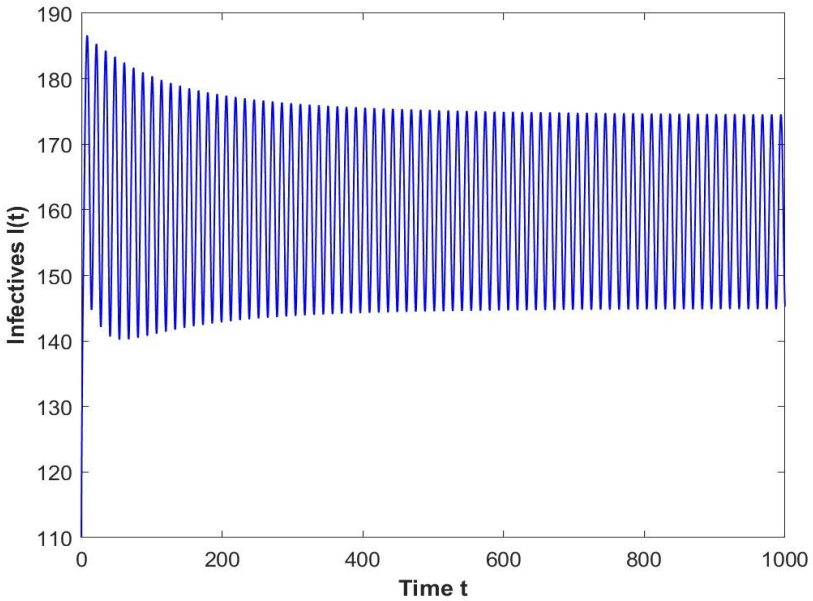

Figure 5.8 Time series for infected population when $\rho = 0.85, \tau = 4.5 > \tau_0$

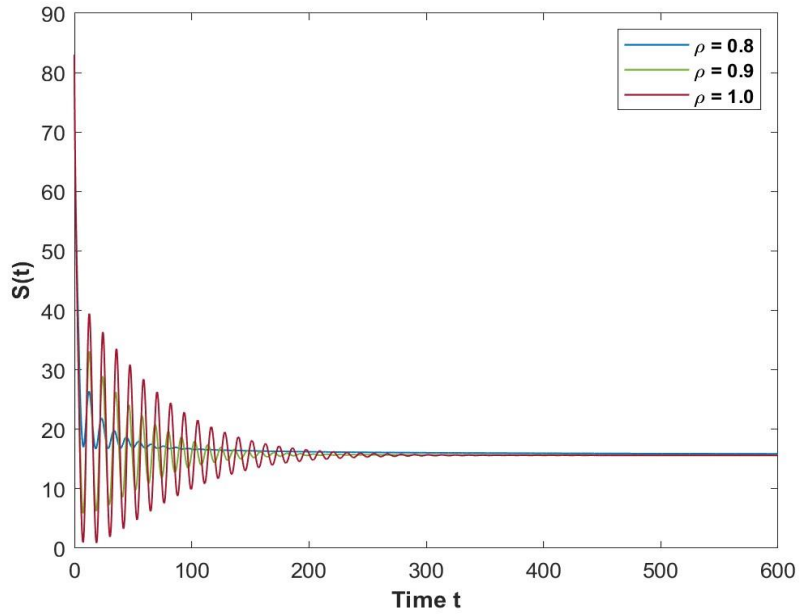

Figure 5.9 Time series for susceptible population when $\rho = 0.8$, 0.9 and 1, $\tau = 3.7$

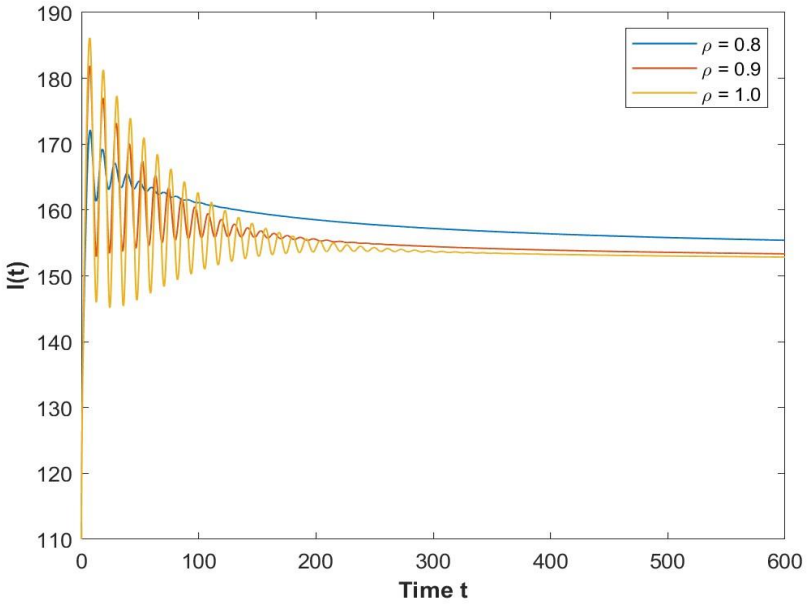

Figure 5.10 Time series for infected population when $\rho = 0.8$, 0.9 and 1, $\tau = 3.7$

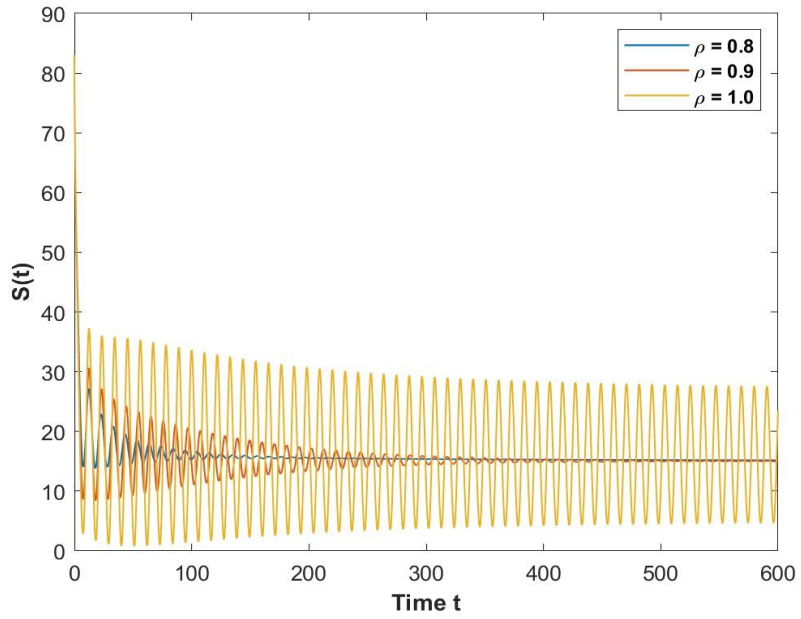

Figure 5.11 Time series for susceptible population when $\rho = 0.8$, 0.9 and 1, $\tau = 4$

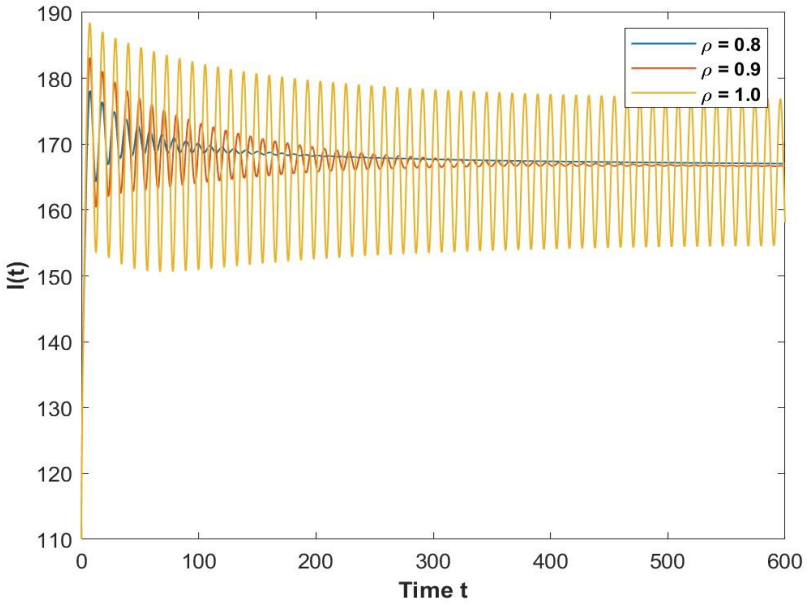

Figure 5.12 Time series for infected population when $\rho = 0.8$, 0.9 and 1, $\tau = 4$

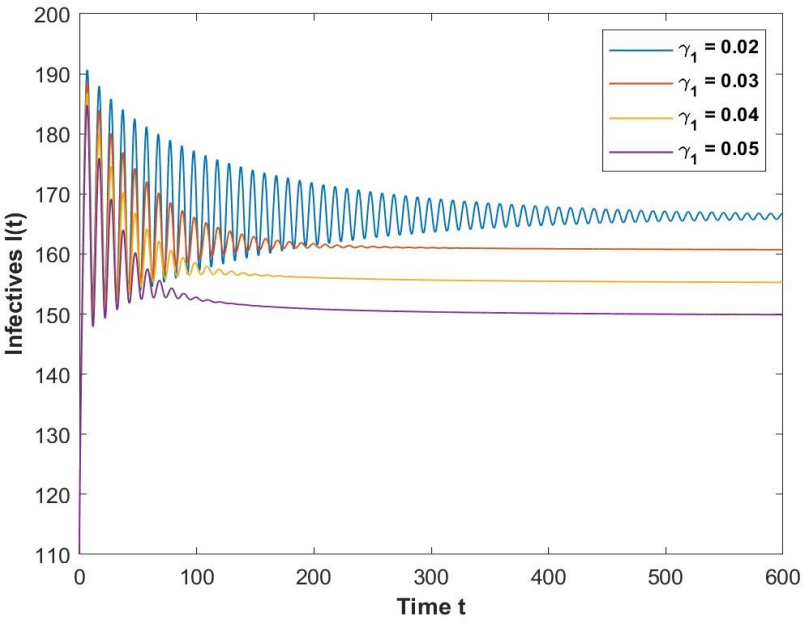

Figure 5.13 Effect of varying γ_1 on infectives when fractional order ρ = 0.8 and $\tau = 3.3$

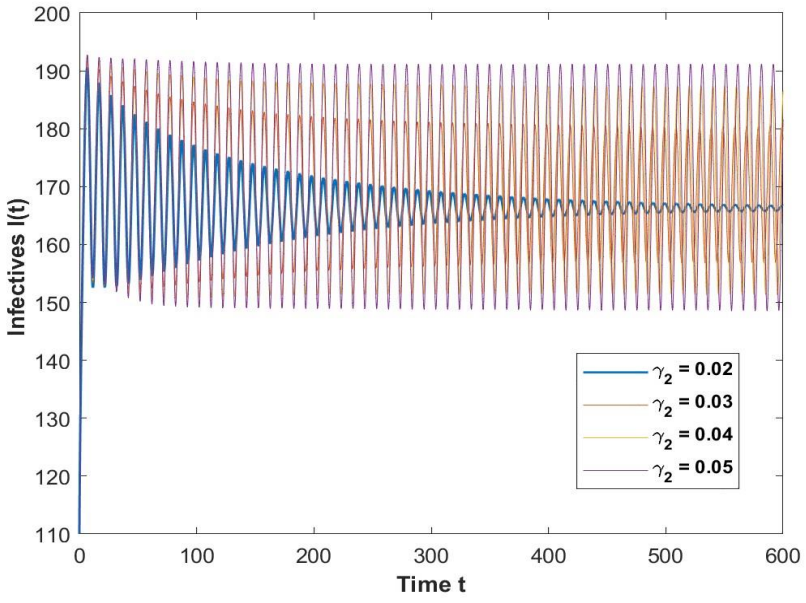

Figure 5.14 Effect of varying γ_2 on infectives when fractional order ρ = 0.8 and $\tau = 3.3$

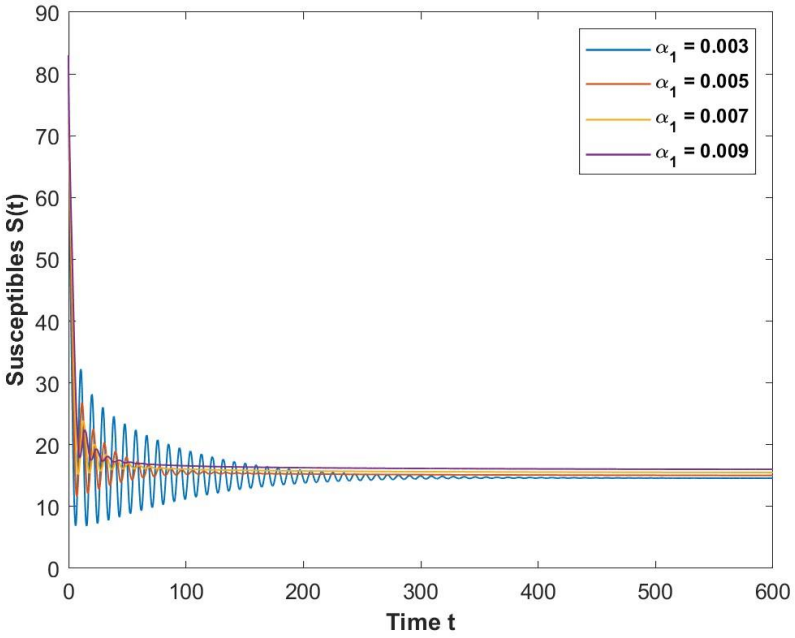

Figure 5.15 Effect of varying α_1 on susceptibles when fractional order ρ = 0.8 and $\tau = 3.3$

5.6 Conclusion

Many biological processes are more accurately modeled by utilizing fractional differential equations with time delay rather than classical order integer systems. We developed and assessed a Caputo fractional order Susceptible-Infectives-Recovered epidemic model with a time delay, Crowley Martin functional type incidence rate, and Holling type II treatment rate. Time delay and fractional order contribute significantly to the model's stability and complexity. We determined the possibility of equilibria in the underlying model and investigated the presence of positive and bounded solutions. By examining the characteristics, some adequate conditions for asymptotic stability in terms of fractional order and time delay were derived. When the time delay approaches critical values, the model undergoes Hopf bifurcation. The transversality condition was obtained to confirm the existence of a Hopf bifurcation for various threshold parameter values.

Furthermore, numerical simulations favouring the analytical work are achieved. As the fractional derivative represents long-term memory, different fractional orders result in varying rates of steady state stabilization. In addition, it is found that infection in society declines as the cure rate increases and the limitation in treatment availability decreases. Additionally, the findings demonstrate that incorporating non-integer order and time delays in the model substantially enhances the dynamics and enriches the model's stability requirement. By implementing time delays as a bifurcation point, one can infer that when time delays increase, the stability at equilibrium gets weakened and Hopf bifurcation develops.

CHAPTER 6

BIFURCATION ANALYSIS OF A DOUBLE DELAYED SIQR FRACTIONAL ORDER MODEL INCORPORATING HOLLING TYPE-II TREATMENT RATE AND MONOD-HALDANE INCIDENCE RATE

Fractional order and time delays are essential for biological systems with memory. A double delayed fractional order susceptible-infected-quarantine-recovered epidemic model with saturated incidence and treatment rates has been examined in this chapter. The model includes two time delays: one for the length of the incubation period, and another for the time delay caused by people's resistance to being placed under quarantine. Specifically, it is established that every solution is bounded and positive. Basic reproduction is computed first, and then the existence and stability of the endemic and disease-free equilibrium points are ascertained by examining the associated characteristic equations along with Hopf bifurcations. A Hopf bifurcation is seen in the model above the threshold parameters. The model experiences Hopf bifurcation when delays exceed critical values. The application of the acquired results is demonstrated by providing a few numerical simulation examples. Numerical simulations confirm that the dynamics and stability requirement of the epidemic model are improved by adding fractional order and time delays.

6.1 Introduction

For many years, infectious diseases produced by pathogens posed a major threat to human health. Several epidemic models have been developed and examined to comprehend the mechanisms of disease spread and forecast future patterns. Kermack and Mckendrick, who are regarded as the pioneers of "compartment modeling," put forth a compartment epidemic model for the spread of the black death in (Kermack & Mckendrick, 1927), which provided fresh insight into the study of infectious illnesses. Subsequently, a number of compartmental models were carried out to investigate how different infectious diseases spread. To illustrate, the well-known SIRS, SIS, and SIR models were developed initially in the 1980s (Li et al., 2014; Wang et al., 2012; Wu & Fu, 2011), where S, I, and R stand for susceptible, infectious, and recovered people, respectively. Many studies have used SEIR models to explore the transmission process (Shu et al., 2012; Yi et al., 2009; Zhou & Cui, 2011), taking into account the possibility that the disease may have minimal early symptoms and may remain dormant in the host for some time during the incubation period (E). Acute infectious infections, on the other hand, might also have symptoms that start appearing up immediately. Isolating affected individuals is one of the quickest and most efficient ways to prevent the infectious disease from progressing. To assess the efficacy of the quarantine strategy, a few SIQR compartmental models (Odagaki, 2021; Pinto & Carvalho, 2015) were developed, in which Q stands for the infectious persons who have been placed under quarantine.

Researchers have discovered through thorough study of the mechanisms underlying the transmission of certain infectious diseases that susceptible individuals do not become infectious instantaneously from contact with infected individuals; rather, a time lag must be taken into account to characterize the interval between contact with the infected and the onset of infectiousness (Li et al., 2012; J. Liu et al., 2018). In fact, there will inevitably be a time lag during various stages of the transmission process, including the incubation and immunity recovery phases. Time delays are therefore crucial variables to consider when researching pandemic diseases. Fractional calculus theory has been extensively used in many fields in the last several decades, including electromagnetic field theory, biology, optical and thermal systems, materials science, mechanical mechanics, and more (Agarwal et al., 2010; Alidousti & Ghaziani, 2017). It has been discovered that the laws and processes governing the evolution of certain natural science phenomena can be precisely described using fractional calculus. Moreover, it becomes apparent that fractional-order differential systems have the benefits of uncomplicated modeling, understandable parameter meaning, and precise characterization for certain materials and processes with memory and genetic properties (Alidousti & Ghahfarokhi, 2019; Auastasio, 1994; Laskin & Zaslavsky, 2006). As a result of this, fractional calculus has gained popularity among researchers as a new mathematical tool. Significant advancements have been made in this field, and the theory of fractional calculus is being introduced through an

increasing number of real-world problem-solving scenarios (Abdeljawad et al., 2017; Abdeljawad & Alzabut, 2018; Chen, 2008; Iswarya et al., 2019; Lin, 2007; Pratap et al., 2020; Rajchakit et al., 2019).

An SIQR compartmental model with an incubation period delay was examined by the authors in(X. Zhou & Cui, 2011). This model measures the time interval between a susceptible person's meet with an infected person and the point at which the person becomes infectious. However, S. Liu, L. Lu and M. Huang in (S. Liu et al., 2020) studied another SIQR model with an additional time delay that quantifies how long it will take for the infected and quarantined people to recover. They investigated how time delays affected the spread of the disease.

6.2 Formulation of Fractional order Mathematical Model

Motivated by the research of (X. Zhou & Cui, 2011) and (S. Liu et al., 2020), we examine the fractional-order SIQR model in this paper along with both time delays considering Monod-Haldane incidence and Holling Type II treatment rate. The Caputo derivative is described in definition 1in Appendix. We suggest the fractional-order delayed SIQR infectious disease model as follows:

$$\left.\begin{aligned} {}_0^C D_t^\rho S(t) &= \omega - \theta_1 S - \frac{\beta S(t-\tau_1) I(t-\tau_1)}{1+\alpha\left(I(t-\tau_1)\right)^2} \\ {}_0^C D_t^\rho I(t) &= \frac{\beta S(t-\tau_1) I(t-\tau_1)}{1+\alpha(I(t-\tau_1))^2} - (\theta_1+\theta_2) I - \delta I(t-\tau_2) - \frac{\sigma I}{1+\vartheta I} \\ {}_0^C D_t^\rho Q(t) &= \delta I(t-\tau_2) - (\theta_1+\theta_3+q) Q \\ {}_0^C D_t^\rho R(t) &= \frac{\sigma I}{1+\vartheta I} + qQ - \theta_1 R \end{aligned}\right\} \tag{6.1}$$

With initial conditions as: $S(t) = \varphi_1(t), I(t) = \varphi_2(t)$, $R(t) = \varphi_3(t)$, $\varphi_i(t) \geq 0, t \in [-\tau, 0]$

Table 6.1 Model parameters and variables

Parameter/ Variables	Description
$S(t)$	Susceptible population at time t
$I(t)$	Infected population at time t
$Q(t)$	Quarantined population at time t
$R(t)$	Recovered population at time t
ω	Recruitment rate
β	Rate of transmission
θ_1	Population's natural death rate

Parameter/ Variables	Description
θ_2	Population's death rate from disease
θ_3	Class Q death rate due to disease
δ	Rate of change from I to Q
q	Rate of change from Q to R
α	Cure rate
ϑ	Limitation rate in the treatment availability
τ_1	Incubation period delay
τ_2	Time delay due to resistance in people for undergoing quarantine

In addition to examining the presence and stability of the endemic and disease-free equilibriums, we also investigate how time delays and fractional order affect the spread of disease. With a fractional order derivative derived using Caputo sense, the memory effects in dynamical systems are characterized by a convolution integral with a power-law memory kernel for $0 < \rho \leq 1$ (see Definition 6.2). The decay rate of the memory kernel (temporal correlation function) is dependent on the fractional order ρ. A lower ρ value indicates that long memory (time-correlation functions) decays more slowly. After then, memory's influence diminishes as ρ approaches 1.

6.3 Basic Properties of the Model

Since model describes the dynamics of human population, therefore the system has non-negative solutions. Furthermore, it can be shown that all the state variables of the model are non-negative and bounded for all ($t \geq 0$). Let $\mathbb{R}^3_+ := \{X \epsilon \mathbb{R}^3 : X \geq 0\}$ and $X(t) = \big(S(t), I(t), R(t)\big)^T$ on non-negative solutions, the lemmas needed to prove the theorem are mentioned in Appendix

Theorem 6.1 All the solutions of the system (6.1) satisfying the initial conditions are non-negative and the solution will remain in region $P = \{(S, I, \mathrm{Q}, R) \in R^4_+ : 0 < S + I + \mathrm{Q} + R \leq \bar{L}\,, \bar{L} \geq C_E \frac{\omega}{\theta_1}\}$ for $t \geq 0$.

Proof. In order to prove the non-negativity of the system (6.1) it is assumed that there exist a $t_* > t_0$ such that $S(t_*) = 0$ and $S(t) < 0$ for $t \in (t_*, t_1]$ where t_1 is sufficiently close to t_*. If $S(t) = 0$, $D_t^\rho S(t_*) = \omega$, thus one obtains , $D_t^\rho S(t) > 0$ for all $t \in [t_*, t_1]$ and $D_t^\rho S(t) > \epsilon\, S(t)$ where $\epsilon > 0$. Hence one derives $S(t) > S(t_*) E_\rho(\epsilon(t - t_*)^\rho), t \in [t_*, t_1]$ where $E_\rho(z) = \sum_{k=0}^{\infty} \frac{z^k}{\Gamma(\rho k+1)}$ is the Mittag Leffler function, which

contradicts the assumption. Hence $S(t) > 0$ for any $t > t_0$. In the same manner $I(t), Q(t)$ and $R(t)$ are non-negative. Now we prove boundedness of solutions. Adding all the equations of the model (6.1), we obtain:

$$D_t^{\rho} N(t) = \omega - \theta_1 N(t) - \theta_2 I(t) - (\theta_1 + \theta_3) Q(t)$$

Where $N(t) = S(t) + I(t) + Q(t) + R(t)$. As $I(t)$and $Q(t) \geq 0$, we have

$$D_t^{\rho} N \leq \omega - \theta_1 N$$

Now consider the initial value problem $D_t^{\rho} \overline{N} = \omega - \theta_1 \overline{N}$, $\overline{N}(0) = \overline{N}_0$. Using comparison principle (Lu & Zhu, 2018), we obtain the following inequality:

$$N(t) \leq \overline{N}(t) \text{ for all } t \geq 0.$$

Now applying Laplace transform to the initial value problem we obtain

$$s^{\rho} L[\overline{N}(t)] - s^{\rho-1} \overline{N}_0 = \frac{\omega^{\rho}}{s} - \theta_1 L[\overline{N}(t)]$$

$$\Rightarrow L[\overline{N}(t)] = \frac{s^{\rho-1} \overline{N}_0}{s^{\rho} + \theta_1} + \frac{\omega^{\rho} s^{-1}}{s^{\rho} + \theta_1}$$

Using Lemma 3, we obtain

$$L\left[E_{\rho,1}(-\theta_1 t^{\rho})\right] = \frac{s^{\rho-1}}{s^{\rho} + \theta_1}$$

$$L\left[t^{\rho} E_{\rho,\rho+1}(-\theta_1 t^{\rho})\right] = \frac{s^{-1}}{s^{\rho} + \theta_1}$$

Applying inverse Laplace transform in the above two equations, we get

$$\overline{N}(t) = \overline{N}_0 E_{\rho,1}(-\theta_1 t^{\rho}) + \omega t^{\rho} E_{\rho,\rho+1}(-\theta_1 t^{\rho}),$$

using $D_t^{\rho} N \leq \omega - \theta_1 N$ we have

$$N(t) \leq N_0 E_{\rho,1}(-\theta_1 t^{\rho}) + \omega t^{\rho} E_{\rho,\rho+1}(-\theta_1 t^{\rho}),$$

By Lemma 4, we obtain

$$|N(t)| \leq \frac{N_0 C_E}{1 + \theta_1 t^{\rho}} + \frac{\omega t^{\rho} C_E}{1 + \theta_1 t^{\rho}}$$

Where C_E is constant given in Lemma 4. Hence, as $t \to \infty$, we have $N(t) \leq \bar{L}$ with $\bar{L} \geq C_E \frac{\omega}{\theta_1}$. Thus, the solutions are bounded and will remain in region P for $t \geq 0$. Therefore, theorem 6.1 is proved and solution remains in $\mathbb{R}_+^4$.

6.4 Mathematical analysis of the model

6.4.1 Stability Analysis and Hopf Bifurcation

We examine the existence and stability of the disease-free equilibrium point in this section. Furthermore, we study how fractional order and time delays affect the dynamics of the disease.

6.4.1.1 Existence and Stability Analysis of Disease Free Equilibrium

System (6.1) always has a disease-free equilibrium, which is easily determined by direct computation, $E_0 = (S_0, 0,0,0)$, where $S_0 = \frac{\omega}{\theta_1}$. Utilizing the next-generation matrix approach (Van Den Driessche & Watmough, 2002), the basic reproduction number is given by

$$R_0 = \frac{\beta\omega}{\theta_1(\theta_1+\theta_2+\delta+\sigma)} \tag{6.2}$$

Now we study the local stability of disease free equilibrium point. The characteristic matrix associated with system (6.1) is given by:

$$\Delta(\lambda) = \begin{bmatrix} -\theta_1 - \lambda & -\frac{\beta\omega}{\theta_1} e^{-\lambda\tau_1} & 0 & 0 \\ 0 & \frac{\beta\omega}{\theta_1} e^{-\lambda\tau_1} - (\theta_1+\theta_2) - \delta e^{-\lambda\tau_2} - \sigma & 0 & 0 \\ 0 & \delta e^{-\lambda\tau_2} & -(\theta_1+\theta_3+q) & 0 \\ 0 & 0 & q & -\theta_1 \end{bmatrix}$$

The corresponding characteristic polynomial at disease-free equilibrium $E_0\left(\frac{\omega}{\theta_1}, 0,0,0\right)$ is

$$(\theta_1 + \lambda^\rho)\left(-\frac{\beta\omega}{\theta_1} e^{-\lambda\tau_1} + (\theta_1+\theta_2) + \delta e^{-\lambda\tau_2} + \sigma + \lambda^\rho\right)(\theta_1+\theta_3+q+\lambda^\rho)(\theta_1 + \lambda^\rho) = 0 \tag{6.3}$$

Case 6.4.1.1.1 $\tau_1 > 0$ and $\tau_2 = 0$, equation (6.3) can be written as

$$(\theta_1 + \lambda^\rho)\left(-\frac{\beta\omega}{\theta_1}\, e^{-\lambda\tau_1} + (\theta_1 + \theta_2) + \delta + \sigma + \lambda^\rho\right)(\theta_1 + \theta_3 + q + \lambda^\rho)(\theta_1 + \lambda^\rho) = 0 \quad (6.4)$$

Three of the roots of the characteristic equation are given by

$$\lambda_1 = -\theta_1\,,\ \lambda_2 = -(\theta_1 + \theta_3 + q)\,,\ \lambda_3 = -\theta_1$$

and the other roots are the solution of the equation

$$-\frac{\beta\omega}{\theta_1}\, e^{-\lambda\tau_1} + (\theta_1 + \theta_2) + \delta + \sigma + \lambda^\rho = 0 \quad (6.5)$$

Suppose the above equation has a purely imaginary roots $\lambda = i\omega, \omega > 0$, then ω satisfy

$$(i\omega)^\rho + (\theta_1 + \theta_2 + \delta + \sigma) - \frac{\beta\omega}{\theta_1}\, e^{-(i\omega)\tau_1} = 0$$

$$\omega^\rho\left(\cos\frac{\rho\pi}{2} + i\sin\frac{\rho\pi}{2}\right) + (\theta_1 + \theta_2 + \delta + \sigma) - \frac{\beta\omega}{\theta_1}(\cos\omega\tau_1 - i\sin\omega\tau_1) = 0$$

Separating the real and imaginary parts of the above equation

$$\omega^\rho \cos\frac{\rho\pi}{2} + (\theta_1 + \theta_2 + \delta + \sigma) = \frac{\beta\omega}{\theta_1}\cos\omega\tau_1$$
$$\omega^\rho \sin\frac{\rho\pi}{2} = -\frac{\beta\omega}{\theta_1}\ \sin\omega\tau_1$$

Squaring and adding both sides, we get

$$\omega^{2\rho} + 2(\theta_1 + \theta_2 + \delta + \sigma)\cos\frac{\rho\pi}{2}\omega^\rho + (\theta_1 + \theta_2 + \delta + \sigma)^2(1 - R_0^2) = 0 \quad (6.6)$$

It is evident that equation (6.6) has no positive root if $R_0 < 1$, however equation (6.6) has a positive root if $R_0 > 1$. Hence equation (6.5) has no purely imaginary roots for $R_0 < 1$ and $\tau_1 > 0$. From (Z. Wang & Wang, 2018) the disease free equilibrium point E_0 is asymptotically stable for $\tau_1 > 0$ and $\tau_2 = 0$.

Case 6.4.1.1.2 $\tau_1 = 0$ and $\tau_2 > 0$, equation (6.3) can be reduced to

$$-\frac{\beta\omega}{\theta_1}\, e^{-\lambda\tau_1} + (\theta_1 + \theta_2) + \delta e^{-\lambda\tau_2} + \sigma + \lambda^\rho = 0 \quad (6.7)$$

Suppose the above equation has a purely imaginary roots $\lambda = i\omega, \omega > 0$, then ω satisfy

$$(i\omega)^{\rho} + (\theta_1 + \theta_2 + \sigma) + \delta e^{-i\omega\tau_2} - \frac{\beta\omega}{\theta_1} = 0$$

$$\omega^{\rho}\left(\cos\frac{\rho\pi}{2} + i\sin\frac{\rho\pi}{2}\right) + (\theta_1 + \theta_2 + \sigma) + \delta(\cos\omega\tau_2 - i\sin\omega\tau_2) - \frac{\beta\omega}{\theta_1} = 0$$

After separating the real and imaginary parts we obtain

$$\omega^{\rho}\cos\frac{\rho\pi}{2} + (\theta_1 + \theta_2 + \sigma) = \frac{\beta\omega}{\theta_1} - \delta\cos\omega\tau_2$$

$$\omega^{\rho}\sin\frac{\rho\pi}{2} = \delta\sin\omega\tau_2$$

Squaring and adding both sides, we get

$$\omega^{2\rho} + 2(\theta_1 + \theta_2 + \sigma)\cos\frac{\rho\pi}{2}\omega^{\rho} + (\theta_1 + \theta_2 + \sigma)^2 - \left(\left(\frac{\beta\omega}{\theta_1}\right)^2 + \delta^2 - 2\frac{\beta\omega}{\theta_1}\delta\cos\omega\tau_2\right) = 0 \quad (6.8)$$

Since $\omega^{\rho} > 0$, $\cos\frac{\rho\pi}{2} > 0$ and the assumption

$$C_1: \left(\left(\frac{\beta\omega}{\theta_1}\right)^2 + \delta^2 - 2\frac{\beta\omega}{\theta_1}\delta\cos\omega\tau_2\right) < (\theta_1 + \theta_2 + \sigma)^2$$

imply that equation (6.8) has no positive real solutions. Furthermore, we can infer that equation (6.7) has no purely imaginary roots for $\tau_2 > 0$. From (Kashkynbayev & Rihan, 2021) the disease free equilibrium point E_0 is asymptotically stable for $\tau_1 = 0$ and $\tau_2 > 0$.

Case 6.4.1.1.3 $\tau_1 > 0$ and $\tau_2 > 0$, equation (6.3) can be reduced to

$$-\frac{\beta\omega}{\theta_1}e^{-\lambda\tau_1} + (\theta_1 + \theta_2) + \delta e^{-\lambda\tau_2} + \sigma + \lambda^{\rho} = 0 \quad (6.9)$$

Suppose the above equation has a purely imaginary roots $\lambda = i\omega, \omega > 0$, then ω satisfy

$$(i\omega)^{\rho} + (\theta_1 + \theta_2 + \sigma) + \delta e^{-i\omega\tau_2} - \frac{\beta\omega}{\theta_1}e^{-i\omega\tau_1} = 0$$

$$\omega^{\rho}\left(\cos\frac{\rho\pi}{2} + i\sin\frac{\rho\pi}{2}\right) + (\theta_1 + \theta_2 + \sigma) + \delta(\cos\omega\tau_2 - i\sin\omega\tau_2) - \frac{\beta\omega}{\theta_1}(\cos\omega\tau_1 - i\sin\omega\tau_1) = 0$$

Separating the real and imaginary parts we get

$$\omega^{\rho}\cos\frac{\rho\pi}{2}+(\theta_1+\theta_2+\sigma)=\frac{\beta\omega}{\theta_1}\cos\omega\tau_1-\delta\cos\omega\tau_2$$

$$\omega^{\rho}\sin\frac{\rho\pi}{2}=\delta\sin\omega\tau_2-\frac{\beta\omega}{\theta_1}\sin\omega\tau_1$$

Squaring and adding both sides, we get

$$\omega^{2\rho}+2(\theta_1+\theta_2+\sigma)\cos\frac{\rho\pi}{2}\omega^{\rho}+(\theta_1+\theta_2+\sigma)^2-\left(\left(\frac{\beta\omega}{\theta_1}\right)^2+\delta^2-2\frac{\beta\omega}{\theta_1}\delta\cos\omega(\tau_2-\tau_1)\right)=0 \quad (6.10)$$

Since $\omega^{\rho}>0$, $\cos\frac{\rho\pi}{2}>0$ and the assumption

$$C_2:\left(\left(\frac{\beta\omega}{\theta_1}\right)^2+\delta^2-2\frac{\beta\omega}{\theta_1}\delta\cos\omega(\tau_2-\tau_1)\right)<(\theta_1+\theta_2+\sigma)^2$$

imply that equation (6.10) has no positive real solutions. Furthermore, we can infer that equation (6.9) has no purely imaginary roots for $\tau_2>0$. From (Kashkynbayev & Rihan, 2021) the disease free equilibrium point E_0 is asymptotically stable for $\tau_1>0$ and $\tau_2>0$.

Case 6.4.1.1.4 $\tau_1=0$ and $\tau_2=0$, equation (6.3) can be changes to

$$(\theta_1+\lambda^{\rho})\left(-\frac{\beta\omega}{\theta_1}+(\theta_1+\theta_2+\delta+\sigma)+\lambda^{\rho}\right)(\theta_1+\theta_3+q+\lambda^{\rho})(\theta_1+\lambda^{\rho})=0$$
$$(\delta_1+\lambda^{\rho})\left((\theta_1+\theta_2+\delta+\sigma)(1-R_0)+\lambda^{\rho}\right)(\theta_1+\theta_3+q+\lambda^{\rho})(\theta_1+\lambda^{\rho})=0 \quad (6.11)$$

It is clear that all the roots of the equation (6.11) will have negative real parts if $R_0<1$. Then, E_0 is locally asymptotically stable if $R_0<1$ and $\tau_1,\tau_2=0$.

Theorem 6.2 Disease free equilibrium is locally asymptotically stable if assumptions C_1, C_2 are satisfied and $R_0<1$ and unstable if $R_0>1$ for $\tau_1,\tau_2\geq 0$.

6.4.1.2 Existence and Stability Analysis of Endemic Equilibrium Point

The endemic equilibria $E^*(S^*,I^*,Q^*,R^*)$ of the system (6.1) can be deduced by the following equations.

$$\left.\begin{array}{c} \omega - \theta_1 S^* - \frac{\beta S^*(t) I^*(t)}{1+\alpha I^*(t)^2} = 0 \\ \frac{\beta S^*(t) I^*(t)}{1+\alpha I^*(t)^2} - (\theta_1 + \theta_2) I^* - \delta I^*(t) - \frac{\sigma I^*}{1+\vartheta I^*} = 0 \\ \delta I^*(t) - (\theta_1 + \theta_3 + q) Q^* = 0 \\ \frac{\sigma I^*}{1+\vartheta I^*} + q Q^* - \theta_1 R^* = 0 \end{array}\right\} \quad (6.12)$$

Which gives

$$S^* = \frac{\omega(1+\alpha I^{*2})}{\beta I^* + \theta_1(1+\alpha I^{*2})},$$

$$Q^* = \frac{\delta I^*}{(\theta_1 + \theta_3 + q)},$$

$$R^* = \frac{\sigma I^*(\theta_1 + \theta_3 + q) + q\delta I^*(1+\vartheta I^*)}{\theta_1(1+\vartheta I^*)(\theta_1 + \theta_3 + q)}$$

And I^* is the positive solution of the equation given below:

$$M_0 + M_1 I^* + M_2 I^{*2} + M_3 I^{*3} + M_4 I^{*4} + M_5 I^{*5} = 0 \quad (6.13)$$

Where

$M_0 = \theta_1(\theta_1 + \theta_2 + \delta + \sigma)(R_0 - 1)$
$M_1 = \beta\omega\vartheta - (\theta_1 + \theta_2 + \delta)\beta - \vartheta\theta_1 - \sigma\beta$

$M_2 = \beta\omega\alpha - (\theta_1 + \theta_2 + \delta)\vartheta\beta - 2\sigma\alpha\theta_1 - 2(\theta_1 + \theta_2 + \delta)\alpha\theta_1$

$M_3 = \alpha\beta(\omega\vartheta - (\theta_1 + \theta_2 + \delta) - \sigma) - 2(\theta_1 + \theta_2 + \delta)\alpha\vartheta\theta_1$

$M_4 = -\theta_1\alpha^2(\theta_1 + \theta_2 + \delta + \sigma) - (\theta_1 + \theta_2 + \delta)\,\vartheta\beta\alpha$

$M_5 = -(\theta_1 + \theta_2 + \delta)\,\vartheta\theta_1\alpha^2$

Using Descartes' rule of sign, the existence of a unique positive real root I^* of equation (6.13) is required to satisfy any of the following conditions:

i. $M_1 > 0, M_2 > 0$ and $M_3 < 0$

ii. $M_1 > 0, M_2 < 0$ and $M_3 < 0$

iii. $M_1 < 0, M_2 < 0$ and $M_3 < 0$

After getting the values of I^*, we can obtain the values of S^*, Q^* and R^*. Hence a unique endemic equilibrium $E^*(S^*, I^*, Q^*, R^*)$ exists if any of the above condition holds true. Assume that

$$(\mathcal{H}_1):\ R_0 = \frac{\beta\omega}{\theta_1(\theta_1 + \theta_2 + \delta + \sigma)} > 1$$

Now to explore the local stability of $E^*(S^*, I^*, Q^*, R^*)$,we linearize the system (6.1) at endemic equilibrium point $E^*(S^*, I^*, Q^*, R^*)$ and obtain the following Jacobian matrix

$$J(E^*) = \begin{bmatrix} -n_1 - n_2 e^{-\lambda\tau_1} & -n_3 e^{-\lambda\tau_1} & 0 & 0 \\ n_2 e^{-\lambda\tau_1} & n_3 e^{-\lambda\tau_1} - n_4 - n_5 e^{-\lambda\tau_2} - n_6 & 0 & 0 \\ 0 & n_5 e^{-\lambda\tau_2} & -n_1 - n_7 & 0 \\ 0 & n_6 & q & -n_1 \end{bmatrix}$$

Where $n_1 = \theta_1, n_2 = \frac{\beta I^*}{1+\alpha I^{*2}}$, $n_3 = \frac{-\beta S^*(1-\alpha I^{*2})}{(1+\alpha I^{*2})^2}$, $n_4 = \theta_1 + \theta_2, n_5 = \delta, n_6 = \frac{\sigma}{(1+\vartheta I^*)^2}$ and $n_7 = \theta_3 + q$

The characteristic equation is

$$\left[\left(\lambda^\rho + n_1 + n_2 e^{-\lambda\tau_1}\right)\left(\lambda^\rho - n_3 e^{-\lambda\tau_1} + n_4 + n_5 e^{-\lambda\tau_2} + n_6\right) + n_2 n_3 e^{-2\lambda\tau_1}\right] \times (\lambda^\rho + n_1 + n_7)(\lambda^\rho + n_1) = 0 \quad (6.14)$$

Suppose that $\tau_1 = \tau_2 = 0$ then the above equation (6.14) reduced to

$$[\lambda^{2\rho} + (A_1 + A_3)\lambda^\rho + (A_2 + A_4)] \times (\lambda^\rho + n_1 + n_7)(\lambda^\rho + n_1) = 0 \quad (6.15)$$

Where

$A_1 = n_1 + n_4 + n_5 + n_6$

$A_3 = n_2 - n_3$

$A_2 = n_1(n_4 + n_5 + n_6)$

$A_4 = n_2(n_4 + n_5 + n_6) - n_1 n_3$

Given that n_1 and n_7 are positive constants, we must take the first factor of (6.15) into account. Suppose that

$(\mathcal{H}_2)$: $(A_1 + A_3) > 0,\ (A_2 + A_4) > 0$, then by the Routh-Hurwitz criterion we have-

Proposition 6.1 For $\tau_1 = \tau_2 = 0$, if assumptions $(\mathcal{H}_1)$ and $(\mathcal{H}_2)$ are satisfied, then the roots of (12) are real and negative. Therefore, the Endemic Equilibrium point $E^*(S^*, I^*, Q^*, R^*)$ is locally asymptotically stable.

Case 6.4.1.2.1 $\tau_1 > 0$ and $\tau_2 = 0$

Since variables Q and R are not included in the first two equations of the system (6.1) and the eigen values corresponding to Q and R are $\lambda^\rho = -n_1 - n_7$ and $\lambda^\rho = -n_1$, therefore we can consider the following subsystem that consists of the first two equations.

$$\left.\begin{aligned} {}_{t_0}^{C}D_t^\rho S(t) &= \omega - \theta_1 S - \frac{\beta S(t-\tau_1)I(t-\tau_1)}{1+\alpha I(t-\tau_1)^2} \\ {}_{t_0}^{C}D_t^\rho I(t) &= \frac{\beta S(t-\tau_1)I(t-\tau_1)}{1+\alpha I(t-\tau_1)^2} - (\theta_1+\theta_2)I - \delta I(t-\tau_2) - \frac{\sigma I}{1+\vartheta I} \end{aligned}\right\} \tag{6.16}$$

Obviously (S^*, I^*) is the unique positive equilibrium point of system (6.1) when $R_0 > 1$ and the characteristic equation (6.14) has the following form

$$\left[\left(\lambda^\rho + n_1 + n_2 e^{-\lambda\tau_1}\right)\left(\lambda^\rho - n_3 e^{-\lambda\tau_1} + n_4 + n_5 + n_6\right) + n_2 n_3 e^{-2\lambda\tau_1}\right] = 0$$

Which can be written as

$$\lambda^{2\rho} + A_1\lambda^\rho + A_2 + A_3\lambda^\rho e^{-\lambda\tau_1} + A_4 e^{-\lambda\tau_1} = 0 \tag{6.17}$$

Let $\lambda = \omega i (\omega > 0)$ be a root of (14) then we have

$$\begin{aligned} \omega^{2\rho}(\cos\rho\pi + i\sin\rho\pi) + A_1\omega^\rho\left(cos\frac{\rho\pi}{2} + i\sin\frac{\rho\pi}{2}\right) + A_2 \\ + A_4(\cos\omega\tau_1 - \sin\omega\tau_1) \\ + A_3\omega^\rho(\cos\omega\tau_1 - \sin\omega\tau_1)\left(cos\frac{\rho\pi}{2} + i\sin\frac{\rho\pi}{2}\right) = 0 \end{aligned}$$

Separating the real and imaginary parts

$$\left.\begin{aligned} B_1 cos\omega\tau_1 + B_2 sin\omega\tau_1 &= -B_3 \\ B_2\, cos\omega\tau_1 - B_1 sin\omega\tau_1 &= -B_4 \end{aligned}\right\} \tag{6.18}$$

Where $B_1 = A_3\omega^\rho cos\frac{\rho\pi}{2} + A_4$, $B_2 = A_3\omega^\rho sin\frac{\rho\pi}{2}$, $B_3 = \omega^{2\rho}cos\rho + A_1\omega^\rho cos\frac{\rho\pi}{2} + A_2$, $B_4 = \omega^{2\rho}sin\rho\pi + A_1\omega^\rho sin\frac{\rho\pi}{2}$.

It follows from (6.18) that

$sin\omega\tau_1 = \frac{B_1B_4 - B_2B_3}{B_1^2 + B_2^2}$, $cos\omega\tau_1 = -\frac{B_1B_3 + B_2B_4}{B_1^2 + B_2^2}$, by $sin^2\omega\tau_1 + cos^2\omega\tau_1 = 1$, we get

$$B_3^2 + B_4^2 = B_1^2 + B_2^2.$$

By simple calculations, we deduce

$$\zeta^4 + C_1\zeta^3 + C_2\zeta^2 + C_3\zeta + C_4 = 0,$$

Where $\zeta = \omega^\rho, C_1 = 2A_1 cos\frac{\rho\pi}{2}$, $C_2 = A_1^2 + 2A_2 cos\rho\pi - A_3^2$, $C_3 = 2(A_1A_2 - A_3A_4)cos\frac{\rho\pi}{2}$, $C_4 = A_2^2 - A_4^2$

Assume that

$$(\mathcal{H}_3)\text{: } C_4 < 0,$$

then (6.17) has at least one positive real root ω_0. Denote

$$\tau_1^i = \frac{1}{\omega_0}\left[arccos\left(\frac{B_1B_3 + B_2B_4}{B_1^2 + B_2^2}\right) + 2i\pi\right], i = 0,1,2 \ldots$$

Define the bifurcation point as

$$\tau_1^0 = \min\left(\tau_1^i\right), \quad i = 0,1,2 \ldots$$

To derive the conditions for the existence of hopf bifurcation, we make the following hypothesis:

$$(\mathcal{H}_4)\text{: } \frac{E_1F_1 + E_2F_2}{F_1^2 + F_2^2} \neq 0,$$

The expressions of E_1, E_2, F_1, F_2 are as follows:

$$E_1 = A_3\omega_0^{\rho+1}\sin\left(\omega_0\tau_1^0 - \frac{\rho\pi}{2}\right) + A_4\omega_0\, sin\omega_0\tau_1^0$$

$$E_2 = A_3\omega_0^{\rho+1}\cos\left(\omega_0\tau_1^0 - \frac{\rho\pi}{2}\right) + A_4\omega_0 cos\omega_0\tau_1^0$$

$$F_1 = 2\rho\omega_0^{2\rho-1}sin\rho\pi + \rho A_1\omega_0^{\rho-1}\sin\frac{\rho\pi}{2} + \rho A_3\omega_0^{\rho-1}\sin\left(\frac{\rho\pi}{2} - \omega_0\tau_1^0\right) - A_3\tau_1^0\omega_0^\rho\cos\left(\frac{\rho\pi}{2} - \omega_0\tau_1^0\right) - A_4\tau_1^0 cos\omega_0\tau_1^0$$

$$F_2 = -2\rho\omega_0^{2\rho-1}cos\rho\pi - \rho A_1\omega_0^{\rho-1}\cos\frac{\rho\pi}{2} - \rho A_3\omega_0^{\rho-1}\cos\left(\frac{\rho\pi}{2} - \omega_0\tau_1^0\right) - A_3\tau_1^0\omega_0^\rho\sin\left(\frac{\rho\pi}{2} - \omega_0\tau_1^0\right) + A_4\tau_1^0 sin\omega_0\tau_1^0$$

Lemma 6.1 Let $\lambda(\tau_1) = \varphi(\tau_1) + i\omega(\tau_1)$ be a root of the characteristic equation (6.17) near $\tau_1 = \tau_1^i$ meeting $\varphi(\tau_1^i) = 0$, $\omega(\tau_1^i) = \omega_0$, then the transversality condition $Re\left[\frac{d\lambda}{d\tau_1}\right]\Big|_{(\tau_1=\tau_1^0,\omega=\omega_0)} \neq 0$ holds.

Proof. Differentiating both sides of (6.14) with respect to τ_1, we get

$$\frac{d\lambda}{d\tau_1} = \frac{\lambda(A_3\lambda^\rho + A_4)e^{-\lambda\tau_1}}{2\rho\lambda^{2\rho-1} + \rho A_1\lambda^{\rho-1} + \rho A_3\lambda^{\rho-1}e^{-\lambda\tau_1} - A_3\tau_1\lambda^\rho e^{-\lambda\tau_1} - A_4\,\tau_1 e^{-\lambda\tau_1}} = \frac{E(\lambda)}{F(\lambda)} \tag{6.19}$$

and

$$\left.\begin{aligned} E(\omega_0 i)|_{\tau_1=\tau_1^0} &= E_1 + iE_2 \\ F(\omega_0 i)|_{\tau_1=\tau_1^0} &= F_1 + iF_2 \end{aligned}\right\} \tag{6.20}$$

By straightforward computation, it can be derived from (6.19) that

$$Re\left[\frac{d\lambda}{d\tau_1}\right]\Big|_{(\tau_1=\tau_1^0,\omega=\omega_0)} = \frac{E_1F_1 + E_2F_2}{F_1^2 + F_2^2} \neq 0$$

The proof is complete.

Theorem 6.3. Suppose $\tau_2 = 0$, if assumptions $(\mathcal{H}_1)$- $(\mathcal{H}_4)$ hold, then :

(i) The endemic equilibrium E^* of system (6.1) is locally asymptotically stable for $\tau_1 \in [0, \tau_1^0)$;

(ii) System (6.1) undergoes hopf bifurcation at E^* when $\tau_1 = \tau_1^0$.

Case 6.4.1.2.2 $\tau_1 = 0$ and $\tau_2 > 0$ then equation (6.14) becomes

$$\left(\lambda^\rho + n_1 + n_2e^{-\lambda\tau_1}\right)\left(\lambda^\rho - n_3e^{-\lambda\tau_1} + n_4 + n_5e^{-\lambda\tau_2} + n_6\right) + n_2n_3e^{-2\lambda\tau_1} = 0 \tag{6.21}$$

Suppose that $\lambda = \omega i(\omega > 0)$ is a root of (6.21), then it follows that

$$\varphi_1(\lambda) + \varphi_2(\lambda)e^{-\lambda\tau_2} = 0 \tag{6.22}$$

where $\varphi_1(\lambda) = \lambda^{2\rho} + (a_1 + a_2)\lambda^\rho + a_1a_2$, $\varphi_2(\lambda) = a_3\lambda^\rho + a_2a_3$

$a_1 = n_4 + n_6 - n_3$
$a_2 = n_2 - n_1$
$a_3 = n_5$

Multiplying both sides of equation (6.22) by $e^{\lambda\tau_2}$, we have

$$\varphi_1(\lambda)e^{\lambda\tau_2} + \varphi_2(\lambda) = 0 \tag{6.23}$$

Substituting $\lambda = \omega i = \omega\left(cos\frac{\pi}{2} + i\, sin\frac{\pi}{2}\right)$ $(\omega > 0)$ in equation (6.23) and separating the real and imaginary parts gives

$$\left.\begin{aligned} \varphi_1^R cos\omega\tau_2 - \varphi_1^I sin\omega\tau_2 = \varphi_2^R \\ \varphi_1^I cos\omega\tau_2 + \varphi_1^R sin\omega\tau_2 = -\varphi_2^I \end{aligned}\right\} \tag{6.24}$$

where φ_i^R, φ_i^I are the real and imaginary parts of φ_i, $i = 1,2$ respectively, and

$$\varphi_1^R = \omega^{2\rho} cos\rho\pi + (a_1 + a_2)\omega^\rho cos\frac{\rho\pi}{2} + a_1 a_2$$
$$\varphi_1^I = \omega^{2\rho} sin\rho\pi + (a_1 + a_2)\omega^\rho sin\frac{\rho\pi}{2}$$
$$\varphi_2^R = a_3\omega^\rho cos\frac{\rho\pi}{2} + a_2 a_3$$
$$\varphi_2^I = a_3\omega^\rho Sin\frac{\rho\pi}{2}$$

It is easy to get

$$\left.\begin{aligned} cos\omega\tau_2 = \frac{-\varphi_2^R\varphi_1^R - \varphi_2^I\varphi_1^I}{(\varphi_1^R)^2 + (\varphi_1^I)^2} = \Phi_1(\omega_1) \\ sin\omega\tau_2 = \frac{-\varphi_1^R\varphi_2^I + \varphi_1^I\varphi_2^R}{(\varphi_1^R)^2 + (\varphi_1^I)^2} = \Phi_2(\omega_1) \end{aligned}\right\} \tag{6.25}$$

Based on (6.25), we obtain that

$$\Phi_1^2(\omega_1) + \Phi_2^2(\omega_1) = 1 \tag{6.26}$$

Assume that equation (6.26) has at least one positive real root ω_1, then it follows from the first equation of (6.25) that

$$\tau_2^i = \frac{1}{\omega_1}[arccos\Phi_1(\omega_1) + 2i\pi], i = 0,1,2 \ldots$$

Define the bifurcation point as

$$\tau_2^0 = \min\left(\tau_2^i\right), \quad i = 0,1,2 \ldots$$

To derive the conditions for the existence of hopf bifurcation, we make the following hypothesis:

$$(\mathcal{H}_5): \frac{P_1Q_1+P_2Q_2}{Q_1^2+Q_2^2} \neq 0,$$

Where P_1, P_2, Q_1, Q_2 are defined as

$$P_1 = \omega_1^{2\rho+1}\sin(\omega_1\tau_2^0 - \rho\pi) + (a_1+a_2)\omega_1^{\rho+1}\sin\left(\omega_1\tau_2^0 + \frac{\rho\pi}{2}\right) + a_1a_2\sin\omega_1\tau_2^0$$

$$P_2 = -\omega_1^{2\rho+1}\cos(\omega_1\tau_2^0 + \rho\pi) - (a_1+a_2)\omega_1^{\rho+1}\cos\left(\frac{\rho\pi}{2} - \omega_1\tau_2^0\right) - a_1a_2\cos\omega_1\tau_2^0$$

$$\begin{aligned} Q_1 = {} & 2\rho\omega_1^{2\rho-1}\cos(\rho\pi + \omega_1\tau_2^0) \\ & + (a_1+a_2)\omega_1^{\rho}\cos\left(\omega_1\tau_2^0 + \frac{\rho\pi}{2}\right) + \tau_2^0\,\omega_1^{2\rho}\cos(\rho\pi + \omega_1\tau_2^0) \\ & + \tau_2^0\,(a_1+a_2)\omega_1^{\rho}\cos\left(\frac{\rho\pi}{2} + \omega_0\tau_1^0\right) + a_1a_2\cos\omega_1\tau_2^0 \\ & + a_3\rho\omega_1^{\rho-1}cos\frac{\rho\pi}{2} \end{aligned}$$

$$\begin{aligned} Q_2 = {} & 2\rho\omega_1^{2\rho-1}\sin(\rho\pi + \omega_1\tau_2^0) \\ & + (a_1+a_2)\omega_1^{\rho}\sin\left(\omega_1\tau_2^0 + \frac{\rho\pi}{2}\right) + \tau_2^0\,\omega_1^{2\rho}\sin(\rho\pi + \omega_1\tau_2^0) \\ & + \tau_2^0\,(a_1+a_2)\omega_1^{\rho}\sin\left(\frac{\rho\pi}{2} + \omega_0\tau_1^0\right) + a_1a_2\sin\omega_1\tau_2^0 \\ & + a_3\rho\omega_1^{\rho-1}sin\frac{\rho\pi}{2} \end{aligned}$$

Lemma 6.2 Let $\lambda(\tau_2) = \varphi(\tau_2) + i\omega(\tau_2)$ be a root of the characteristic equation (6.23) near $\tau_2 = \tau_2^i$ meeting $\varphi(\tau_2^i) = 0$, $\omega(\tau_2^i) = \omega_1$, then the transversality condition $Re\left[\frac{d\lambda}{d\tau_2}\right]\Big|_{(\tau_2=\tau_2^0,\omega=\omega_1)} \neq 0$ holds.

Proof. Differentiating both sides of (6.23) with respect to τ_2, we get

$$\frac{d\lambda}{d\tau_2} = -\frac{\lambda\varphi_1(\lambda)e^{\lambda\tau_2}}{\varphi_1'(\lambda)e^{\lambda\tau_2} + \tau_2\varphi_1(\lambda)e^{\lambda\tau_2} + \varphi_2'(\lambda)} = \frac{P(\lambda)}{Q(\lambda)}$$

Where $\varphi_i'(\lambda)$ are the derivatives of $\varphi_i(\lambda)$ $(i = 1,2)$.

$$\left.\begin{aligned} P(\omega_1 i)|_{\tau_2=\tau_2^0} &= P_1 + iP_2 \\ Q(\omega_1 i)|_{\tau_2=\tau_2^0} &= Q_1 + iQ_2 \end{aligned}\right\} \tag{6.27}$$

By straightforward computation, it can be derived from (6.23) that

$$Re\left[\frac{d\lambda}{d\tau_2}\right]\Big|_{(\tau_2=\tau_2^0,\omega=\omega_1)} = \frac{P_1Q_1+P_2Q_2}{Q_1^2+Q_2^2} \neq 0.$$

This completes the proof.

Theorem 6.4 Suppose $\tau_1 = 0$, if assumptions (H_1),(H_2) and (H_5) hold, then :

(i) The endemic equilibrium E^* of system (6.1) is locally asymptotically stable for $\tau_2 \in [0, \tau_2^0)$;

(ii) System (6.1) undergoes hopf bifurcation at E^* when $\tau_2 = \tau_2^{(0)}$.

Case 6.4.1.2.3 $\tau_1 > 0$ and $\tau_2 > 0$

Case (6.4.1.2.3 a) $\tau_1 > 0$ and $\tau_2 > 0$ and $\tau_1 \in (0, \tau_1^0)$

For any $\tau_1 = \widehat{\tau_1} \in (0, \tau_1^0)$, let $\lambda = i\omega(\widehat{\tau_1}, \tau_2)(\omega(\widehat{\tau_1}, \tau_2) > 0)$ be a root of equation (6.14). Obviously $\lambda = i\omega(\widehat{\tau_1}, \tau_2)(\omega(\widehat{\tau_1}, \tau_2) > 0)$ is also a root of

$$\left[\left(\lambda^\rho + n_1 + n_2 e^{-\lambda\tau_1}\right)\left(\lambda^\rho - n_3 e^{-\lambda\tau_1} + n_4 + n_5 e^{-\lambda\tau_2} + n_6\right) + n_2 n_3 e^{-2\lambda\tau_1}\right] = 0 \tag{6.28}$$

Rearranging equation (6.28) leads to

$$\mathrm{f}_1(\lambda, \widehat{\tau_1}) + \mathrm{f}_2(\lambda, \widehat{\tau_1}) e^{-\lambda\widehat{\tau_1}} + \mathrm{f}_3(\lambda, \widehat{\tau_1}) e^{-\lambda\tau_2} + \mathrm{f}_4(\lambda, \widehat{\tau_1}) e^{-\lambda\tau_1} e^{-\lambda\tau_2} = 0 \tag{6.29}$$

Where

$$\left.\begin{aligned} \mathrm{f}_1(\lambda, \widehat{\tau_1}) &= \lambda^{2\rho} + b_1\lambda^\rho + b_2 \\ \mathrm{f}_2(\lambda, \widehat{\tau_1}) &= b_3\lambda^\rho + b_4 \\ \mathrm{f}_3(\lambda, \widehat{\tau_1}) &= b_5\lambda^\rho + b_6 \\ \mathrm{f}_4(\lambda, \widehat{\tau_1}) &= b_7 \end{aligned}\right\} \tag{6.30}$$

and $b_i (i = 1,2, \ldots 7)$ are defined as

$b_1 = n_1 + n_4 + n_6$
$b_2 = n_1(n_4 + n_6)$
$b_3 = n_2 - n_3$
$b_4 = n_2(n_4 + n_6) - n_1 n_3$
$b_5 = n_5$
$b_6 = n_1 n_5$
$b_7 = n_2 n_5$

Multiplying both sides of (6.29) by $e^{\lambda\tau_2}$, we obtain

$$\mathrm{f}_1(\lambda, \widehat{\tau_1}) e^{\lambda\tau_2} + \mathrm{f}_2(\lambda, \widehat{\tau_1}) e^{-\lambda\tau_1} e^{\lambda\tau_2} + \mathrm{f}_3(\lambda, \widehat{\tau_1}) + \mathrm{f}_4(\lambda, \widehat{\tau_1}) e^{-\lambda\tau_1} = 0 \tag{6.31}$$

Suppose that $\lambda = \omega i(\omega > 0)$ is a root of equation (6.31). Substituting it into (6.31) and separating the imaginary and real parts, we get

$$\Omega_1 \cos\omega\tau_2 + \Omega_2 \sin\omega\tau_2 = -\Omega_3$$

$$\Omega_4 \cos\omega\tau_2 + \Omega_5 \sin\omega\tau_2 = -\Omega_6$$

where

$$\left.\begin{aligned} \Omega_1 &= \mathrm{f}_1^R + \mathrm{f}_2^R cos\omega\widehat{\tau_1} + \mathrm{f}_2^I sin\omega\widehat{\tau_1} \\ \Omega_2 &= -\mathrm{f}_1^I - \mathrm{f}_2^I cos\omega\widehat{\tau_1} + \mathrm{f}_2^R sin\omega\widehat{\tau_1} \\ \Omega_3 &= \mathrm{f}_3^R + \mathrm{f}_4^R cos\omega\widehat{\tau_1} + \mathrm{f}_4^I sin\omega\widehat{\tau_1} \\ \Omega_4 &= \mathrm{f}_1^I + \mathrm{f}_2^I cos\omega\widehat{\tau_1} - \mathrm{f}_2^R sin\omega\widehat{\tau_1} \\ \Omega_5 &= \mathrm{f}_1^R + \mathrm{f}_2^R cos\omega\widehat{\tau_1} + \mathrm{f}_2^I sin\omega\widehat{\tau_1} \\ \Omega_6 &= \mathrm{f}_3^I + \mathrm{f}_4^I cos\omega\widehat{\tau_1} - \mathrm{f}_4^R sin\omega\widehat{\tau_1} \end{aligned}\right\} \quad (6.32)$$

and $\mathrm{f}_\mathrm{i}^R, \mathrm{f}_\mathrm{i}^I$ are the real and imaginary part of $\mathrm{f}_\mathrm{i}(\lambda, \widehat{\tau_1})(i = 1,2, \ldots 6)$ are given as

$$\mathrm{f}_1^R = \omega^{2\rho} cos\rho\pi + b_1\omega^\rho cos\frac{\rho\pi}{2} + b_2$$

$$\mathrm{f}_1^I = \omega^{2\rho} sin\rho\pi + b_1\omega^\rho sin\frac{\rho\pi}{2}$$

$$\mathrm{f}_2^R = b_3\omega^\rho cos\frac{\rho\pi}{2} + b_4$$

$$\mathrm{f}_2^I = b_3\omega^\rho sin\frac{\rho\pi}{2}$$

$$\mathrm{f}_3^R = b_5\omega^\rho cos\frac{\rho\pi}{2} + b_6$$

$$\mathrm{f}_3^I = b_5\omega^\rho sin\frac{\rho\pi}{2}$$

$$\mathrm{f}_4^R = b_7$$

$$\mathrm{f}_4^I = 0$$

By simple calculation, we get

$$\cos\omega\tau_2 = \frac{-\Omega_3\Omega_5 + \Omega_2\Omega_6}{\Omega_1\Omega_5 - \Omega_2\Omega_4}$$

$$\sin\omega\tau_2 = \frac{-\Omega_3\Omega_4 + \Omega_1\Omega_6}{\Omega_2\Omega_4 - \Omega_1\Omega_5}$$

Since $cos^2\ \omega\tau_2 + sin^2\ \omega\tau_2 = 1$ (6.33)

Assume that equation (6.33) has at least one positive real root ω_2, then it follows that $\tau_3^i = \frac{1}{\omega_2}[arccos\ \omega_2\tau_2 + 2i\pi], i = 0,1,2 \ldots$

Define the bifurcation point as

$$\tau_3^0 = \min\left(\tau_3^i\right), \quad i = 0,1,2 \ldots$$

To derive the conditions for the existence of hopf bifurcation, we make the following hypothesis:

$$(\mathcal{H}_6): \frac{M_1N_1+M_2N_2}{N_1^2+N_2^2} \neq 0,$$

Where M_1, M_2, N_1, N_2 are defined as

$$\begin{aligned}
M_1 = {} & -b_3\omega_2^{\rho+1}\cos\left(\frac{\rho\pi}{2} + (\widehat{\tau_1} - \tau_3^0)\omega_2\right) - \omega_2 b_4 \sin\left((\widehat{\tau_1} - \tau_3^0)\omega_2\right) \\
& + \omega_2^{2\rho+1}\sin(\rho\pi + \omega_2\tau_3^0) + b_1\omega_2^{\rho+1}\sin\left(\frac{\rho\pi}{2} + \omega_2\tau_3^0\right) \\
& + \omega_2 b_2 \sin\omega_2\tau_3^0 \\
M_2 = {} & -b_3\omega_2^{\rho+1}\cos(\rho\pi + \omega_2\tau_3^0) - \omega_2 b_4 \cos\left((\widehat{\tau_1} - \tau_3^0)\omega_2\right) \\
& - \omega_2^{2\rho+1}\cos(\rho\pi + \omega_2\tau_3^0) - b_1\omega_2^{\rho+1}\cos\left(\frac{\rho\pi}{2} + \omega_2\tau_3^0\right) \\
& - \omega_2 b_2 \cos\omega_2\tau_3^0 \\
N_1 = {} & 2\,\rho\omega_2^{2\rho-1}\cos(\rho\pi + \omega_2\tau_3^0) + \rho b_1\omega_2^{\rho-1}\cos\left(\frac{\rho\pi}{2} + \omega_2\tau_3^0\right) \\
& + \tau_3^0\omega_2^{2\rho}\cos(\rho\pi + \omega_2\tau_3^0) + b_1\tau_3^0\omega_2^{\rho}\cos\left(\frac{\rho\pi}{2} + \omega_2\tau_3^0\right) \\
& + \tau_3^0 b_2\cos\omega_2\tau_3^0 + b_3\rho\omega_2^{\rho-1}\cos\left(\frac{\rho\pi}{2} + (\tau_3^0 - \widehat{\tau_1})\omega_2\right) \\
& + \tau_3^0 b_3\omega_2^{\rho}\cos\left(\frac{\rho\pi}{2} + (\tau_3^0 - \widehat{\tau_1})\omega_2\right) + \tau_3^0 b_4\cos(\tau_3^0 - \widehat{\tau_1})\omega_2 \\
& + b_5\rho\omega_2^{\rho-1}\cos\frac{\rho\pi}{2} - \widehat{\tau_1} b_3\omega_2^{\rho}\cos\left(\frac{\rho\pi}{2} + (\tau_3^0 - \widehat{\tau_1})\omega_2\right) \\
& - \widehat{\tau_1} b_4\cos(\tau_3^0 - \widehat{\tau_1})\omega_2 + \widehat{\tau_1} b_7 cos\omega_2\widehat{\tau_1} \\
N_2 = {} & 2\,\rho\omega_2^{2\rho-1}\sin(\rho\pi + \omega_2\tau_3^0) + \rho b_1\omega_2^{\rho-1}\sin\left(\frac{\rho\pi}{2} + \omega_2\tau_3^0\right) \\
& + \tau_3^0\omega_2^{2\rho}\sin(\rho\pi + \omega_2\tau_3^0) + b_1\tau_3^0\omega_2^{\rho}\sin\left(\frac{\rho\pi}{2} + \omega_2\tau_3^0\right) \\
& + \tau_3^0 b_2\sin\omega_2\tau_3^0 + b_3\rho\omega_2^{\rho-1}\sin\left(\frac{\rho\pi}{2} + (\tau_3^0 - \widehat{\tau_1})\omega_2\right) \\
& + \tau_3^0 b_3\omega_2^{\rho}\sin\left(\frac{\rho\pi}{2} + (\tau_3^0 - \widehat{\tau_1})\omega_2\right) + \tau_3^0 b_4\sin(\tau_3^0 - \widehat{\tau_1})\omega_2 \\
& + b_5\rho\omega_2^{\rho-1}\sin\frac{\rho\pi}{2} + \widehat{\tau_1} b_3\omega_2^{\rho}\sin\left(\frac{\rho\pi}{2} + (\tau_3^0 - \widehat{\tau_1})\omega_2\right) \\
& + \widehat{\tau_1} b_4\sin(\tau_3^0 - \widehat{\tau_1})\omega_2 - \widehat{\tau_1} b_7\, sin\omega_2\widehat{\tau_1}
\end{aligned}$$

Lemma 6.3 Let $\lambda(\tau_2) = \varphi(\tau_2) + i\omega(\tau_2)$ be a root of the characteristic equation (6.31) near $\tau_2 = \tau_3^{(i)}$ meeting $\varphi\left(\tau_3^i\right) = 0$, $\omega\left(\tau_3^i\right) = \omega_2$, then the transversality condition $Re\left[\frac{d\lambda}{d\tau_2}\right]\Big|_{(\tau_2=\tau_3^0,\omega=\omega_2)} \neq 0$ holds.

Proof. Differentiating both sides of (6.31) with respect to τ_2, we get

$$\frac{d\lambda}{d\tau_2} = \frac{M(\lambda)}{N(\lambda)}$$

where $M(\lambda) = (-f_1 e^{\lambda\tau_2} - f_2 e^{-\lambda\widehat{\tau_1}} e^{\lambda\tau_2})\lambda$

$$N(\lambda) = \left(f_1{}' + \tau_2 f_1 + f_2{}' e^{-\lambda\widehat{\tau_1}} + \tau_2 f_2 e^{-\lambda\widehat{\tau_1}}\right)e^{\lambda\tau_2} + f_3{}' + f_4{}' e^{-\lambda\widehat{\tau_1}} - \widehat{\tau_1}(f_2 e^{\lambda\tau_2} - f_4)e^{-\lambda\widehat{\tau_1}}$$

Where $f_i'(\lambda)$ are the derivatives of $f_i(\lambda)$ $(i = 1,2,3,4)$

$$\left.\begin{aligned} M(\omega_2 i)|_{\tau_2=\tau_3^0} &= M_1 + iM_2 \\ N(\omega_2 i)|_{\tau_2=\tau_3^0} &= N_1 + iN_2 \end{aligned}\right\} \tag{6.34}$$

Where M_1, M_2, N_1, N_2 are the real and imaginary parts of $M(\lambda)$ and $N(\lambda)$.

By straightforward computation we get

$$Re\left[\frac{d\lambda}{d\tau_2}\right]\Big|_{(\tau_2=\tau_3^0,\omega=\omega_2)} = \frac{M_1N_1+M_2N_2}{N_1^2+N_2^2} \neq 0.$$

This completes the proof.

Theorem 6.5 For any $\tau_1 = \widehat{\tau_1} \in (0, \tau_1^0)$ if assumptions $(\mathcal{H}_1)$, $(\mathcal{H}_2)$ and $(\mathcal{H}_6)$ hold, then:

(i) The endemic equilibrium E^* of system (6.1) is locally asymptotically stable for $\tau_2 \in [0, \tau_3^0)$;

(ii) System (6.1) undergoes hopf bifurcation at E^* when $\tau_2 = \tau_3^0$.

Case (6.4.1.2.3 b) $\tau_1 > 0$ and $\tau_2 > 0$ and $\tau_2 \in (0, \tau_2^0)$

For any $\tau_2 = \widehat{\tau_2} \in (0, \tau_2^0)$, let $\lambda = i\omega(\tau_1, \widehat{\tau_2})(\omega(\tau_1, \widehat{\tau_2}) > 0)$ be a root of equation (6.14). Obviously $\lambda = i\omega(\widehat{\tau_1}, \tau_2)(\omega(\widehat{\tau_1}, \tau_2) > 0)$ is also a root of (6.31)

Rearranging equation (6.31) leads to

$$\mathrm{f}_1(\lambda, \tau_1) + \mathrm{f}_2(\lambda, \tau_1)e^{-\lambda\tau_1} + \mathrm{f}_3(\lambda, \tau_1)e^{-\lambda\widehat{\tau_2}} + \mathrm{f}_4(\lambda, \tau_1)e^{-\lambda\tau_1}e^{-\lambda\widehat{\tau_2}} = 0 \tag{6.35}$$

Where $\mathrm{f_i}, i = 1,2,3$ and 4 are defined in (6.30)

Multiplying both sides of (6.35) by $e^{\lambda\widehat{\tau_2}}$, we obtain

$$\mathrm{f}_1(\lambda, \tau_1)e^{\lambda\widehat{\tau_2}} + \mathrm{f}_2(\lambda, \tau_1)e^{-\lambda\tau_1}e^{\lambda\widehat{\tau_2}} + \mathrm{f}_3(\lambda, \tau_1) + \mathrm{f}_4(\lambda, \tau_1)e^{-\lambda\tau_1} = 0 \tag{6.36}$$

Suppose that $\lambda = \omega i(\omega > 0)$ is a root of equation (6.36). Substituting it into (6.36) and separating the imaginary and real parts, we get

$$\Omega_7 \cos\omega\tau_1 + \Omega_8 \sin\omega\tau_1 = -\Omega_9$$
$$\Omega_{10} \cos\omega\tau_1 + \Omega_{11} \sin\omega\tau_1 = -\Omega_{12}$$

where

$$\left.\begin{aligned}
\Omega_7 &= \mathrm{f}_4^R + \mathrm{f}_2^R cos\omega\widehat{\tau_2} - \mathrm{f}_2^I sin\omega\widehat{\tau_2} \\
\Omega_8 &= \mathrm{f}_4^I + \mathrm{f}_2^I cos\omega\widehat{\tau_2} + \mathrm{f}_2^R sin\omega\widehat{\tau_2} \\
\Omega_9 &= \mathrm{f}_3^R + \mathrm{f}_1^R cos\omega\widehat{\tau_2} - \mathrm{f}_1^I sin\omega\widehat{\tau_2} \\
\Omega_{10} &= \mathrm{f}_4^I + \mathrm{f}_2^I cos\omega\widehat{\tau_2} + \mathrm{f}_2^R sin\omega\widehat{\tau_2} \\
\Omega_{11} &= -\mathrm{f}_4^R - \mathrm{f}_2^R cos\omega\widehat{\tau_2} + \mathrm{f}_2^I sin\omega\widehat{\tau_2} \\
\Omega_{12} &= \mathrm{f}_3^I + \mathrm{f}_1^I cos\omega\widehat{\tau_2} + \mathrm{f}_1^R sin\omega\widehat{\tau_2}
\end{aligned}\right\} \quad (6.37)$$

By simple calculation, we get

$$\cos\omega\tau_1 = \frac{-\Omega_9\Omega_{11} + \Omega_8\Omega_{12}}{\Omega_7\Omega_{11} - \Omega_8\Omega_{10}}$$
$$\sin\omega\tau_2 = \frac{-\Omega_9\Omega_{10} + \Omega_7\Omega_{12}}{\Omega_8\Omega_{10} - \Omega_7\Omega_{11}}$$

Since $cos^2\ \omega\tau_1 + sin^2\ \omega\tau_1 = 1$ (6.38)

Assume that equation (6.38) has at least one positive real root ω_3, then it follows that

$$\tau_4^i = \frac{1}{\omega_3}[arccos\ \omega_3\tau_1 + 2i\pi], i = 0,1,2 \ldots$$

Define the bifurcation point as

$$\tau_4^0 = \min\left(\tau_4^i\right), \quad i = 0,1,2 \ldots$$

To derive the conditions for the existence of hopf bifurcation, we make the following hypothesis:

$$(\mathcal{H}_7): \frac{R_1S_1 + R_2S_2}{S_1^2 + S_2^2} \neq 0,$$

Where R_1, R_2, S_1, S_2 are defined as

$$R_1 = b_3\omega_3^{\rho+1} \sin\left(\frac{\rho\pi}{2} + (\widehat{\tau_2} - \tau_4^0)\omega_3\right) + b_4\omega_3 \sin\left((\widehat{\tau_2} - \tau_4^0)\omega_3\right) + b_7\omega_3 \sin\omega_3\tau_4^0$$

$$R_2 = -b_3\omega_3^{\rho+1}\cos\left(\frac{\rho\pi}{2} + (\widehat{\tau_2} - \tau_4^0)\omega_3\right) - b_4\omega_3\cos\left((\widehat{\tau_2} - \tau_4^0)\omega_3\right) + b_7\omega_3\cos\omega_3\tau_4^0$$

$$\begin{aligned} S_1 = {} & 2\,\rho\omega_3^{2\rho-1}\cos(\rho\pi + \omega_3\widehat{\tau_2}) + \rho b_1\omega_3^{\rho-1}\cos\left(\frac{\rho\pi}{2} + \omega_3\widehat{\tau_2}\right) \\ & + \widehat{\tau_2}\omega_3^{2\rho}\cos(\rho\pi + \omega_3\widehat{\tau_2}) + b_1\widehat{\tau_2}\omega_3^{\rho}\cos\left(\frac{\rho\pi}{2} + \omega_3\widehat{\tau_2}\right) \\ & + \widehat{\tau_2}b_2\cos\omega_3\widehat{\tau_2} + b_3\rho\omega_3^{\rho-1}\cos\left(\frac{\rho\pi}{2} + (\widehat{\tau_2} - \tau_4^0)\omega_3\right) \\ & + (\widehat{\tau_2} - \tau_4^0)b_3\omega_3^{\rho}\cos\left(\frac{\rho\pi}{2} + (\widehat{\tau_2} - \tau_4^0)\omega_3\right) \\ & + (\widehat{\tau_2} - \tau_4^0)b_4\cos(\widehat{\tau_2} - \tau_4^0)\omega_3 + b_5\rho\omega_3^{\rho-1}\cos\frac{\rho\pi}{2} - \tau_4^0 b_7 cos\omega_3\tau_4^0 \end{aligned}$$

$$\begin{aligned} S_2 = {} & 2\,\rho\omega_3^{2\rho-1}\sin(\rho\pi + \omega_3\widehat{\tau_2}) + \rho b_1\omega_3^{\rho-1}\sin\left(\frac{\rho\pi}{2} + \omega_3\widehat{\tau_2}\right) \\ & + \widehat{\tau_2}\omega_3^{2\rho}\sin(\rho\pi + \omega_3\widehat{\tau_2}) + b_1\widehat{\tau_2}\omega_3^{\rho}\sin\left(\frac{\rho\pi}{2} + \omega_3\widehat{\tau_2}\right) \\ & + \widehat{\tau_2}b_2\sin\omega_3\widehat{\tau_2} + b_3\rho\omega_3^{\rho-1}\sin\left(\frac{\rho\pi}{2} + (\widehat{\tau_2} - \tau_4^0)\omega_3\right) \\ & + (\widehat{\tau_2} - \tau_4^0)b_3\omega_3^{\rho}\sin\left(\frac{\rho\pi}{2} + (\widehat{\tau_2} - \tau_4^0)\omega_3\right) \\ & + (\widehat{\tau_2} - \tau_4^0)b_4\sin(\widehat{\tau_2} - \tau_4^0)\omega_3 + b_5\rho\omega_3^{\rho-1}\sin\frac{\rho\pi}{2} + \tau_4^0 b_7\sin\omega_3\tau_4^0 \end{aligned}$$

Lemma 6.4 Let $\lambda(\tau_1) = \varphi(\tau_1) + i\omega(\tau_1)$ be a root of the characteristic equation (6.35) near $\tau_1 = \tau_4^{(i)}$ meeting $\varphi(\tau_4^i) = 0$, $\omega(\tau_4^i) = \omega_3$, then the transversality condition $Re\left[\frac{d\lambda}{d\tau_1}\right]\Big|_{(\tau_1=\tau_4^0,\omega=\omega_3)} \neq 0$ holds.

Proof. Differentiating both sides of (6.36) with respect to τ_1, we get

$$\frac{d(\lambda, \widehat{\tau_2})}{d\tau_1} = \frac{R(\lambda)}{S(\lambda)}$$

where $R(\lambda) = (f_4 e^{-\lambda\tau_1} - f_2 e^{-\lambda\tau_1}e^{\lambda\widehat{\tau_2}})\lambda$

$$S(\lambda) = \left(f_1' + \widehat{\tau_2}f_1\right)e^{\lambda\widehat{\tau_2}} + \left(f_2' + (\widehat{\tau_2} - \tau_1)f_2\right)e^{-\lambda\tau_1}e^{\lambda\widehat{\tau_2}} + f_3' + (f_4' - \tau_1 f_4)e^{-\lambda\tau_1}$$

Where $f_i'(\lambda)$ are the derivatives of $f_i(\lambda)$ $(i = 1,2,3,4)$.

$$\left.\begin{aligned} R(\omega_2 i)|_{\tau_2=\tau_3^0} &= R_1 + iR_2 \\ S(\omega_2 i)|_{\tau_2=\tau_3^0} &= S_1 + iS_2 \end{aligned}\right\} \tag{6.39}$$

Where R_1, R_2, S_1, S_2 are the real and imaginary parts of $R(\lambda)$ and $S(\lambda)$

By straightforward computation we get

$$Re\left[\frac{d\lambda}{d\tau_2}\right]\Big|_{(\tau_1=\tau_4^0,\omega=\omega_3)} = \frac{R_1S_1+R_2S_2}{S_1^2+S_2^2} \neq 0.$$

This completes the proof.

Theorem 6.6 For any $\tau_2 = \widehat{\tau_2} \in (0, \tau_2^0)$ if assumptions $(\mathcal{H}_1)$, $(\mathcal{H}_2)$ and $(\mathcal{H}_7)$ hold, then:

(i) The endemic equilibrium E^* of system (6.1) is locally asymptotically stable for $\tau_1 \in [0, \tau_4^0)$;

(ii) System (6.1) undergoes Hopf Bifurcation at E^* when $\tau_1 = \tau_4^0$.

6.5 Numerical Simulations

In this section, numerical simulations are performed to verify our theoretical results of stability and bifurcation of system (6.1).
We take $\omega = 0.009,\ \beta = 0.009,\ \theta_1 = 0.05,\ \theta_2 = 0.01, \theta_3 = 0.02,\ \delta = 0.002, q = 0.02, \alpha = 0.0007, \vartheta = 0.002, \sigma = 0.02$ and by simple calculations , we get the unique endemic equilibrium point $E^*(S^*, I^*, Q^*, R^*) = (75.3331, 103.8889, 2.3086, 35.3301)$.

6.5.1 $\tau_1 > 0$ and $\tau_2 = 0$

First, we study the impact of the incubation delay τ_1 on the dynamical behaviours of the system. Here we fix the fractional order $\rho = 0.85$. We easily obtain critical value $\tau_1^0 = 21.8372$. Figures 6.1(i), 6.1(ii), 6.1(iii) and 6.1(iv) shows the endemic equilibrium E^* is asymptotically stable when $\tau_1 = 13.2 < \tau_1^0$ which agrees with Theorem 6.3. Figures 6.2(i), 6.2(ii), 6.2(iii) and 6.4(iv) shows that the endemic equilibrium E^* is unstable when $\tau_1 = 22.3 > \tau_1^0$ and a Hopf Bifurcation occurs.

We also evaluate the impact of the fractional order ρ on the dynamics of the system. When choosing $\tau_1 = 9$, it can be seen from Figures 6.3(i), 6.3(ii), 6.3(iii) and 6.3(iv) that with the decrease of the fractional order ρ can speed up the convergence rate of the system. Fixing $\tau_1 = 12$, system demonstrates an unstable behavior when $\rho = 1$(i.e. system is when integer order system), however the endemic equilibrium of the system is locally asymptotically stable when $\rho = 0.7$ or $\rho = 0.8$ or ρ

= 0.9 (see Figures 6.4(i), 6.4(ii), 6.4(iii) and 6.4(iv)). This implies that the unstable equilibrium of an integer order system may become stable in a fractional order system.

6.5.2 $\tau_1 = 0$ and $\tau_2 > 0$

Fixing $\rho = 0.85$, we can get critical values $\omega_1 = 0.0534$ and $\tau_2^0 = 20.77$. Figures 6.5(i), 6.5(ii), 6.5(iii) and 6.5(iv) shows that state trajectories of the system converge to the endemic equilibrium E^* when $\tau_2 = 15.5 < \tau_2^0$, while it can seen from Figure 6.6(i), 6.6(ii), 6.6(iii) and 6.6(iv) that the endemic equilibrium $E^*$of the system becomes unstable and a periodic solution bifurcates from a Hopf bifurcation when $\tau_2 = 26.2 > \tau_2^0$. These numerical results are consistent with Theorem 6.4.

We also study how the fractional order ρ affects the convergence rate of the system. Choosing $\tau_2 = 8$, we find from figures 6.7(i), 6.7(ii), 6.7(iii) and 6.7(iv) that with decreasing the value of fractional order can accelerate the speed of the system. When fixing $\tau_2 = 12$ (i.e. the system is an integer order system), while it becomes locally stable if $\rho = 0.7, 0.8, 0.9$ (Figures 6.8(i), 6.8(ii), 6.8(iii) and 6.8(iv)). This implies that the introduction of fractional order may convert an oscillatory system into a stable one.

6.5.3 $\tau_1 > 0$ and $\tau_2 > 0$

6.5.3.1 $\tau_1 > 0, \tau_2 > 0$ and $\tau_1 \in (0, \tau_1^0)$

For the sake of convenience, we fix $\tau_1 = \hat{\tau_1} = 9$. Choosing $\rho = 0.85$, we obtain $\tau_3^0 = 23.4$. Our numerical simulations can verify theoretical results in Theorem 6.7. To be more specific, Figures 6.9(i), 6.9(ii), 6.9(iii) and 6.9(iv) shows that the endemic equilibrium E^* of the system is asymptotically stable when $\tau_2 = 18 < \tau_3^0$, while it becomes unstable and Hopf bifurcation occurs when $\tau_2 = 24.5 > \tau_3^0$ (see Figures 6.10(i), 6.10(ii), 6.10(iii) and 6.10(iv)).

When the fractional order is chosen as $\rho =$ 0.6, 0.7, 0.8 and 0.9 with $\tau_2 =$ 13.5 , it can be seen from Figures 6.11(i), 6.11(ii), 6.11(iii) and 6.11(iv) that the decrease of the fractional order fasten the convergence rate of the system and the endemic equilibrium of system is unstable when fractional order reaches unity .Setting $\tau_2 = 19.5$ and choosing fractional order as $\rho =$ 0.7, 0.8, 0.85 and 0.86, we observe that decrease of the fractional order speed up the convergence rate of the system (see Figures 6.12(i), 6.12(ii), 6.12(iii) and 6.12(iv)).

6.5.3.2 $\tau_1 > 0, \tau_2 > 0$ and $\tau_2 \in (0, \tau_2^0)$

In the same way, we fix $\tau_2 = \widehat{\tau_2} = 18 \in (0, \tau_2^0]$. By setting $\rho = 0.85$, we get $\tau_4^0 = 17.6$. The endemic equilibrium of the system is asymptotically stable when $\tau_1 = 9.1 < \tau_4^0$ (see Figures 6.13(i), 6.13(ii), 6.13(iii) and 6.13(iv)) and it becomes unstable and Hopf bifurcation occurs when $\tau_1 = 18.6 > \tau_4^0$ (see Figures 6.14(i), 6.14(ii), 6.14(iii) and 6.14(iv)), which agrees with theorem 6.8.

By choosing $\rho = 0.7$, 0.8, 0.9 and 1.0 with $\tau_1 = 9$, we find the similar impact of the fractional order on the convergence rate of the system (see Figures 6.15(i), 6.15(ii), 6.15(iii) and 6.15(iv)). Setting $\tau_1 = 15$ with fractional orders $\rho = 0.8$, 0.9 and 1.0, the endemic equilibrium of the system is unstable when fractional order $\rho = 1$ (i.e. the system is an integer order system), while it becomes asymptotically stable when $\rho = 0.7$ or 0.8 (see Figures 6.16(i), 6.16(ii), 6.16(iii) and 6.16(iv)).

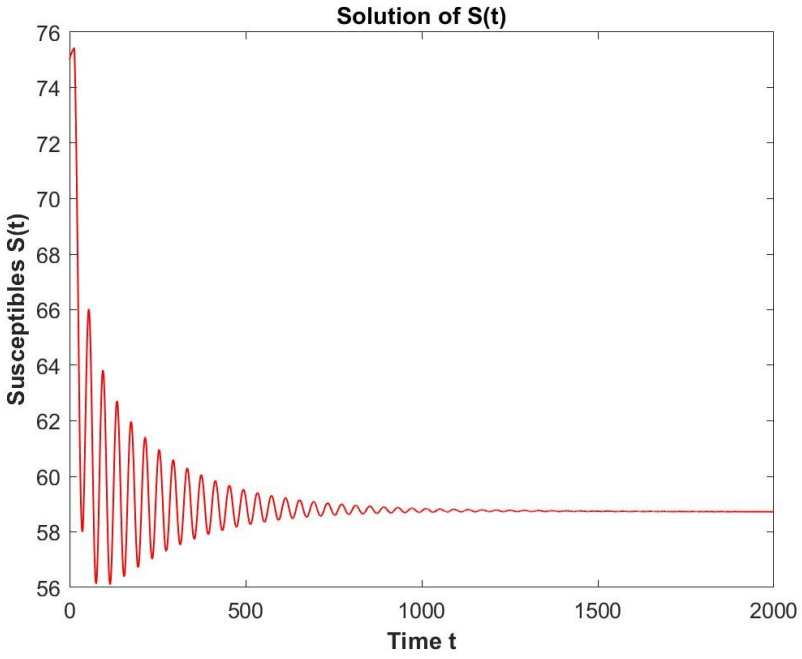

Figure 6.1 (i) Time series for the susceptible population when $\rho = 0.85, \tau_1 = 13.2 < \tau_1^0$

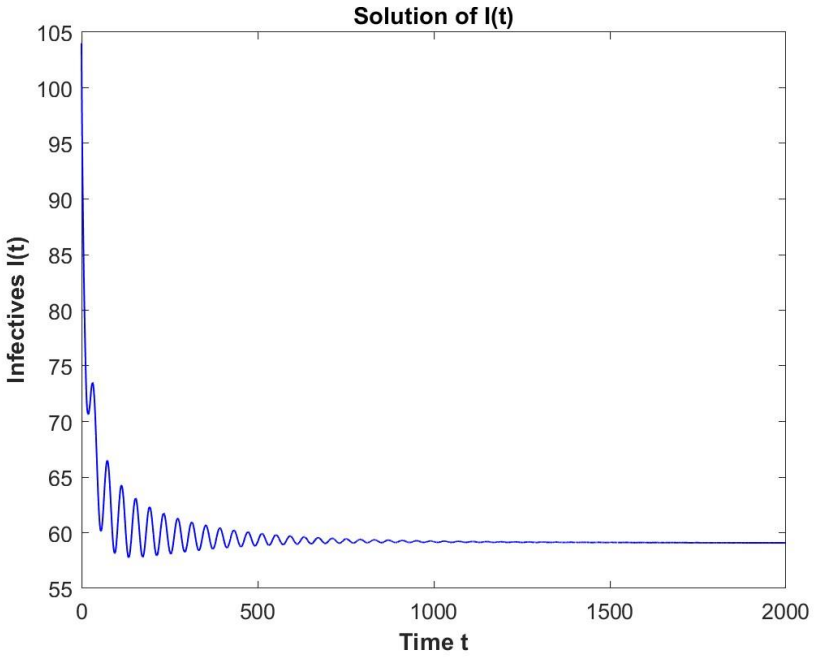

Figure 6.1 (ii) Time series for the infected population when $\rho = 0.85, \tau_1 = 13.2 \ < \tau_1^0$

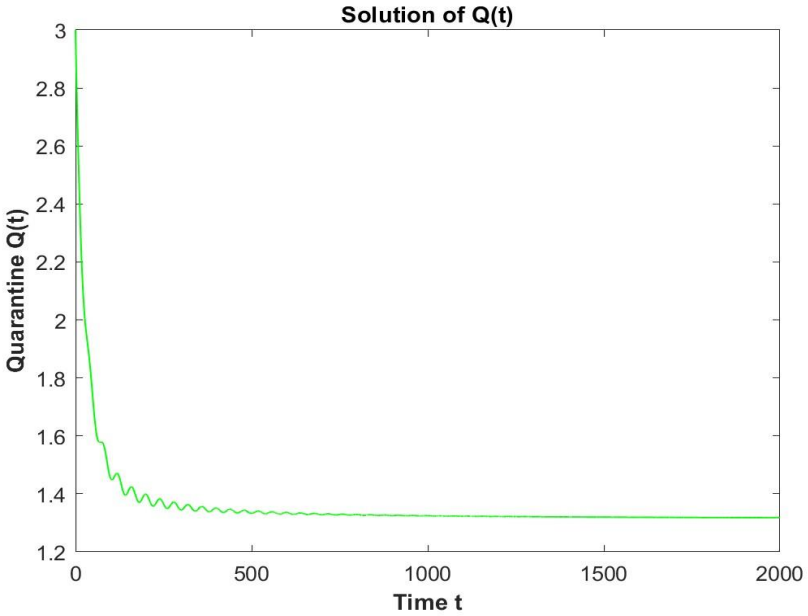

Figure 6.1 (iii) Time series for the quarantine population when $\rho = 0.85, \tau_1 = 13.2 \ < \tau_1^0$

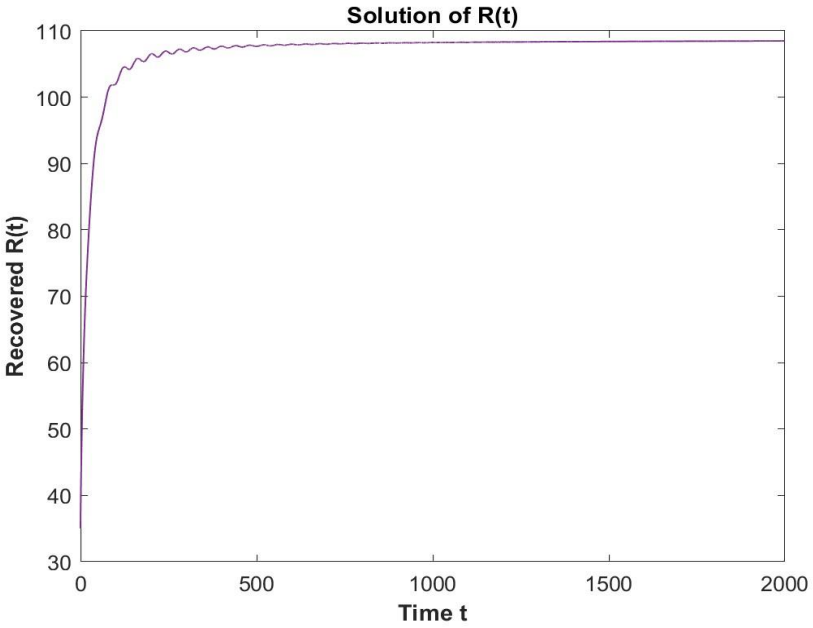

Figure 6.1 (iv) Time series for the recovered population when $\rho = 0.85, \tau_1 = 13.2 < \tau_1^0$

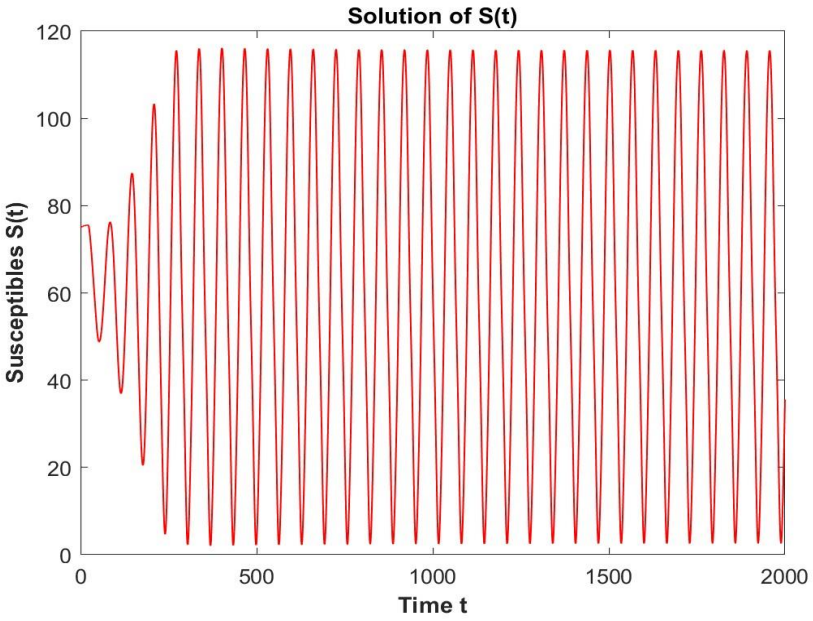

Figure 6.2 (i) Time series for the susceptible population when $\rho = 0.85, \tau_1 = 22.3 > \tau_1^0$

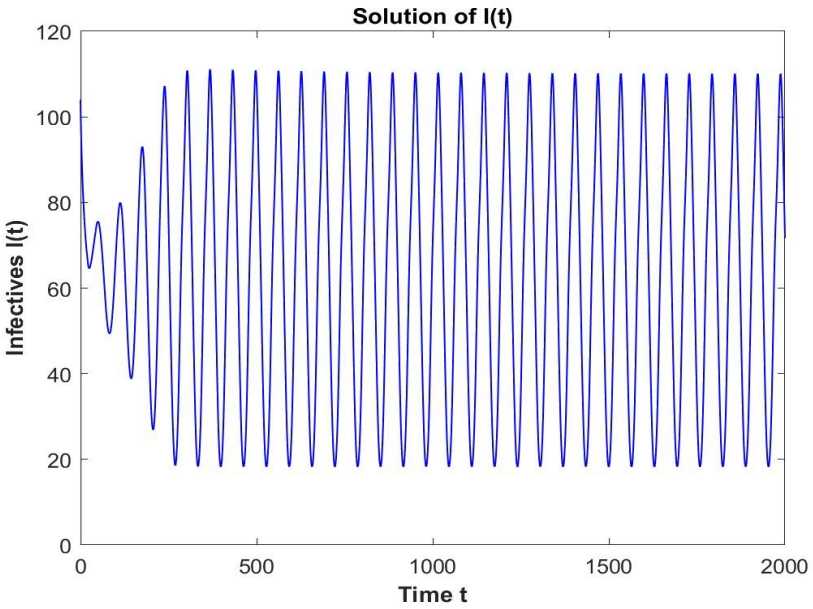

Figure 6.2 (ii) Time series for the infected population when $\rho = 0.85, \tau_1 = 22.3 \ > \tau_1^0$

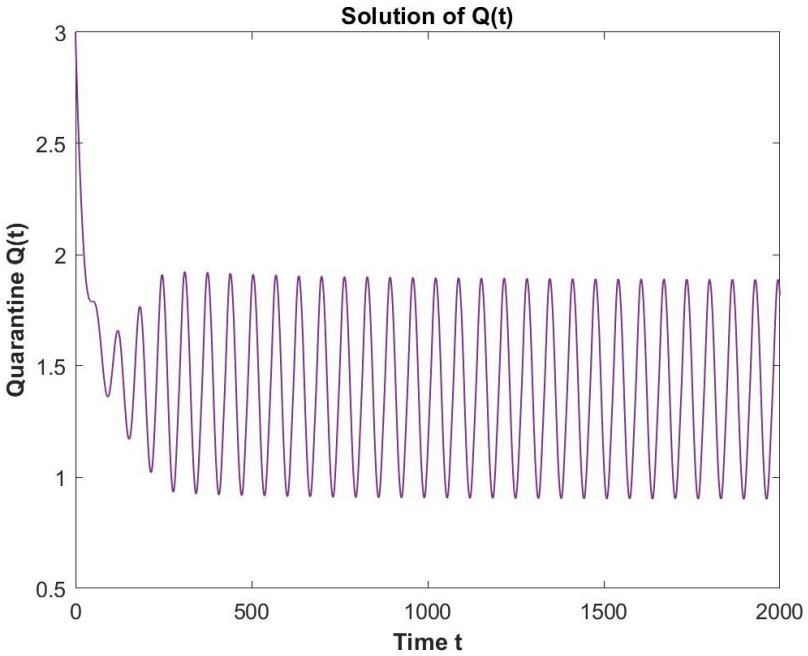

Figure 6.2 (iii) Time series for the quarantine population when $\rho = 0.85, \tau_1 = 22.3 \ > \tau_1^0$

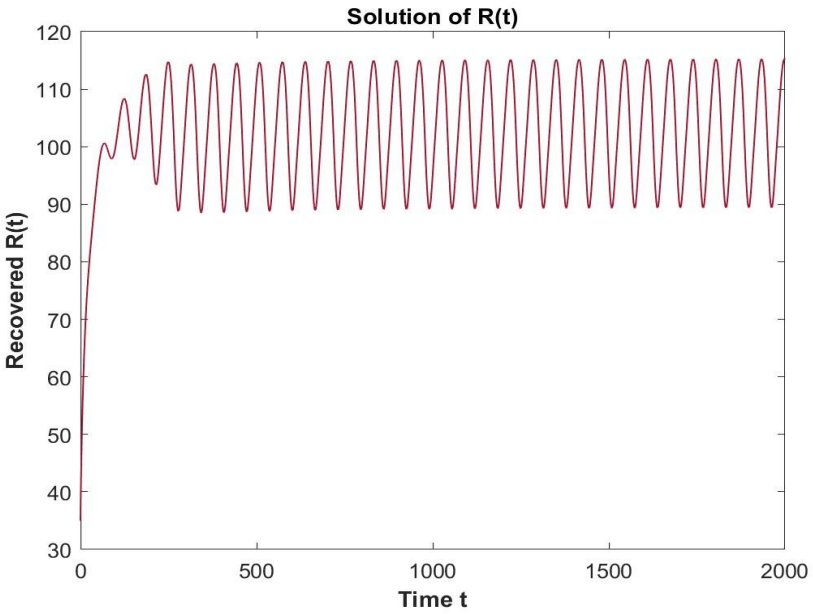

Figure 6.2 (iv) Time series for the recovered population when $\rho = 0.85, \tau_1 = 22.3 > \tau_1^0$

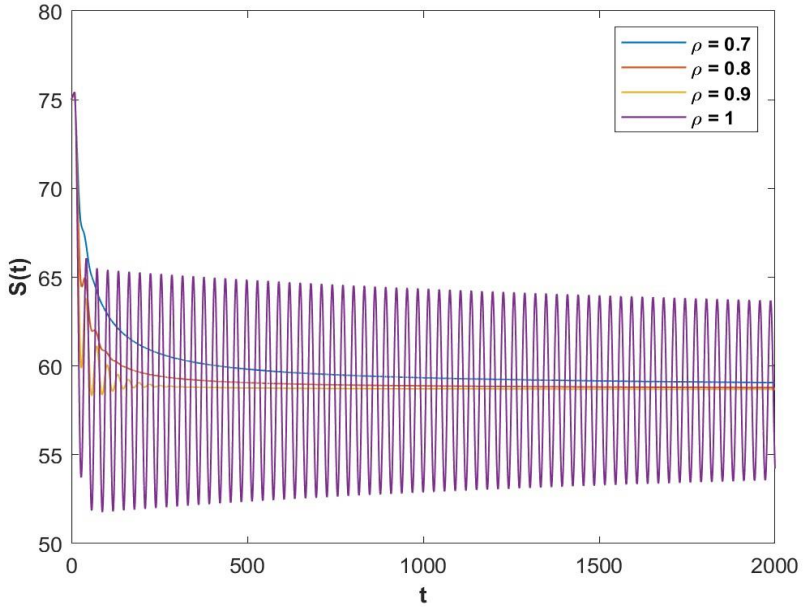

Figure 6.3 (i) Time series for the susceptible population when $\rho = 0.7, 0.8, 0.9 \; and \; 1, \tau_1 = 9$

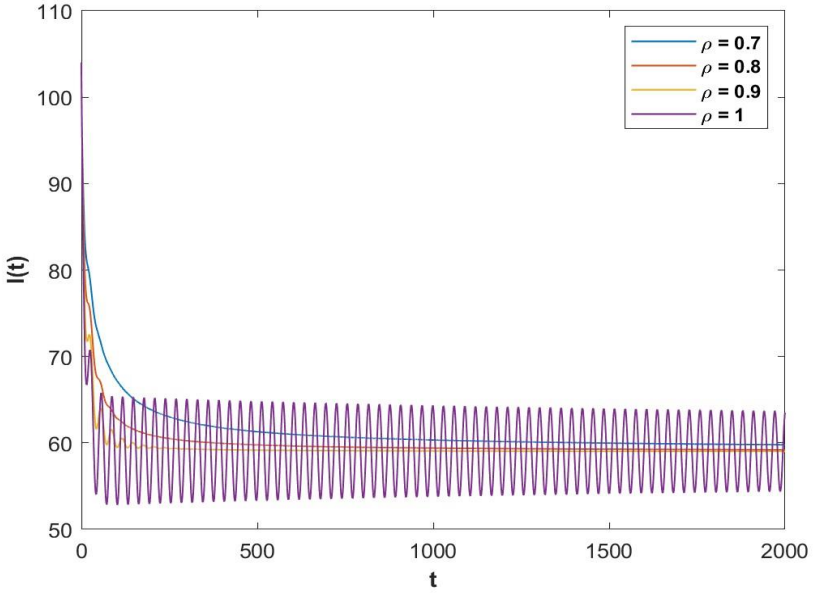

Figure 6.3 (ii) Time series for the infected population when $\rho = 0.7, 0.8, 0.9\ and\ 1, \tau_1 = 9$

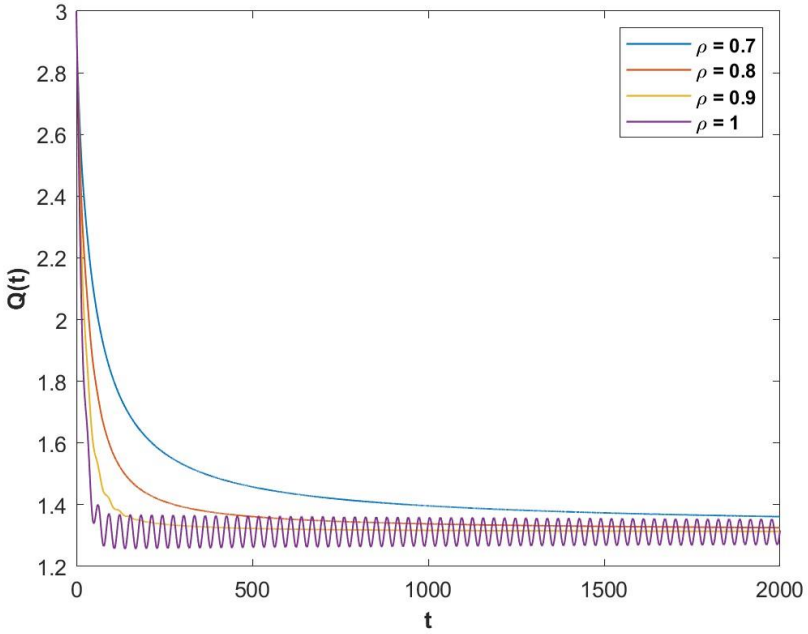

Figure 6.3 (iii) Time series for the quarantine population when $\rho = 0.7, 0.8, 0.9\ and\ 1, \tau_1 = 9$

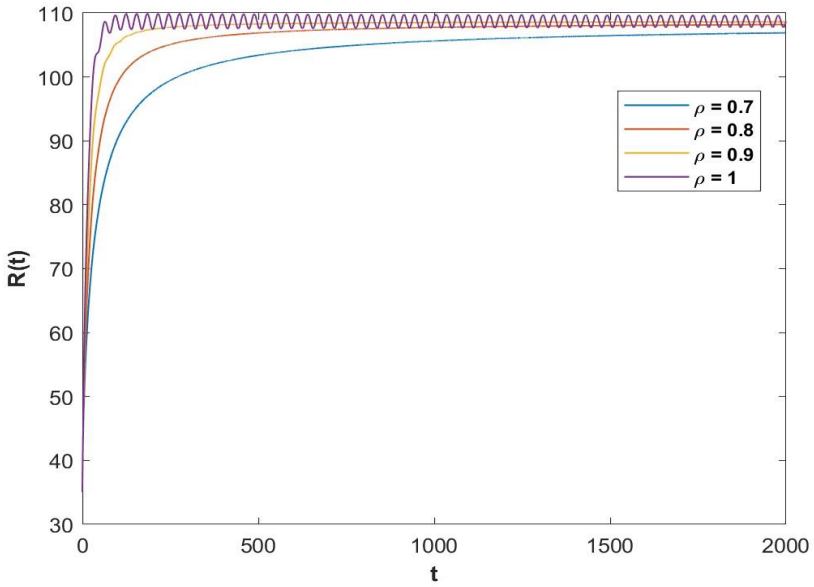

Figure 6.3 (iv) Time series for the recovered population when $\rho = 0.7, 0.8, 0.9\ and\ 1, \tau_1 = 9$

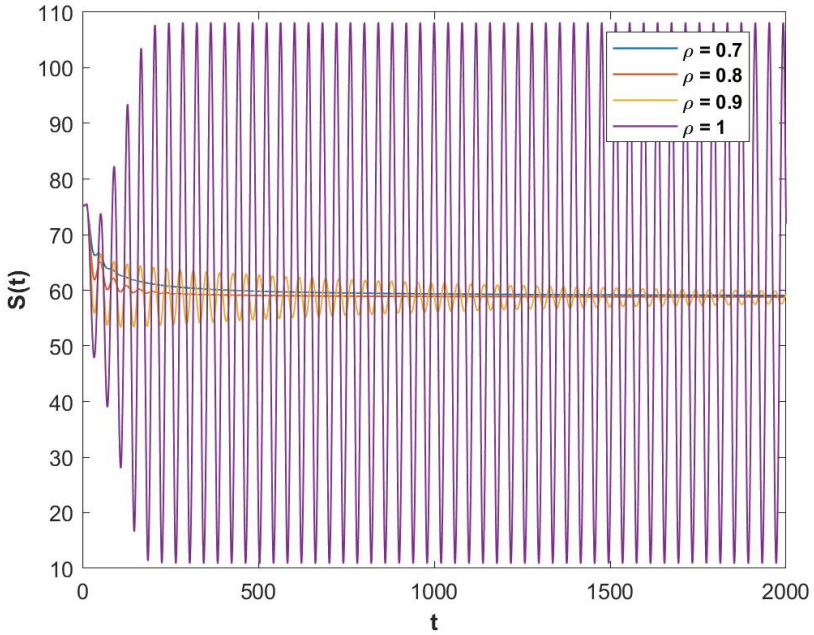

Figure 6.4 (i) Time series for the susceptible population when $\rho = 0.7, 0.8, 0.9\ and\ 1, \tau_1 = 12$

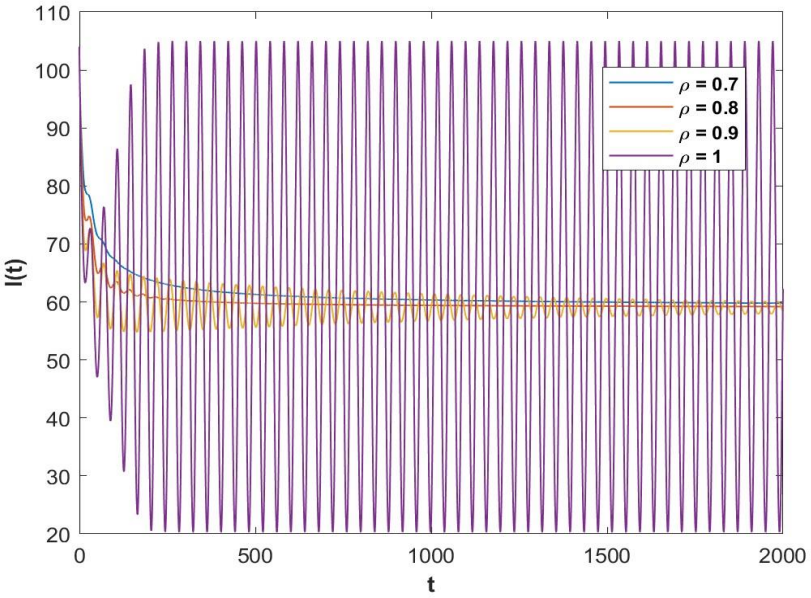

Figure 6.4 (ii) Time series for the infected population when $\rho = 0.7, 0.8, 0.9\ and\ 1, \tau_1 = 12$

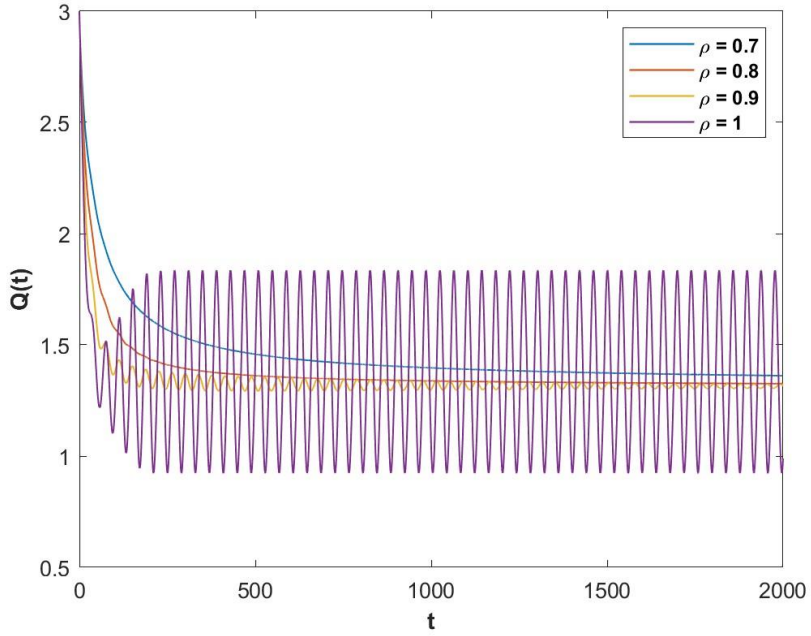

Figure 6.4 (iii) Time series for the quarantine population when $\rho = 0.7, 0.8, 0.9\ and\ 1, \tau_1 = 12$

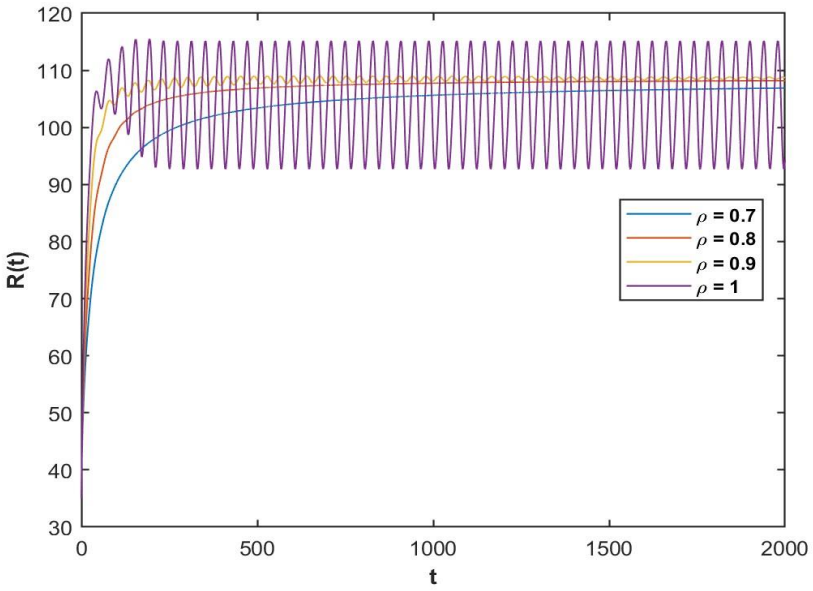

Figure 6.4 (iv) Time series for the recovered population when $\rho = 0.7, 0.8, 0.9\ and\ 1, \tau_1 = 12$

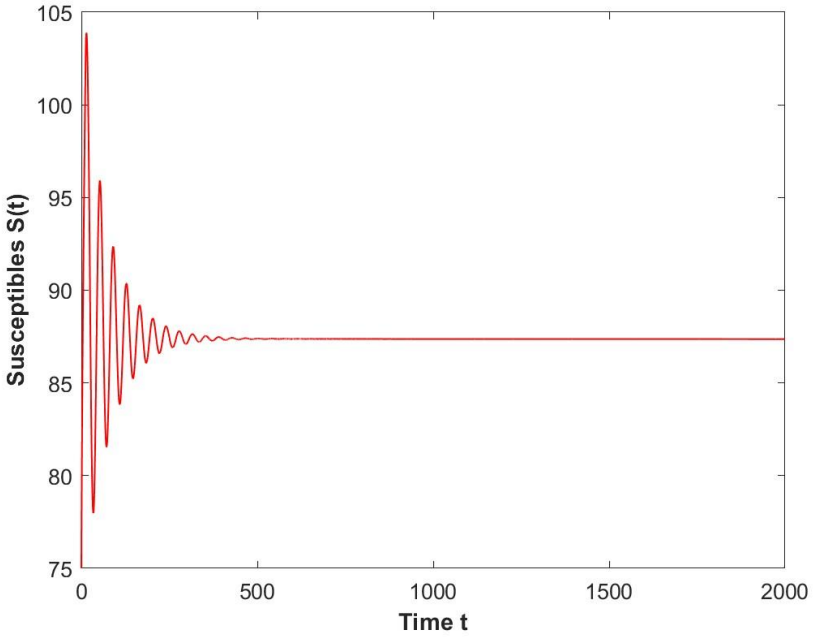

Figure 6.5 (i) Time series for the susceptible population when $\rho = 0.85, \tau_2 = 15\ < \tau_2^0$

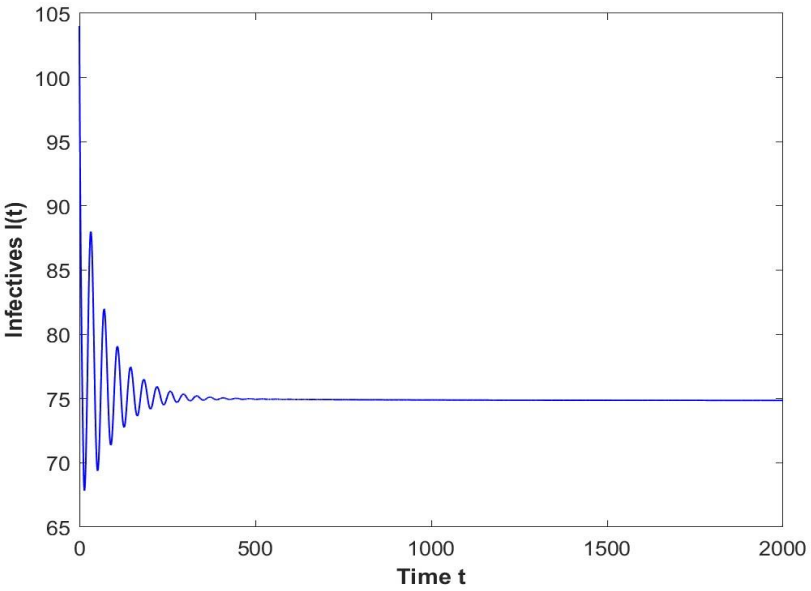

Figure 6.5 (ii) Time series for the infected population when $\rho = 0.85, \tau_2 = 15 \ < \tau_2^0$

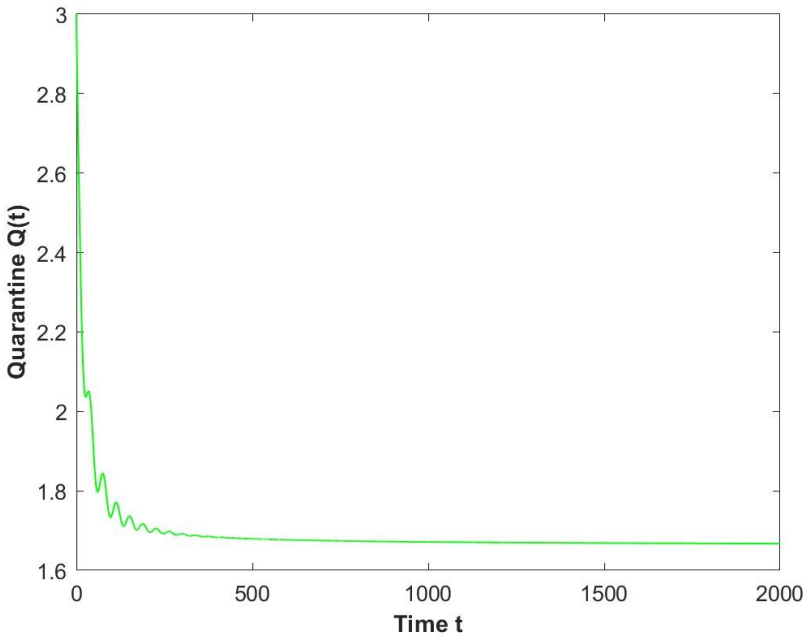

Figure 6.5 (iii) Time series for the quarantine population when $\rho = 0.85, \tau_2 = 15 \ < \tau_2^0$

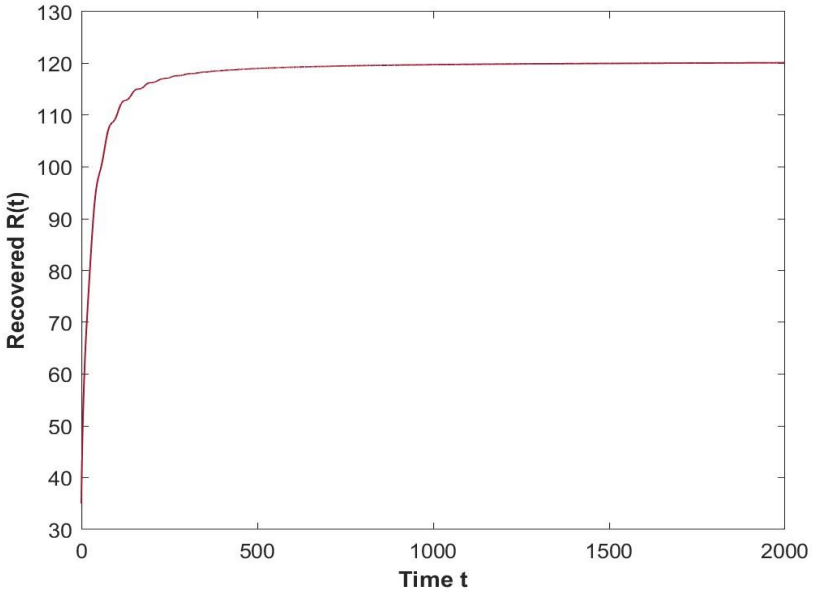

Figure 6.5 (iv) Time series for the recovered population when $\rho = 0.85, \tau_2 = 15 \ < \tau_2^0$

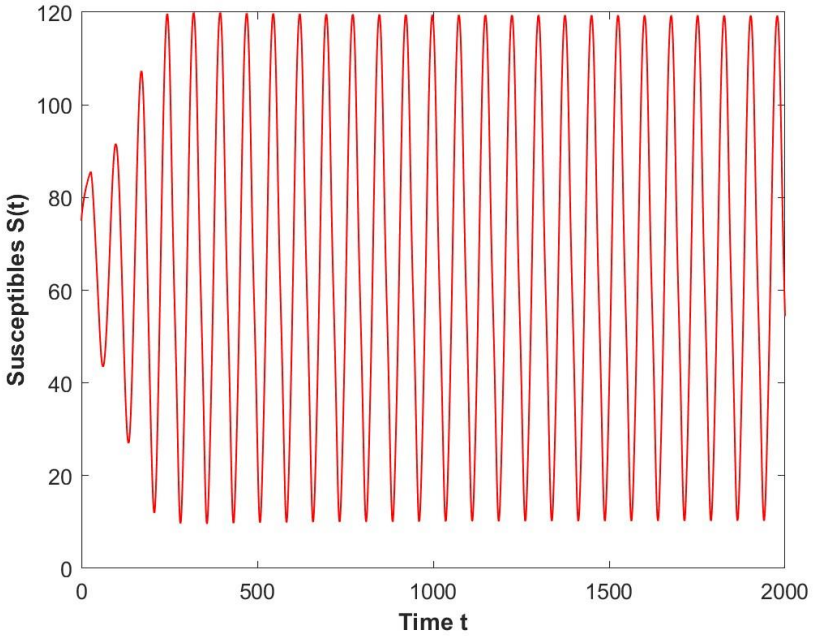

Figure 6.6 (i) The time series of the system when $\rho = 0.85, \tau_2 = 26 \ > \tau_2^0$

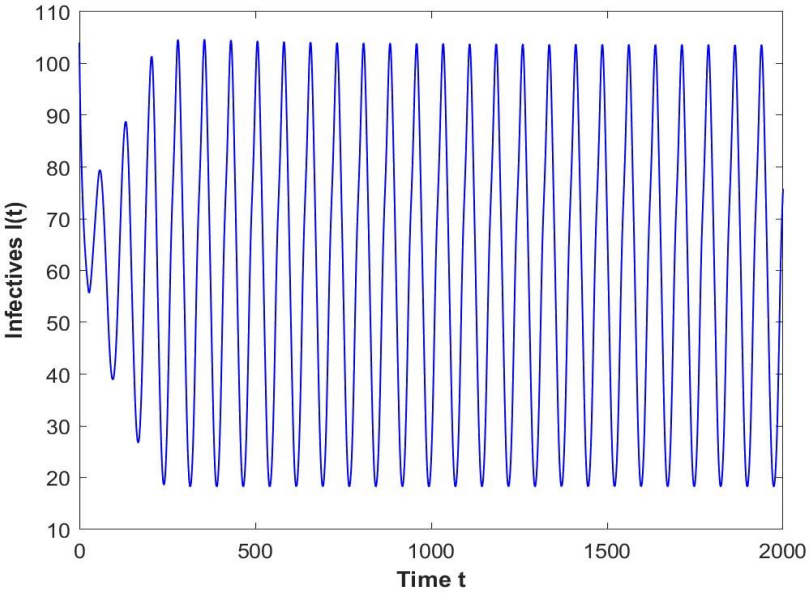

Figure 6.6 (ii) Time series for the infected population when $\rho = 0.85, \tau_2 = 26 \ > \tau_2^0$

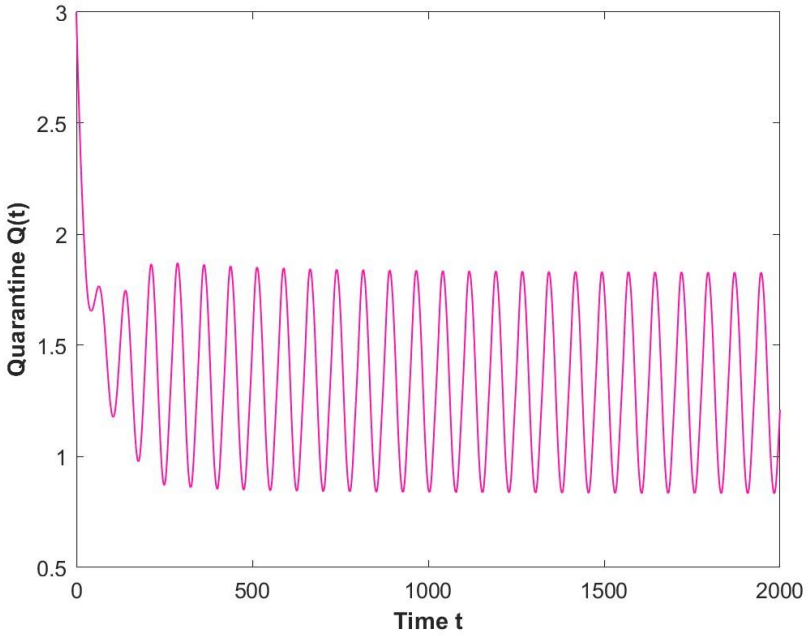

Figure 6.6 (iii) Time series for the quarantine population when $\rho = 0.85, \tau_2 = 26 \ > \tau_2^0$

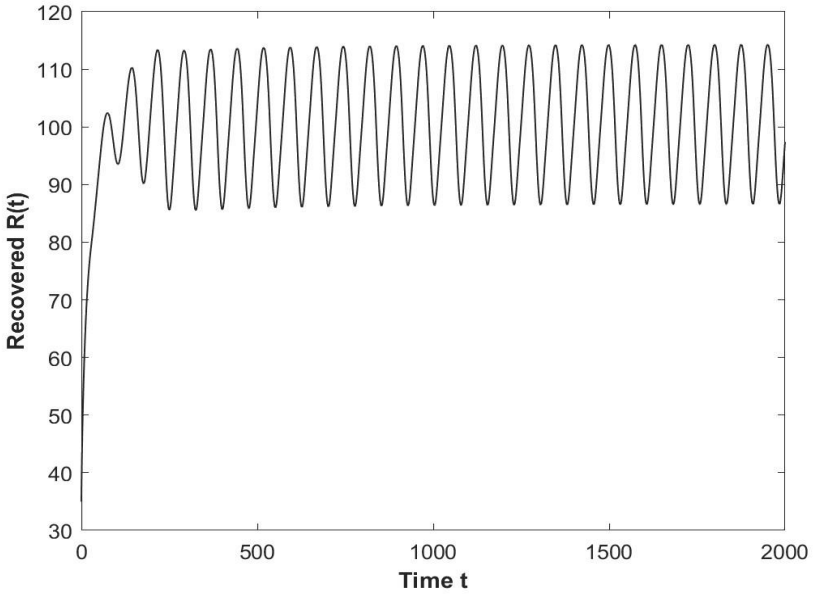

Figure 6.6 (iv) Time series for the recovered population when $\rho = 0.85, \tau_2 = 26 > \tau_2^0$

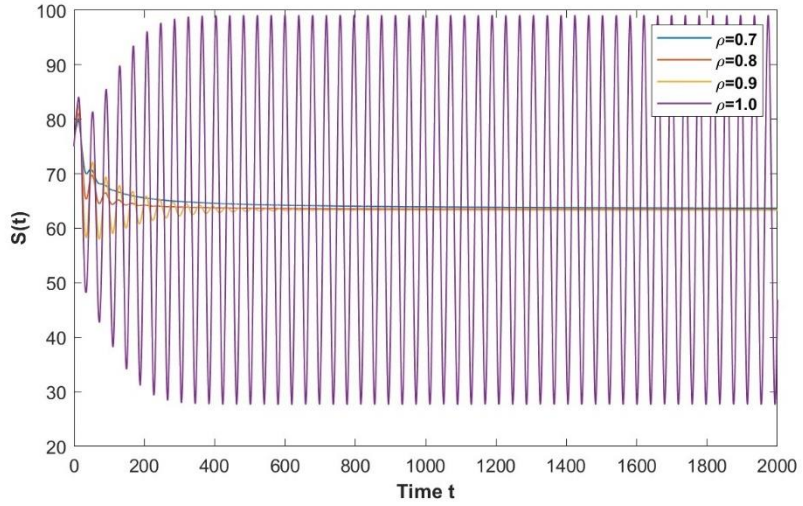

Figure 6.7 (i) Time series for the susceptible population when $\rho = 0.7, 0.8, 0.9 \; and \; 1, \tau_2 = 8$

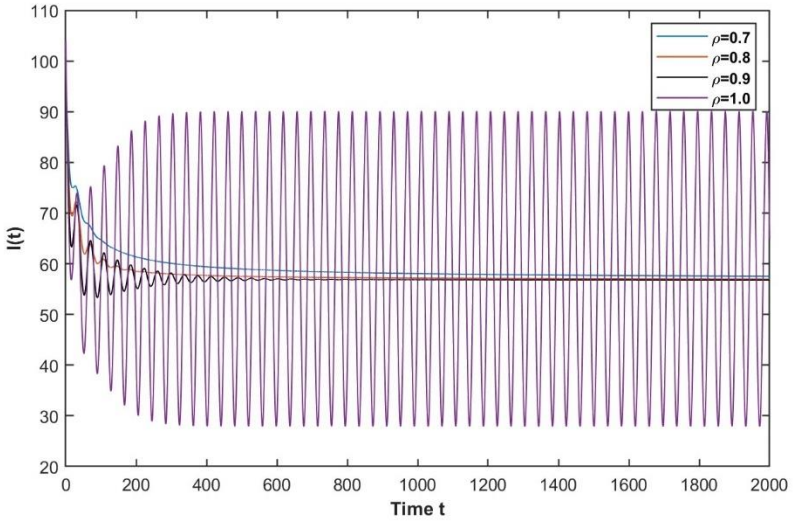

Figure 6.7 (ii) Time series for the infected population when $\rho = 0.7, 0.8, 0.9\ and\ 1, \tau_2 = 8$

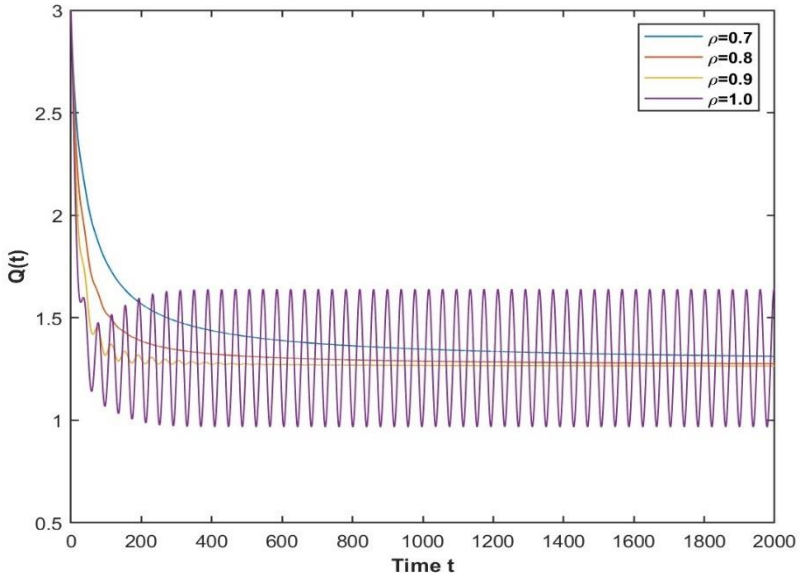

Figure 6.7 (iii) Time series for the quarantine population when $\rho = 0.7, 0.8, 0.9\ and\ 1, \tau_2 = 8$

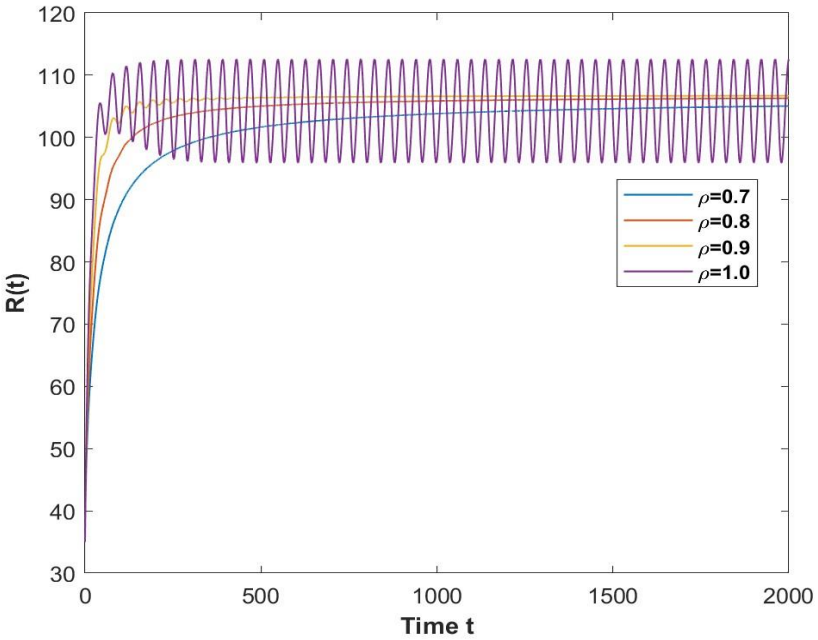

Figure 6.7 (iv) Time series for the recovered population when $\rho = 0.7, 0.8, 0.9\ and\ 1, \tau_2 = 8$

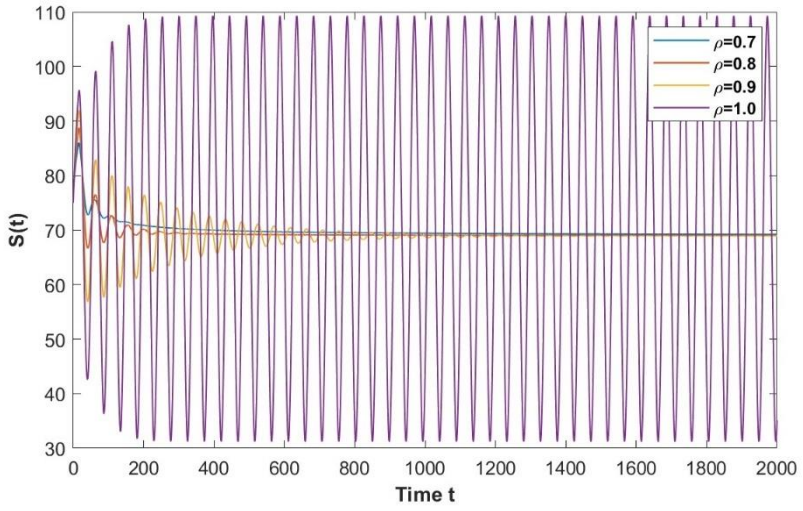

Figure 6.8 (i) Time series for the susceptible population when $\rho = 0.7, 0.8, 0.9\ and\ 1, \tau_2 = 12$

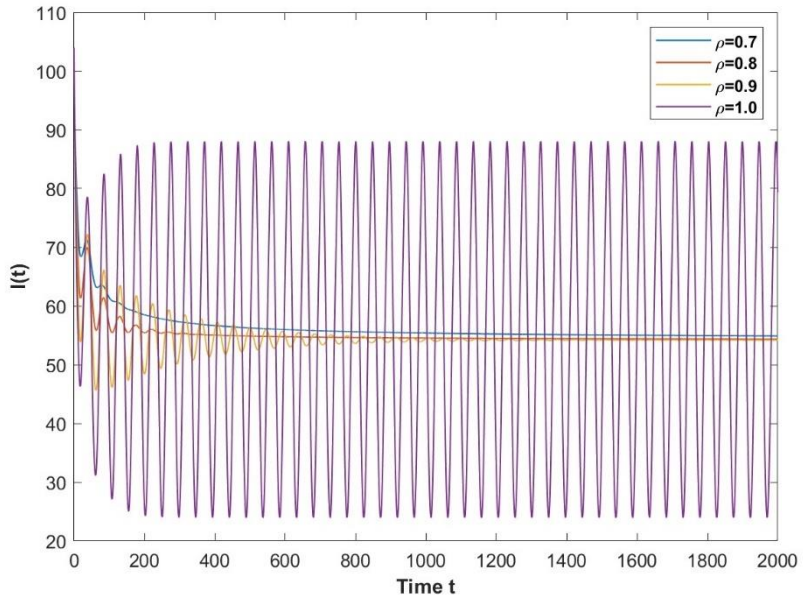

Figure 6.8 (ii) Time series for the infected population when $\rho = 0.7, 0.8, 0.9 \; and \; 1, \tau_2 = 12$

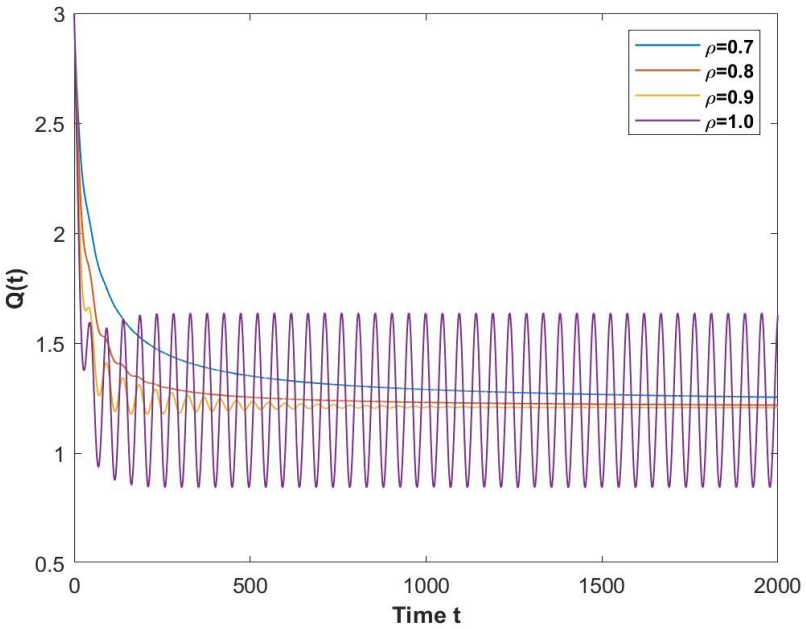

Figure 6.8 (iii) Time series for the quarantine population when $\rho = 0.7, 0.8, 0.9 \; and \; 1, \tau_2 = 12$

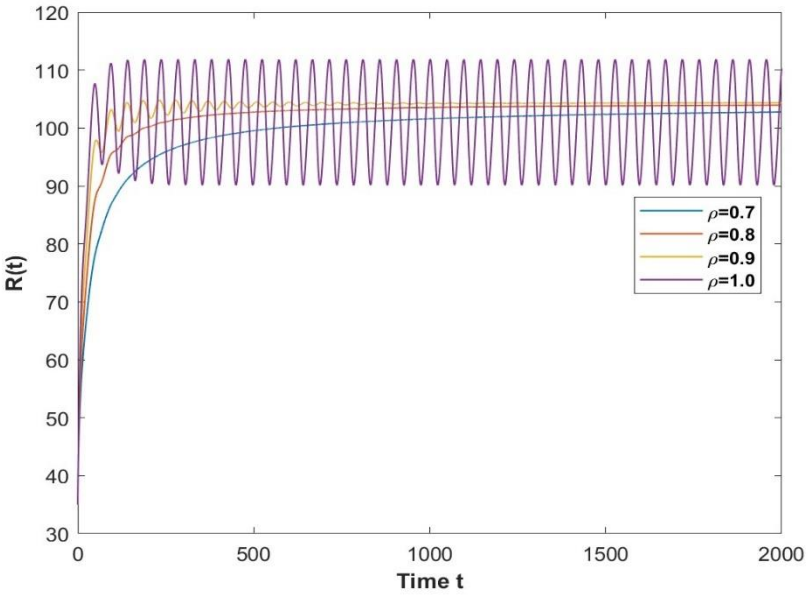

Figure 6.8 (iv) Time series for the recovered population when $\rho = 0.7, 0.8, 0.9\ and\ 1, \tau_2 = 12$

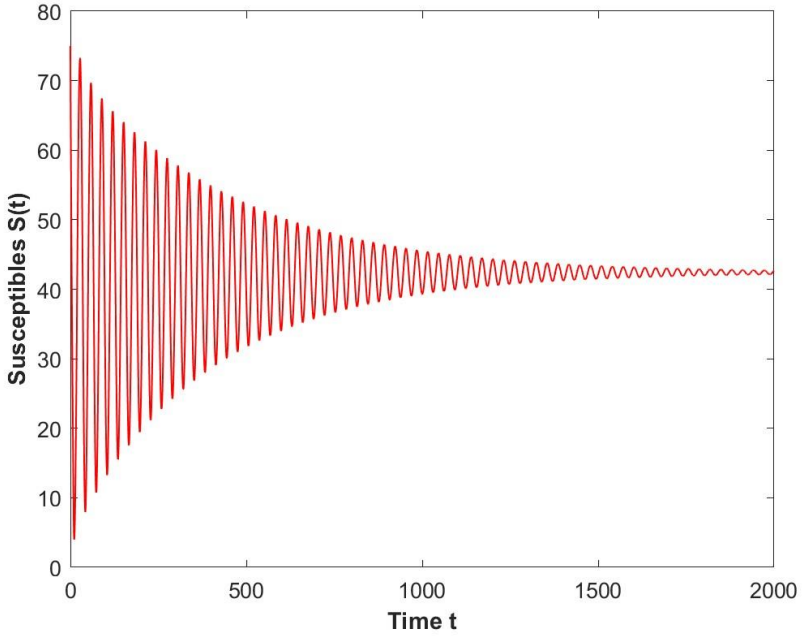

Figure 6.9 (i) Time series for the susceptible population when $\rho = 0.85, \tau_1 = 9, \tau_2 = 18 < \tau_3^0$

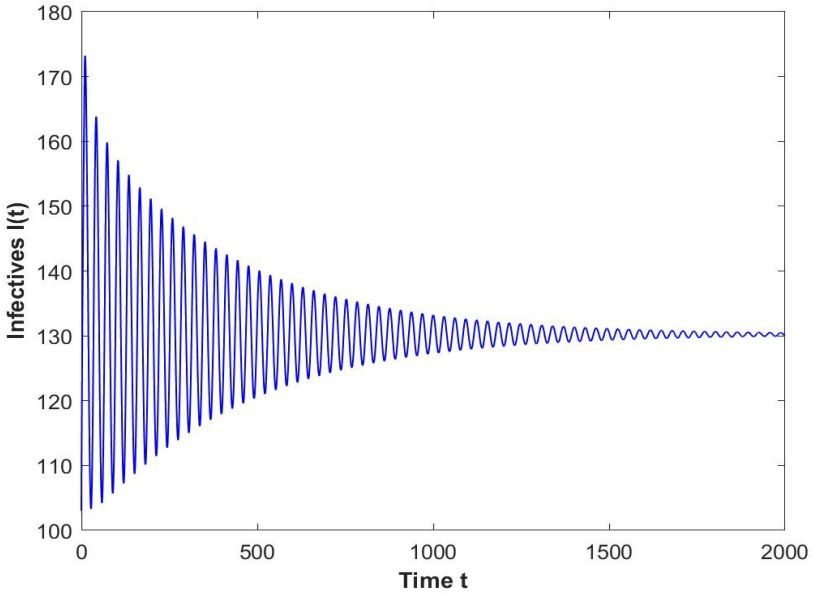

Figure 6.9 (ii) Time series for the infected population when $\rho = 0.85, \tau_1 = 9, \tau_2 = 18 < \tau_3^0$

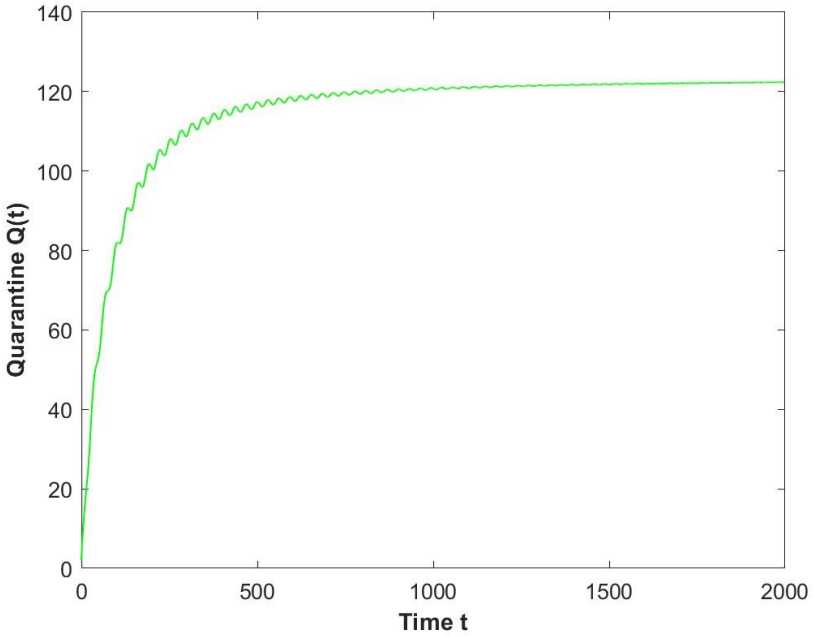

Figure 6.9 (iii) Time series for the quarantine population when $\rho = 0.85, \tau_1 = 9, \tau_2 = 18 < \tau_3^0$

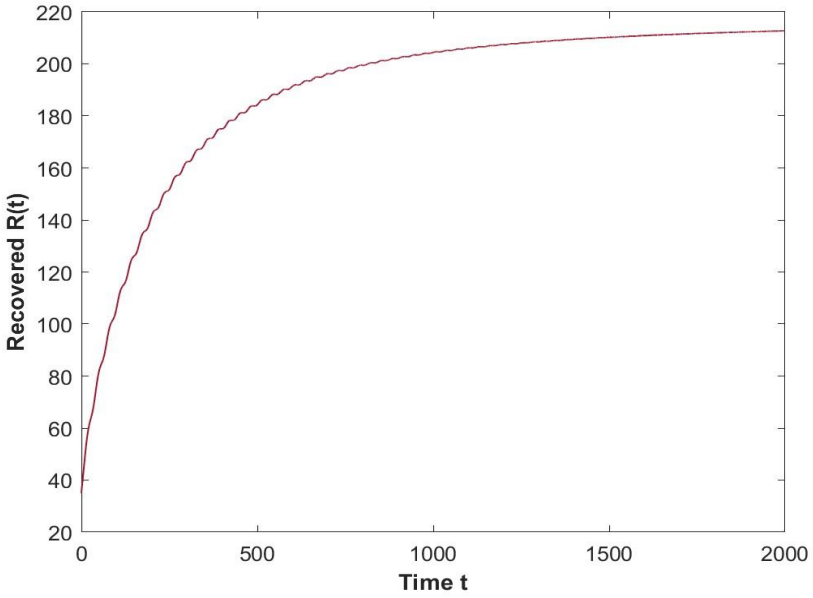

Figure 6.9 (iv) Time series for the recovered population when $\rho = 0.85, \tau_1 = 9, \tau_2 = 18 < \tau_3^0$

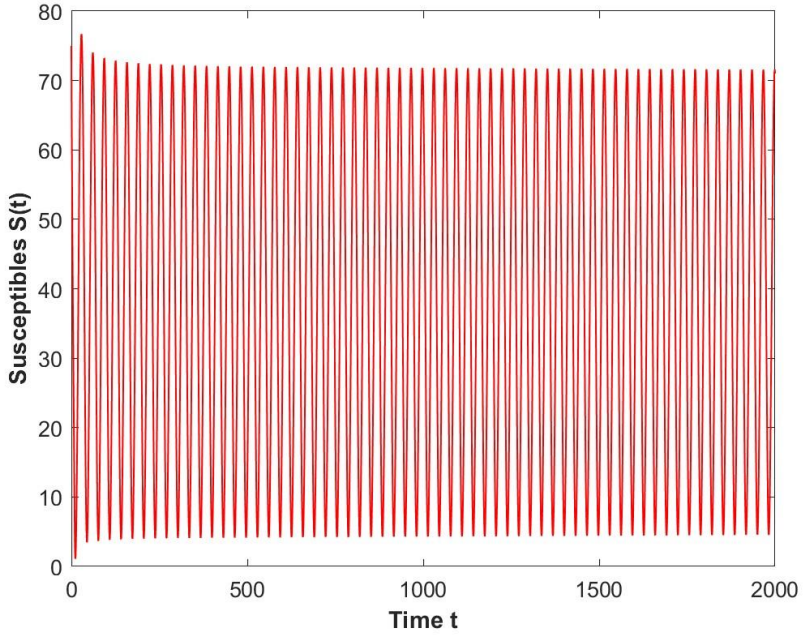

Figure 6.10 (i) Time series for the susceptible population when $\rho = 0.85, \tau_1 = 9, \tau_2 = 24.5 > \tau_3^0$

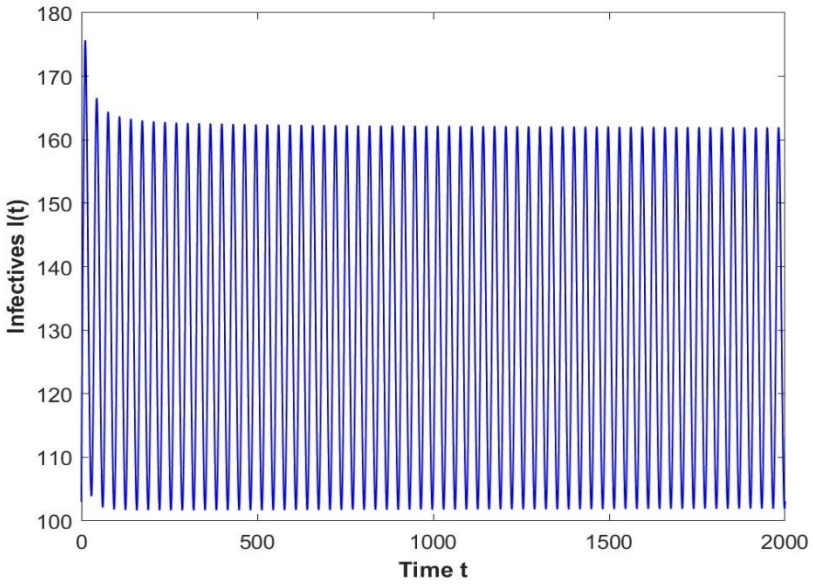

Figure 6.10 (ii) Time series for the infected population when $\rho = 0.85, \tau_1 = 9, \tau_2 = 24.5 > \tau_3^0$

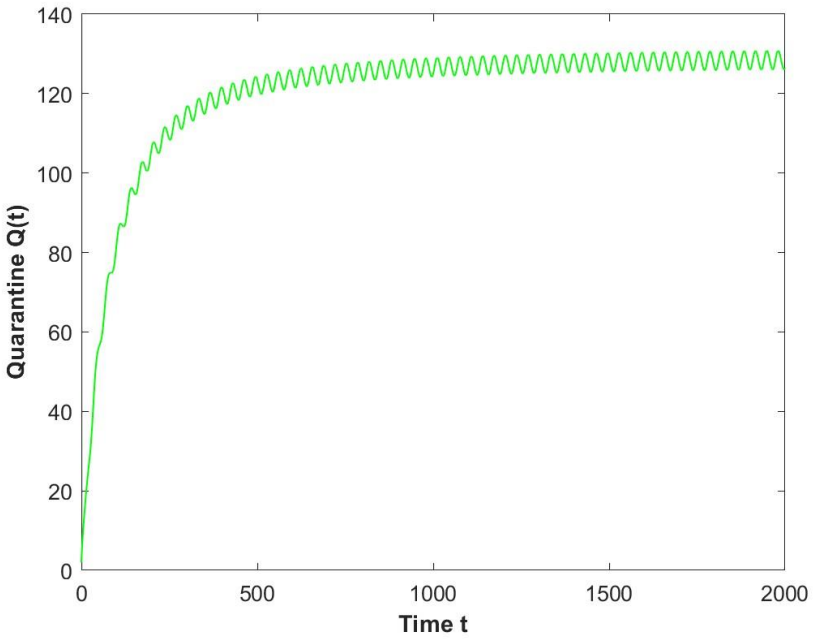

Figure 6.10 (iii) Time series for the quarantine population when $\rho = 0.85, \tau_1 = 9, \tau_2 = 24.5 > \tau_3^0$

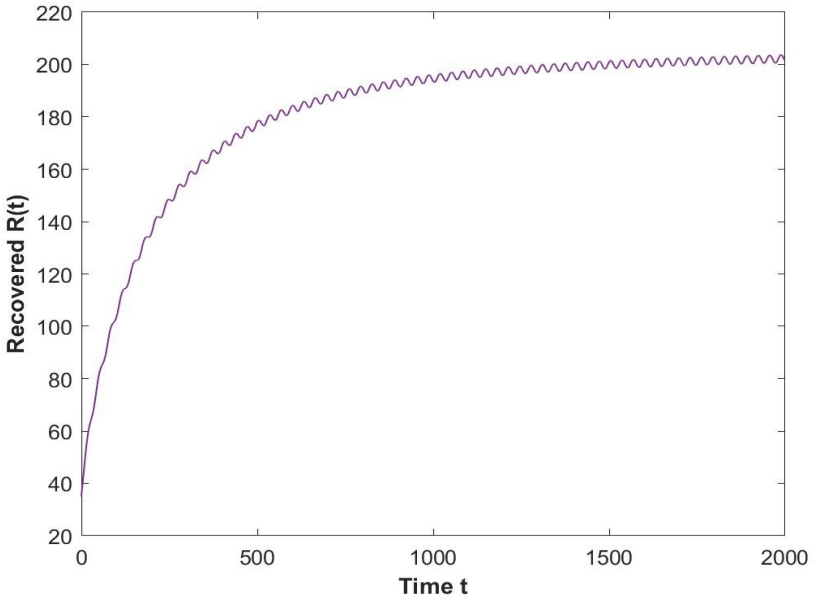

Figure 6.10 (iv) Time series for the recovered population when $\rho = 0.85, \tau_1 = 9, \tau_2 = 24.5 > \tau_3^0$

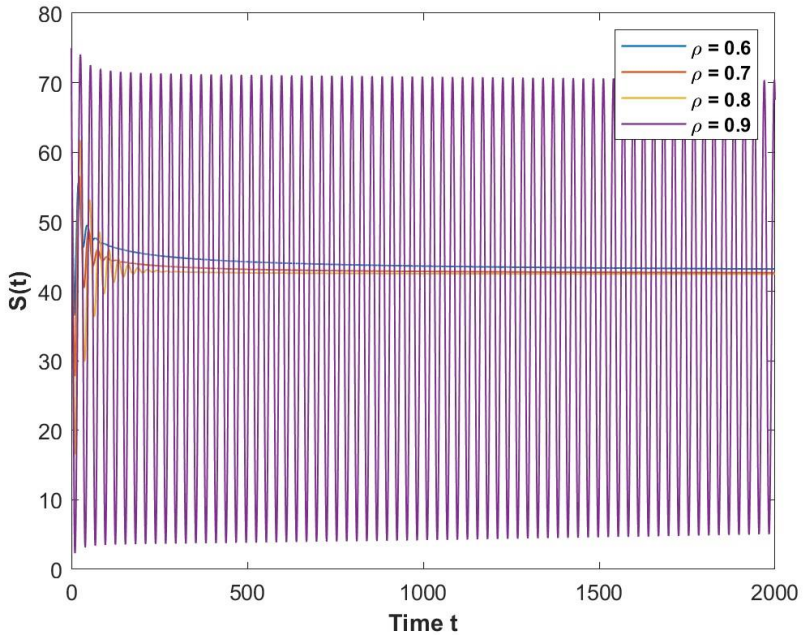

Figure 6.11 (i) Time series for the susceptible population when $\rho = 0.6, 0.7, 0.8 \; and \; 0.9, \tau_2 = 13.5$

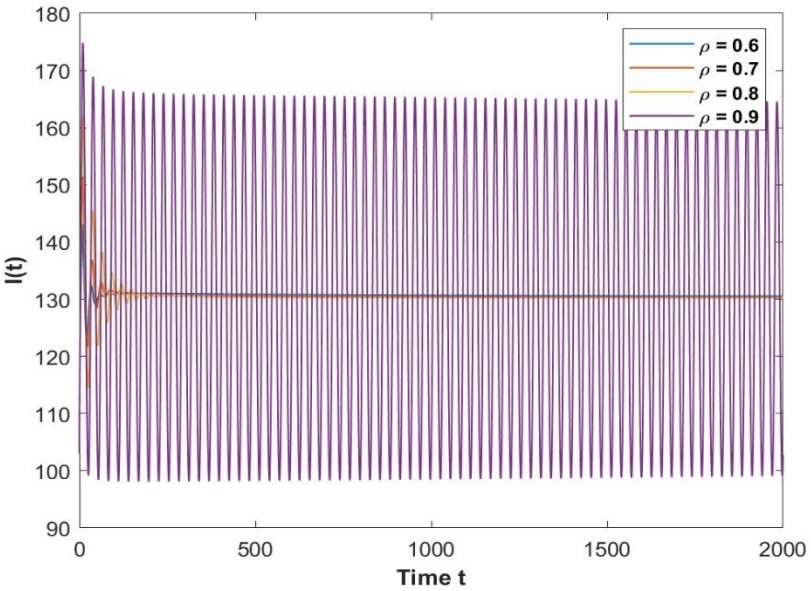

Figure 6.11 (ii) Time series for the infected population when $\rho = 0.6, 0.7, 0.8 \; and \; 0.9, \tau_2 = 13.5$

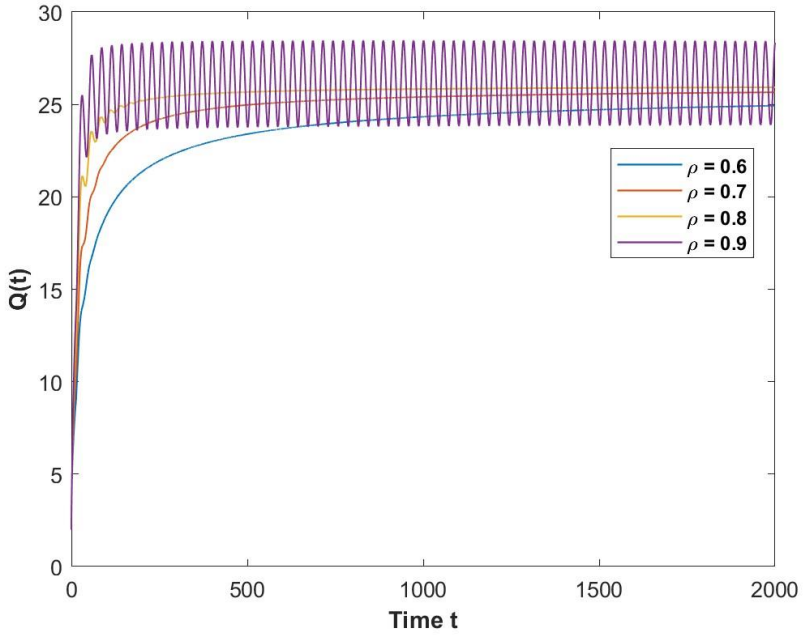

Figure 6.11 (iii) Time series for the quarantine population when $\rho = 0.6, 0.7, 0.8 \; and \; 0.9, \tau_2 = 13.5$

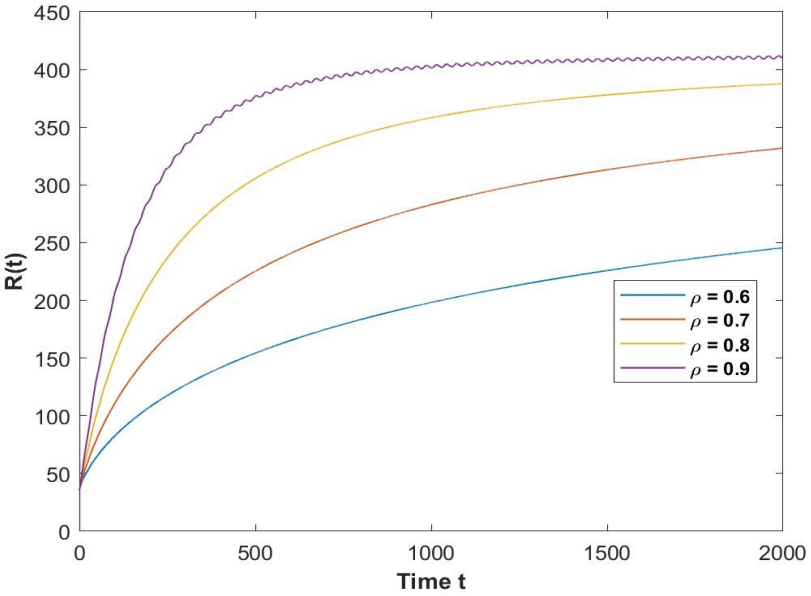

Figure 6.11 (iv) Time series for the recovered population when $\rho = 0.6, 0.7, 0.8 \; and \; 0.9, \tau_2 = 13.5$

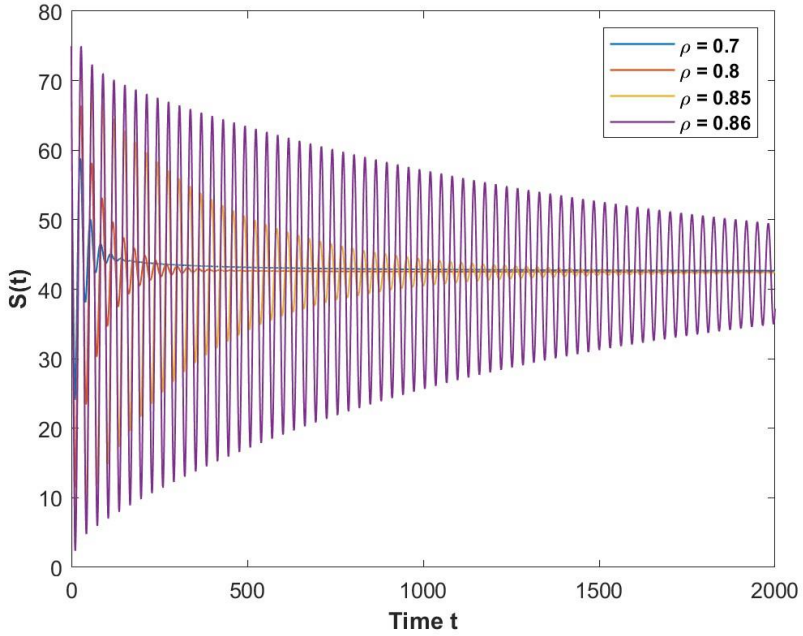

Figure 6.12 (i) Time series for the susceptible population when $\rho = 0.7, 0.8, 0.85 \; and \; 0.86, \tau_2 = 19.5$

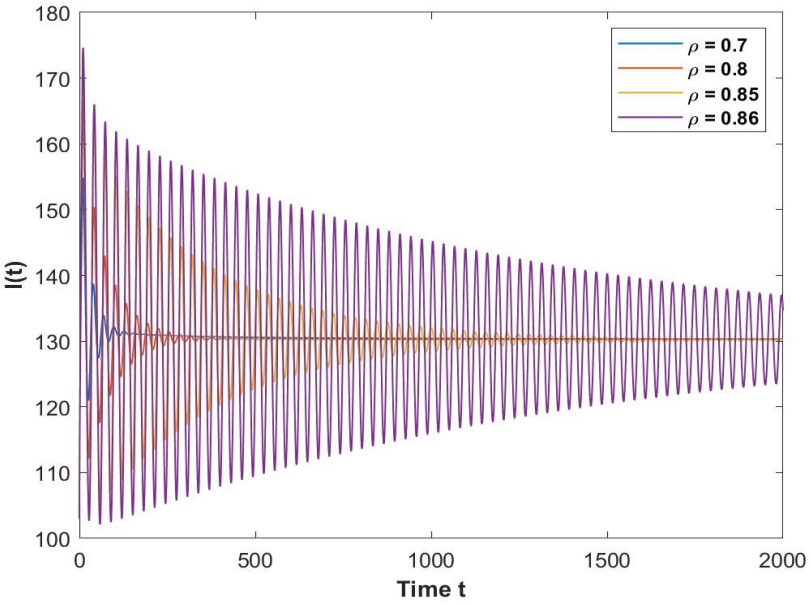

Figure 6.12 (ii) Time series for the infected population when $\rho = 0.7, 0.8, 0.85 \; and \; 0.86, \tau_2 = 19.5$

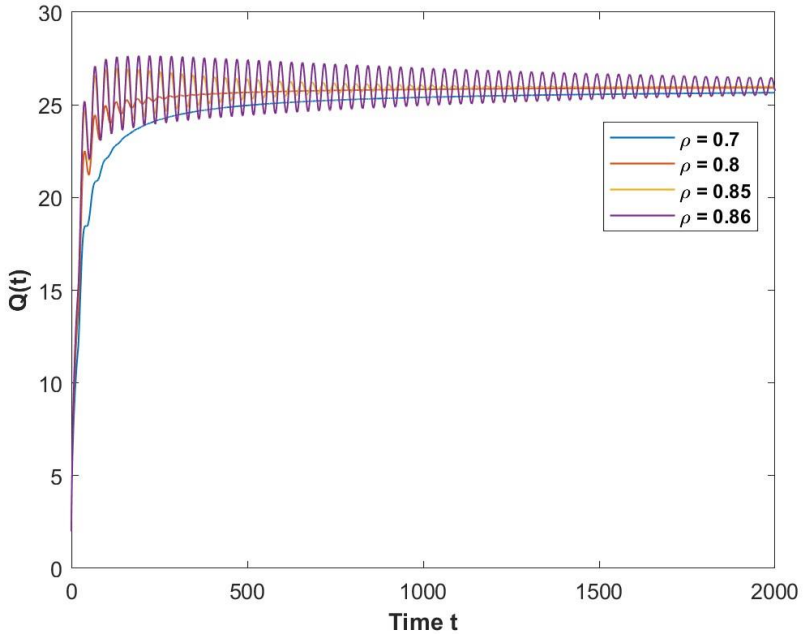

Figure 6.12 (iii) Time series for the quarantine population when $\rho = 0.7, 0.8, 0.85 \; and \; 0.86, \tau_2 = 19.5$

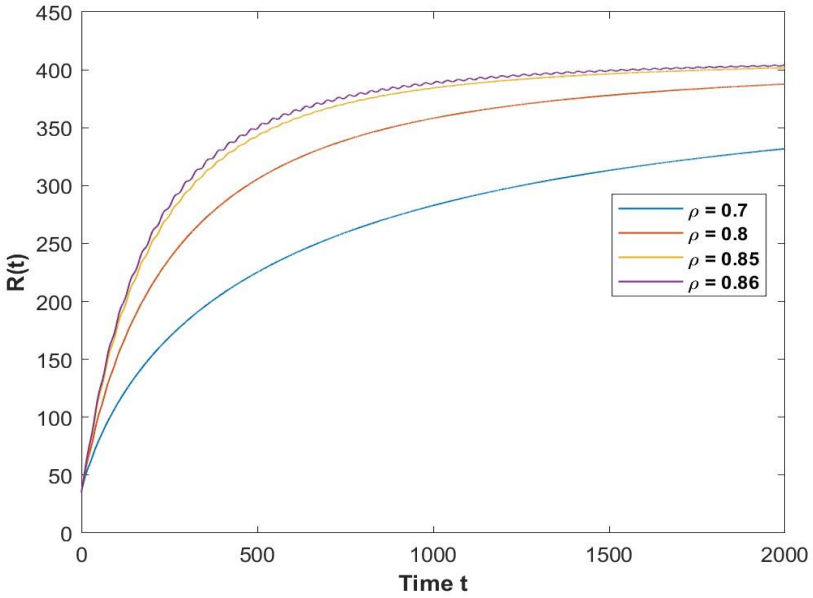

Figure 6.12 (iv) Time series for the recovered population when $\rho = 0.7, 0.8, 0.85 \; and \; 0.86, \tau_2 = 19.5$

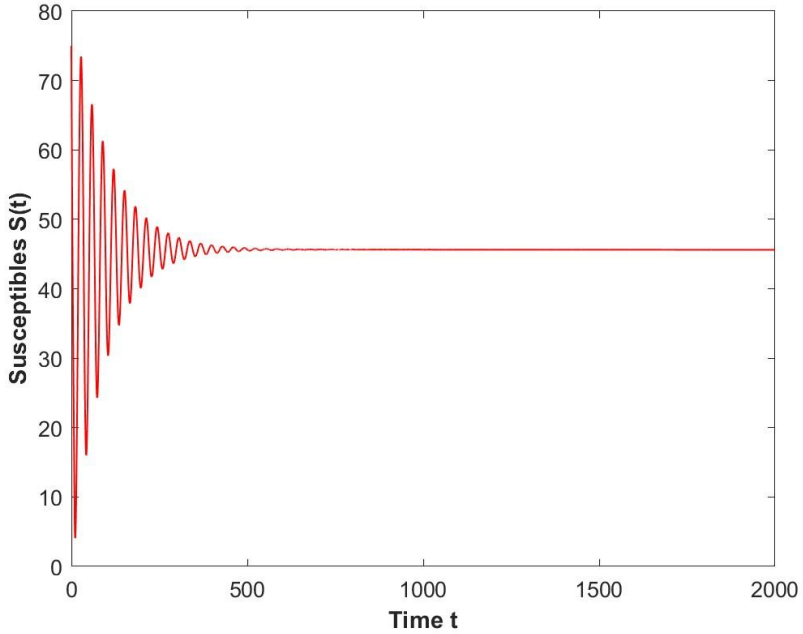

Figure 6.13 (i) Time series for the susceptible population when $\rho = 0.85, \tau_2 = 18, \tau_1 = 9 < \tau_4^0$

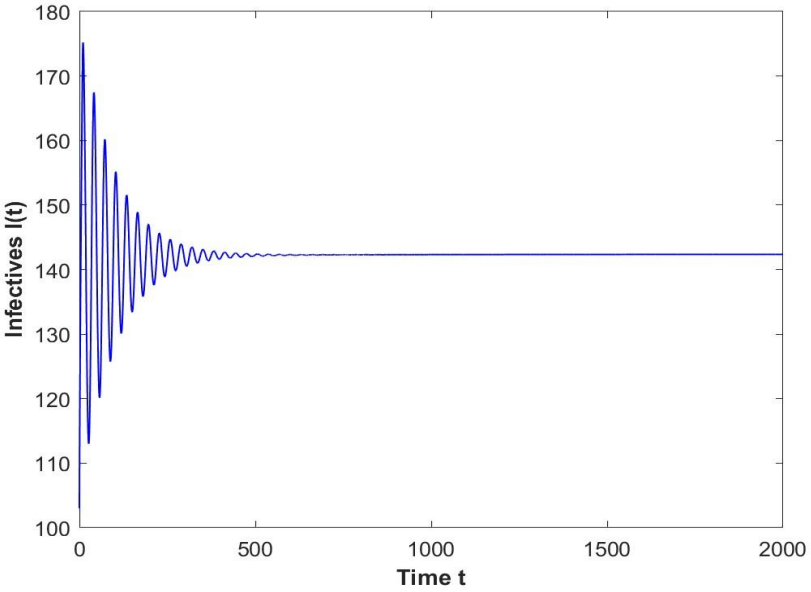

Figure 6.13 (ii) Time series for the infected population when $\rho = 0.85, \tau_2 = 18, \tau_1 = 9 < \tau_4^0$

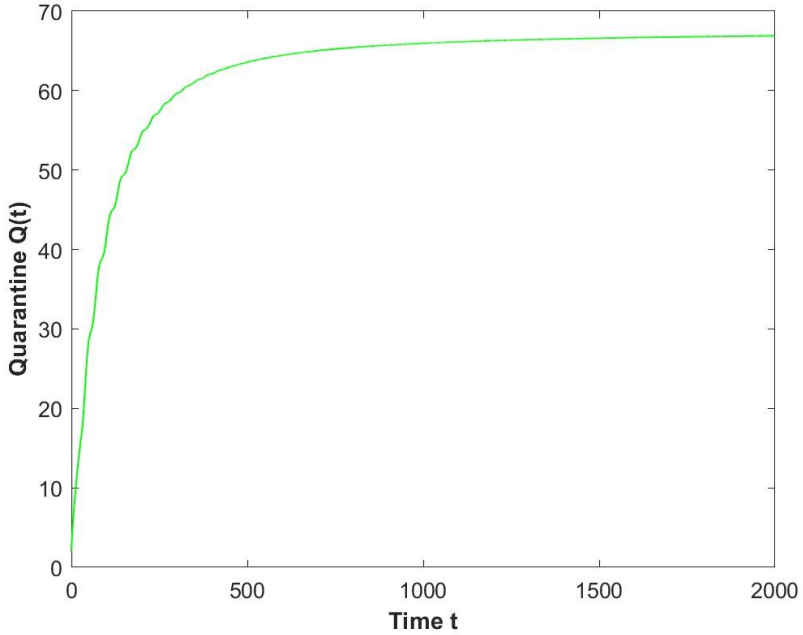

Figure 6.13 (iii) Time series for the quarantine population when $\rho = 0.85, \tau_2 = 18, \tau_1 = 9 < \tau_4^0$

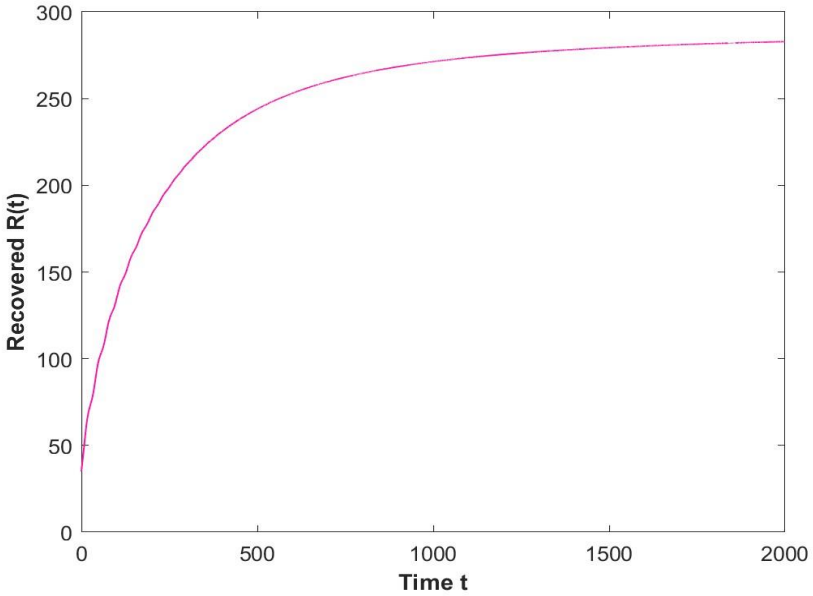

Figure 6.13 (iv) Time series for the recovered population when $\rho = 0.85, \tau_2 = 18, \tau_1 = 9 < \tau_4^0$

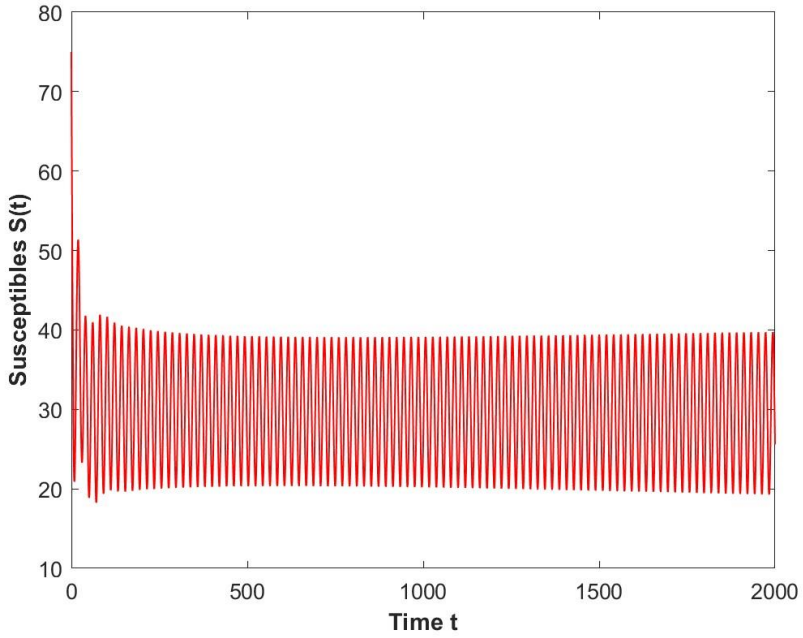

Figure 6.14 (i) Time series for the susceptible population when $\rho = 0.85, \tau_2 = 18, \tau_1 = 23 > \tau_4^0$

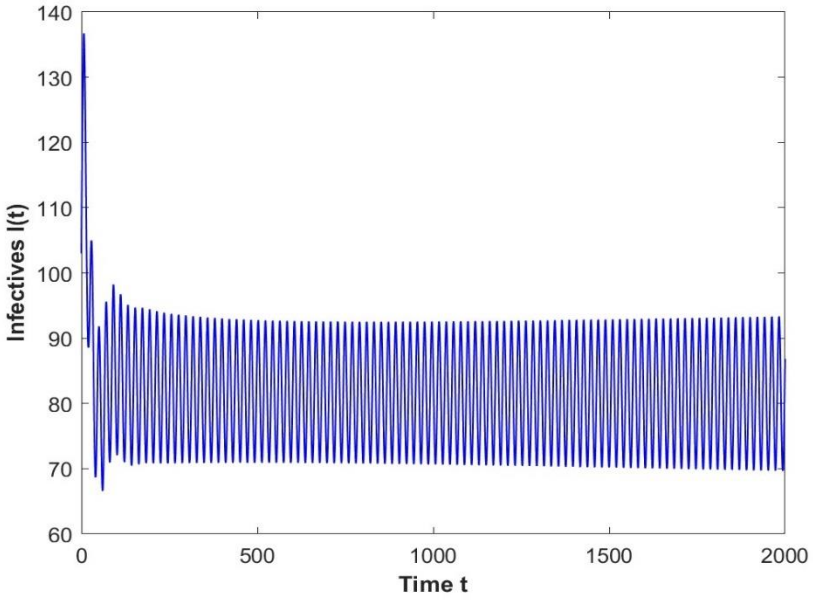

Figure 6.14 (ii) Time series for the infected population when $\rho = 0.85, \tau_2 = 18, \tau_1 = 23 > \tau_4^0$

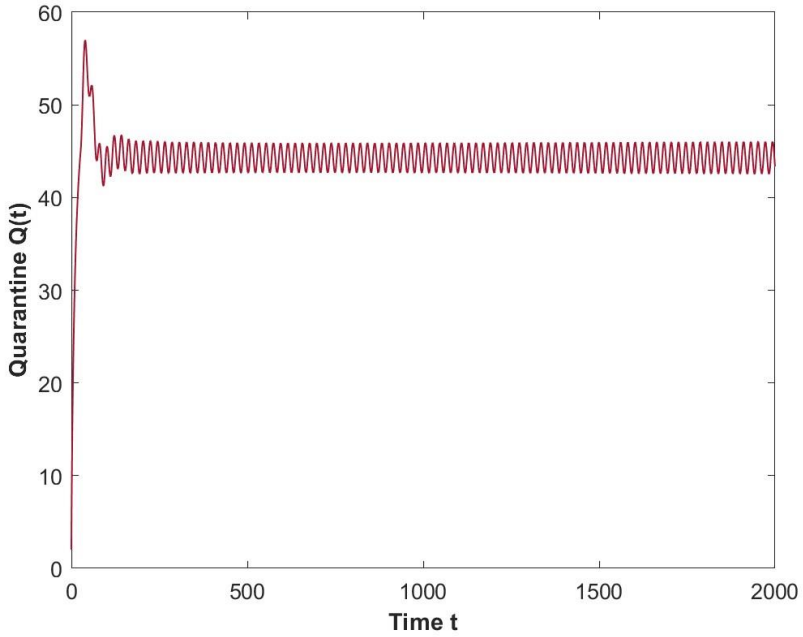

Figure 6.14 (iii) Time series for the quarantine population when $\rho = 0.85, \tau_2 = 18, \tau_1 = 23 > \tau_4^0$

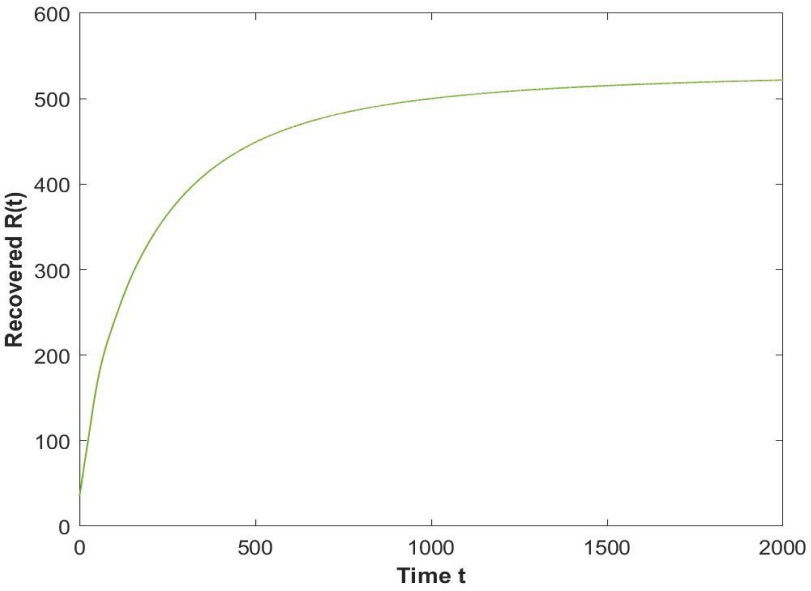

Figure 6.14 (iv) Time series for the recovered population when $\rho = 0.85, \tau_2 = 18, \tau_1 = 23 > \tau_4^0$

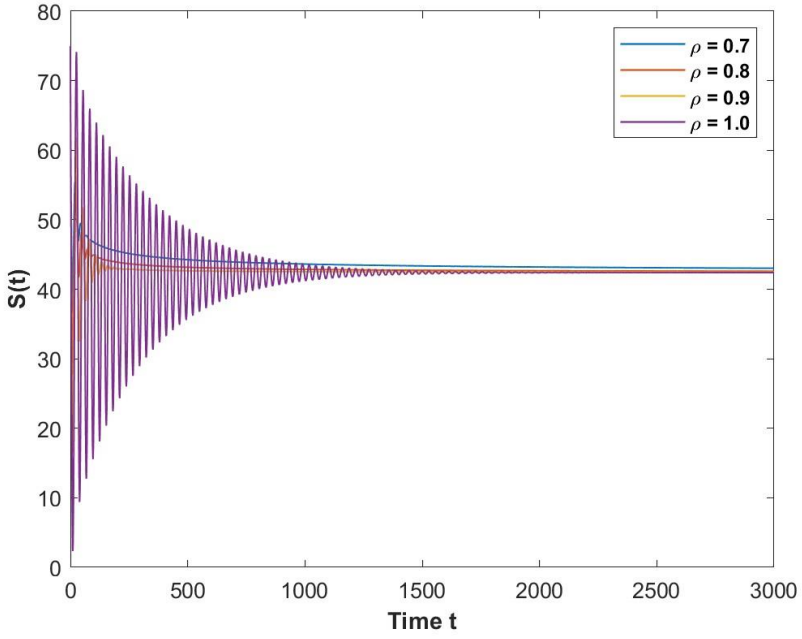

Figure 6.15 (i) Time series for the susceptible population when $\rho = 0.7, 0.8, 0.9 \; and \; 1.0, \tau_1 = 9$

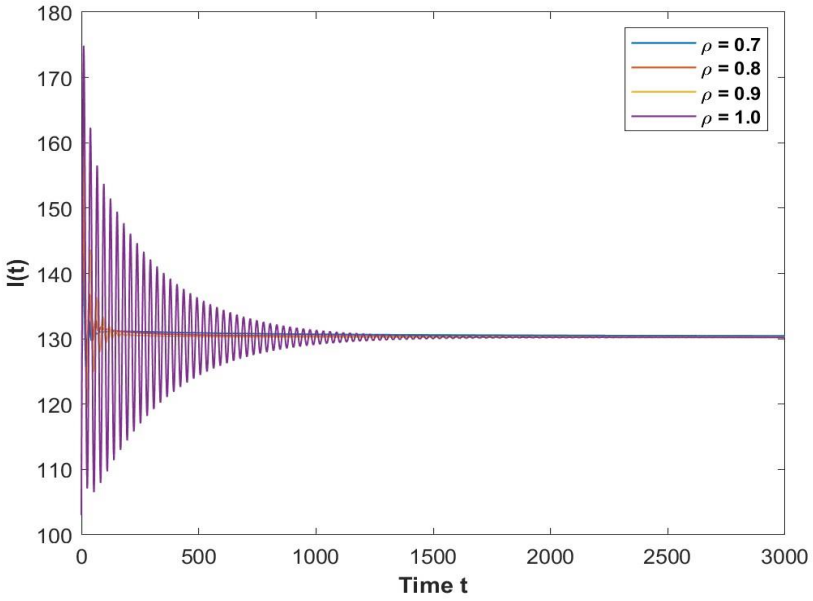

Figure 6.15 (ii) Time series for the infected population when $\rho = 0.7, 0.8, 0.9 \; and \; 1.0, \tau_1 = 9$

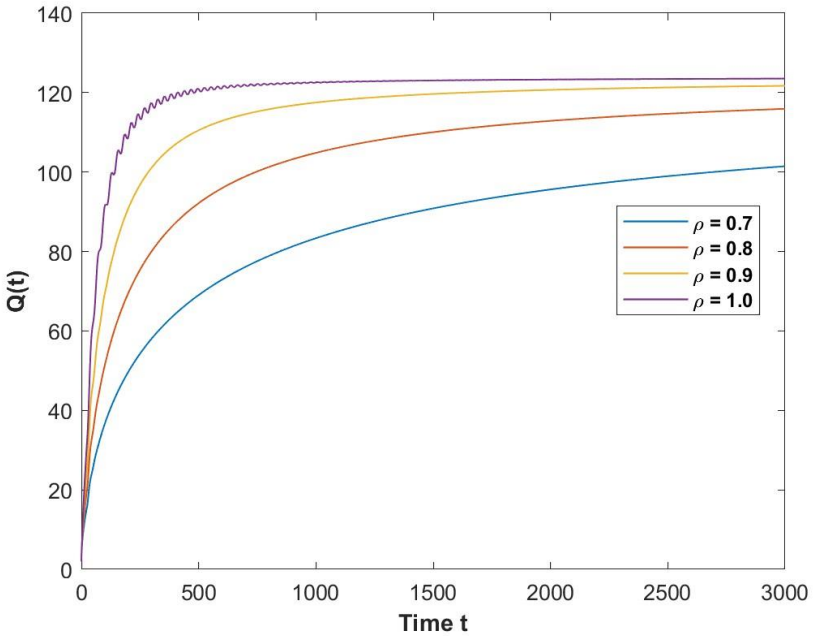

Figure 6.15 (iii) Time series for the quarantine population when $\rho = 0.7, 0.8, 0.9 \; and \; 1.0, \tau_1 = 9$

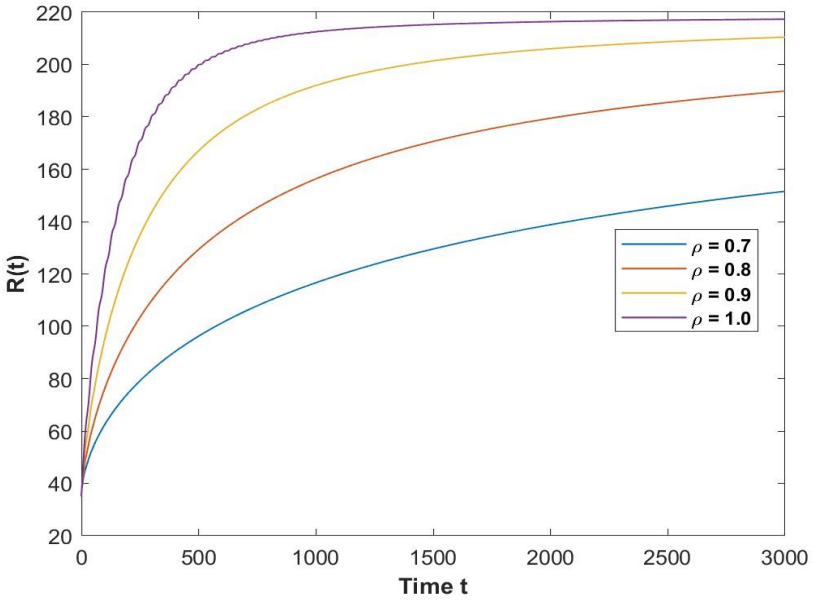

Figure 6.15 (iv) Time series for the recovered population when $\rho = 0.7, 0.8, 0.9 \; and \; 1.0, \tau_1 = 9$

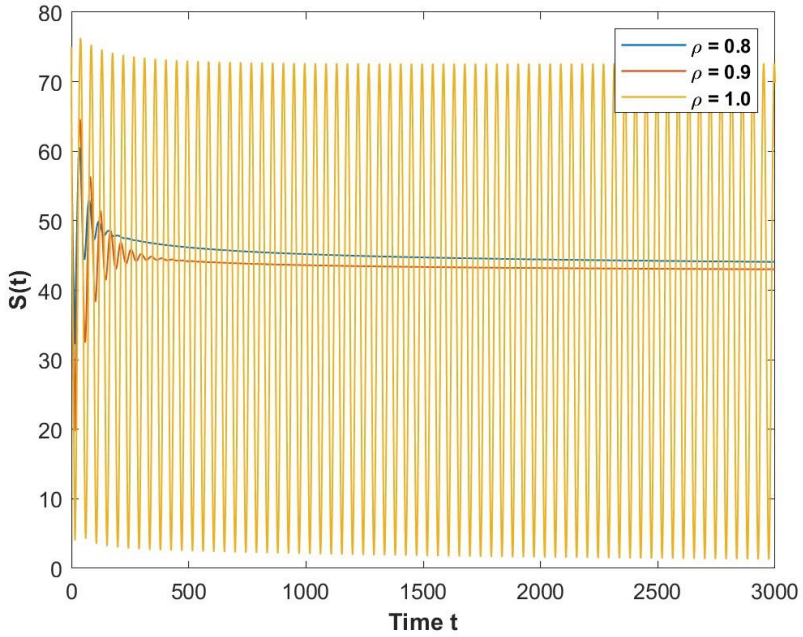

Figure 6.16 (i) Time series for the susceptible population when $\rho = 0.7, 0.8, 0.9 \; and \; 1.0, \tau_1 = 15$

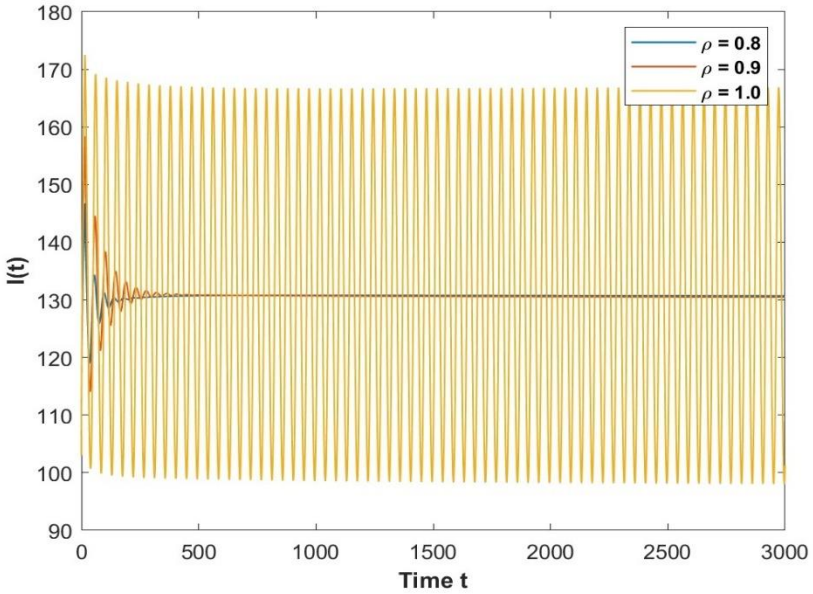

Figure 6.16 (ii) Time series for the infected population when $\rho = 0.7, 0.8, 0.9 \; and \; 1.0, \tau_1 = 15$

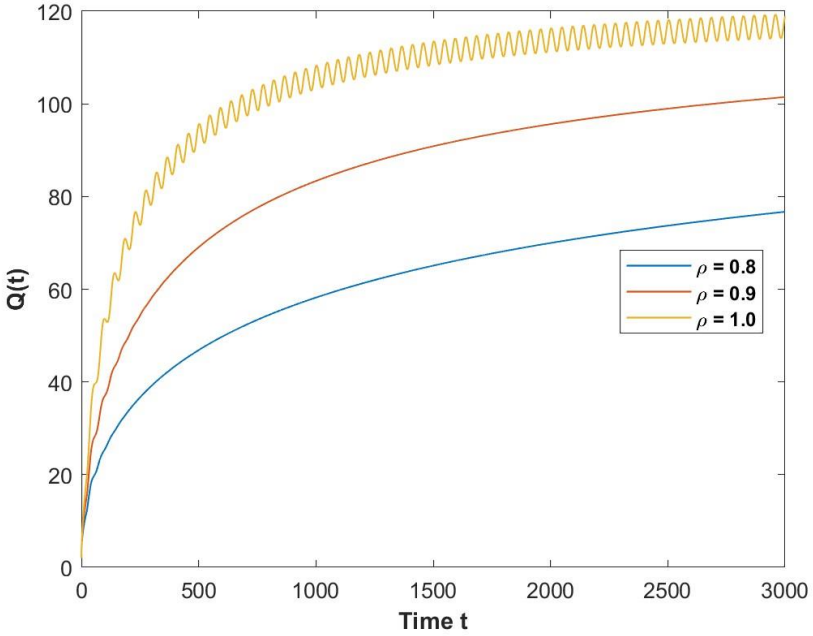

Figure 6.16 (iii) Time series for the quarantine population when $\rho = 0.7, 0.8, 0.9 \; and \; 1.0, \tau_1 = 15$

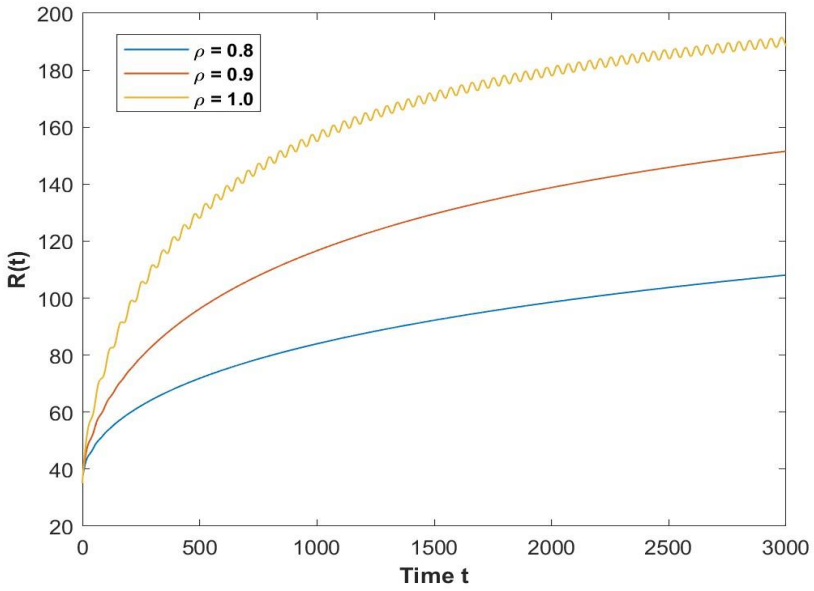

Figure 6.16 (iv) Time series for the recovered population when $\rho = 0.7, 0.8, 0.9 \; and \; 1.0, \tau_1 = 15$

6.6 Conclusion

This chapter examines a fractional order SIQR model that has two distinct time delays and a saturated incidence rate and treatment rate. We generalized the integer order system into a fractional order system, which more precisely captures the disease's process. We acquire the characteristics of the system. A number of adequate conditions have been determined based on the derived characteristics to ensure the stability of the endemic equilibrium points and the disease free equilibrium, as well as the existence of the Hopf bifurcation. We find that when the time delays cross the critical thresholds of τ_1^* and τ_2^*, the model exhibits Hopf bifurcation.

Some numerical simulations have been used to validate the theoretical results. Our numerical results confirm the theoretical work that the endemic equilibrium is locally stable when time delays are smaller than the critical value, and that the endemic equilibrium becomes unstable and undergoes Hopf bifurcation when the bifurcation parameter crosses the critical value. Additionally, numerical simulations suggest that because of the long run memory embodied by the fractional derivative, varying fractional orders result in different rates of steady state stabilization. The system's dynamics are improved by including memory in the model, which is represented by the fractional derivative and time delay.

CHAPTER 7

CONCLUSION, FUTURE SCOPE AND SOCIAL IMPACT

In this final chapter, we summarize the main outcomes of the thesis and present some potential directions for further research along with its social impact.

7.1 Conclusion

Compared to traditional integer-order models, the development of a fractional mathematical model for the dynamics of infectious diseases offers a more precise and adaptable method of simulating the spread of diseases. These models provide a more accurate representation of the dynamics of disease transmission in real life by capturing memory effects and more intricate interactions within a population using fractional-order derivatives. The accuracy and adaptability of epidemiological modeling for infectious disease dynamics are significantly enhanced by including time delay in the fractional mathematical model. By incorporation of fractional derivatives and time delays, the model covers more realistic disease spread than with classical models. Fractional derivatives represent the long-term memory and hereditary nature of the disease, while time delays may reflect real-world phenomena such as incubation periods, delayed immune responses or lags in applying social measures. The model formed by the amalgamation of these two phenomena reflects a more realistic mechanism of disease dynamics in time series and is thus better for forecasting about the diseases which will help suggest predictive measures, thereby supporting sensible planning etc., regarding public health interventions.

In the thesis, we formulated and analyzed Caputo fractional order mathematical models to investigate the transmission and preventive mechanisms of infectious diseases with non-linear incidence and treatment rates. Models have been categorized based on the outbreak, transmission, and expansion of the disease by integrating numerous aspects, such as psychological impacts, population density of susceptible individuals, and constraints on treatment techniques. The model has also incorporated novel combinations of various non-linear incidence and treatment rates according to the disease's requirements. The infection incidence rates have a non-linear functional form that facilitates the required dynamics of transmission in a large population. It is demonstrated that the proposed models are epidemiologically valid. The model’s equilibrium analysis confirms and demonstrates the existence and uniqueness of equilibria. Numerical simulations were used to analyse and validate the equilibria's local and global stability characteristics. For each model, we have

determined the basic reproduction number R_0,which serves as threshold value for assessing disease persistence in the endemic domain. Suitable incidence and treatment rates for different diseases can capture the various unknown aspects of the dynamics of the disease. Public health organizations may use the suggested combinations to keep an eye on the outbreak, better preventive suggestions and proper treatment planning to tackle the situation according to the severity of the condition. Therefore, a lot of precaution has been taken in choosing suitable form of incidence and treatment rates according to the need of the dynamics of a particular situation of the diseases.

In chapter two, we explore the Caputo fractional order SIR epidemic model with Beddington-De Angelis incidence and Holling type II treatment rate for COVID-19. The local and global stability of the disease free & endemic equilibrium points has been investigated. The results suggests that better convergence can be accomplished by reducing the order of fractional derivatives. Also, the rate of transmission decreases if there is less contact between susceptibles and infectives which could be achieved by taking adequate safety measures both by susceptibles and infectives, as well as imposing lockdown. Chapter three studies fractional order model using Caputo fractional derivative to analyse the effects of social media on mental health during COVID-19 considering Holling type II saturated cure rate and the Beddington-De Angelis incidence rate, discussing the stability behavior of local and endemic equilibrium points. It concludes that on reducing the fractional order, number of infectives decreases. Also, number of infectives decreases by optimum and control use of social media in case of any situation like COVID-19 where the possibility of panic is very high. From this study we suggest that as the infected individuals take more precautions such as switching to traditional media use, reducing online time, practicing yoga, exercise and meditation, appropriate use of social media etc, number of infectives decreases. Chapter four presents Caputo fractional derivative model for impact of awareness on infectious disease with Holling type III treatment rate and Monod-Haldane incidence rate and it has been discovered that increasing media awareness decreases the number of infected individuals and consequently reduces the peak of the epidemic. In chapter five, we examine the dynamics of fractionally ordered delay differential Susceptible-Infectives-Recovered epidemiological model with Holling functional type II treatment rate and Crowley-Martin (CM) functional type incidence. To make ourselves acquainted with more practical understanding of the epidemic's dynamics, the incidence rate was delayed by the latency time, studies the sufficient requirements for steady-state stability and Hopf bifurcation in the presence of time delay. The model exhibits a Hopf bifurcation at the threshold parameters. When time delays exceed critical values, the model goes through Hopf bifurcation. Numerical studies demonstrate that combining fractional order with time delays in the epidemic model affects the behavior and improves the model's stability. Chapter six is an extension of chapter five. A double delayed fractional order susceptible-infected-quarantine-recovered epidemic model with saturated incidence and treatment rates is examined in this chapter. The model includes two time delays: one for the length of the incubation period, and another for the time delay caused by people's resistance to being placed under quarantine. The model experiences Hopf bifurcation when delays exceed critical values. Our numerical results confirm the theoretical work that the

endemic equilibrium is locally stable when time delays are smaller than the critical value, and that the endemic equilibrium becomes unstable and undergoes Hopf bifurcation when the bifurcation parameter crosses the critical value. Additionally, numerical simulations suggest that because of the long run memory embodied by the fractional derivative, varying fractional orders result in different rates of steady state stabilization. The system's dynamics are improved by including memory in the model, which is represented by the fractional derivative and time delay.

7.2 Future Scope

We have solely suggested deterministic models for the spread of disease in this thesis. To account for randomness in disease transmission, fractional models can be coupled with stochastic processes as future research and directions. This will increase possibility of accuracy in forecast and may make the models more sensitive to real-world uncertainty. The inclusion of control theory can provide improved instruments for the control of infectious diseases.

7.3 Social Impact

Fractional models can be used to improve planning and response strategies, which will help society in better management of pandemics and minimize their overall effects. By offering more accurate predictions of disease spread and the effectiveness of interventions, fractional models may help in lessening the financial impact of infectious disease outbreaks by facilitating more effective resource allocation. By educating the public on the need of prompt actions, such as adhering to preventative measures, seeking treatment early, and the consequences of delays, the results of these models can help to mould into a society that is more informed and proactive even in more critical situation.

REFERENCES

Abdeljawad, T., & Alzabut, J. (2018). On Riemann-Liouville fractional q–difference equations and their application to retarded logistic type model. Mathematical Methods in the Applied Sciences, 41(18), 8953–8962. https://doi.org/10.1002/mma.4743

Abdeljawad, T., Alzabut, J., & Jarad, F. (2017). A generalized Lyapunov-type inequality in the frame of conformable derivatives. Advances in Difference Equations, 2017(1). https://doi.org/10.1186/s13662-017-1383-z

Agarwal, R. P., Benchohra, M., & Hamani, S. (2010). A survey on existence results for boundary value problems of nonlinear fractional differential equations and inclusions. Acta Applicandae Mathematicae, 109(3), 973–1033. https://doi.org/10.1007/s10440-008-9356-6

Aghdaoui, H., Lamrani Alaoui, A., Nisar, K. S., & Tilioua, M. (2021). On analysis and optimal control of a SEIRI epidemic model with general incidence rate. Results in Physics, 20, 103681. https://doi.org/10.1016/j.rinp.2020.103681

Akdim, K., Adil Ez-Zetouni, & Zahid, Mehdi. (2022). The influence of awareness campaigns on the spread of an infectious disease: a qualitative analysis of a fractional epidemic model. 8, 1311–1319. https://doi.org/10.1007/s40808-021-01158-9

Al-Dmour, H., Masa'deh, R., Salman, A., Abuhashesh, M., & Al-Dmour, R. (2020). Influence of social media platforms on public health protection against the COVID-19 pandemic via the mediating effects of public health awareness and behavioral changes: Integrated model. Journal of Medical Internet Research, 22(8). https://doi.org/10.2196/19996

Alidousti, J., & Ghaziani, R. K. (2017). Spiking and bursting of a fractional order of the modified FitzHugh-Nagumo neuron model. Mathematical Models and Computer Simulations, 9(3), 390–403. https://doi.org/10.1134/S2070048217030036

Alidousti, J., & Mostafavi Ghahfarokhi, M. (2019). Dynamical behavior of a fractional three-species food chain model. Nonlinear Dynamics, 95(3), 1841–1858. https://doi.org/10.1007/s11071-018-4663-6

Allgaier, J., & Svalastog, A. L. (2015). The communication aspects of the Ebola virus disease outbreak in Western Africa – do we need to counter one, two, or many epidemics? Croatian Medical Journal, 56(5), 496. https://doi.org/10.3325/CMJ.2015.56.496

Alshorman, A., Wang, X., Joseph Meyer, M., & Rong, L. (2017). Analysis of HIV models with two-time delays. Journal of Biological Dynamics, 11, 40–64. https://doi.org/10.1080/17513758.2016.1148202

Angstmann, C. N., Henry, B. I., & McGann, A. V. (2016). A fractional-order infectivity SIR model. Physica A: Statistical Mechanics and Its Applications, 452, 86–93. https://doi.org/10.1016/j.physa.2016.02.029

Anastasio, T. J. (1994). The fractional-order dynamics of brainstem vestibulo-oculomotor neurons. Biological Cybernetics, 72(1), 69-79. https://doi.org/10.1007/BF00206239

Awais, M., Alshammari, F. S., Ullah, S., Khan, M. A., & Islam, S. (2020). Modeling and simulation of the novel coronavirus in Caputo derivative. Results in Physics, 19(November), 103588. https://doi.org/10.1016/j.rinp.2020.103588

Baleanu, D., Jajarmi, A., Sajjadi, S. S., & Mozyrska, D. (2019). A new fractional model and optimal control of a tumor-immune surveillance with non-singular derivative operator. Chaos: An Interdisciplinary Journal of Nonlinear Science, 29(8), 083127. https://doi.org/10.1063/1.5096159

Bardina, X., Ferrante, M., & Rovira, C. (2020). A stochastic epidemic model of COVID-19 disease. AIMS Mathematics, 2020, 5(6): 7661-767. https://doi: 10.3934/math.2020490

Beddington, J. R. (1975). Mutual Interference Between Parasites or Predators and its Effect on Searching Efficiency. The Journal of Animal Ecology, 44(1), 331. https://doi.org/10.2307/3866

Bontcheva, K., Gorrell, G., & Wessels, B. (2013). Social Media and Information Overload: Survey Results. *ArXiv, abs/1306.0813*.

Boudaoui, A., El hadj Moussa, Y., Hammouch, Z., & Ullah, S. (2021). A fractional-order model describing the dynamics of the novel coronavirus (COVID-19) with nonsingular kernel. Chaos, Solitons & Fractals, 110859. https://doi.org/10.1016/j.chaos.2021.110859

Chen, W. C. (2008). Nonlinear dynamics and chaos in a fractional-order financial system. Chaos, Solitons and Fractals, 36(5), 1305–1314. https://doi.org/10.1016/j.chaos.2006.07.051

Chinnathambi, R., & Rihan, F. A. (2018). Stability of fractional-order prey–predator system with time-delay and Monod–Haldane functional response. Nonlinear Dynamics, 92(4), 1637–1648. https://doi.org/10.1007/s11071-018-4151-z

Crowley, P. H., & Martin, E. K. (1989). Functional Responses and Interference within and between Year Classes of a Dragonfly. Journal of the North American Benthological Society, 8(3), 211–221. https://doi.org/10.2307/1467324

Cui, J. A., Tao, X., & Zhu, H. (2008). An SIS Infection Model Incorporating Media Coverage. Rocky Mountain Journal of Mathematics, 38, 1323-1334. https://doi.org/10.1216/RMJ-2008-38-5-1323

Cui, J., Sun, Y., & Zhu, H. (2008). The impact of media on the control of infectious diseases. Journal of Dynamics and Differential Equations, 20(1), 31–53. https://doi.org/10.1007/S10884-007-9075-0

Deangelis, D. L., Goldstein, R. A., & O'neill, R. V. (1975). A model for trophic interaction'. Ecology, 56,881-892. http://dx.doi.org/10.2307/1936298

Debasis Mukherjee, D. M., & Maji, C. (2020). Dynamical analysis of a fractional order model incorporating fear in the disease transmission rate of COVID-19. Mathematics in Applied Sciences and Engineering, 99(99), 1–17. https://doi.org/10.5206/mase/10745

Deng, W., Li, C., & Lü, J. (2007). Stability analysis of linear fractional differential system with multiple time delays. Nonlinear Dynamics, 48(4), 409–416. https://doi.org/10.1007/s11071-006-9094-0

Diekmann, O., Heesterbeek, J. A. P., & Metz, J. A. J. (1990). On the definition and the computation of the basic reproduction ratio R0 in models for infectious diseases in heterogeneous populations. J Math Biol. 1990;28(4):365-82. doi: 10.1007/BF00178324. PMID: 2117040.

Diekmann, O., Heesterbeek, J. A. P., & Roberts, M. G. (2010). The construction of next-generation matrices for compartmental epidemic models. Journal of the Royal Society Interface, 7(47), 873–885. https://doi.org/10.1098/rsif.2009.0386

Diethelm, K., Ford, N. J., & Freed, A. D. (2002). A predictor-corrector approach for the numerical solution of fractional differential equations. Nonlinear Dynamics, 29(1–4), 3–22. https://doi.org/10.1023/A:1016592219341

Din, R. ud, & Algehyne, E. A. (2021). Mathematical Analysis of COVID-19 by Using SIR Model with Convex Incidence Rate. Results in Physics, 103970. https://doi.org/10.1016/j.rinp.2021.103970

Driver, R.D. (1977) Ordinary and Delay Differential Equations. Applied Mathematical Sciences, Vol. 20, Springer-Verlag, Berlin. https://doi.org/10.1007/978-1-4684-9467-9

Dubey, B., Dubey, P., & Dubey, U. S. (2015). Dynamics of an SIR Model with Nonlinear Incidence and Treatment Rate. An International Journal (AAM), 10(2), 718–737. http://pvamu.edu/aam

Dubey, B., Patra, A., Srivastava, P. K., & Dubey, U. S. (2013). Modeling and analysis of an seir model with different types of nonlinear treatment rates. Journal of Biological Systems, 21(3). https://doi.org/10.1142/S021833901350023X

Dubey, P. (2016). Stability Analysis and Simulation of Deterministic Models in Epidemiology and Immunology. https://www.researchgate.net/publication/325767063

El-Sayed, A. M. A., El-Mesiry, A. E. M., & El-Saka, H. A. A. (2007). On the fractional-order logistic equation. Applied Mathematics Letters, 20(7), 817–823. https://doi.org/10.1016/j.aml.2006.08.013

Fauci, A. S., & Morens, D. M. (2012). The Perpetual Challenge of Infectious Diseases. N Engl J Med. 2012 Feb 2;366(5):454-61. doi: 10.1056/NEJMra1108296.

Funk, S., Gilad, E., Watkins, C., & Jansen, V. A. A. (2009). The spread of awareness and its impact on epidemic outbreaks. https://doi.org/10.1073/pnas.0810762106

Garfin, D. R., Silver, R. C., & Holman, E. A. (2020). The novel coronavirus (COVID-2019) outbreak: Amplification of public health consequences by media exposure. Health Psychology, 39(5), 355–357. https://doi.org/10.1037/hea0000875

Goel, K., Kumar, A., & Nilam. (2020). Nonlinear dynamics of a time-delayed epidemic model with two explicit aware classes, saturated incidences, and treatment. Nonlinear Dynamics, 101(3), 1693–1715. https://doi.org/10.1007/s11071-020-05762-9

Goel, K., & Nilam. (2019). A mathematical and numerical study of a SIR epidemic model with time delay, nonlinear incidence and treatment rates. Theory in Biosciences, 138(2), 203–213. https://doi.org/10.1007/s12064-019-00275-5

Gómez Alcaraz, G., & Vargas-De-León, C. (2012). Modeling control strategies for influenza A H1N1 epidemics: SIR models. Revista Mexicana de Física S (Vol. 58, Issue 1). http://www.redalyc.org/articulo.oa?id=57030391007

Guckenheimer, J., & Holmes, P. (1983). Nonlinear Oscillations, Dynamical Systems, and Bifurcations of Vector Fields, 42. https://doi.org/10.1007/978-1-4612-1140-2

Hao, K., & Basu, T. (2020). The coronavirus is the first true social-media “infodemic” | CEJC 2023; 16 (2 (34)): 209-223; 10.51480/1899-5101.16.2(34).272

Hattaf, K., Lashari, A., … Y. L.-E. J. of, & 2013, undefined. (2013). A delayed SIR epidemic model with a general incidence rate. Electronic Journal of Qualitative Theory of Differential Equations, (3)1-9. http://real.mtak.hu/22731/1/p1851.pdf

Hattaf, K., & Yousfi, N. (2016). A class of delayed viral infection models with general incidence rate and adaptive immune response. International Journal of Dynamics and Control, 4(3), 254–265. https://doi.org/10.1007/s40435-015-0158-1

Hattaf, K., Yousfi, N., & Tridane, A. (2013). Stability analysis of a virus dynamics model with general incidence rate and two delays. https://doi.org/10.1016/j.amc.2013.07.005

Hethcote, H. W. (2006). The Mathematics of Infectious Diseases. SIAM Review 42(4), 599–653. https://doi.org/10.1137/S0036144500371907

Hilfer, R. (Ed.). (2000). Applications of fractional calculus in physics. World scientific.

Hoan, L. V. C., Akinlar, M. A., Inc, M., Gómez-Aguilar, J. F., Chu, Y. M., & Almohsen, B. (2020). A new fractional-order compartmental disease model. Alexandria Engineering Journal, 59(5), 3187–3196. https://doi.org/10.1016/j.aej.2020.07.040

Holling, C. S. (1959). Some Characteristics of Simple Types of Predation and Parasitism. The Canadian Entomologist, 91(7), 385–398. https://doi.org/10.4039/Ent91385-7

Iswarya, M., Raja, R., Rajchakit, G., Cao, J., Alzabut, J., & Huang, C. (2019). A perspective on graph theory-based stability analysis of impulsive stochastic recurrent neural networks with time-varying delays. Advances in Difference Equations, 2019(1). https://doi.org/10.1186/s13662-019-2443-3

Ji, Qihang. (2022). The Influence of Social Media on Mental Health During COVID-19 Pandemic: Benefits and Risks. 10.2991/assehr.k.220504.233.

Jones, J. H., & Salathé, M. (2009). Early Assessment of Anxiety and Behavioral Response to Novel Swine-Origin Influenza A(H1N1). https://doi.org/10.1371/journal.pone.0008032

Kashkynbayev, A., & Rihan, F. A. (2021). Dynamics of fractional-order epidemic models with general nonlinear incidence rate and time-delay. Mathematics, 9(15). https://doi.org/10.3390/math9151829

Kermack, W. 0, & Mckendrick, A. G. (1927). A contribution to the mathematical theory of epidemics. Proceedings of the Royal Society of London. Series A, Containing Papers of a Mathematical and Physical Character, 115(772), 700–721. https://doi.org/10.1098/rspa.1927.0118

Kimid, L., Fast, S. M., & Markuzon, N. (2019). Incorporating media data into a model of infectious disease transmission. https://doi.org/10.1371/journal.pone.0197646

Kozioł, K., Stanisławski, R., & Bialic, G. (2020). Fractional-order sir epidemic model for transmission prediction of COVID-19 disease. Applied Sciences (Switzerland), 10(23), 1–9. https://doi.org/10.3390/app10238316

Kumar, A. (2020). Stability of a Fractional-Order Epidemic Model with Nonlinear Incidences and Treatment Rates. Iranian Journal of Science and Technology, Transaction A: Science, 44(5), 1505–1517. https://doi.org/10.1007/s40995-020-00960-x

Kumar, A., Goel, K., & Nilam. (2020). A deterministic time-delayed SIR epidemic model: mathematical modeling and analysis. Theory in Biosciences, 139(1), 67–76. https://doi.org/10.1007/s12064-019-00300-7

Kumar, A., Kumar, M., & Nilam. (2020). A study on the stability behavior of an epidemic model with ratio-dependent incidence and saturated treatment. Theory in Biosciences, 139(2), 225–234. https://doi.org/10.1007/s12064-020-00314-6

Kumar, A., & Nilam. (2019). Dynamic Behavior of an SIR Epidemic Model along with Time Delay; Crowley–Martin Type Incidence Rate and Holling Type II Treatment Rate. International Journal of Nonlinear Sciences and Numerical Simulation, 20(7–8), 757–771. https://doi.org/10.1515/ijnsns-2018-0208

Kumar, A., Nilam, & Kishor, R. (2019). A short study of an SIR model with inclusion of an alert class, two explicit nonlinear incidence rates and saturated treatment rate. SeMA Journal, 76(3), 505–519**.** https://doi.org/10.1007/s40324-019-00189-8

Kumar, A., & Nilam, N. (2018). Stability of a Time Delayed SIR Epidemic Model Along with Nonlinear Incidence Rate and Holling Type-II Treatment Rate. International Journal of Computational Methods, 15(6). https://doi.org/10.1142/S021987621850055X

Kumar, S., Sandhu, H. A. S., Awasthi, U., Singh, S. K., & Agarwal, P. (2023). Analysis of COVID-19 outbreak using GIS and SEIR model. Fractional Order Systems and Applications in Engineering, 215–225**.** https://doi.org/10.1016/B978-0-32-390953-2.00020-7

La Salle, J. P. (1976). The Stability of Dynamical Systems. Society for Industrial and Applied Mathematics. https://doi.org/10.1137/1.9781611970432

Laskin, N., & Zaslavsky, G. (2006). Nonlinear fractional dynamics on a lattice with long range interactions. Physica A: Statistical Mechanics and Its Applications, 368(1), 38–54. https://doi.org/10.1016/j.physa.2006.02.027

Li, C. H., Tsai, C. C., & Yang, S. Y. (2012). Analysis of the permanence of an SIR epidemic model with logistic process and distributed time delay. Communications in Nonlinear Science and Numerical Simulation, 17(9), 3696–3707. https://doi.org/10.1016/j.cnsns.2012.01.018

Li, C. H., Tsai, C. C., & Yang, S. Y. (2014). Analysis of epidemic spreading of an SIRS model in complex heterogeneous networks. Communications in Nonlinear Science and Numerical Simulation, 19(4), 1042–1054. https://doi.org/10.1016/j.cnsns.2013.08.033

Li, C., Jia Chen, L., Chen, X., Zhang, M., Pui Pang, C., Chen, H., Cuilian, L., Li Jia, C., Xueyu, C., Mingzhi, Z., Chi Pui, P., & Haoyu, C. (2020). Retrospective analysis of the possibility of predicting the COVID-19 outbreak from Internet searches and social media data, China, 2020. https://doi.org/10.2807/1560-7917.ES.2020.25.10.2000199

Li, M., & Liu, X. (2014). An SIR epidemic model with time delay and general nonlinear incidence rate. Abstract and Applied Analysis, Article ID 131257, 7 pages. https://doi.org/10.1155/2014/131257

Li, M. Y., Graef, J. R., Wang, L., & Karsai, J. (1999). Global dynamics of a SEIR model with varying total population size. Mathematical Biosciences, 160(2), 191–213. https://doi.org/10.1016/S0025-5564(99)00030-9

Li, Z., Ge, J., Yang, M., Feng, J., Qiao, M., Jiang, R., Bi, J., Zhan, G., Xu, X., Wang, L., Zhou, Q., Zhou, C., Pan, Y., Liu, S., Zhang, H., Yang, J., Zhu, B., Hu, Y., Hashimoto, K. Yang, C. (2020). Vicarious traumatization in the general public, members, and non-members of medical teams aiding in COVID-19 control. Brain, Behavior, and Immunity, 88(March), 916–919. https://doi.org/10.1016/j.bbi.2020.03.007

Lin, W. (2007). Global existence theory and chaos control of fractional differential equations. Journal of Mathematical Analysis and Applications, 332(1), 709–726. https://doi.org/10.1016/j.jmaa.2006.10.040

Liu, J., Bai, Z., & Zhang, T. (2018). A periodic two-patch SIS model with time delay and transport-related infection. Journal of Theoretical Biology, 437, 36–44. https://doi.org/10.1016/j.jtbi.2017.10.011

Liu, S., Yu, L., & Huang, M. (2020). Bifurcation analysis of a fractional-order SIQR model with double time delays. International Journal of Biomathematics, 13(7). https://doi.org/10.1142/S1793524520500679

Liu, Y., & Cui, J. A. (2012). The impact of media coverage on the dynamics of infectious disease. International Journal of Biomathematics. 1(1), 65–74. https://doi.org/10.1142/S1793524508000023

Longini, I. M., & Halloran, M. E. (2005). Strategy for distribution of influenza vaccine to high-risk groups and children. American Journal of Epidemiology, 161(4), 303–306. https://doi.org/10.1093/AJE/KWI053

Lu, Z., & Zhu, Y. (2018). Comparison principles for fractional differential equations with the Caputo derivatives. Advances in Difference Equations, 2018(1). https://doi.org/10.1186/s13662-018-1691-y

Mammeri, Y. (2020). A reaction-diffusion system to better comprehend the unlockdown: Application of SEIR-type model with diffusion to the spatial spread of COVID-19 in France. Computational and Mathematical Biophysics, 8(1), 102–113. https://doi.org/10.1515/cmb-2020-0104

Mandal, M., Jana, S., Nandi, S. K., & Kar, T. K. (2020). Modelling and control of a fractional-order epidemic model with fear effect. Energy, Ecology and Environment, 5(6), 421–432. https://doi.org/10.1007/S40974-020-00192-0

Manzoni, G. M., Nazaré, B., Li, Z., Landa-Blanco, M., Landa-Blanco, A., Mejía-Suazo, C. J., & Martínez-Martínez, C. A. (2021). Coronavirus Awareness and Mental Health: Clinical Symptoms and Attitudes Toward Seeking Professional Psychological Help. Front. Psychol, 12, 549644. https://doi.org/10.3389/fpsyg.2021.549644

Matignon, D., & Matignon, D. (1996). Stability Results for Fractional Differential Equations With Applications To Control Processing. In computational engineering in systems applications, 963-968. doi.org/10.1.1.40.4859

Meng, X., Chen, L., & Wu, B. (2010). A delay SIR epidemic model with pulse vaccination and incubation times. Nonlinear Analysis: Real World Applications, 11(1), 88–98. https://doi.org/10.1016/j.nonrwa.2008.10.041

Merchant, R. M., & Lurie, N. (2020). Social Media and Emergency Preparedness in Response to Novel Coronavirus. JAMA - Journal of the American Medical Association, 323(20), 2011–2012. https://doi.org/10.1001/jama.2020.4469

Ministry of Health. (2021). Ministry of Health, the official website of the Jordanian Ministry of Health | Coronavirus disease. Ministry of Health. https://corona.moh.gov.jo/en

Misra, A. K., Sharma, A., & Shukla, J. B. (2011). Modeling and analysis of effects of awareness programs by media on the spread of infectious diseases. Mathematical and Computer Modelling, 53(5–6), 1221–1228. https://doi.org/10.1016/J.MCM.2010.12.005

Murray, J. D. (1989). Mathematical Biology. Springer-Verlag. https://doi.org/10.1007/978-3-662-08539-4

Musa, S. S., Qureshi, S., Zhao, S., Yusuf, A., Mustapha, U. T., & He, D. (2021). Mathematical modeling of COVID-19 epidemic with effect of awareness programs. Infectious Disease Modelling, 6, 448–460. https://doi.org/10.1016/J.IDM.2021.01.012

Naik, P. A. (2020). Global dynamics of a fractional-order SIR epidemic model with memory. International Journal of Biomathematics, 13(8). https://doi.org/10.1142/S1793524520500710

Naim, M., Sabbar, Y., Zahri, M., Ghanbari, B., Zeb, A., Gul, N., Djilali, S., & Lahmidi, F. (2022). The impact of dual time delay and Caputo fractional derivative on the long-run behavior of a viral system with the non-cytolytic immune hypothesis. Physica Scripta, 97(12), 124002. https://doi.org/10.1088/1402-4896/AC9E7A

Odagaki, T. (2021). Exact properties of SIQR model for COVID-19. Physica A, 564, 125564**.** https://doi.org/10.1016/j.physa.2020.125564

Odibat, Z. M., & Shawagfeh, N. T. (2007). Generalized Taylor's formula. Applied Mathematics and Computation, 186(1), 286–293. https://doi.org/10.1016/j.amc.2006.07.102

Otto, S. P., & Day, T. (2019). A Biologist's Guide to Mathematical Modeling in Ecology and Evolution. Princeton University Press. https://doi.org/10.2307/j.ctvcm4hnd

Owoyemi, A. E., Sulaiman, I. M., Mamat, M., Olowo, S. E., Adebiyi, O. A., & Zakaria, Z. A. (2020). Analytic numeric solution of coronavirus (Covid−19) pandemic model in fractional-order. Communications in Mathematical Biology and Neuroscience, 2020(0), 1–18. https://doi.org/10.28919/cmbn/4885

Palladino, A., Nardelli, V., Atzeni, L. G., Cantatore, N., Cataldo, M., Croccolo, F., Estrada, N., & Tombolini, A. (2020). Modelling the spread of Covid19 in Italy using a revised version of the SIR model. doi:10.3204/PUBDB-2020-03341

Pinto, C. M. A., & Carvalho, A. (2015). Virus propagation in a SIQR model with impulse quarantine. AIP Conference Proceedings, 1648. https://doi.org/10.1063/1.4912582

Podlubny, I. (1999) Fractional Differential Equations. Academic Press, San Diego.

Pratap, A., Raja, R., Cao, J., Alzabut, J., & Huang, C. (2020). Finite-time synchronization criterion of graph theory perspective fractional-order coupled

discontinuous neural networks. Advances in Difference Equations, 2020(1). https://doi.org/10.1186/s13662-020-02551-x

Pruyt, E., Auping, W. L., & Kwakkel, J. H. (2015). Ebola in West Africa: Model-Based Exploration of Social Psychological Effects and Interventions. Systems Research and Behavioral Science, 32(1), 2–14. https://doi.org/10.1002/SRES.2329

Rajagopal, K., Hasanzadeh, N., Parastesh, F., Hamarash, I. I., Jafari, S., & Hussain, I. (2020). A fractional-order model for the novel coronavirus (COVID-19) outbreak. Nonlinear Dynamics, 101(1), 711–718. https://doi.org/10.1007/s11071-020-05757-6

Rajchakit, G., Pratap, A., Raja, R., Cao, J., Alzabut, J., & Huang, C. (2019). Hybrid control scheme for projective lag synchronization of Riemann-Liouville sense fractional order memristive BAM neural networks with mixed delays. Mathematics, 7(8). https://doi.org/10.3390/math7080759

Rakkiyappan, R., Preethi Latha, V., & Rihan, F. A. (2019). A Fractional-Order Model for Zika Virus Infection with Multiple Delays. https://doi.org/10.1155/2019/4178073

Rezapour, S., Mohammadi, H., & Samei, M. E. (2020). SEIR epidemic model for COVID-19 transmission by Caputo derivative of fractional order. Advances in Difference Equations, 2020(1). https://doi.org/10.1186/s13662-020-02952-y

Rihan, F. A., Al-Mdallal, Q. M., AlSakaji, H. J., & Hashish, A. (2019). A fractional-order epidemic model with time-delay and nonlinear incidence rate. Chaos, Solitons and Fractals, 126, 97–105. https://doi.org/10.1016/j.chaos.2019.05.039

Rihan, F. A., Sheek-Hussein, M., Tridane, A., & Yafia, R. (2017). Dynamics of Hepatitis C Virus Infection: Mathematical Modeling and Parameter Estimation. Mathematical Modelling of Natural Phenomena, 12(5), 33–47. https://doi.org/10.1051/MMNP/201712503

Ross, B. (1975). A brief history and exposition of the fundamental theory of fractional calculus. Springer, Berlin, Heidelberg. https://doi.org/10.1007/BFb0067096

Rostamy, D., & Mottaghi, E. (2016). Stability analysis of a fractional-order epidemics model with multiple equilibriums. 2016, 170. https://doi.org/10.1186/s13662-016-0905-4

Roth, F., & Brönnimann, G. (2013). Using the Internet for Public Risk Communication. Risk and Resilience Reports.

Roy M. A., Robert M. M. (1992) Infectious Diseases of humans - Oxford University Press.

Scholarship, W., Ashrafur Rahman, S., & Zou, X. (2016). Study of Infectious Diseases by Mathematical Models: Study of Infectious Diseases by Mathematical Models: Predictions and Controls Predictions and Controls. https://ir.lib.uwo.ca/etd://ir.lib.uwo.ca/etd/3487

Sene, N. (2021). Introduction to the fractional-order chaotic system under fractional operator in Caputo sense. Alexandria Engineering Journal, 60(4), 3997–4014. https://doi.org/10.1016/j.aej.2021.02.056

Shu, H., Fan, D., & Wei, J. (2012). Global stability of multi-group SEIR epidemic models with distributed delays and nonlinear transmission. Nonlinear Analysis: Real World Applications, 13(4), 1581–1592. https://doi.org/10.1016/j.nonrwa.2011.11.016

Shuai, Z., & Van Den Driessche, P. (2013). Global stability of infectious disease models using lyapunov functions. SIAM Journal on Applied Mathematics, 73(4), 1513–1532. https://doi.org/10.1137/120876642

Shulgin, B., Stone, L., & Agur, Z. (1998). Pulse vaccination strategy in the SIR epidemic model. Bulletin of Mathematical Biology, 60(6), 1123–1148. https://doi.org/10.1016/S0092-8240(98)90005-2

Strogatz, S. H. (2018). Nonlinear dynamics and chaos: With Applications to Physics, Biology, Chemistry, and Engineering. Nonlinear Dynamics and Chaos: With Applications to Physics, Biology, Chemistry, and Engineering, 1–513. https://doi.org/10.1201/9780429492563

Swati, & Nilam. (2022). Fractional order SIR epidemic model with Beddington–De Angelis incidence and Holling type II treatment rate for COVID-19. Journal of Applied Mathematics and Computing, 68, 3835-3859. https://doi.org/10.1007/S12190-021-01658-Y

Tipsri, S., & Chinviriyasit, W. (2014). Stability Analysis of SEIR Model with Saturated Incidence and Time Delay. International Journal of Applied Physics and Mathematics, 4(1), 42–45. https://doi.org/10.7763/ijapm.2014.v4.252

Usher, J. R. (1994). Some mathematical models for cancer chemotherapy. Computers & Mathematics with Applications, 28(9), 73–80. https://doi.org/10.1016/0898-1221(94)00179-0

Van Den Driessche, P., & Watmough, J. (2002). Reproduction numbers and sub-threshold endemic equilibria for compartmental models of disease transmission. Mathematical Biosciences, 180(1–2), 29–48**.** https://doi.org/10.1016/S0025-5564(02)00108-6

Van Seventer, J. M., & Hochberg, N. S. (2016). Principles of Infectious Diseases: Transmission, Diagnosis, Prevention, and Control. International Encyclopedia of Public Health, 22–39. https://doi.org/10.1016/B978-0-12-803678-5.00516-6

Wang, K., Wang, W., Pang, H., & Liu, X. (2007). Complex dynamic behavior in a viral model with delayed immune response. Physica D: Nonlinear Phenomena, 226(2), 197–208. https://doi.org/10.1016/J.PHYSD.2006.12.001

Wang, W. (2006). Backward bifurcation of an epidemic model with treatment. Mathematical Biosciences, 201(1–2), 58–71. https://doi.org/10.1016/j.mbs.2005.12.022

Wang, W., & Ruan, S. (2004). Bifurcations in an epidemic model with constant removal rate of the infectives. Journal of Mathematical Analysis and Applications, 291(2), 775–793. https://doi.org/10.1016/j.jmaa.2003.11.043

Wang, Y., Jin, Z., Yang, Z., Zhang, Z. K., Zhou, T., & Sun, G. Q. (2012). Global analysis of an SIS model with an infective vector on complex networks. Nonlinear Analysis: Real World Applications, 13(2), 543–557. https://doi.org/10.1016/j.nonrwa.2011.07.033

Wang, Z., & Wang, X. (2018). Stability and hopf bifurcation analysis of a fractional-order epidemic model with time delay. Mathematical Problems in Engineering, 2018. https://doi.org/10.1155/2018/2308245

Wei, H. M., Li, X. Z., & Martcheva, M. (2008). An epidemic model of a vector-borne disease with direct transmission and time delay. Journal of Mathematical Analysis and Applications, 342(2), 895–908. https://doi.org/10.1016/J.JMAA.2007.12.058

Wu, Q., & Fu, X. (2011). Modelling of discrete-time SIS models with awareness interactions on degree-uncorrelated networks. Physica A: Statistical Mechanics and Its Applications, 390(3), 463–470. https://doi.org/10.1016/j.physa.2010.10.006

Yadav, S., Kumar, D., Singh, J., & Baleanu, D. (2021). Analysis and Dynamics of Fractional Order Covid-19 Model with Memory Effect. Results in Physics, 104017. https://doi.org/10.1016/j.rinp.2021.104017

Ye, X., & Xu, C. (2019). A fractional order epidemic model and simulation for avian influenza dynamics. Mathematical Methods in the Applied Sciences, 42(14), 4765–4779. https://doi.org/10.1002/mma.5690

Yi, N., Zhang, Q., Mao, K., Yang, D., & Li, Q. (2009). Analysis and control of an SEIR epidemic system with nonlinear transmission rate. Mathematical and Computer Modelling, 50(9–10), 1498–1513. https://doi.org/10.1016/j.mcm.2009.07.014

Zarocostas, J. (2020). How to fight an infodemic. Lancet (London, England), 395(10225), 676. https://doi.org/10.1016/S0140-6736(20)30461-X

Zhonghua, Z., & Yaohong, S. (2010). Qualitative analysis of a SIR epidemic model with saturated treatment rate. Journal of Applied Mathematics and Computing, 34(1–2), 177–194. https://doi.org/10.1007/s12190-009-0315-9

Zhou, L., & Fan, M. (2012). Dynamics of an SIR epidemic model with limited medical resources revisited. Nonlinear Analysis: Real World Applications, 13(1), 312–324. https://doi.org/10.1016/j.nonrwa.2011.07.036

Zhou, X., & Cui, J. (2011). Analysis of stability and bifurcation for an SEIR epidemic model with saturated recovery rate. Communications in Nonlinear Science and Numerical Simulation, 16(11), 4438–4450. https://doi.org/10.1016/j.cnsns.2011.03.026

APPENDIX

Definition 1(Podlubny, I. (1999)) "The Caputo fractional derivative of order ρ of a function $f(t) \in C^n([t_0, +\infty), \mathbb{R})$ is defined as

$$D_t^{\rho} f(t) = \frac{1}{\Gamma(n-\rho)} \int_{t_0}^{t} \frac{f^{(n)}(\tau)}{(t-\tau)^{\rho+1-n}} \, d\tau$$

Where $t_0 \geq t, \Gamma.$ is the Gamma Function and n is the positive integer such that $n - 1 < \rho < n$. When $0 < \rho < 1$, we have

$$D_t^{\rho} f(t) = \frac{1}{\Gamma(1-\rho)} \int_{t_0}^{t} \frac{f'(\tau)}{(t-\tau)^{\rho}} \, d\tau$$

We have the following definition for the Riemann-Liouville case:

$$D_t^{\rho} f(t) = \frac{1}{\Gamma(n-\rho)} \frac{d^n}{dt^n} \int_{t_0}^{t} (t-\tau)^{\rho+1-n} f(\tau) d\tau \quad "$$

Lemma 1(Matignon & Matignon, 1996) "Consider the fractional-order system
$D_t^{\rho} x(t) = f\big(t, x(t)\big)$
with initial condition $x(t_0) = x_{t_0}$where $\rho \in (0,1]$. The equilibrium points of system are locally asymptotically stable if all eigenvalues λ_i of the Jacobian matrix $\frac{\partial f(t,x)}{\partial x}$ evaluated at the equilibrium points satisfy $|arg(\lambda i)| > \frac{\rho\,\pi}{2}$ "

Lemma 2. "Generalized mean value theorem (Odibat & Shawagfeh, 2007) Let $f(x) \epsilon\, C[a,b]$ and $D^{\rho} f(x) \epsilon\, C(a,b]$ for $0 < \rho \leq 1$. Then we have
$f(x) = f(a) + \frac{1}{\Gamma(\alpha)} D^{\rho} f(\xi)\, (x-a)^{\rho}$ where $0 \leq \xi \leq x$, $\forall\, x \epsilon\, (a,b]$"

Lemma 3 (El-Sayed et al., 2007) "Let $\alpha_1 > 0, \alpha_2 > 0, and\ c \in C$. Define $y(t) = t^{\alpha_2 - 1} E_{\alpha_1,\alpha_2}(\pm c t^{\alpha_1})$, where E_{α_1,α_2}(z) denotes the two-parameter Mittag–Leffler function with parameters α_1 and α_2, then the Laplace transformation of y is given by $L[y(t)] = \frac{s^{\alpha_1 - \alpha_2}}{s^{\alpha_1 \mp c}}$ ".

Lemma 4 (El-Sayed et al., 2007) "Let α_2 is an arbitrary real number. If $\alpha_1 < 2$, then there is a constant C_E such that, for all z in the complex plane, $\left|E_{\alpha_1,\alpha_2}(z)\right| \leq \frac{C_E}{1+|z|}$".

LIST OF PUBLICATIONS

1. **Swati**, Nilam, Fractional order SIR epidemic model with Beddington–De Angelis incidence and Holling type II treatment rate for COVID-19. J. Appl. Math. Comput. 68, 3835–3859 (2022), **https://doi.org/10.1007/s12190-021-01658-y**, Impact Factor-2.4, Indexing: SCIE.

2. **Swati**, Nilam, Fractional order model using Caputo fractional derivative to analyse the effects of social media on mental health during Covid-19, Alexandria Engineering Journal, 92, 336-345 (2024), **https://doi.org/10.1016/j.aej.2024.02.049**, Impact Factor-6.2, Indexing: SCIE

3. **Swati,** Nilam "Caputo Fractional derivative model for impact of awareness on infectious disease" (Communicated)

4. **Swati,** Nilam **"**The behavior of the fractional order delay differential SIR epidemic model with Holling type II treatment rate and Crowley-Martin rate of incidence" (Communicated)

5. **Swati,** Nilam, Ankit Sharma "Bifurcation analysis of a double Delayed SIQR fractional order model incorporating Holling Type-II treatment rate and Monod-Haldane incidence rate" (Communicated)

LIST OF CONFERENCES

1. **Swati,** Nilam "Fractional order SIR epidemic model for COVID-19" presented at International Nonlinear Dynamics Conference (NODYCON 2021) organised by Department of Structural and Geotechnical Engineering, SAPIENZA, University of Rome, Italy, February 16-19, 2021.

2. **Swati,** Nilam "Role of fractional differential equations in epidemiology" presented at International Conference on Mathematical Modeling and Simulation (MMSPS 2021) organised by Applied Mathematics and Humanities Department & Department of Physics, SVNIT, Gujrat, India, April 17-18, 2021.

Journal of Applied Mathematics and Computing
https://doi.org/10.1007/s12190-021-01658-y

ORIGINAL RESEARCH

Fractional order SIR epidemic model with Beddington–De Angelis incidence and Holling type II treatment rate for COVID-19

Swati[1] · **Nilam**[1]

Received: 28 July 2021 / Revised: 25 October 2021 / Accepted: 26 October 2021
© Korean Society for Informatics and Computational Applied Mathematics 2021

Abstract
In this paper, an attempt has been made to study and investigate a non-linear, non-integer SIR epidemic model for COVID-19 by incorporating Beddington–De Angelis incidence rate and Holling type II saturated cure rate. Beddington–De Angelis incidence rate has been chosen to observe the effects of measure of inhibition taken by both: susceptible and infective. This includes measure of inhibition taken by susceptibles as wearing proper mask, personal hygiene and maintaining social distance and the measure of inhibition taken by infectives may be quarantine or any other available treatment facility. Holling type II treatment rate has been considered for the present model for its ability to capture the effects of available limited treatment facilities in case of Covid 19. To include the neglected effect of memory property in integer order system, Caputo form of non-integer derivative has been considered, which exists in most biological systems. It has been observed that the model is well posed i.e., the solution with a positive initial value is reviewed for non-negativity and boundedness. Basic reproduction number R_0 is determined by next generation matrix method. Routh Hurwitz criteria has been used to determine the presence and stability of equilibrium points and then stability analyses have been conducted. It has been observed that the disease-free equilibrium Q^d is stable for $R_0 < 1$ i.e., there will be no infection in the population and the system tends towards the disease-free equilibrium Q^d and for $R_0 > 1$, it becomes unstable, and the system will tend towards endemic equilibrium Q^e. Further, global stability analysis is carried out for both the equilibria using R_0. Lastly numerical simulations to assess the effects of various parameters on the dynamics of disease has been performed.

Keywords Equilibrium points · Local stability · Global stability · Basic reproduction number · Memory effect · Caputo non-integer order differential equations

✉ Nilam
drnilam@dce.ac.in

[1] Department of Applied Mathematics, Delhi Technological University, Delhi 110042, India

Published online: 06 January 2022

Alexandria Engineering Journal 92 (2024) 336–345

Contents lists available at ScienceDirect

Alexandria Engineering Journal

journal homepage: www.elsevier.com/locate/aej

Fractional order model using Caputo fractional derivative to analyse the effects of social media on mental health during Covid-19

Swati [a,b], Nilam [a,*]

[a] Department of Applied Mathematics, Delhi Technological University, Delhi 110042, India
[b] Department of Mathematics, Ramjas College, University of Delhi, Delhi 110007, India

ARTICLE INFO

JEL classification:
34D20
34D23
37C75
92B05

Keywords:
Caputo fractional derivative
Lyapunov functions
Routh Hurwitz's criteria
Basic reproduction number
Holling type II incidence rate
Monod Haldane treatment rate
Memory effect
Social media

ABSTRACT

During the COVID-19 outbreak, a large population was exposed to social media. Since it was a new virus and no specific information was available about its dynamics, therefore people were dependent on social media to gather more and more information. Social media has its pros and cons, which have an impact on the life of human beings which was more in the case of COVID-19 due to restricted interaction during the period of pandemic. In this article, the effects of social media on the mental health of people have been investigated with the help of Holling type II and Monod Haldane rates in the form of incidence and treatment rates, respectively. The model exhibits two types of equilibria: disease-free equilibrium (DFE) and endemic equilibrium (EE), which has been confirmed by the Fractional Routh-Hurwitz criterion. Further stability behavior has been also analyzed under certain sufficient conditions that depend on threshold R_0, a Basic Reproduction number, which is determined by the next generation approach. The findings indicate that the fractional order has a considerable influence on the dynamic process. The difference between fractional and integer order derivatives is illustrated by the memory effect. Finally, numerical simulations have been performed to validate our analytical findings and to examine the effect of various parameters on the dynamics of social media on mental health.

1. Introduction

Severe Acute Respiratory Syndrome Corona Virus-2 (SARS CoV-2), 2019-nCoV is a new coronavirus capable of causing coronavirus disease, a severe respiratory illness similar to SARS and MERS, originally first identified in Wuhan, China, in December 2019. The World Health Organization first declared the COVID-19 outbreak as a Concern of International Public Health Emergency and then a pandemic. As a result of the outbreak, rigorous laws prohibiting massive gatherings and social activities have been implemented across the world. Because of the stringent social distancing restrictions, people were heavily relying on media, particularly social media, for up-to-date information regarding the outbreak and to maintain connectivity. Among the most widely utilized resources of information is social media networks; they are one of the simplest and most effective techniques for transmitting information.

The World Health Organization has revealed that they are currently fighting not only with a global pandemic but also with a social media infodemic, with some media organizations claiming that the coronavirus is the first true social media infodemic because it has exacerbated information and misinformation globally, causing panic and confusion among people [1]. The term infodemic [2] has been coined to outline the perils of misinformation phenomena during the management of disease outbreaks since it could even speed up the epidemic process by influencing and fragmenting social response [3].

Indeed, Li et al. [4] found that the general public reported even higher levels of vicarious traumatization than front-line nurses fighting COVID-19. According to an ABC News poll, anxiety due to the coronavirus spreads faster on social media than the virus itself, triggering mass chaos [5].

Compared with traditional media, social media has played a multitude of positive roles in information exchange during the COVID-19 crisis, including disseminating health-related recommendations and enabling connectivity and psychological first aid [6]. On the other hand, social media has also fueled the rapid spread of misinformation and rumors, which can create a sense of panic and confusion among the public [7]. In China, the peak of information searches on the Internet and social media platforms came 10-14 days before the peak of COVID-19 cases, suggesting that searches on the Internet and social media networks are linked to disease occurrence [8].

* Correspondence to: Department of Applied Mathematics, Delhi Technological University, Delhi, India.
E-mail address: drnilam@dce.ac.in (Nilam).

https://doi.org/10.1016/j.aej.2024.02.049
Received 6 June 2023; Received in revised form 4 February 2024; Accepted 22 February 2024
Available online 8 March 2024
1110-0168/© 2024 The Author(s). Published by Elsevier BV on behalf of Faculty of Engineering, Alexandria University This is an open access article under the CC BY-NC-ND license (http://creativecommons.org/licenses/by-nc-nd/4.0/).

DELHI TECHNOLOGICAL UNIVERSITY
(Formerly Delhi College of Engineering)
Shahbad Daulatpur, Main Bawana Road, Delhi-42

PLAGIARISM VERIFICATION

Title of the Thesis **FRACTIONAL MATHEMATICAL MODEL FOR DYNAMICS OF INFECTIOUS DISEASES**.

Total Pages: 213

Name of the Scholar: Ms. Swati

Supervisor: Dr. Nilam

Department: Applied Mathematics

This is to report that the above thesis was scanned for similarity detection. Process and outcome is given below:

Software used: Turnitin

Similarity Index: 8%

Total Word Count: 45882

Date: 30 October 2024

Swati

Dr. Nilam
Associate Professor
Supervisor

Turnitin Originality Report

Processed on: 29-Oct-2024 17:52 IST
ID: 2501365889
Word Count: 45882
Submitted: 1

Swati Thesis By Sunil MEENA

Similarity Index	Similarity by Source
8%	Internet Sources: 7% Publications: 8% Student Papers: 0%

3% match (Internet from 17-Feb-2023)
https://www.researchgate.net/publication/263804626_Modeling_and_analysis_of_an_seir_model_with_different_types_of_nonlinear_treatr

2% match (Shouzong Liu, Ling Yu, Mingzhan Huang. "Bifurcation analysis of a fractional-order SIQR model with double time delays", International Journal of Biomathematics, 2020)
Shouzong Liu, Ling Yu, Mingzhan Huang. "Bifurcation analysis of a fractional-order SIQR model with double time delays", International Journal of Biomathematics, 2020

1% match (Rahman, Sm Ashrafur. "Study of Infectious Diseases by Mathematical Models: Predictions and Controls", The University of Western Ontario (Canada), 2022)
Rahman, Sm Ashrafur. "Study of Infectious Diseases by Mathematical Models: Predictions and Controls", The University of Western Ontario (Canada), 2022

1% match (Parvaiz Ahmad Naik. "Global Dynamics of a Fractional order SIR Epidemic Model with Memory", International Journal of Biomathematics, 2020)
Parvaiz Ahmad Naik. "Global Dynamics of a Fractional order SIR Epidemic Model with Memory", International Journal of Biomathematics, 2020

1% match (Abhishek Kumar. "Stability of a Fractional-Order Epidemic Model with Nonlinear Incidences and Treatment Rates", Iranian Journal of Science and Technology, Transactions A: Science, 2020)
Abhishek Kumar. "Stability of a Fractional-Order Epidemic Model with Nonlinear Incidences and Treatment Rates", Iranian Journal of Science and Technology, Transactions A: Science, 2020

1% match (Internet from 27-Sep-2022)
https://www.hindawi.com/journals/complexity/2019/4178073/

1% match (Internet from 18-Mar-2023)
https://ebin.pub/mathematical-modelling-and-analysis-of-infectious-diseases-1st-ed-9783030498955-9783030498962.html

vi FRACTIONAL MATHEMATICAL MODEL FOR DYNAMICS OF INFECTIOUS DISEASES SWATI ABSTRACT This thesis presents a comprehensive study of fractional-order differential models used for analysing the dynamics of infectious diseases. The fractional-order framework generalizes classical models with the inclusion of derivatives not being integer, thus capturing memory effects that describe long-term dependencies in disease spread and dynamics. We have also introduced time delays to account for incubation periods or delayed interventions seen in the real- world delay between disease spread and treatment. Such delays have major impacts on both epidemic progress and the timing of control measures, such as quarantine, vaccination or therapeutic intervention. In this work, we developed and evaluated fractional-order models for infectious diseases, including delayed versions of SIR and SIQR models. We investigated the

CURRICULUM VITAE

SWATI
E-mail: swati@ramjas.du.ac.in
Mob. 8447783711

TEACHING EXPERIENCE:

- Working as an Assistant Professor in Ramjas College, University of Delhi, Delhi since 21st November 2022.
- Worked as an Assistant Professor in Swami Shraddhanand College, University of Delhi, Alipur, Delhi from 29th July 2013- 20th November 2022.

AREA OF SPECIALIZATION:

Differential Equations, Numerical Methods, Mathematical Modelling and Simulation, Linear Algebra, Calculus.

RESEARCH:

- Area - Dynamics of Infectious Diseases
- Pursuing Ph.D. from Delhi Technological University, Delhi under the supervision of Dr. Nilam.

EDUCATIONAL QUALIFICATION:

- Pursuing Ph.D. from Delhi Technological University, Delhi since Oct 2019 under the supervision of Dr. Nilam on "Fractional Mathematical Model for dynamics of infectious diseases".
- CSIR-JRF June -2011 AIR-113
- Gate Qualified-2011,12
- M.Phil (Mathematics) from the department of Mathematics, Dayalbagh Educational Institute, Agra in 2010
- M.Sc. (Mathematics) with specialization in computer applications from the department of Mathematics, Dayalbagh Educational Institute, Agra in 2009
- B.Sc. from Agra College, Dr. B.R. University Agra, U.P. in 2007.

PAPER PUBLISHED

- Swati, Nilam, Fractional order model using Caputo fractional derivative to analyse the effects of social media on mental health during Covid-19, Alexandria Engineering Journal, Volume 92, 2024, Pages 336-345, ISSN 1110-0168, https://doi.org/10.1016/j.aej.2024.02.049.

- Swati, Nilam Fractional order SIR epidemic model with Beddington–De

Angelis incidence and Holling type II treatment rate for COVID-19. J. Appl. Math. Comput. 68, 3835–3859 (2022). https://doi.org/10.1007/s12190-021-01658-y

CONFERENCE PROCEEDINGS:

- Presented a paper titled “Fractional order SIR epidemic model for COVID-19” in an international conference Nonlinear Dynamics Conference (NODYCON2021), SAPIENZA University of Rome, Italy on February 19,2021.
- Presented a paper titled “Role of Fractional differential equations in epidemiology” in an international conference on Mathematical Modeling and Simulation in Physical Sciences (MMSPS-2021), Sardar Vallabhbhai National Institute of Technology on April 18, 2021.

FDPS/REFRESHER COURSES/WORKSHOPS

- Completed 2-week Refresher Course in “Mathematical Sciences-Theme-Python and Vedic Mathematics”, from 01- 14 September 2023, organized by Teaching Learning Centre, Ramanujan College, University of Delhi.
- Three days online workshop on “LaTeX and R” organised by Atma Ram Sanatan Dharm College, from 20-22 October 2023, University of Delhi, Delhi.
- Completed a 4-Week Faculty Induction/Orientation Programme for “Faculty in Universities/Colleges/Institutes of Higher Education” from 21 December 2022 – 19 January 2023, organized by Teaching Learning Centre, Ramanujan College, University of Delhi.
- Completed an Online 2-week Refresher Course in “Mathematical Sciences”, from 28 January 11 February 2023, organized by Teaching Learning Centre, Ramanujan College, University of Delhi.
- FDP on Mathematical Modeling of biosystems with special focus on epidemiology, by Mizoram University, 22 August-27 August 2022.
- One day workshop on “Google Classroom: Teaching, Learning and Managing” by Swami Shradhhanand College, University of Delhi, Delhi, 24 May 2020.
- One-week online FDP on “Moodle Learning Management System”, Atal Bihari Vajpayee University, Bilaspur (C.G.), 12 May 2020- 17 May 2020
- 2 days FDP on "Introduction to R programming", Janki Devi Memorial College, University of Delhi, Delhi, 6 Sep 2018-7 Sep 2018.